

Self-Assembling Molecular Capsules

by

Brendan M. O'Leary

B.A., Chemistry
Middlebury College, 1994

SUBMITTED TO THE DEPARTMENT OF CHEMISTRY IN PARTIAL
FULFILLMENT OF THE REQUIREMENTS FOR THE DEGREE OF

DOCTOR OF PHILOSOPHY

at the
MASSACHUSETTS INSTITUTE OF TECHNOLOGY

September 1999

© 1999 Massachusetts Institute of Technology. All rights reserved.

Signature of Author: _____
Department of Chemistry
June 7, 1999

Certified by: _____
Professor Julius Rebek, Jr.
Thesis Supervisor

Accepted by: _____
Professor Robert W. Field
Chairman, Departmental Committee on Graduate Students in Chemistry

This doctoral thesis has been examined by a Committee of the Department of Chemistry as follows:

Professor Daniel S. Kemp: _____ Chairman

Professor Julius Rebek, Jr.: _____ Thesis Supervisor

Professor Peter H. Seeberger: _____

Self-Assembling Molecular Capsules

by

Brendan M. O'Leary

Submitted to the Department of Chemistry on June 7, 1999
in Partial Fulfillment of the Requirements for the Degree of
Doctor of Philosophy

Abstract

Host complexes formed through non-covalent interactions comprise a rapidly growing area of supramolecular chemistry. In particular, three-dimensional hosts which reversibly encapsulate guests hold great potential as both novel tools in chemistry and as biological models. Here, we describe the design, synthesis, and study of several self-assembling molecular capsules. In particular, we discuss how challenges encountered with earlier capsules were overcome using a modular strategy based upon unique glycoluril building blocks. This method generated capsules approaching nanoscale dimensions that were studied using a combination of NMR and ESI-mass spectrometry. Progress toward novel supramolecular capsules which utilize both hydrogen bonds and metal-ligand interactions is reported and new ferric iron sequestering agents are introduced.

Thesis Supervisor: Professor Julius Rebek, Jr.
Title: Director, The Skaggs Institute for Chemical Biology and
Professor, Department of Chemistry
The Scripps Research Institute

for

Trystan

Acknowledgements

At both MIT and Scripps, Professor Rebek created an incredible environment for the study of science. He granted me considerable freedom to pursue challenging research projects and generously supported all of my efforts both financially and intellectually. Over the past five years, I have deeply admired Professor Rebek's unique, broad vision and I will continue to do so throughout my career.

Professor Dmitry M. Rudkevich has contributed significantly to my development as a scientist. For being both a knowledgeable mentor and a good friend, I offer Dmitry sincere thanks.

My undergraduate advisor, Professor Jeffrey H. Byers, introduced me to organic chemistry and gave me my first opportunity to perform research. His friendship and encouraging words were also constants during my graduate career.

During the past five years, I had the pleasure of collaborating with numerous members of the Rebek Group. Although I mention each by name throughout my thesis, I wish to thank them collectively here for all of the skills and knowledge they shared with me. A fellow graduate student, Kent E. Pryor, is not mentioned specifically in the ensuing chapters, but his thoughtful advice throughout the years was greatly appreciated.

Finally, I wish to thank my family: Mom, Niamh, Sean, Dad, Clif, Jan, Jim, Linnie, and Tamsyn. In particular, I thank my wife, Trystan, for her constant encouragement.

Table of Contents

Chapter 1

Supramolecular Capsules

1.1 Introduction.....	15
1.2 A Natural System: Ferritin	15
1.3 Synthetic Systems: Covalent Hosts.....	17
1.4 Synthetic Systems: Self-Assembled Capsules.....	20

Chapter 2

A D_{3d} -Symmetric Self-Assembling Capsule The “Jelly Doughnut”

2.1 Introduction.....	27
2.2 Synthesis.....	28
2.3 Characterization	31
2.2 Encapsulation Studies.....	32
2.4.1 Benzene as a Guest.....	32
2.4.2 Ring Inversion Dynamics of Encapsulated Cyclohexane.....	33
2.4.3 Other Encapsulation Studies	39
2.5 Experimental.....	40
2.5.1 General Apparatus, Materials, and Methods.....	40
2.5.2 Calculations / Error Analysis for Cyclohexane Ring Inversion Experiments ..	41
2.5.3 Procedures.....	42

Chapter 3

Glycolurils: Synthesis and Modification

3.1 Introduction.....	47
3.2 <i>cis</i> -Bisprotected Glycoluril.....	48

3.3 Soluble Glycolurils.....	49
3.4 Alkylation Reactions	52
3.5 Experimental.....	52
3.5.1 Apparatus, Materials, and Methods.....	52
3.5.2 Procedures.....	52

Chapter 4

A Modular Approach to Self-Assembling Systems

4.1 Introduction.....	65
4.2 Nolte Methodology	65
4.3 New Modules	68
4.4 Hydroxyl Module.....	68
4.5 Acid Module	72
4.6 Amine Module	74
4.7 Experimental.....	75
4.7.1 Apparatus, Materials, and Methods.....	75
4.7.2 Procedures.....	75

Chapter 5

Flexible, Dimeric Assemblies “Flexiballs”

5.1 Introduction.....	103
5.2 Benzene-Based Spacers.....	103
5.3 Triethylbenzene-Based Flexiballs.....	107
5.3.1 Amide Flexiballs	107
5.3.2 Ester Flexiball	115
5.4 Larger Flexiballs	116

5.4.1 Calix[4]arene Flexiball	116
5.4.2 Cavitand Flexiball	117
5.5 Capsule Characterization by ESI-MS	122
5.5.1 Introduction.....	122
5.5.2 ESI-MS of Triethylbenzene Flexiballs	124
5.5.3 ESI-MS of the Cavitand Flexiball	128
5.5.4 Ion-Pairing in ESI-MS Experiments	130
5.6 Experimental.....	131
5.6.1 Apparatus, Materials, and Methods.....	131
5.6.2 Procedures.....	131

Chapter 6

Ferric Iron Sequestering Agents

6.1 Introduction.....	141
6.2 Truxene-Based Ligand	143
6.3 Pseudopeptide-Based Ligand.....	145
6.4 Triphenylene-Based Ligand.....	147
6.5 Future Work.....	148
6.6 Experimental.....	149
6.6.1 Apparatus, Materials, and Methods.....	149
6.6.2 Procedures.....	149

Chapter 7

Toward Glycoluril Modules as Transition-Metal Ligands

7.1 Introduction.....	157
7.2 Design Considerations.....	159

7.3 Dipyridyl Ligand Modules	160
7.4 Aminophenol Ligand Modules	164
7.5 Catechol Ligand Modules.....	167
7.6 Experimental.....	171
7.7.1 Apparatus, Materials, and Methods.....	171
7.7.2 Procedures.....	171

Chapter 1 **Supramolecular Capsules**

1.1 Introduction

The physical separation between self and the non-self is a common characteristic throughout all aspects of life. On the cellular level, phospholipid membranes define boundaries by encapsulating cellular components and excluding extra-cellular material. Protein coats serve the same functions for viruses.¹ Insufficient genetic material exists in either case, however, to encode for biological capsules consisting of a single, complex molecule. Instead, nature utilizes multiple copies of relatively small molecules that assemble through non-covalent interactions.² This economical solution reserves valuable genetic material for the encoding of other structures required for diverse function. Over the past two decades, research devoted to synthetic capsules has attempted to mimic the elegance and efficiency of this minimalist strategy developed by nature.

1.2 A Natural System: Ferritin³

Ferritin is one of the most ubiquitous structures throughout nature and a poignant example of a sub-cellular level biological capsule. Present in living organisms from plants to microbes to mammals, ferritin is an iron storage protein whose three-dimensional structure is highly conserved across species. All ferritins possess 24 proteins assembled *via* hydrogen bonds and salt bridges into an octahedral capsule. The resulting cavity, with approximate volume of 268 nm³, can accommodate up to 4500 iron(III)

¹ Wessells, N.K.; Hopson, J.L. *Biology*; Random House, Inc.: New York, 1988.

² Stryer, L. *Biochemistry*, 3rd ed.; W.H. Freeman and Co.: New York, 1988.

³ For a recent review on ferritin, see: Harrison, P.M.; Arosio, P. *Biochim. Biophys. Acta* **1996**, *1275*, 161-203.

atoms in the form of FeO(OH). This iron sequestering ability manifests itself in ferritin's dual functions of iron reserve and iron detoxification.

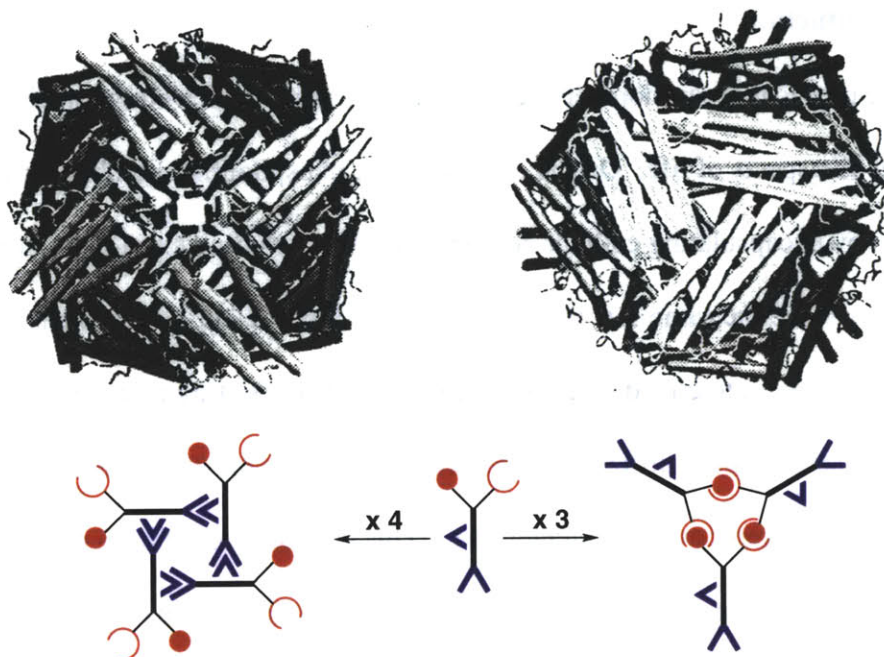


Figure 1-1.⁴ (top) Human H-chain ferritin as viewed down the C_4 (left) and C_3 (right) axes of the complex. (bottom) The H-chain protein assembles *via* different binding schemes giving tetrameric and trimeric subunits.

In humans, several isoferritins exist and are composed of two types of proteins, H- and L- chains. The composition of a particular ferritin ($H_{24}L_0$, $H_{23}L_1$,... H_0L_{24}) varies dependent upon body location. Figure 1-1 illustrates recombinant human H-chain ferritin as viewed down its two types of rotational axes.⁵ The H-chain proteins assemble through two binding motifs producing tetrameric and trimeric subunits with C_4 and C_3 axes, respectively. The overall symmetry of ferritin must be octahedral since only this shape can accommodate both types of rotational axes and the stoichiometric requirements of the complex.⁴

⁴ Caulder, D.L.; Raymond, K.N. *J. Chem. Soc., Dalton Trans.* **1999**, 1185-1200.

Current research focuses on the complex mechanisms by which ferritin accomplishes efficient, reversible iron encapsulation and modulates the reactivity of its metallic guests.³ In the latter case, ferritin prevents the iron(III)-mediated catalysis of hydroxyl radical production⁶ by inhibiting ferric iron's reduction to iron(II), a key step in the process.⁷ The complex functions and simplicity of design exemplified by ferritin have inspired bioorganic and supramolecular chemists for decades.

1.3 Synthetic Systems: Covalent Hosts

Although biological systems provide compelling models for supramolecular capsules, the ability to design the requisite functional building blocks (i.e. polypeptides with programmed tertiary structures) is still in its infancy.⁸ Relatively simple organic compounds, however, can serve as useful model systems and demonstrate unique functions.

The first generation of three-dimensional hosts with central cavities were covalent, polycyclic structures. Figure 1-2 illustrates four representatives. Building upon the development of crown ethers, Lehn introduced the cryptands in the 1970's and demonstrated their affinity for a variety of small guests such as alkali metal cations and

⁵ Lawson, D.M.; Artymiuk, P.J.; Yewdall, S.J.; Smith, J.M.A.; Livingstone, J.C.; Treffry, A.; Luzzago, A.; Levi, S.; Arosio, P.; Cesareni, G.; Thomas, C.D.; Shaw, W.V.; Harrison, P.M. *Nature* **1991**, *349*, 541-544.

⁶ For a review of biomolecule degradation by hydroxyl radicals, see: Halliwell, B.; Gutteridge, J.M.C. *Biochem. J.* **1984**, *219*, 1-14.

⁷ For further information about the iron catalyzed Haber-Weiss reaction, see: Haber, F.; Weiss, J. *Proc. Roy. Soc. Ser. A.* **1934**, *147*, 332-333.

⁸ (a) Vogtle, F. *Supramolecular Chemistry*; John Wiley and Sons: New York, 1993. (b) Dugas, H. In *Bioorganic Chemistry: A Chemical Approach to Enzyme Action*, 3rd ed.; Cantor, C.R., Ed.; Springer Advanced Texts in Chemistry; Springer-Verlag: New York, 1996.

ammonium ions.⁹ However, while high yields of some cryptands were possible through template effects, many of these hosts still required significant synthetic effort.¹⁰

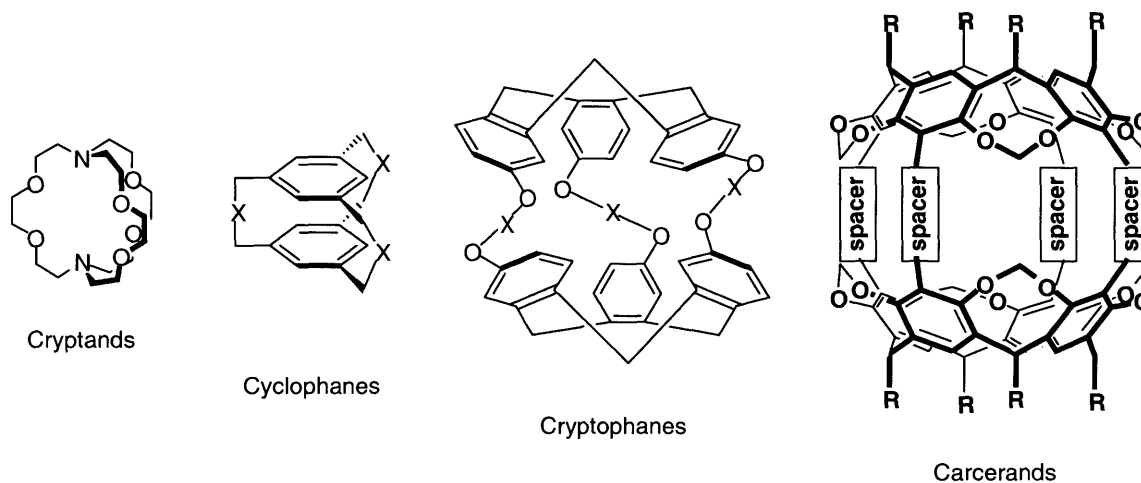


Figure 1-2. Some representative covalent hosts.

An alternative strategy employing multiple, readily available subunits overcame many of these synthetic difficulties. Mimicking the efficiency of biological systems, covalent hosts derived from “molecular building blocks”¹¹ or “molecular LEGOs”¹² were created. Consisting of two spacers and three bridges, triply-bridged cyclophanes¹³ were some of the earliest examples of such structures. Soon thereafter, cryptophane hosts based upon cyclotrimeratrylene spacers were utilized as new tools in the studies of host-guest complexation,¹⁴ chiroselective recognition,¹⁵ and intermolecular forces.¹⁶

⁹ Lehn, J.-M. *Acc. Chem. Res.* **1978**, *11*, 49-57.

¹⁰ See ref. 8a, pp 27-83.

¹¹ Ebmeyer, F.; Vögtle, F. In *Inclusion Compounds, Vol. 4*; Atwood, J.L., Davies, J.E.D., MacNicol, D.D., Eds.; Oxford Science Publications: Oxford, U.K., 1991; pp 263-282.

¹² Kohnke, F.E.; Mathias, J.P.; Stoddart, J.F. *Angew. Chem. Int. Ed. Engl. Adv. Mater.* **1989**, *28*, 1126-1133.

¹³ (a) Seel, C.; Vögtle, F. *Angew. Chem. Int. Ed. Engl.* **1992**, *31*, 528-549; (b) *Comprehensive Supramolecular Chemistry, Vol. 2*; Atwood, J.L, Davies, J.E.D., Lehn, J.-M. MacNicol, D.D., Vögtle, F., Eds.; Elsevier Science Inc.: New York, 1996; pp 195-266.

¹⁴ See ref. 8a, pp142-154.

Larger, more complex hosts such as Cram's carcerands¹⁷ or structurally-related calixarene systems¹⁸ also arose from this convergent strategy and were shown to encapsulate a variety of organic guests. Among other uses, these "molecule-within-molecule" complexes¹⁹ provided physical organic chemistry with the means to study reactive intermediates,²⁰ novel phases of matter,²¹ and new forms of stereoisomerism. (The latter results from severe restrictions on guest motions imposed by some covalently-sealed container hosts.^{22,23})

Although proven as useful receptors, these covalent systems still differ markedly from biological capsules such as ferritin. In the case of many cyclophanes, for instance, insufficient boundaries exist to slow the rapid exchange of guests. Hosts such as the carcerands, in contrast, usually imprison guests irreversibly so no exchange is possible. In biological systems, a compromise between these two extremes is reached by constructing hosts out of self-assembled building blocks rather than covalently linked systems.

¹⁵ (a) Collet, A. Cryptophanes. In *Comprehensive Supramolecular Chemistry, Vol. 2*; Atwood, J.L., Davies, J.E.D., Lehn, J.-M., MacNicol, D.D., Vögtle, F., Eds.; Elsevier Science Inc.: New York, 1996; pp 325-366.

(b) Collet, A.; Dutasta, J.-P.; Lozach, B.; Canceill, J. *Top. Curr. Chem.* **1993**, *165*, 103-129.

¹⁶ Garel, L.; Dutasta, J.-P.; Collet, A. *Angew. Chem., Int. Ed. Engl.* **1993**, *32*, 1169-1171.

¹⁷ *Container Molecules and Their Guests*; Cram, D.J., Cram, J.M., Eds.; Royal Society of Chemistry: Cambridge, UK, 1997.

¹⁸ Higler, I.; Timmerman, P.; Verboom, W.; Reinhoudt, D.N. *Eur. J. Org. Chem.* **1998**, *12*, 2689-2702.

¹⁹ This phrase first appeared as the title of a lecture by D. J. Cram at the C. David Gutsche Symposium, Washington University, St. Louis, Missouri, May 5, 1990.

²⁰ (a) Beno, B.R.; Sheu, C.; Houk, K.N.; Warmuth, R.; Cram, D.J. *Chem. Commun.* 301-302 (1998). (b) Cram, D.J.; Tanner, M.E.; Thomas, R. *Angew. Chem., Int. Ed. Engl.* **1991**, *30*, 1024-1027.

²¹ Sherman, J.C.; Cram, D.J. *J. Am. Chem. Soc.* **1989**, *117*, 4527-4528.

²² a) van Wageningen, A.M.A.; Timmerman, P.; van Duynhoven, J.P.M.; Verboom, W.; van Veggel, F.C.J.M.; Reinhoudt, D.N. *Chem. Eur. J.* **1997**, *3*, 639-654. b) Timmerman, P.; Verboom, W.; van Veggel, F.C.J.M.; van Duynhoven, J.P.M.; Reinhoudt, D.N. *Angew. Chem., Int. Ed. Engl.* **1994**, *33*, 2345-2348.

²³ a) Helgeson, R.C.; Paek, K.; Knobler, C.B.; Maverick, E.F.; Cram, D.J. *J. Am. Chem. Soc.* **1996**, *118*, 5590-5604. b) Sherman, J.C.; Knobler, C.B.; Cram, D.J. *J. Am. Chem. Soc.* **1991**, *113*, 2194-2204.

1.4 Synthetic Systems: Self-Assembled Capsules²⁴

In the construction of large biomolecules such as ferritin, nature chose the process of self-assembly over the use of single supermolecules united entirely by covalent bonds. The advantages of this solution also apply to synthetic, self-assembled capsules in comparison to their covalent counterparts.²⁵ Self-assembly provides for:

- dynamic error correction *en route* to the targeted, lowest energy structure;
- relatively fast structure formation; and
- economical use of both the time and material required for synthesis.

However, in contrast to the wide variety of covalently-linked hosts available, relatively few artificial, self-assembled capsules exist. The difficulty of incorporating design features which lead to assembly within synthetically-accessible structures underlies this scarcity. In regard to supramolecular capsules, these features include:

- programming of sufficient information, or complementary recognition sites, to instruct the formation of the desired complex;
- mitigating the entropic costs of assembly by *minimizing* the number of components while *maximizing* structural preorganization; and
- providing avenues for reversible encapsulation of desired guests.

Given these requirements, metal-ligand complexes offer intriguing possibilities for the design of supramolecular capsules. For instance, Figure 1-3 illustrates a

²⁴ For extensive reviews on this topic, see: (a) Conn, M.M.; Rebek, J., Jr. *Chem. Rev.* **1997**, *97*, 1647-1668; (b) Rebek, J., Jr. *Pure Appl. Chem.* **1996**, *68*, 1261-1266; (c) Rebek, J., Jr. *Chem. Soc. Rev.* **1996**, 255-264; (d) Rebek, J., Jr. *Acc. Chem. Res.* **1999**, *32*, 278-286; (e) de Mendoza, J. *Chem. Eur. J.* **1998**, *4*, 1373-1377.

²⁵ Lawrence, D.S.; Jiang, T.; Levett, M. *Chem. Rev.* **1995**, *95*, 2229-2260.

tetrahedral cluster formed from six bis-bidentate ligands and four gallium(III) ions.²⁶ In contrast to many of the cyclophanes, the cavity of this host is completely enclosed by virtue of the naphthalene units. Nonetheless, a variety of alkylammonium guests can be encapsulated due to the dynamic nature of the assembly.²⁷

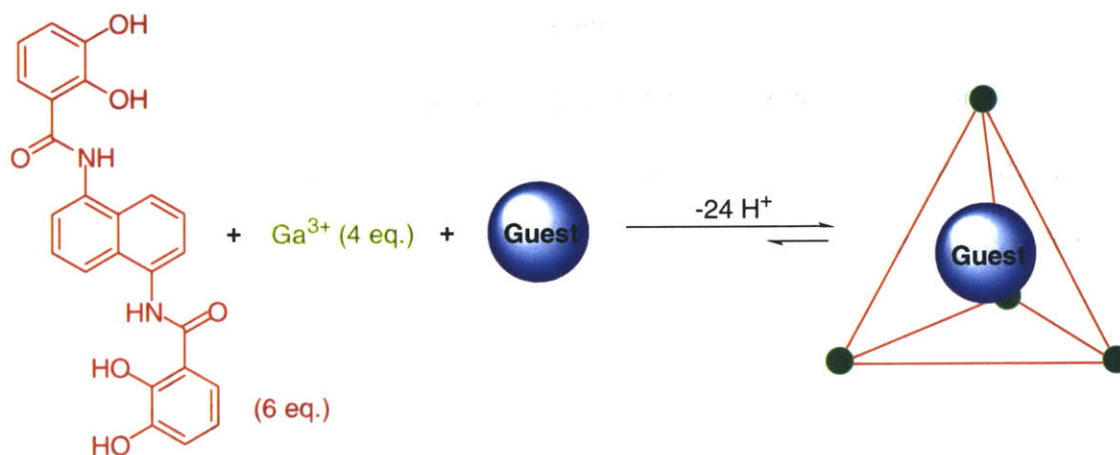


Figure 1-3. Example of a tetrahedral organometallic cluster complex capable of guest encapsulation.

While metal-ligand interactions are non-covalent, their strong nature can still inhibit facile error correction and exchange of guests. Capsules formed from the hydrophobic effect in polar media are much weaker assemblies in comparison. The non-directional nature of the hydrophobic effect and low binding energies, however, have limited the number of such capsules.^{24a} Other systems rely upon the selective, directional, and relatively strong nature of hydrogen bonds to promote capsule assembly. Mediating between the extremes of capsules based upon transition-metal complexes and

²⁶ (a) Caulder, D.L.; Powers, R.E.; Parac, T.; Raymond, K.N. *Angew. Chem. Int. Ed. Engl.* **1998**, *37*, 1840-1843. (b) Parac, T.; Caulder, D.L.; Raymond, K.N. *J. Am. Chem. Soc.* **1998**, *120*, 8003-8004.

²⁷ For other examples of capsules based upon organometallic clusters, see: (a) Saalfrank, R. W.; Burak, R.; Breit, A.; Stalke, D.; Herbst-Irmer, R.; Daub, J.; Porsch, M.; Bill, E.; Muther, M.; Trautwein, A.X. *Angew. Chem. Int. Ed. Engl.* **1994**, *33*, 1621-1623; (b) Mann, S.; Huttner, G.; Zsolnai, L.; Heinze, K. *Angew. Chem. Int. Ed. Engl.* **1996**, *35*, 2808-2809; (c) Fujita, M.; Oguro, D.; Miyazawa, M.; Oka, H.; Yamaguchi, K.; Ogura, K. *Nature* **1995**, *378*, 469-470; (d) Fujita, M.; Nagao, S.; Ogura, K. *J. Am. Chem. Soc.* **1995**, *117*,

hydrophobic interactions, hydrogen-bonded systems represent the largest class of supramolecular capsules.

An example of the evolution from covalent hosts to hydrogen-bonded capsules is illustrated in Figure 1-4. Sherman demonstrated that the tetrahydroxycavitand spacers used in Cram's carceplexes dimerize in non-competitive solvents following partial deprotonation.²⁸ Surprisingly, the resulting dynamic capsule was sufficiently rigid to constrain the motions of an encapsulated pyrazine, yet dynamic enough to permit reversible encapsulation.

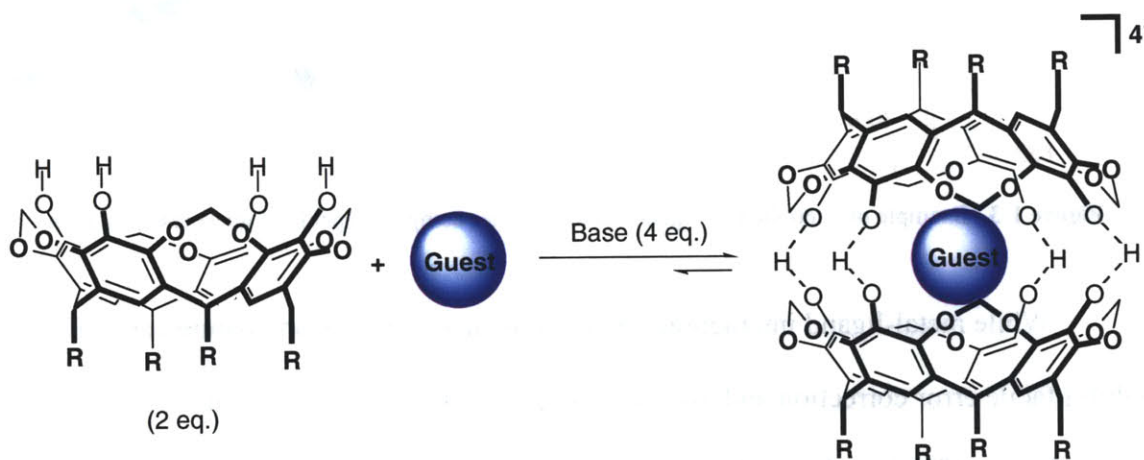


Figure 1-4. Guest encapsulation within a hydrogen-bonded cavitand dimer.

Hydrogen-bonded capsules trace their roots to the introduction of the “Tennis Ball” in 1993 by Rebek *et al.*²⁹ As shown in Figure 1-5, monomer **1.1** consists of a durene spacer adorned with two glycolurils. *The latter impart the necessary self-complementary curvature and hydrogen-bonding surfaces to encode for dimerization into*

1649-1650; (e) Harrison, R.G.; Fox, O.D.; Dalley, N.K.; Harrison, R.G. *J. Am. Chem. Soc.* **1998**, *120*, 7111-7112; (f) Albrecht, M.; Schneider, M.; Rottele, H. *Angew. Chem. Int. Engl.* **1999**, *38*, 557-559.

²⁸ (a) Chapman, R.G.; Sherman, J.C. *J. Am. Chem. Soc.* **1995**, *117*, 9081-9082. (b) Chapman, R.G.; Olovsson, G.; Trotter, J.; Sherman, J.C. *J. Am. Chem. Soc.* **1998**, *120*, 6252-6260. (c) Chapman, R.G.; Sherman, J.C. *J. Am. Chem. Soc.* **1998**, *120*, 9818-9826.

²⁹ Wyler, R.; de Mendoza, J.; Rebek, J., Jr. *Angew. Chem. Int. Ed. Engl.* **1993**, *32*, 1699-1701.

a capsule. Molecular modeling analysis predicted **1.1** would dimerize through eight hydrogen bonds with N-O bond lengths (2.84 Å) and N-H-O bond angles (176.5°) mirroring ideal values.³⁰ In fact, capsule formation was observed exclusively³¹ in non-competitive solvents such as chloroform and a variety of small guests such as methane were encapsulated. Used to uncover fundamental rules governing the assembly of hydrogen-bonded capsules, the Tennis Ball and its derivatives initiated a new area of supramolecular chemistry.^{24c}

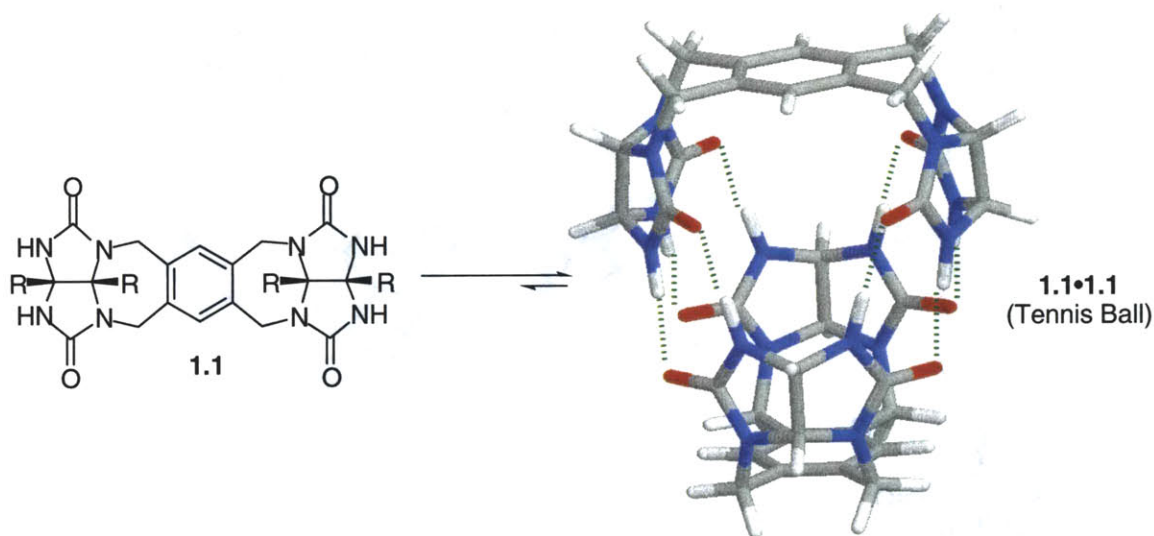


Figure 1-5. Monomer **1.1** dimerizes *via* eight strong hydrogen bonds to give a D_{2d} capsule **1.1•1.1** which is similar in design to a tennis ball. [R groups removed for clarity.]

Success with the Tennis Ball encouraged the development of numerous hydrogen-bonded capsules. For example, a larger glycoluril-based capsule,³² the Softball (**1.2•1.2**),

³⁰ Jeffrey, G.A.; Saenger, W. *Hydrogen Bonding in Biological Structures*; Springer-Verlag: New York, 1994; pp 71-135.

³¹ A large dimerization constant ($K_D \approx 3.2 \times 10^9 \text{ M}^{-1}$) and free energy of dimerization ($\Delta G^\circ \approx -12.6 \text{ kcal/mol}$) were estimated using a Tennis Ball derivative (Szabo, T.; Hilmersson, G.; Rebek, J., Jr. *J. Am. Chem. Soc.* **1998**, *120*, 6193-6194).

³² For a discussion of the structural characteristics of the Softball series, see: Rivera, J.M.; Martin, T.; Rebek, J., Jr. *J. Am. Chem. Soc.* **1998**, *120*, 819-820.

was synthesized and shown to encapsulate guests such as adamantane. Later versions of the Softball, in display of increasing functional complexity, were used to accelerate the Diels-Alder reaction,³³ demonstrate enantioselective guest encapsulation,³⁴ and explore the “sociology” of co-encapsulated guests.³⁵

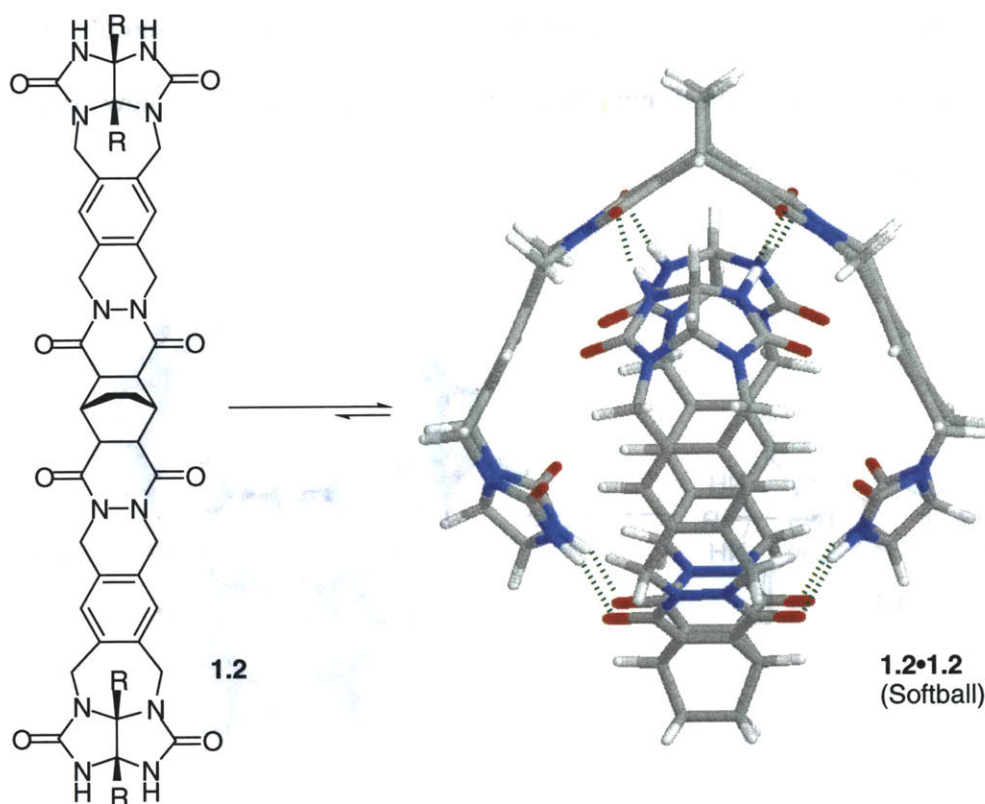


Figure 1-6. Monomer **1.2** dimerizes *via* eight hydrogen bonds to give a larger capsule **1.2•1.2** reminiscent of a softball. [R groups removed for clarity.]

Several capsules utilizing recognition elements other than glycolurils have been prepared as well. For instance, calix[4]arene modules functionalized with aryl³⁶ or

³³ (a) Kang, J.; Santamaria, J.; Hilmersson, G.; Rebek, J., Jr. *J. Am. Chem. Soc.* **1998**, *120*, 7389-7390. (b) Kang, J.; Hilmersson, G.; Santamaria, J.; Rebek, J., Jr. *J. Am. Chem. Soc.* **1998**, *120*, 3650-3656. (c) Kang, J.; Rebek, J., Jr. *Nature* **1997**, *385*, 50-52.

³⁴ Rivera-Ortiz, J.; Martin, T.; Rebek, J., Jr. *Science* **1998**, *279*, 1021-1023.

³⁵ Meissner, R.; Garcias, X.; Mecozzi, S.; Rebek, J., Jr. *J. Am. Chem. Soc.* **1997**, *119*, 77-85.

³⁶ (a) Shimizu, K.D.; Rebek, J., Jr. *Proc. Natl. Acad. Sci. USA* **1995**, *92*, 12403-12407. (b) Hamann, B.; Shimizu, K.D.; Rebek, J., Jr. *Angew. Chem. Int. Ed. Engl.* **1996**, *35*, 1326-1329. (c) Castellano, R.K.; Rudkevich, D.M.; Rebek, J., Jr. *J. Am. Chem. Soc.* **1996**, *108*, 10002-10003. (d) Mogck, O.; Böhmer, V.;

sulfonyl ureas,³⁷ dimerized to form discrete capsules.³⁸ Further elaboration gave rise to informational polymers³⁹ and novel materials.⁴⁰ Other capsules were derived from the dimerization of resorcinarenes functionalized with four imides.⁴¹ These assemblies exhibited highly selective discrimination between similar guests and helped define stereochemical relationships between encapsulated species.⁴²

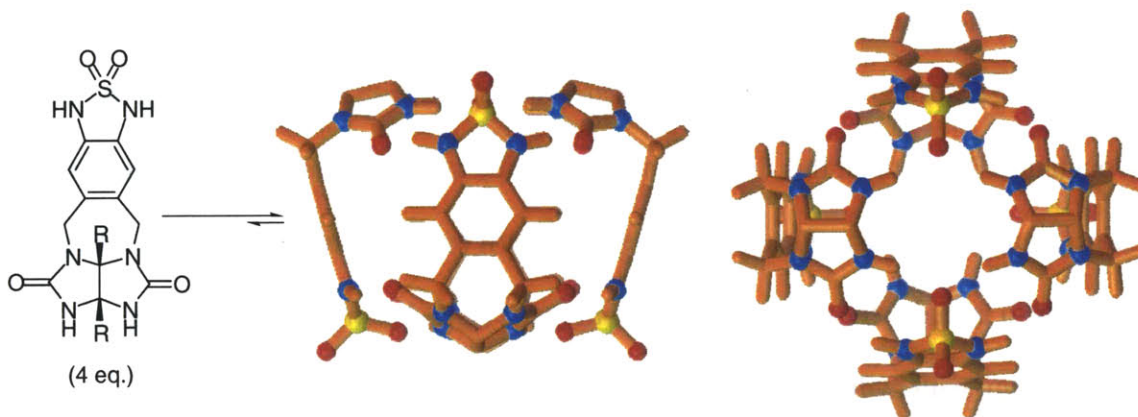


Figure 1-7. In non-competitive solvents, the monomer shown exists as a nearly insoluble, disordered aggregate. However, upon the addition of an appropriate guest like adamantane, the monomer assembles into a tetrameric capsule possessing 16 hydrogen bonds. Two views of the capsule are displayed with R groups and guests removed for clarity.

While the aforementioned capsules exhibited diverse behaviors, their simple dimeric structures present some limitations. Ghadiri's peptide nanotubes⁴³ and Rebek's

Vogt, W. *Tetrahedron*, **1996**, 52, 8489-8496. (e) Mogck, O.; Paulus, E.F.; Böhmer, V.; Thondorf, I.; Vogt, W. *J. Chem. Soc. Chem. Commun.* **1996**, 2533-2534. (f) Mogck, O.; Pons, M.; Böhmer, V.; Vogt, W. *J. Am. Chem. Soc.* **1997**, 119, 5706-5712.

³⁷ Castellano, R.K.; Kim, B.H.; Rebek, J., Jr. *J. Am. Chem. Soc.* **1997**, 119, 12671-12672.

³⁸ Other self-assembling calix[4]arene systems have been reported by Reinhoudt (Vreekamp, R.H.; Verboom, W.; Reinhoudt, D.N. *J. Org. Chem.* **1996**, 61, 4282-4288) and Shinkai (Koh, K.; Araki, K.; Shinkai, S. *Tetrahedron Lett.* **1994**, 35, 8255-8258), but were not shown to encapsulate guests.

³⁹ (a) Castellano, R.K.; Rudkevich, D.M.; Rebek, J., Jr. *Proc. Natl. Acad. Sci. U.S.A.* **1997**, 94, 7132-7137.

(b) Castellano, R.K.; Rebek, J., Jr. *J. Am. Chem. Soc.* **1998**, 120, 3657-3663. (c) Castellano, R. K.; Rebek, J., Jr. *Polym. Mater. Sci. Eng.* **1999**, 80, 16-17.

⁴⁰ Castellano, R. K.; Nuckolls, C.; Eichhorn, S. H.; Wood, M. R.; Lovinger, A. J.; Rebek, J., Jr. *Angew. Chem. Int. Ed.*, submitted.

⁴¹ (a) Heinz, T.; Rudkevich, D.M.; Rebek, J., Jr. *Nature* **1998**, 394, 764-766. (b) Heinz, T.; Rudkevich, D.M.; Rebek, J., Jr. *Angew. Chem. Int. Ed. Engl.* **1999**, 38, 1136-1139.

⁴² Tucci, F.C.; Rudkevich, D.M.; Rebek, J., Jr. *J. Am. Chem. Soc.* **1999**, 121, 4928-4929.

⁴³ Hartgerink, J.D.; Clark, T.D.; Ghadiri, M.R. *Chem. Eur. J.* **1998**, 4, 1367-1372.

recently introduced tetrameric capsules⁴⁴ (Figure 1-7), however, are two members of an increasingly diverse pool of structures. These new systems promise a fuller understanding of the rules governing self-assembly and the design requirements of functional architectures.

In the following chapters, we discuss several self-assembling systems related to the glycoluril-based capsules described above. First, the reader is acquainted with the assembly, encapsulation, and synthetic issues associated with a capsule named the Jelly Doughnut. Based upon this discussion, we describe a strategy for the rapid synthesis of larger, more diverse capsules using novel glycoluril building blocks. The focus then expands to include structures resulting from metal-ligand interactions alone and in combination with hydrogen bonds. Taken as a whole, this work describes an evolutionary path of glycoluril capsules from “classical” to future structures.

⁴⁴ (a) Martin, T.; Obst, U.; Rebek, J., Jr. *Science*, **1998**, *281*, 1842-1845. (b) Schalley, C.A.; Martin, T.; Obst, U.; Rebek, J., Jr. *J. Am. Chem. Soc.* **1999**, *121*, 2133-2138.

Chapter 2

A D_{3d} -Symmetric Self-Assembling Capsule The “Jelly Doughnut”

2.1 Introduction

A thorough understanding of the host-guest chemistry of molecular capsules relies upon the availability of hosts with diverse sizes and shapes. As described in Chapter 1, the first capsules possessed roughly spherical cavities which encapsulated guests such as methane and adamantane. Non-spherical guests of intermediate size, however, were also interesting targets for our studies. For instance, a host with a disc-shaped cavity could encapsulate a variety of complementary guests.

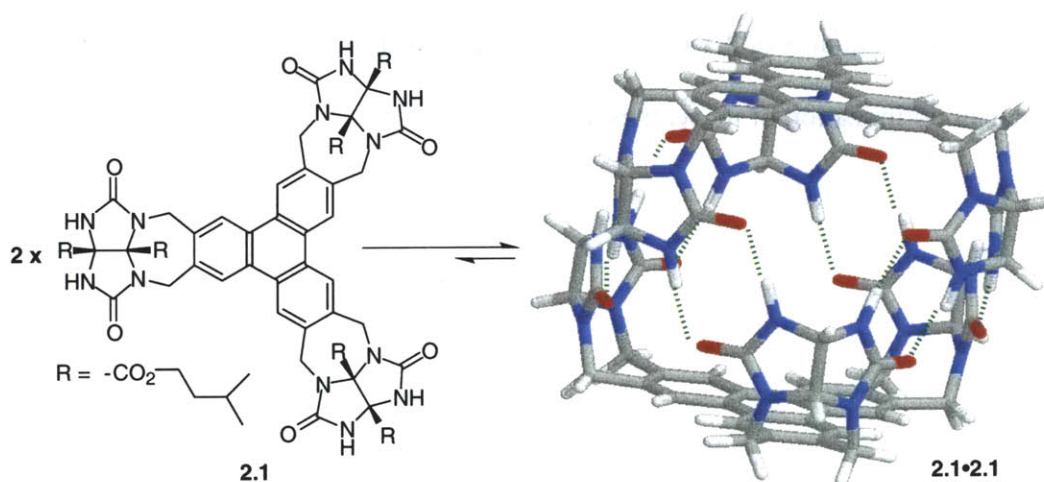


Figure 2-1. Structural diagram of Jelly Doughnut monomer **2.1** and energy-minimized structure of dimer **2.1•2.1**. [Note: R groups have been removed from the dimer for clarity.]

One such host arose from the dimerization of monomer **2.1**, composed of a triphenylene spacer adorned with three glycoluril units.¹ Dimerization to form the D_{3d} -

¹ This host was designed by Robert M. Grotzfeld and Neil Branda. For a complete discussion regarding the design of **2.1** and similar structures, see: Grotzfeld, R.M. *Studies in Molecular Recognition: Self-Assembling Molecular Host-Guest Systems*. Ph.D. Thesis, Massachusetts Institute of Technology, Cambridge, MA, May 1996.

symmetric capsule occurs by virtue of the monomer's self-complementary shape and the network of twelve hydrogen bonds between glycolurils.² The overall structure of **2.1•2.1** is a flattened sphere and, given its central cavity, the dimer resembles a molecular-level jelly doughnut. Molecular modeling³ predicts a cavity volume of approximately 240 Å³. In this chapter, we will discuss the synthesis of **2.1** and the host-guest properties of the dimer.

2.2 Synthesis

The original synthesis of **2.1** was carried out by Robert Grotzfeld and reported elsewhere.^{1,4} This synthesis suffered from three inefficient steps (Figure 2-2, steps a-d) which limited available amounts of **2.1** to sub-milligram quantities per reaction sequence. Since the small amounts of **2.1** hindered our ability to study this novel system, we pursued an optimization of its synthesis.

² The hydrogen-bonding pattern is highly symmetric giving average H-bond lengths of 2.8 Å and N-H-O bond angles of 172°.

³ All structural models were created using MacroModel v.5.5 and energy-minimized with the Amber* forcefield. [See: Mohamadi, F.; Richards, N.G.J.; Guida, W.C.; Liskamp, R.; Caulfield, C.; Chang, G.; Hendrickson, T.; Still, W.C. *J. Comput. Chem.* **1990**, *11*, 440.] All volumes were calculated using either MacroModel or Grasp. [See: Mecozzi, S.; Rebek, J., Jr. *Chem. Eur. J.* **1998**, *4*, 1016-1022.]

⁴ Grotzfeld, R.M.; Branda, N.; Rebek, J., Jr. *Science* **1996**, *271*, 487-489.

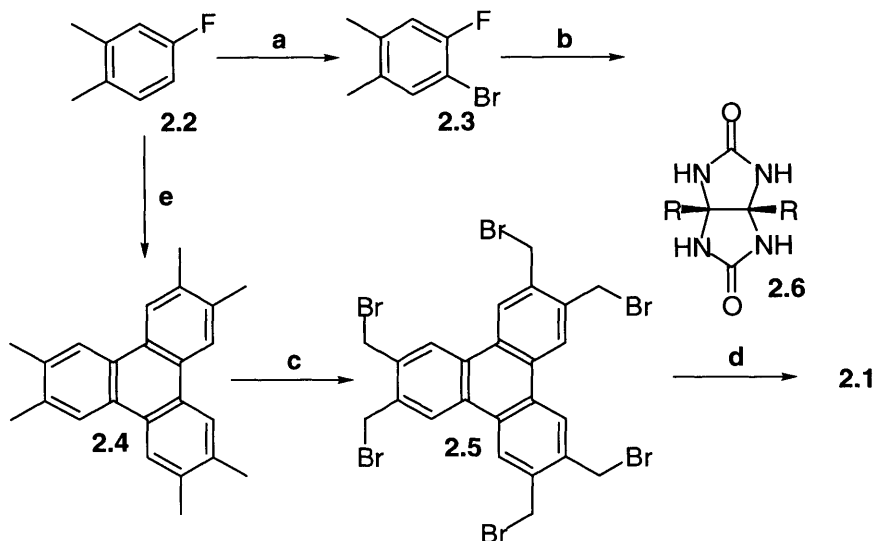


Figure 2-2. Synthesis of monomer **2.1**: a) Br₂, Fe, FeCl₃, CH₂Cl₂ (59%); b) Mg, I₂, BrCH₂CH₂Br, THF (8% adj.); c) Br₂, BrCH₂CH₂Br, hv, Δ (38% crude); d) iso-amylglycoluril **2.6**, KO^tBu, DMSO (<1%); e) i. n-BuLi, THF, -78 °C; ii. KO^tBu, -100 to -28 °C (39%).

The first low-yielding step of the synthesis was the trimerization of dihaloxylene **2.3** to hexamethyltriphenylene **2.4** (step b). Adapted from an analogous synthesis of triphenylene,⁵ this reaction proceeded in only 8% yield based upon reacted starting material. After several attempts to optimize this step failed, another route was evaluated. Directed lithiation of 4-fluoro-*o*-xylene **2.2** using n-BuLi (-78 °C) followed by treatment with NaO^tBu (-100 °C) gave the sodiated fluoroxylylene. This salt decomposes more readily than the Grignard reagent generated in step b to give larger concentrations of 4,5-dimethylbenzyne, a key intermediate in the stepwise trimerization leading to **2.4**.⁶ This increased the yield of the cyclization to 39% and removed a step from the reaction sequence.

The next reaction requiring optimization was step c, the bromination of **2.4**. Several bromination strategies failed due to the insolubility of intermediates *en route* to

⁵ Bartle, K.D.; Heaney, H.; Jones, D.W.; Lees, P. *Tetrahedron* **1965**, *21*, 3289-3296.

hexabromide **2.5**. For example, under typical conditions for radical NBS bromination (AIBN, CCl₄), partially brominated products precipitated from solution and no hexabromide could be isolated. As described in the Experimental section, we eventually identified the conditions⁷ shown in step c which produced the crude hexabromide, although purification was hindered by its poor solubility.

The last step of the synthesis of **2.1** suffered from several complicating factors which are listed below.

- 1) The insolubility of spacer **2.5** limited alkylation conditions to the use of hot DMSO. Under these conditions and in the presence of strong base, Swern oxidations or hydroxide displacement (from trace water) were highly competitive with the desired alkylation reactions.
- 2) A large excess of glycoluril was necessary to overcome poor solubility and to reduce undesirable *trans* alkylations (i.e. one glycoluril alkylated by spacers on both sides). This complicated purification of the final product.
- 3) The formation of three seven-membered rings competes against the above two side reactions.
- 4) Given the crude mixture of **2.5** (and the aforementioned degradation reactions), many side products were produced which complicated purification.
- 5) Since three glycolurils must all alkylate on one side of a spacer (*syn* alkylation), the maximum theoretical yield of the desired product is 25%. The remaining will be undesired *anti* product (2 glycolurils up, one down).

⁶ Fossatelli, M.; Brandsma, L. *Synthesis* **1992**, 756.

⁷ (a) Stephenson, E.F.M. *Organic Syntheses Collective Volume 4*; Wiley: New York; pp 984-986. (b) Tashiro, M.; Mataka, S.; Takezaki, Y.; Takeshita, M.; Arimura, T.; Tsuge, A.; Yamato, T. *J. Org. Chem.* **1989**, *54*, 451-458.

These factors combined to produce very low yields of **2.1**. However, employing a purer version of crude **2.5** and optimizing purification procedures (see Experimental section) led to larger yields of **2.1**. Since large amounts of triphenylene **2.4** were now available, only the last two steps of the synthesis needed to be repeated to produce several milligrams of monomer **2.1** per sequence.

2.3 Characterization

Monomer **2.1** was shown to exist as the predicted assembly **2.1•2.1** through a variety of means. For instance, the ^1H NMR spectra of the monomer dissolved in non-competitive solvents such as CDCl_3 showed a single set of sharp peaks for all protons including a far-downfield signal (≈ 9 ppm) for the glycoluril NH 's (Figure 2-3). These characteristics are indicative of a highly symmetric, hydrogen-bonded structure.⁸

Furthermore, no concentration dependence on chemical shift was detected over a range of 15.0 mM^{-1} (saturation) to 0.3 mM^{-1} (detection limit) for any of the resonances of **2.1•2.1**.⁹ This evidence of a large dimerization constant was further supported by titration experiments with highly competitive solvents. Addition of up to 25% CD_3OH to a CDCl_3 solution of **2.1** gave no change in shift for the glycoluril NH .¹⁰ Similarly, the discrete dimer was the sole species in solution at up to 30% $\text{DMSO-}d_6$ and 40% $\text{DMF-}d_7$.

⁸ Rebek, J., Jr. *Chem. Soc. Rev.* **1996**, 255-264.

⁹ UV dilution experiments failed to show significant changes in the spectra of the assembly from 2.2×10^{-2} to $8.5 \times 10^{-5} \text{ mM}^{-1}$.

¹⁰ After this point, the solute precipitated from solution.

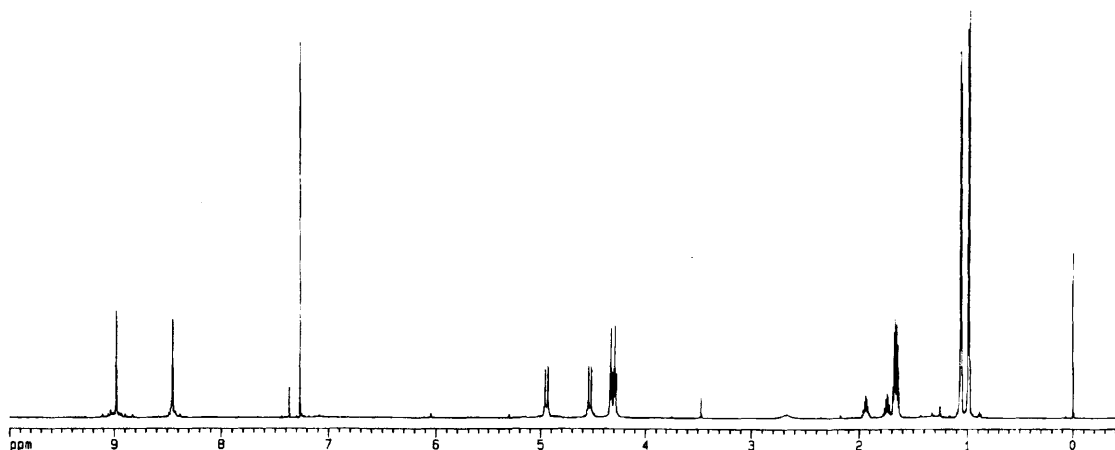


Figure 2-3. ^1H NMR spectrum (CDCl_3 , 600 MHz) of the dimer **2.1•2.1**.

Further evidence for the dimeric structure arose from IR and mass spectroscopic data. The IR spectrum of **2.1** in CH_2Cl_2 gave two strong absorbances at 3214.2 and 3094.9 cm^{-1} (N-H stretching) as expected in the presence of amide hydrogen-bonding.¹¹ In addition, plasma desorption (PD) mass spectrometry found ion peaks corresponding to the dimer plus one molecule of solvent (CH_2Cl_2 or CHCl_3).

2.4 Encapsulation Studies

2.4.1 Benzene as a Guest

Some of the most compelling evidence for the assembly of the dimer arose from guest encapsulation studies. In a CDCl_3 solution of **2.1•2.1**, each dimer likely encapsulates chloroform.¹² Upon titrating benzene- d_6 into such a solution, Grotzfeld^{1,4}

¹¹ Pretsch, E.; Clerc, T.; Seibl, J.; Simon, W. In *Spectral Data for Structure Determination of Organic Compounds, 2nd edition* (Engl. Transl. by K. Biemann); Fresenius, W., Huber, J.F.K., Pungor, E., Rechnitz, G.A., Simon, W., West, Th. S., Eds.; Chemical Laboratory Practice; Springer-Verlag: New York, 1989; p 1-145.

¹² Two chloroforms (71\AA^3 each) can fit within the Jelly Doughnut by modeling giving a packing coefficient of ≈ 0.58 which is within the "ideal" range of 0.55 ± 0.09 for such systems. [See ref. 3] However, ^1H NMR experiments using a mixture of $\text{CDCl}_3/\text{CHCl}_3$ (9:1) and employing either binomial peak suppression or solvent presaturation failed to give meaningful integrations of encapsulated CHCl_3 ($\delta = 5.69$ ppm). Therefore, while it is likely that the Jelly Doughnut encapsulates chloroform, the stoichiometry of the complex remains unclear.

found that a second set of dimer peaks developed which suggested the presence of a new complex containing benzene. A van't Hoff analysis of his titrations showed benzene to be the preferred guest of the dimer by approximately 0.75 kcal/mol.¹³ Direct evidence of encapsulation came from the use of ¹³C₆H₆ (15% v/v) in a CDCl₃ solution of the assembly. In the ¹³C NMR spectra, a new peak ascribed to encapsulated benzene arose 2 ppm upfield from the peak for free benzene. This shift resulted from the shielded environment created by the capsule's triphenylene spacers. These results supported our initial hypothesis that the Jelly Doughnut was a suitable system to evaluate disc-shaped guests.

2.4.2 Ring Inversion Dynamics of Encapsulated Cyclohexane¹⁴

Molecular capsules assemble reversibly on time scales that range from hours to milliseconds.¹⁵ Given their dynamic nature, a question arises: Are capsules sufficiently rigid to constrain the motions of molecules trapped inside? Surprisingly, little had been published on this topic despite its fundamental importance. The most relevant work, as discussed in Chapter 1, was a study by Sherman¹⁶ describing hindered rotation for pyrazine encapsulated within a hydrogen-bonded host. We offered further insights to this question by examining the ring inversion of cyclohexane within two of our capsules.

Cyclohexane can be encapsulated in the Jelly Doughnut as shown in Figure 2-4.

At room temperature in a *p*-xylene-*d*₁₀ solution, a slightly broadened NMR signal at -

¹³ From the analysis, $\Delta H = -3.7$ kcal/mol and $\Delta S = -9.9$ cal/K•mol. The negative entropy change suggests that two benzenes are displacing a single chloroform. However, modeling indicates that two stacked benzenes within the dimer result in π - π distances of only ≈ 3.2 Å. Instead, the negative value probably indicates that a single benzene displaces a single chloroform, but the new guest experiences fewer degrees of rotational freedom compared to its free state. Modeling, for instance, shows that sufficient room does not exist for an edge-to-face (benzene-to-triphenylenes) orientation.

¹⁴ Reproduced with permission from O'Leary, B.M.; Grotzfeld, R.M.; Rebek, J., Jr. *J. Am. Chem. Soc.* **1997**, *119*, 11701-11702. Copyright 1997 American Chemical Society.

¹⁵ Rebek, J.-Jr. *Chem. Soc. Rev.* **1996**, 255-264.

0.87 ppm for bound cyclohexane appeared. On cooling, this signal further broadened and flattened into the baseline at 283 K (10° C). Since the solution froze at lower temperatures, we chose CD₂Cl₂ as an alternative solvent for our studies. Dissolving the Jelly Doughnut in a mixture of cyclohexane-*d*₁₁ and CD₂Cl₂ (15%, v:v) resulted in cyclohexane encapsulation within roughly half the capsules at room temperature.

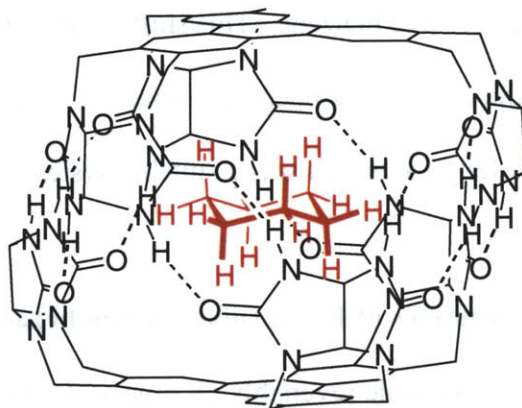


Figure 2-4. Cyclohexane encapsulated by the Jelly Doughnut. [R groups have been removed for clarity.]

Figure 2-5 shows the appropriate region of the ¹H NMR spectra (600 MHz) of encapsulated cyclohexane-*d*₁₁ at different temperatures.¹⁷ The low temperature extreme was reached at 203 K where a spacing ($\delta\nu$) of almost 600 Hz or 1 ppm was observed between the equatorial (downfield) and axial (upfield) positions of the lone proton.¹⁸ Since the $\delta\nu$ value was less than 0.5 ppm for "free" cyclohexane-*d*₁₁, the environment inside the Jelly Doughnut produces a magnetic field corresponding to a spectrometer operating at 1.2 GHz! The larger chemical shift difference between protons of the

¹⁶ Chapman, R.G.; Sherman, J.C. *J. Am. Chem. Soc.* **1995**, *117*, 9081-9082.

¹⁷ Partially deuterated cyclohexane was chosen because of the large amounts needed to effect encapsulation and to eliminate complications from proton-proton coupling.

¹⁸ All spectra were recorded with simultaneous deuterium decoupling. Prior to acquisition, the instrument and samples were allowed to equilibrate at the various temperatures for at least one hour and thermostat values fluctuated by no more than 0.5 K.

encapsulated cyclohexane resulted from the anisotropy created by the host's triphenylene floor and ceiling.

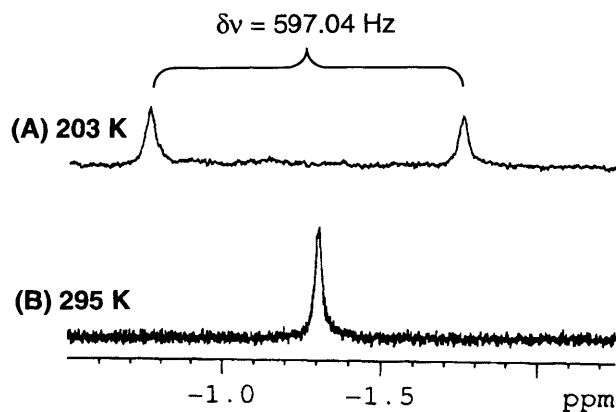


Figure 2-5. Portions of ^1H NMR spectra (600 MHz) showing the resonance(s) of cyclohexane- d_{11} encapsulated within the Jelly Doughnut at (A) the low temperature, no-exchange limit and (B) room temperature.

Given the $\delta\nu$ value and assuming a similar ring-inversion barrier for free¹⁹ and encapsulated cyclohexane- d_{11} , a coalescence temperature (T_c) of about 241 K was predicted for the guest by the Eyring equation.²⁰ Surprisingly, an even higher T_c was found (248 ± 0.5 K). This corresponds to a free energy of activation at coalescence (ΔG^*) of 10.55 ± 0.05 kcal/mole. For the free cyclohexane derivative, we observed a ΔG^* of 10.25 ± 0.05 kcal/mole at $T_c = 233.5 \pm 0.5$ K, a value in excellent agreement with those found in a number of other studies (10.1-10.3 kcal/mole).¹⁹

What caused the increased barrier for the guest's ring inversion process? Perhaps "cramped quarters" restrict cyclohexane's internal motions, thus raising the transition state for inversion. Molecular modeling³ predicts that the volume of space inside the empty jelly doughnut (243 \AA^3) shrinks slightly upon placing cyclohexane inside (229 \AA^3).

¹⁹ For a review, see: Anet, F.A.L.; Anet, R. In *Dynamic Nuclear Magnetic Resonance Spectroscopy*; Jackman, L.M., Cotton, F.A., Eds. Academic: New York, 1975, pp 574-580.

This appears to be driven by favorable van der Waals contacts between the six axial hydrogens of the guest and the π systems above and below.²¹

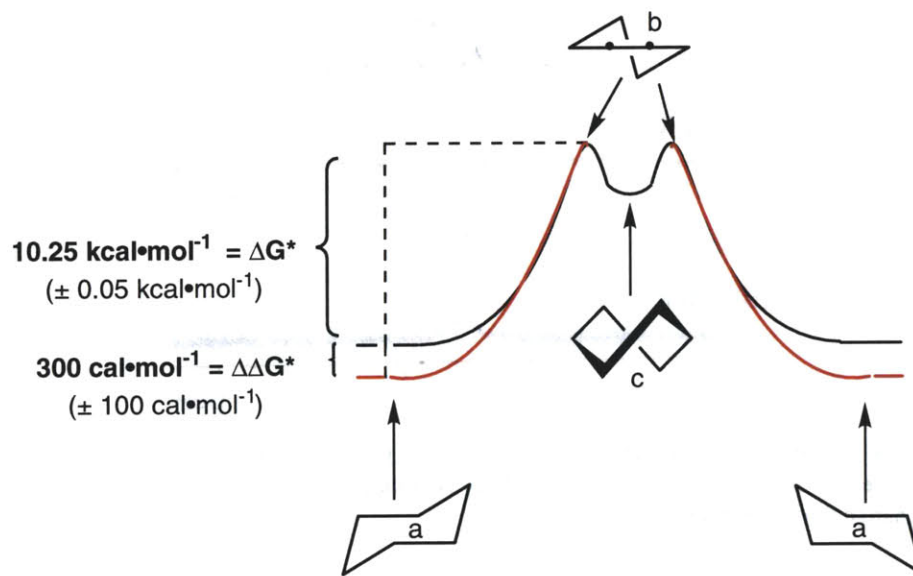


Figure 2-6. Energy diagram for cyclohexane ring inversion. The different conformers are a) chair, b) half-chair, and c) twisted boat. The red line illustrates the ground state stabilization of encapsulated cyclohexane as described in the text.

Since the transition state for ring inversion ('half-chair' conformer **b**) involves a partial planarization of cyclohexane,²² we doubt steric effects are responsible for the modest increase observed in activation energy. Another possibility is that encapsulation lowers the ground state of cyclohexane through favorable contacts (Figure 2-6). The process leading from the chair-conformer to the transition state can reduce the number and quality of favorable C-H (and C-D) to π contacts that *stabilize* the ground state.

²⁰ See section 2.5.2 for calculations and error analysis. For analogous calculations involving cyclohexane- d_{11} , see: Friebolin, H. *Basic One- and Two-Dimensional NMR Spectroscopy*; VCH Publishers: New York, 1991, pp 267-274.

²¹ For a review, see: Nishio, M.; Umezawa, Y.; Hirota, M.; Takeuchi, Y. *Tetrahedron* **1995**, *51*, 8665-8701.

²² Volumes were calculated for three conformers of cyclohexane: chair = 87.2 Å³; twisted boat = 86.4 Å³; and half-chair = 87.2 Å³.

These contacts, worth a few hundred calories, are of the magnitude first measured by Wilcox with a molecular torsion balance.²³

A second, smaller capsule was available from a calix[4]arene functionalized with aryl ureas that dimerizes *via* hydrogen bonding (Fig. 2-7).²⁴ Calculations and a crystal structure²⁵ converged on a value of 190 Å³ for the cavity, large enough to accommodate cyclohexane.

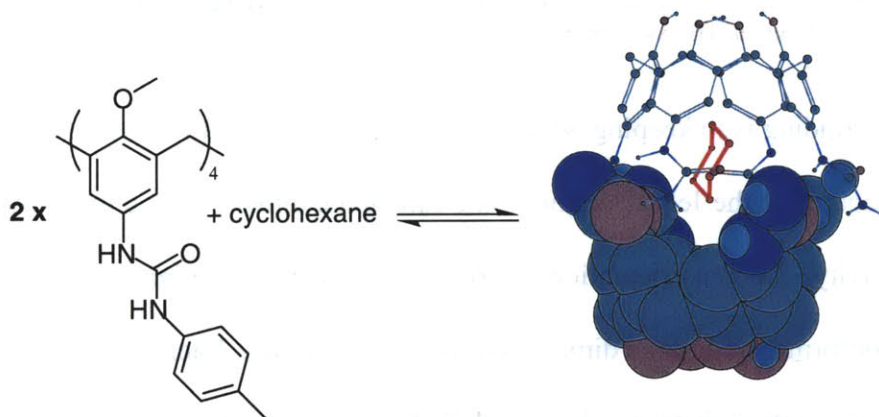


Figure 2-7. A functionalized calix[4]arene self-assembles forming a dimer capable of encapsulating cyclohexane. The split view of the dimer shows one of the minimized structures for this system. [Some groups have been removed from the dimer for clarity.]

Indeed, a 1% solution of cyclohexane-d₁₁ in toluene-d₈ (v:v) resulted in the encapsulation of cyclohexane in almost 50% of the dimers (Fig. 2-8). Despite this relatively high affinity, no significant difference in activation energies was found for the ring inversions of free and encapsulated cyclohexane species ($\Delta G^* = 10.24$ and 10.27 ± 0.05 kcal/mol, respectively).

²³ Paliwal, S.; Geib, S.; Wilcox, C.S. *J. Am. Chem. Soc.* **1994**, *116*, 4497-4498.

²⁴ Castellano, R.K.; Rudkevich, D.M.; Rebek, J., Jr. *J. Am. Chem. Soc.* **1996**, *118*, 10002-10003.

²⁵ Mogck, O.; Paulus, E.F.; Bohmer, V.; Thondorf, I.; Vogt, W. *J. Chem. Soc. Chem. Commun.* **1996**, 2533-2534.

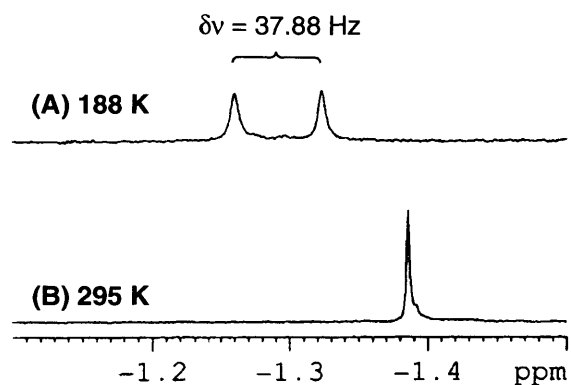


Figure 2-8. Portions of ^1H NMR spectra (600 MHz) showing the resonance(s) of cyclohexane- d_{11} encapsulated within the calixarene dimer at (A) the low temperature, no-exchange limit and (B) room temperature.

This finding is in keeping with the differences between the cavities of the two hosts. Compared to the Jelly Doughnut, the calixarene dimer boasts a much more spherical cavity. Several orientations corresponding to energy-minima are possible for the chair conformer within the dimer according to modeling. Each offers the possibility of CH to π interactions between the cyclohexane and the cavity's phenyl rings located in the “poles”. However, there are a similar number of such contacts when the dimer is modeled while encapsulating the half-chair conformer of cyclohexane. There is no special stabilization of the ground state and, accordingly, no change in the activation energy.

Our original question asked if molecular capsules were rigid enough to constrain guest motion. For guests, the rigidity of capsules can magnify positive interactions with the host relative to the solvent and this leads to encapsulation. In some instances, these interactions may be favorable enough to restrict guest motions. Such should be the case in the contacts between the polarized C-H bonds of pyrazine and the electron rich phenoxide surfaces in Sherman’s capsule.¹⁶ In our case, C-H to π interactions likely affect the intramolecular dynamics of encapsulated cyclohexane.

In hydrogen bonded capsules, unfavorable interactions (i.e. sterics, Coulombic repulsion) are not likely to be major contributors in the restriction of guest motion. Sizeable interactions of this nature probably would preclude encapsulation all together. In contrast, the possibility of guest expulsion from covalently sealed hosts is severely limited, so guest motions may be hindered by other forces. Steric effects, for example, are probably responsible for the hindered rotation of certain guests in Cram's carceplexes.²⁶ In contrast, gentle coercion is required to constrain guests of molecular capsules.

2.4.3 Other Encapsulation Studies

Following successful encapsulation studies involving benzene and cyclohexane, other disc-shaped guests were examined in a variety of solvents. In order for encapsulation to be observed, non-competitive solvents were sought which dissolved reasonable amounts of the Jelly Doughnut and would not compete with prospective guests for encapsulation despite much greater concentrations.²⁷ Table 2-1 lists the solvents and guests we evaluated.

<u>Solvents</u>		<u>Guests</u>	
CDCl ₃	<i>p</i> -Xylene- <i>d</i> ₁₀	C ₆ F ₆	Phenol
CD ₂ Cl ₂	<i>o</i> -Xylene- <i>d</i> ₁₀	Anisole	Inositol
C ₆ D ₆	Fluorobenzene- <i>d</i> ₅	<i>cis,cis</i> -1,3,5-Cyclo-	Allyl vinyl ether
Toluene- <i>d</i> ₈	Diglyme- <i>d</i> ₁₄	hexanetriol	Fluorocyclohexane
Ethylbenzene- <i>d</i> ₁₀	1,4-Dioxane- <i>d</i> ₈		
THF- <i>d</i> ₈			

Table 2-1. Several solvents and guests evaluated during encapsulation studies with the Jelly Doughnut. Note that several solvents were also evaluated as guests and guests were typically evaluated using several solvents. All guests were predicted to have affinity for the capsule by modeling.

²⁶ (a) Helgeson, R.C.; Paek, K.; Knobler, C.B.; Maverick, E.F.; Cram, D.J. *J. Am. Chem. Soc.* **1996**, *118*,

Due to the limited quantity of available Jelly Doughnut, parallel studies were not possible. Following each test, the capsule was recycled by purification prior to the next study which resulted in a laborious process. Unfortunately, various combinations of the solvents and guests listed in the table gave no positive encapsulation results. Some solvents (e.g. toluene- d_8) could not be displaced because of their high affinity for the capsule despite predictions that some guests should be tight binders.²⁸ Other solvents (e.g. 1,4-dioxane- d_8 and several not listed) did not dissolve sufficient amounts of the assembly.

Given that the majority of commercially-available guests suitable for the Jelly Doughnut were evaluated, we turned our sights upon other possible hosts. As described in the next three chapters, we sought capsules that were available in larger amounts and possessed diverse sizes and shapes.

2.5 Experimental

2.5.1 General Apparatus, Materials, and Methods

NMR spectra were recorded on Varian Unity 300, Varian Unity 500, Bruker AC-250, Bruker AC-300, or Bruker DRX-600 spectrometers in various solvents as indicated. ^1H and ^{13}C chemical shifts (δ) are listed as parts per million (ppm) from tetramethylsilane ($\delta = 0$). IR spectra were recorded on a Perkin-Elmer Paragon 1000PC FT-IR spectrometer. Mass spectra were recorded on the following instruments: plasma desorption (PD) on an Applied Biosystems Biopolymer Mass Analyzer BioIon 20

5590-5604. (b) Sherman, J.C.; Knobler, C.B.; Cram, D.J. *J. Am. Chem. Soc.* **1991**, *113*, 2194-2204.

²⁷ Rebek, J., Jr. *Chem. Soc. Rev.* **1996**, 255-264.

²⁸ MacroModel minimization of host-guest complexes were performed and specific binding interactions such as hydrogen bonds or stacking interactions were identified. Guests were then removed, separated from the capsule by several nanometers, minimizations repeated, and final energies subtracted to give a

spectrometer from nitro-cellulose wafers; fast atom bombardment (FAB) on a VG ZAB-VSE magnetic sector; MALDI (TOF) on a PerSeptive DE; electrospray (ESI) [< 3000 amu] on a Perkin Elmer API 100 Sciex single quadrupole; electrospray (ESI) [> 3000 amu] on a Finnigan LCQ ion trap.

Unless otherwise stated, commercially-available chemicals were used without further purification. Anhydrous conditions entailed the use of flame-dried glassware under inert atmosphere (N_2 or Ar) with solvents that were generally dried by passage through packed alumina. DMSO was dried by sequential drying over 4Å molecular sieves. Flash chromatography was performed using E. Merck Silica Gel 60 (230-400 mesh) following standard procedures.²⁹

2.5.2 Calculations / Error Analysis for Cyclohexane Ring Inversion Experiments

- 1) $\delta\nu$ = peak separation in Hz at low temperature, typically 188 - 203 K.
(Reported $\delta\nu$ values did not change significantly over this temperature range.)
- 2) Rate constant (k_c) was calculated from $\delta\nu$ as follows: $k_c = 2k_{obs} = 2(\pi \cdot \delta\nu) / 2^{1/2}$.
(This system meets all criteria required to calculate k_c in this manner. See ref. 20.)
- 3) The activation energy (ΔG^*) for cyclohexane- d_{11} ring inversion was calculated using the Eyring equation: $\Delta G^* = 4.58T_c[10.32 + \log(T_c/k_c)] \text{ cal}\cdot\text{mol}^{-1}$.
- 4) To account for any experimental errors, ΔG^* values were calculated using the observed $T_c \pm 1$ K. We feel this is a generous error estimation given that:
 - a) the maximum thermostat fluctuation was ± 0.5 K;
 - b) the experimental ΔG^* values for free cyclohexane- d_{11} closely match literature values¹⁹ thereby demonstrating accurate measurement conditions; and

binding energy. The value found for cyclohexane inclusion (≈ -18 kcal/mol) was used as a benchmark

c) fairly constant (< 1Hz variations) $\delta\nu$ values were obtained at a variety of low temperatures.

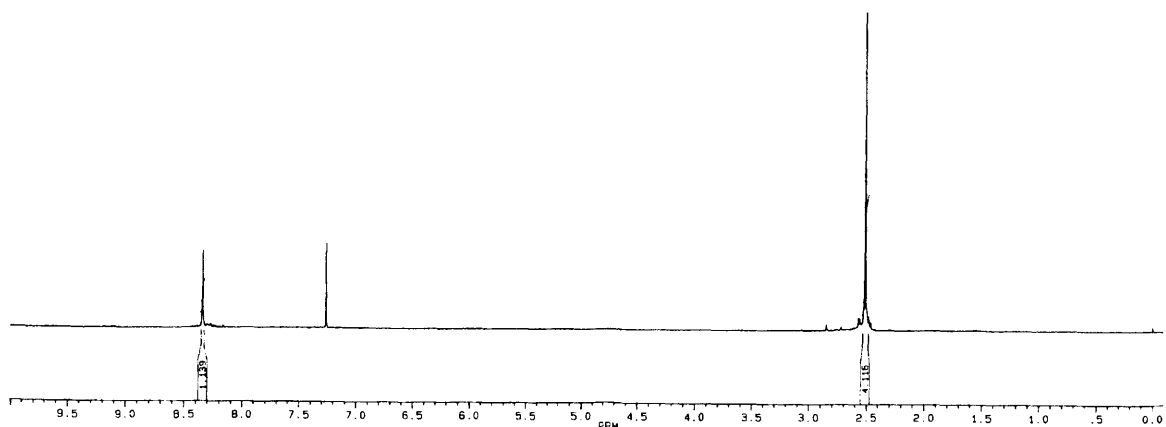
Using $T_c \pm 1$ K gives ΔG^* values with an error range of ± 0.05 kcal \cdot mol $^{-1}$.

2.5.3. Procedures (^1H NMR spectra follow each preparation.)

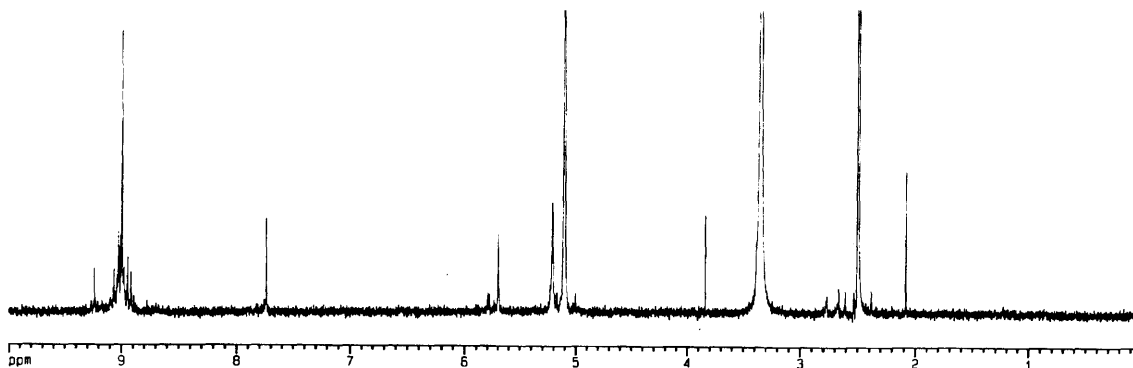
2,3,6,7,10,11-Hexamethyltriphenylene (2.4). Under anhydrous conditions, n-butyl lithium [1.6M in hexanes] (62.5 mL, 100.0 mmol) was cooled to -78 $^\circ\text{C}$. While maintaining temperature, **2.2** (14.90 g, 120.0 mmol) was added by syringe. The solution was cooled further with a liquid nitrogen to -120 $^\circ\text{C}$ and then removed from the bath. A solution of NaO^tBu (9.63 g, 100.0 mmol) in 100 mL freshly distilled THF was added dropwise over 3 min. After approximately 20 minutes, the temperature of the brown solution reached -28 $^\circ\text{C}$ and a strongly exothermic reaction began. The solution turned black and the reaction flask was submerged in liquid nitrogen immediately. The bath was then removed and the solution allowed to reach rt over 1 h at which point 200 g of crushed ice was added. After 30 min, the solution was filtered and washed with water. The off-white precipitate was taken up in 100 mL CCl_4 , heated to reflux, cooled to rt, collected by filtration, and dried under vacuum. Yield: 4.04 g (39%). ^1H NMR (CDCl_3 , 300 MHz) δ 8.34 (s, 6Har), 2.51 (s, 18H) ppm; ^{13}C NMR (CDCl_3 , 300 MHz) δ 135.3, 127.6, 123.6, 20.3 ppm.

against which lower values were considered favorable.

²⁹ Still, W.C.; Kahn, M.; Mitra, A. *J. Org. Chem.* **1978**, *43*, 2923-2925.



2,3,6,7,10,11-Hexakis(bromomethyl)triphenylene (2.5). Prior to use, the solvent 1,2-dibromoethane (Aldrich, 99+%) was purified according to the following procedure. Washing with conc. HCl (2 x 75 mL), saturated NaHCO_{3(aq)} (100 mL), and water (75 mL) removed some color into the aqueous phases. The organic layer was then dried with CaCl₂, filtered, and vacuum distilled (aspirator, 40 °C) to provide a clear liquid which was dried further over 4 Å molecular sieves overnight. Under anhydrous conditions, triphenylene **2.4** (0.50 g, 1.60 mmol) was mixed with the solvent (60 mL) in a flask fitted with a gas inlet, reflux condenser, and a dropping funnel. The latter was filled with solvent (5 mL) and bromine (0.58 mL, 11.20 mmol) and fitted with a teflon tube which extended into the reaction solution. While refluxing (heating mantle) and irradiating (sunlamp) the reaction solution, the bromine solution was added dropwise over 15 min. The reaction solution was allowed to stir under these conditions until all the brown color had dissipated (\approx 5 min) and then stirred at rt for 2 h without the sunlamp. The resulting white precipitate was collected by filtration and washed thoroughly with THF. Crude Yield: 0.48 g (38%). ¹H NMR (DMSO-*d*₆, 600 MHz) δ 9.00 (s, 6H), 5.11 (s, 12H) ppm.



Jelly Doughnut Monomer (2.1). Under anhydrous conditions, glycoluril **2.6** (5.13 g, 13.85 mmol) was dissolved in DMSO (120 mL) with vigorous stirring. KO^tBu (3.11 g, 27.70 mmol) was added and the solution became slightly cloudy and yellow. Crude **2.5** (0.45 g, 0.58 mmol) was sonicated in DMSO (50 mL) to give a fine suspension and then heated until a homogenous, yellow solution developed. This hot solution was then added to the glycoluril mixture dropwise over 10 min during which time the reaction mixture became homogenous and purple. After stirring for an additional 15 min, the solution was poured into a mixture of water (1400 mL) and conc. HCl (200 mL). Stirring for a few minutes generated a precipitate that was collected by filtration and washed with water. The yellowish filter cake was sonicated thoroughly in CH₂Cl₂ (300 mL), filtered, and the filtrate evaporated. This filtrate residue was then dissolved in a minimum amount of CHCl₃ (0.5 mL) and mixed with MeOH (10 mL) which produced a cloudy solution. After chilling overnight, a white precipitate was isolated by filtration and collected using CHCl₃. Yield: 10.6 mg (1.3%). ¹H NMR of dimer **2.1•2.1** (CDCl₃, 600 MHz) δ 8.98 (s, 12H), 8.45 (s, 12Har), 4.94 (d, 12H, *J* = 15.8 Hz), 4.53 (d, 12H, *J* = 15.6 Hz), 4.33 (t, 12H, *J* = 7.0 Hz), 4.29 (t, 12H, *J* = 6.7 Hz), 1.94 (m, 6H), 1.74 (m, 6H), 1.66 (m, 24H), 1.06 (d, 36H, *J* = 6.5 Hz), 0.99 (d, 36H, *J* = 6.4 Hz) ppm; IR (CH₂Cl₂) 3214.2, 3094.9, 1754.2, 1715.7 cm⁻¹; MS (PD) Calc'd for C₇₂H₉₁N₁₂O₁₈⁺ [Monomer+H]⁺ 1413, found

1413; Calc'd for $C_{72}H_{90}N_{12}O_{18} \cdot Na^+$ [Monomer+Na]⁺ 1435, found 1435; Calc'd for $C_{144}H_{181}N_{24}O_{36}^+ \cdot CHCl_3$ [Dimer+H+CHCl₃]⁺ 2943, found 2943; Calc'd for $C_{144}H_{180}N_{24}O_{36} \cdot Na^+ \cdot CH_2Cl_2$ [Dimer+Na+CH₂Cl₂]⁺ 2931, found 2931.

[See Figure 2-3 for the ¹H spectrum of **2.1•2.1.**]

Chapter 3

Glycolurils: Synthesis and Modification

3.1 Introduction

As discussed in Chapter 2, the difficult synthesis of the Jelly Doughnut limited its availability. The other glycoluril-based capsules, such as the Tennis Ball and Softballs, shared similar low-yielding steps featuring glycoluril alkylation of brominated spacers (Figure 3-1A). The synthetic complications with this reaction may be distilled to three key problems: glycoluril reactivity, spacer reactivity, and isomer formation.¹ In this chapter, we will discuss efforts to address the first issue in terms of glycoluril protection and solubility.

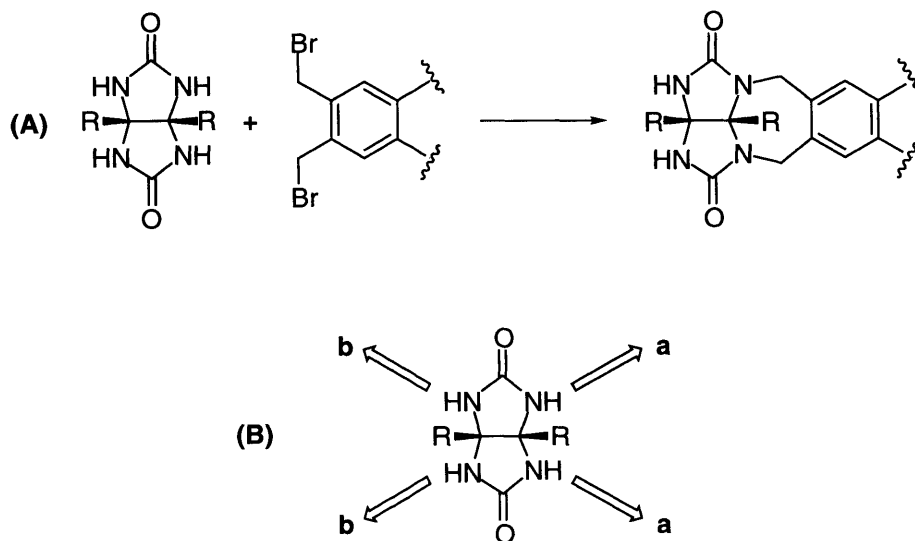


Figure 3-1. (A) Common alkylation step for glycoluril-based capsules. (B) Undesirable *trans* byproducts result from alkylation on both the **a** and **b** sides lowering yields for this step.

Figure 3-1B denotes the four alkylation sites on a glycoluril. Capsules are derived from *cis* (either **a,a** or **b,b**) dialkylation. Undesirable *trans* alkylation (**a,b**) consumes

¹ With the Softballs, isomer formation actually occurs at a step following glycoluril alkylation.

both glycoluril and spacer units and these can no longer produce desired products. The glycolurils we employed exhibited poor solubility in the typical alkylation conditions (KO^tBu, DMSO), but became more soluble upon spacer alkylation. [Initial glycoluril solubility depended primarily upon choice of R groups.] Unfortunately, this led to a preference for *trans* alkylated species which lowered desired product yields. Using large excesses of glycoluril compared to spacers reduced this problem, however purification became more difficult and yields were still low.

3.2 *cis*-Bisprotected Glycoluril

Given the above considerations, the best way to prevent *trans* alkylation was *cis*-bisprotection of the glycoluril. After the evaluation of numerous protection strategies, the efforts of several group members led to the *p*-methoxybenzyl (PMB) protecting group.² As shown in Figure 3-2, condensation of two equivalents of PMB-urea³ **3.1** with benzil derivatives usually provides the *cis*-substituted glycoluril **3.3** as the major product.

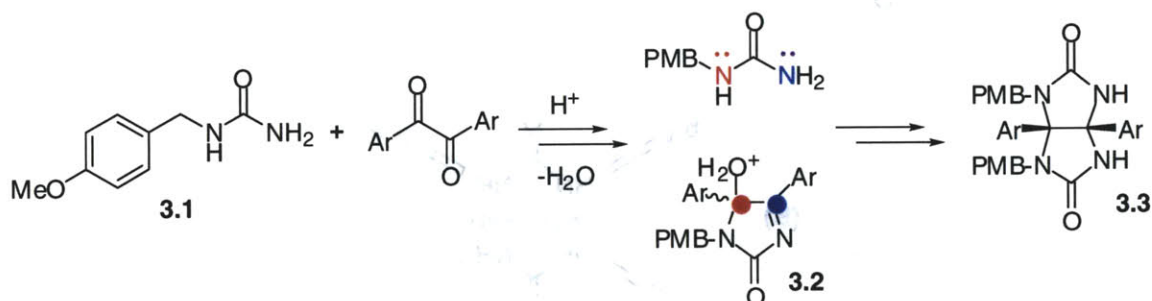


Figure 3-2. Formation of *cis*-bisprotected (PMB) glycoluril **3.3**.

Previous studies⁴ proposed that the regioselectivity of this reaction arises from protonated intermediate **3.2**. In acidic solution, loss of water produces a stabilized

² Dr. Dmitry M. Rudkevich and Dr. Tomas Szabo first identified the PMB protection strategy.

³ Moschel, R.C.; Hudgins, W.R.; Dipple, A. *J. Org. Chem.* **1986**, *51*, 4180-4185.

⁴ (a) Butler, A.R.; Leitch, E. *J. Chem. Soc., Perkin Trans. 2* **1980**, 103-105. (b) Butler, A. R.; Hussain, I.; Leitch, E. *J. Chem. Soc., Perkin Trans. 2* **1981**, 106-109.

carbonium ion at the red position that is attacked by the most nucleophilic nitrogen (red) on the second equivalent of urea. Subsequent ring closure provides the *cis*-bisprotected glycoluril **3.3**. However, given the steric encumbrances of this pathway, an alternative mechanism is likely. Protonation of the amide functionality on **3.2** rather than the hydroxyl can produce a carbonium ion at the blue position. This site is more reactive due to less hindrance and less stabilization compared to the alternative. The less hindered nitrogen of PMB-urea (blue) then attacks in S_N1 fashion which, after ring closure, gives **3.3**.

Following alkylation reactions, the PMB-groups may be removed under mild oxidation conditions using cerium ammonium nitrate (CAN).⁵ However, the solvent system used for this step (CH₃CN / H₂O; 5:1) made the identification of solubilizing groups imperative. Otherwise, complete deprotection could not be accomplished due to precipitation of intermediates.

3.3 Soluble Glycolurils

Several 1,2-diketones were evaluated in the synthesis of *cis*-bis-PMB-protected glycolurils (Figure 3-3). The commercially-available 4,4'-dimethylbenzil **3.4a** gave the desired glycoluril **3.3a** in good yield. However, following alkylation of spacers, complete deprotection proved difficult because of poor solubility. Benzil **3.4b**, formed from Heck ethynylation,⁶ decomposed under the glycoluril condensation conditions. Benzil **3.4c** gave the desired glycoluril **3.3c** in fair yield, but the glycol chains made subsequent products somewhat water-soluble after CAN deprotection and complicated

⁵ (a) Yoshimura, J.; Yamaura, M.; Suzuki, T.; Hashimoto, H. *Chem. Lett.* **1983**, 1001-1002. (b) Yamaura, M.; Suzuki, T.; Hashimoto, H.; Yoshimura, J.; Okamoto, T.; Shin, C. *Bull. Chem. Soc. Jpn.* **1985**, *58*, 1413-1420.

reaction work-ups.⁷ Condensation using the diketone substituted with two isoamyl esters⁸ **3.4d** gave the *trans*-substituted glycoluril as the major product.

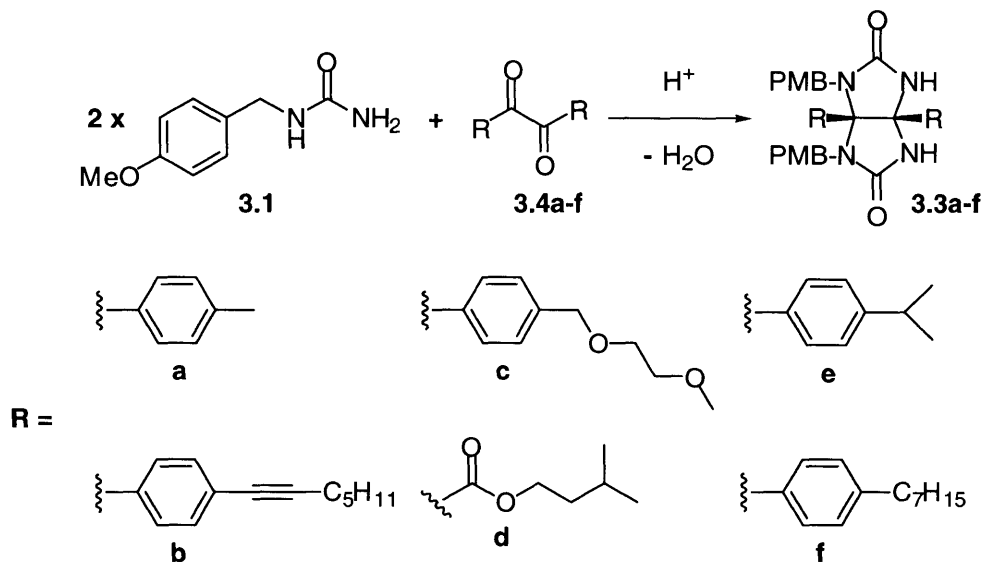


Figure 3-3. Diketones tested in the synthesis of **3.3**.

The glycoluril derived from 4,4'-diisopropylbenzil **3.4e** gave the *cis*-protected product **3.3e** in good yield and, following alkylation steps, could be CAN-deprotected cleanly. Although this derivative appeared promising, the starting benzil synthesis required four steps (Figure 3-4) and it imparted only moderate solubility to the glycoluril.

⁶ Method adapted from Singh, R.; Just, G. *J. Org. Chem.* **1989**, *54*, 4453-4457.

⁷ Studies of glycol-substituted glycolurils were done in collaboration with Dr. Tomas Szabo. T.S. synthesized the PMB-protected glycoluril **3.3c** and I synthesized the non-PMB protected version. We performed various reactions using both derivatives.

⁸ Used in the synthesis of the unprotected glycoluril **2.6**, this "diketone" actually exists as the tetrahydrate.

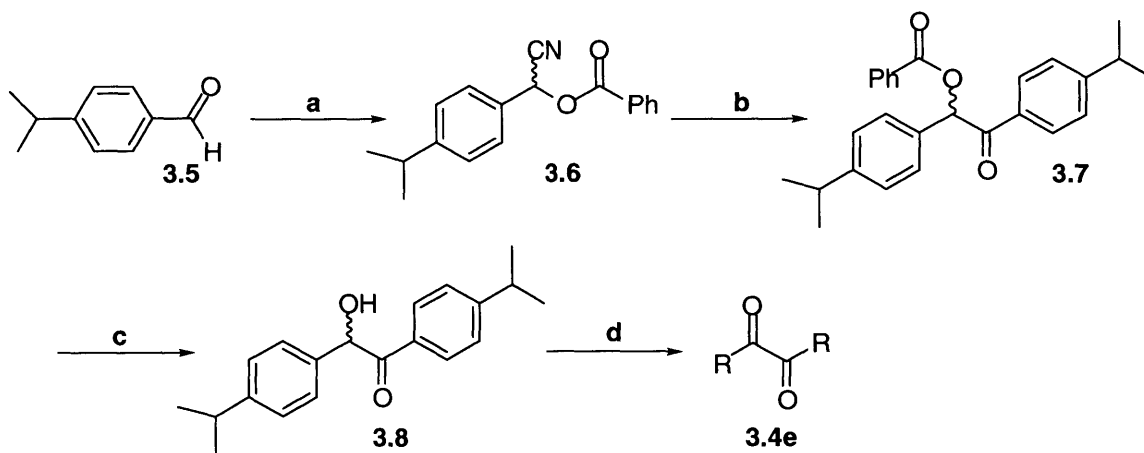


Figure 3-4. Synthesis of 4,4'-diisopropylbenzil **3.4e**: a) BnNEt₃Cl, KCN, BzCl, CH₂Cl₂, H₂O; b) **3.5**, KO^tBu, THF; c) KOH, CH₃CN, H₂O; d) CuSO₄·5H₂O, pyr, H₂O.

Therefore, a one step synthesis of the more lipophilic 4,4'-di-*n*-heptylbenzil **3.4f** was sought (Figure 3-5). Jose M. Rivera-Ortiz had previously synthesized **3.4f** via a double Friedel-Crafts acylation involving oxalyl chloride and 1-phenylheptane.⁹ This reaction proceeded in fair yield, but involved a difficult purification. Reductive coupling of 4-*n*-heptylbenzoyl chloride promoted by samarium diiodide¹⁰ gave a fair yield of **3.4f** and involved a much simpler work-up. However, the analogous reaction involving 4-*n*-heptylbenzoic acid and lithium¹¹ gave a higher yield of the desired product and had the added benefit of using a more stable reducing agent. The *cis*-protected glycoluril **3.3f** derived from this benzil demonstrated increased solubility over glycoluril **3.3e** and was used in several successful synthetic routes (see later chapters).

⁹ Prepared analogously to the octyl derivative, see: Mohr, B.; Enkelmann, V.; Wegner, G. *J. Org. Chem.* **1994**, *59*, 635-638.

¹⁰ Adapted from: (a) Girad, P.; Couffignal, R.; Kagan, H.B. *Tetrahedron Lett.* **1981**, *22*, 3959-3960. (b) Soupe, J.; Namy, J.-L.; Kagan, H.B. *Tetrahedron Lett.* **1984**, *25*, 2869-2872.

¹¹ Method adapted from Karaman, R.; Fry, J.L. *Tetrahedron Lett.* **1989**, *30*, 6267-6270 and optimized by Dr. Göran Hilmersson.

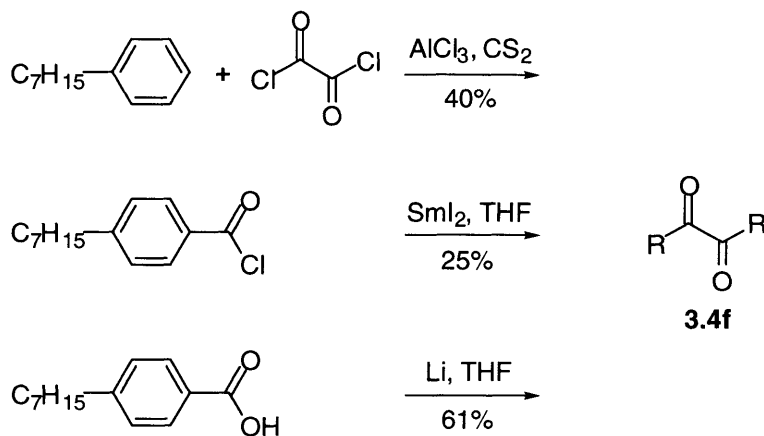


Figure 3-5. Three approaches to 4,4'-di-*n*-heptylbenzil **3.4f**.

3.4 Alkylation Reactions

Using the protected glycoluril **3.3a**, Dr. Dmitry Rudkevich succeeded in synthesizing a Tennis Ball derivative.¹² However, analogous attempts to synthesize the Jelly Doughnut using glycolurils **3.3a** and **3.3e** failed because of poor solubility during deprotection and apparent cleavage of the triphenylene spacer. Due to the latter issue, the more soluble glycoluril **3.3f** was not evaluated in this context and other synthetic strategies were explored.

3.5 Experimental

3.5.1 Apparatus, Materials, and Methods

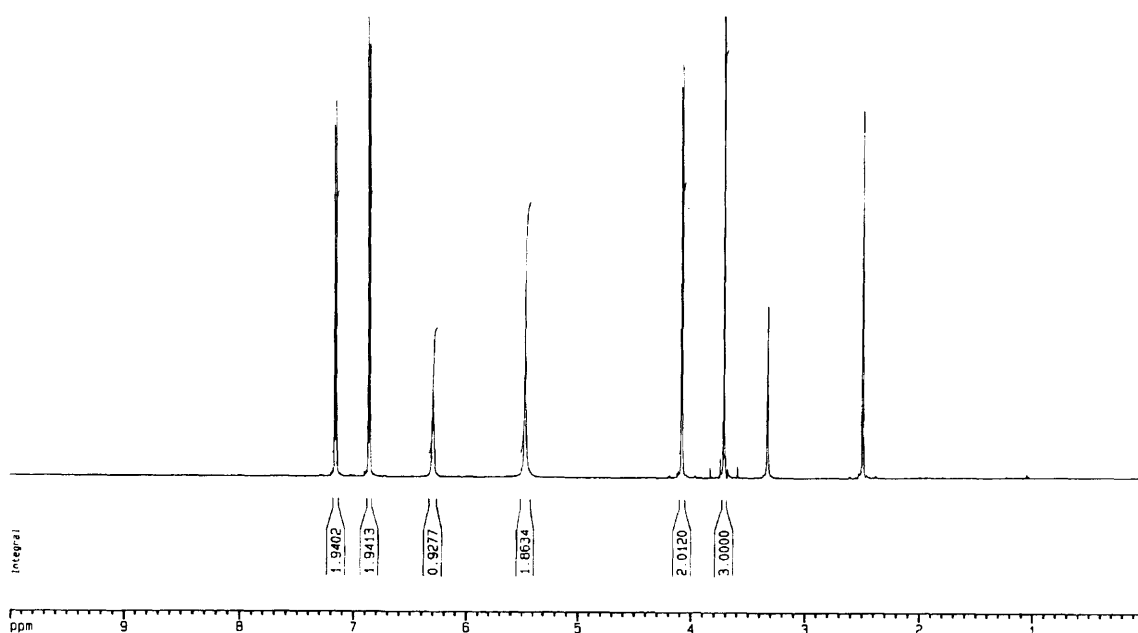
See section 2.5.1.

3.5.2 Procedures (¹H NMR spectra follow each preparation.)

***p*-Methoxybenzylurea (3.1).** A solution of *p*-methoxybenzylamine (19.60 mL, 150 mmol) in 300 mL water was brought to pH \approx 4 using 1 N HCl_{aq}. A second solution of KOCN (18.25 g, 225 mmol) in 100 mL water was added to the first and the mixture

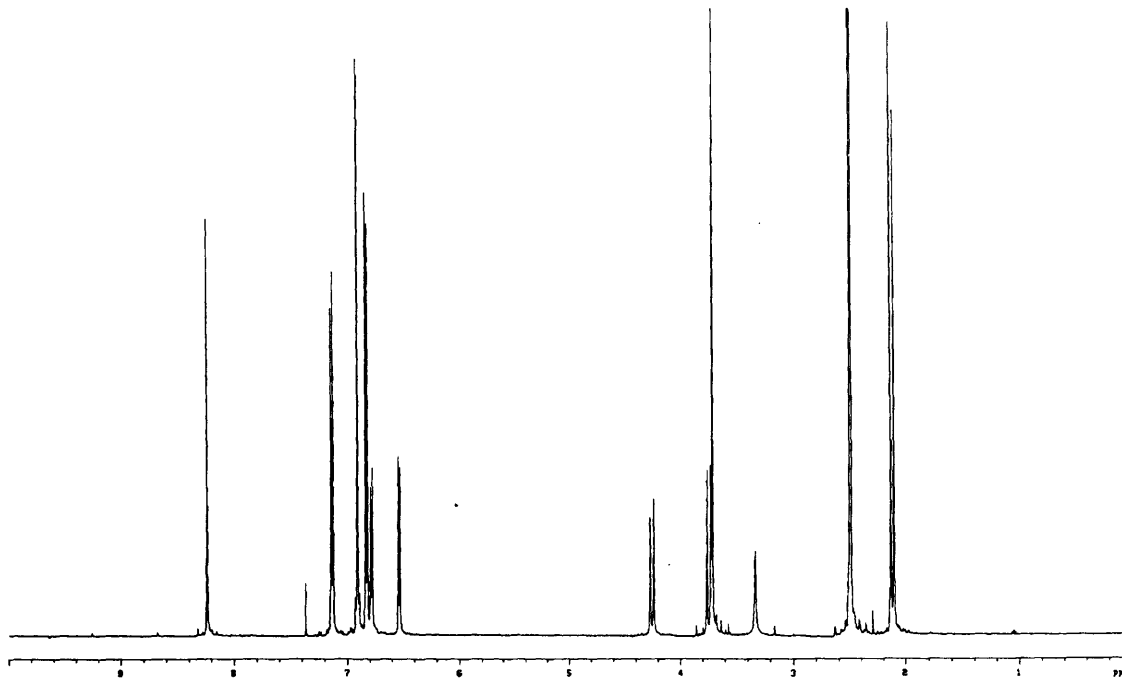
¹² Rudkevich, D.M. Unpublished results.

was stirred for 48 h. The resulting precipitate was collected by filtration, recrystallized with EtOH / H₂O (1:1), and washed with EtOH / H₂O (1:10) to yield white, needle-like crystals. Yield: 23.74 g (89%). ¹H NMR (DMSO-*d*₆, 600 MHz) δ 7.16 (d, 2H, *J* = 8.47 Hz), 6.87 (d, 2H, *J* = 8.56 Hz), 6.30 (m, 1H), 5.47 (s, 2H), 4.09 (d, 2H, *J* = 5.96 Hz), 3.72 (s, 3H) ppm; ¹³C NMR (DMSO-*d*₆, 600 MHz) δ 158.86, 158.28, 132.99, 128.52, 113.75, 55.08, 42.28 ppm; HRMS (FAB) Calc'd for [M+H]⁺ C₉H₁₃N₂O₂⁺ 181.0977, found 181.0970.



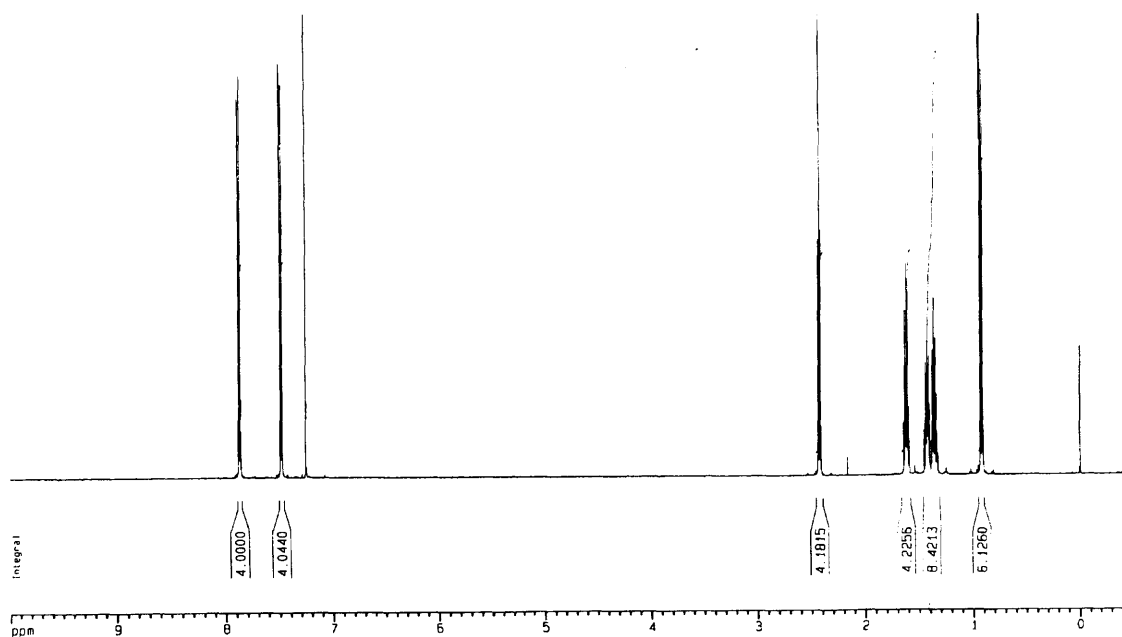
PMB-Glycoluril (3.3a). (R = *p*-Me-C₆H₅) Benzil **3.4a** (2.98 g, 12.51 mmol), PMB-urea (4.51 g, 25.03 mmol), and TFA (2 mL) were mixed in benzene (100 mL). The mixture was refluxed overnight and the generated water was collected in a Dean-Stark trap. After cooling to rt, ether (100 mL) was added and the mixture cooled in an ice bath. The resulting precipitate was collected by filtration and washed with ether. Stirring this crude product in refluxing 1:1 toluene/MeOH (200 mL) for 30 min followed by filtration gave a clean, white powder. Yield: 5.44 g (77%). ¹H NMR (DMSO-*d*₆, 500 MHz) δ 8.23

(s, 2H), 7.14 (d, 4Har, $J = 9.0$ Hz), 6.89 (m, 4Har), 6.83 (m, 4Har), 6.79 (d, 2Har, $J = 8.0$ Hz), 6.54 (d, 2Har, $J = 8.0$ Hz), 4.25 (d, 2H, $J = 17.0$ Hz), 3.74 (d, 2H, $J = 17.0$ Hz), 3.72 (s, 6H), 2.13 (s, 3H), 2.10 (s, 3H) ppm.



Ethynyl benzil (3.4b). ($R = -CC(CH_2)_4CH_3$) 4, 4'-Dibromobenzil (Aldrich, tech. grade) was purified by dissolving in benzene, washing with 1N KOH, and drying over $MgSO_4$. Filtering and concentrating the filtrate provided a yellow powder which was recrystallized in benzene to give fine yellow needles. This starting benzil (5.09 g, 13.83 mmol) was dissolved under anhydrous conditions by a refluxing mixture of benzene (250 mL) and triethylamine (150 mL), both freshly distilled from CaH_2 . 1-Heptyne (3.81 mL, 29.04 mmol) was added followed by $Pd(PPh_3)_4$ (0.64 g, 0.55 mmol) and CuBr (0.24 g, 1.66 mmol). The clear yellow solution immediately turned black and substantial precipitate developed. After refluxing for 30 min with efficient stirring, the mixture was cooled and filtered. The filtrate was concentrated in vacuo, taken up in ether (250 mL), and washed with saturated NH_4Cl (aq) solution (4 x 100 mL) and water (100 mL). The

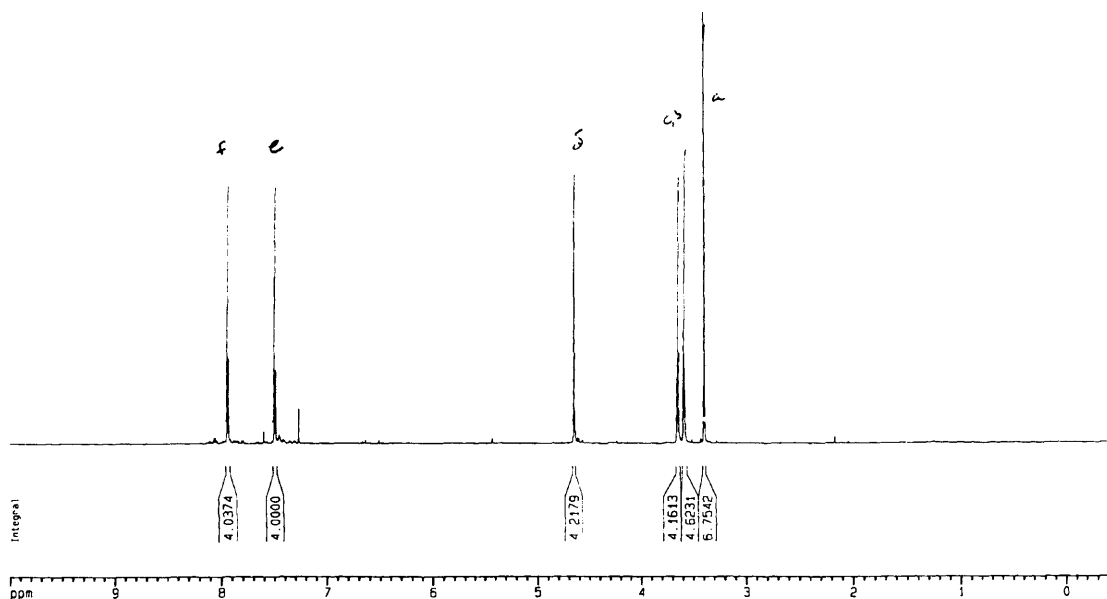
organic layer was dried over MgSO_4 and stirred with activated charcoal. This mixture was filtered, concentrated, and purified by flash chromatography (2% EtOAc/Hex) to give a yellow powder. Yield: 2.93 g (53%). ^1H NMR (CDCl_3 , 600 MHz) δ 7.87 (d, 4H, $J = 8.4$ Hz), 7.49 (d, 4H, $J = 8.4$ Hz), 2.43 (t, 4H, $J = 7.2$ Hz), 1.62 (m, 4H), 1.40 (m, 4H), 1.37 (m, 4H), 0.92 (t, 6H, $J = 7.2$ Hz) ppm; ^{13}C NMR (CDCl_3 , 600 MHz) δ 193.93, 132.35, 131.75, 131.52, 130.04, 96.42, 80.31, 31.25, 28.31, 22.31, 19.69, 14.07 ppm; HRMS (FAB) Calc'd for $[\text{M}+\text{Na}]^+$ $\text{C}_{28}\text{H}_{30}\text{O}_2\cdot\text{Na}^+$ 421.2144, found 421.2154.



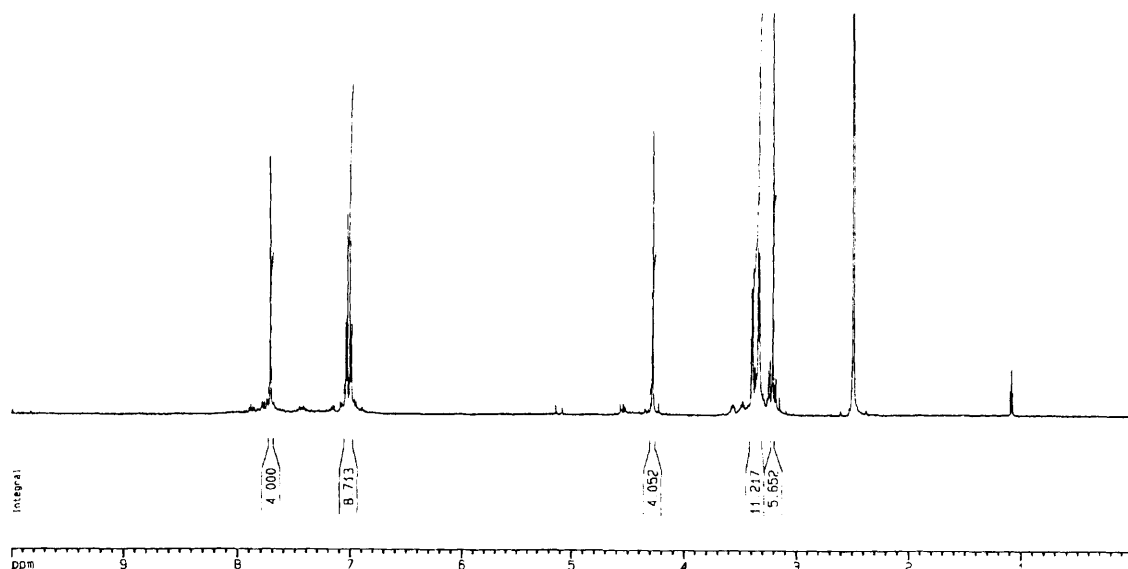
Glycol benzil (3.4c). ($\text{R} = -\text{CH}_2\text{OCH}_2\text{CH}_2\text{OCH}_3$) KOH (1.60 g, 28.50 mmol) was dissolved in 2-methoxyethanol (25 mL) with stirring. 4,4-bisbromomethylbenzil¹³ (3.96 g, 10.00 mmol) was dissolved in benzene (10 mL) and this solution was added to the reaction mixture. After refluxing for 30h, the solution was poured into 1M HCl_{aq} (100 mL) and extracted with CHCl_3 (2 x 100 mL). The combined organic layers were

¹³ Available from NBS bromination of 4,4'-dimethylbenzil; see: Wang, C.; Bryce, M.R.; Batsanov, A.S.; Howard, J.A.K. *Chem. Eur. J.* **1997**, *3*, 1679-1690.

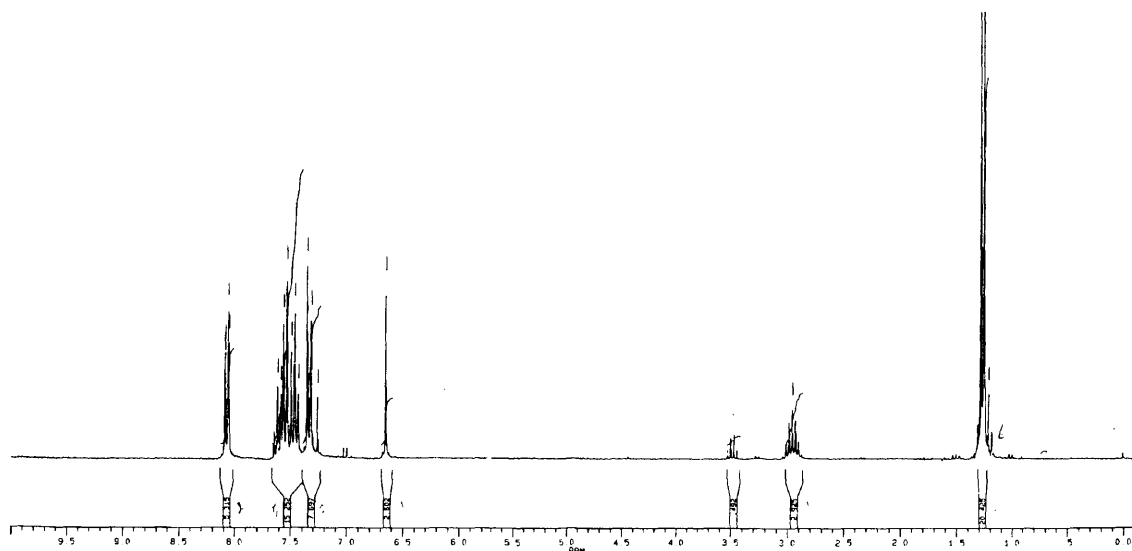
dried (Na_2SO_4), filtered, and concentrated by rotary evaporation. This residue was purified by repetitive flash chromatography (3 times; 30 \rightarrow 50% EtOAc/Hex) to give a yellow oil. Yield: 1.41 g (36%). ^1H NMR (CDCl_3 , 600 MHz) δ 7.94 (d, 4Har, $J = 8.2$ Hz), 7.49 (d, 4Har, $J = 8.2$ Hz), 4.65 (s, 4H), 3.65 (m, 4H), 3.60 (m, 4H), 3.40 (s, 6H) ppm; HRMS (FAB) Calc'd for $[\text{M}+\text{Na}]^+$ $\text{C}_{22}\text{H}_{26}\text{O}_6\cdot\text{Na}^+$ 409.1627, found 409.1627.



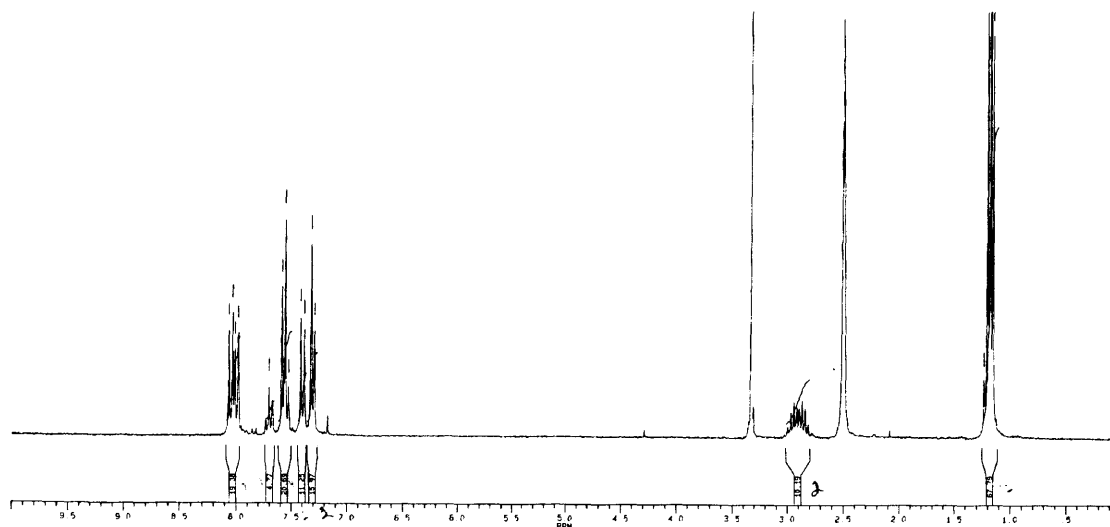
Glycol glycoluril. (non-PMB protected, $\text{R} = -\text{CH}_2\text{OCH}_2\text{CH}_2\text{OCH}_3$) Benzil **3.4c** (5.27 g, 13.64 mmol), urea (2.46 g, 40.92 mmol), and TFA (2 mL) were mixed in benzene (75 mL). After refluxing the solution overnight with water removal *via* a Dean-Stark trap, the volatiles were removed by rotary evaporation. The residue was sonicated in EtOH (50 mL) to produce a fine suspension to which water (250 mL) was added. Further sonication followed by overnight refrigeration produced a yellow precipitate that was collected by filtration. This crude material was further purified by sonication in ether (200 mL) and filtration to give an off-white powder. Yield: 2.28 g (36%). ^1H NMR ($\text{DMSO}-d_6$, 600 MHz) δ 7.72 (s, 4H), 7.02 (d, 4Har, $J = 8.1$ Hz), 6.99 (d, 4Har, $J = 8.2$ Hz), 4.29 (s, 4H), 3.35 (m, 8H), 3.22 (s, 6H) ppm.



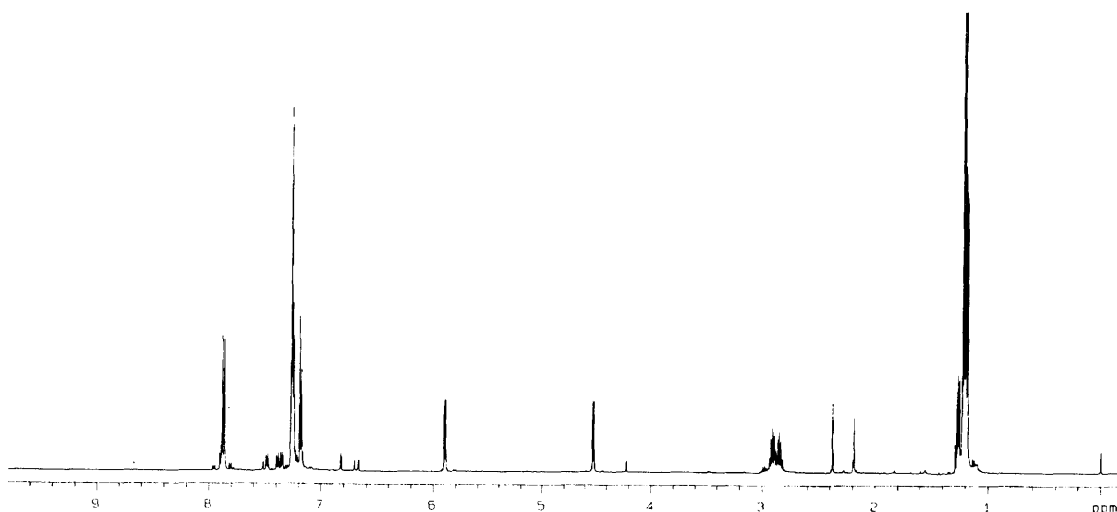
Cyanobenzoate (3.6). Benzyl triethylammonium chloride (2.93 g, 12.87 mmol), 4-isopropylbenzaldehyde **3.5** (15.00 mL, 98.88 mmol), and KCN (25.94 g, 398.35 mmol) were mixed in water (110 mL) and CH_2Cl_2 . Benzoyl chloride (13.8 mL, 118.89 mmol) was dissolved in CH_2Cl_2 (70 mL) and added dropwise to the reaction mixture over 30 min at rt. After an additional 30 min, the dark red mixture was transferred to a separatory funnel and the layers separated. The organic phase was washed with saturated aqueous K_2CO_3 (3 x 30 mL), water (2 x 200 mL), and brine (50 mL). After drying (MgSO_4) and filtration, the solution was concentrated *in vacuo* to a dark red oil which solidified upon standing. Crude Yield: 30.01 g (108%). ^1H NMR (CDCl_3 , 250 MHz) δ 8.07 (m, 2Har), 7.55 (m, 5Har), 7.33 (m, 2Har), 2.95 (m, 1H), 1.26 (d, 6H, $J = 7.0$ Hz) ppm.



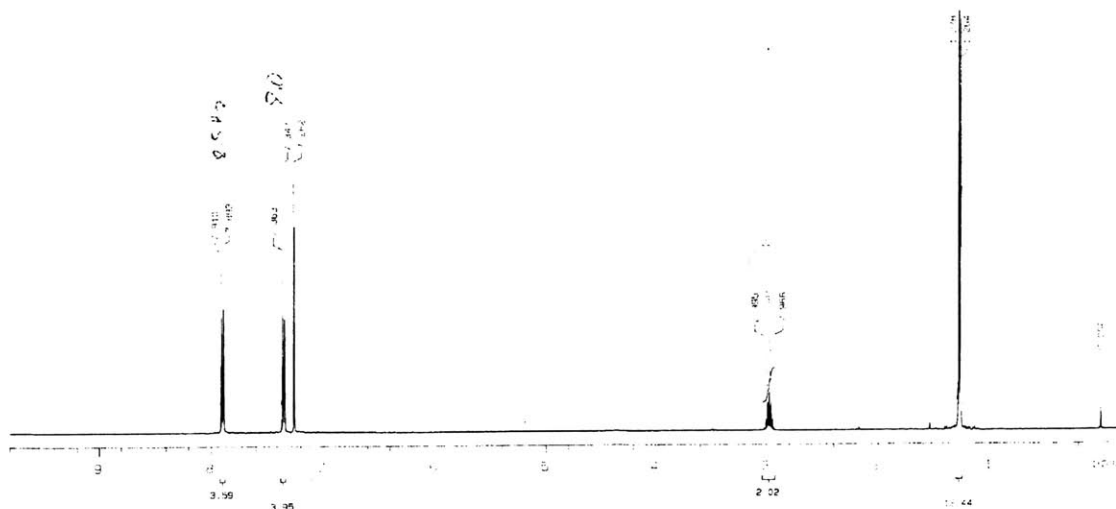
Alpha-benzoate ketone (3.7). Under anhydrous conditions, cyanobenzoate **3.6** (30.01 g, 107.43 mmol) and 4-isopropylbenzaldehyde **3.5** (15.92 mL, 107.43 mmol) were dissolved in THF (150 mL). A mixture of KO^tBu (13.26 g, 118.17 mmol) and THF (150 mL) was added to the stirring reaction solution *via* a dropping funnel over 45 min at rt. The resulting mixture turned black over the course of 2 h after which time the volatiles were removed under vacuum to give an orange residue. The residue was triturated in EtOAc (500 mL) and filtered to remove solids. The filtrate was washed with water (2 x 100 mL) and brine (50 mL) followed by drying with MgSO₄, filtration, and evaporation to give an orange powder. Yield: 40.46 g (94%). ¹H NMR (DMSO-*d*₆, 250 MHz) δ 8.01 (m, 4Har), 7.71 (m, 5Har), 7.40 (m, 2Har), 7.31 (m, 2Har), 2.91 (m, 2H), 1.19 (m, 12H) ppm.



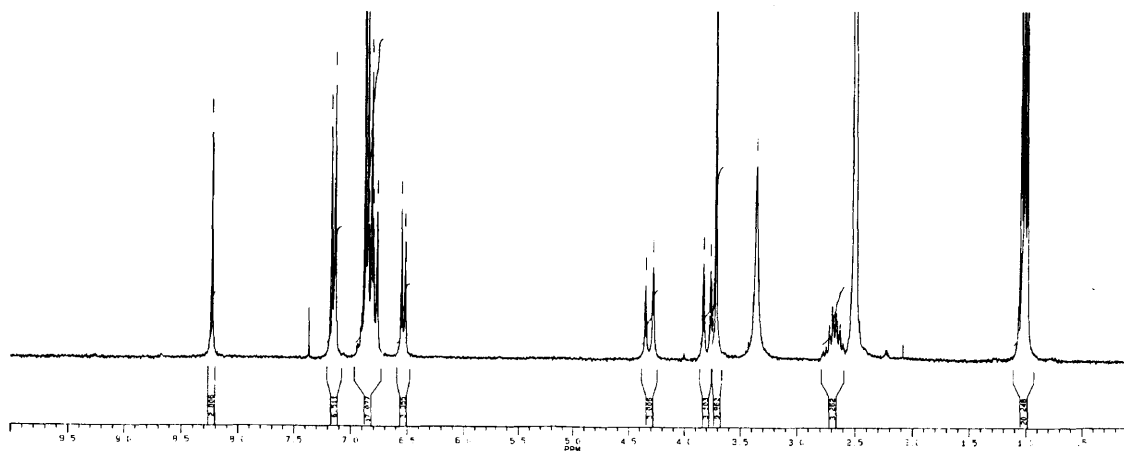
Benzoin (3.8). Ketone **3.7** (40.46 g, 101.02 mmol) was dissolved in CH₃CN with the assistance of sonication and mild heating. An aqueous solution (150 mL) of KOH (11.34 g, 202.04 mmol) was added dropwise over 30 min to the orange solution. The resulting mixture was allowed to stir at rt overnight and then neutralized using HCl. Water (100 mL) was added and the CH₃CN removed by rotary evaporation. The mixture was then poured into 500 mL ether and shaken thoroughly until no solids remained. The organic layer was then washed with 1M NaOH_{aq} (4 x 75 mL), water (100 mL), and brine (50 mL). After drying (MgSO₄) and filtration, the solution was evaporated and dried further under high vacuum for 24 h. Crude Yield: 23.94 g (80%). ¹H NMR (CDCl₃, 500 MHz) δ 7.87 (d, 2Har, *J* = 8.0 Hz), 7.25 (m, 4Har), 7.18 (d, 2Har, *J* = 8.5 Hz), 5.91 (d, 1H, *J* = 6.5 Hz), 4.53 (d, 1H, *J* = 6.5 Hz), 2.88 (m, 2H), 1.20 (m, 12H) ppm.



Isopropyl benzil (3.4e). (R = *p*-isopropylphenyl) Benzoin **3.8** (23.94 g, 80.77 mmol) was dissolved in pyridine (125 mL) with the aid of sonication. $\text{CuSO}_4 \cdot 5\text{H}_2\text{O}$ (42.35 g, 169.68 mmol) and water (90 mL) were added and the blue mixture was then brought to reflux. After 16 h, the pyridine was removed by rotary evaporation and the sludge taken up in ether (250 mL) and water (100 mL). The layers were separated and the organic phase was washed further with water (100 mL), 1M HCl_{aq} (2 x 50 mL), and brine (50 mL). Drying (MgSO_4), filtration, and evaporation of the filtrate gave a brown residue which was triturated with MeOH (100 mL) and cooled to give a light yellow precipitate. The powder was collected by filtration. Yield: 14.86 g (63%). ^1H NMR (CDCl_3 , 500 MHz) δ 7.90 (d, 4H, $J = 8.5$ Hz), 7.35 (d, 4H, $J = 8.0$ Hz), 2.98 (m, 2H), 1.27 (d, 12H, $J = 7.0$ Hz) ppm.



PMB-Glycoluril (3.3e). (R = *p*-isopropylphenyl) Benzil **3.4e** (12.5 mmol, 3.68 g), PMB-urea (25 mmol, 4.51 g), and 2 mL of trifluoroacetic acid were added to 300 mL of benzene and the solution was refluxed overnight with a Dean-Stark trap. After removal of the benzene *in vacuo*, the residue was taken up in 100 mL EtOH, refluxed for 30 min, cooled for 1 h, and then filtered. Washing with some cold EtOH and drying produced a fine white powder. Yield: 4.40 g (57%) ^1H NMR (DMSO- d_6 , 250 MHz) δ 8.23 (s, 2H), 7.15 (d, 4Har, $J = 8.6$ Hz), 6.85 (m, 10Har), 6.53 (d, 2Har, $J = 8.3$ Hz), 4.31 (d, 2H, $J = 16.5$ Hz), 3.80 (d, 2H, $J = 16.5$ Hz), 3.72 (s, 6H), 2.68 (m, 2H), 1.02 (m, 12H) ppm; ^{13}C NMR (DMSO- d_6 , 300 MHz) δ 160.15, 157.82, 148.83, 148.38, 134.58, 130.93, 130.49, 127.78, 126.86, 125.48, 125.03, 113.39, 90.38, 79.29, 54.90, 44.16, 32.87, 32.80, 23.61, 23.50 ppm.

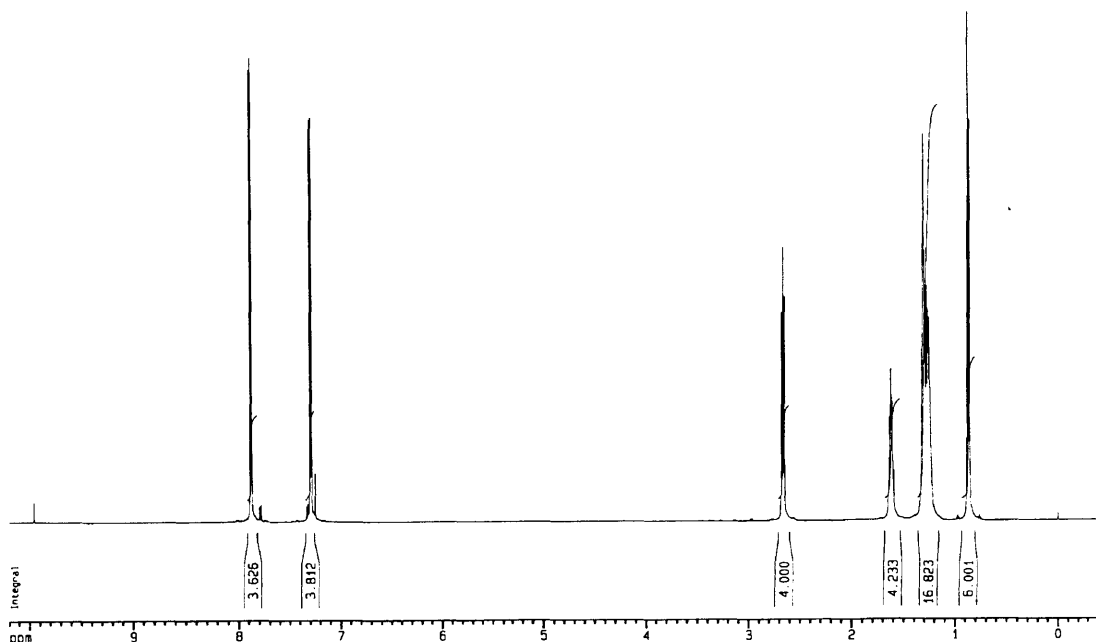


***N*-heptyl benzil (3.4f).** (R = *p*-*n*-heptylphenyl via *p*-*n*-heptylbenzoyl chloride)

Under anhydrous conditions, powdered samarium metal (5.39 g, 35.86 mmol) was suspended in 300 mL THF. To the suspension was added CH₂I₂ (3.05 mL, 12.80 mmol) and the mixture was stirred in the dark under N₂ overnight to give a dark blue solution. The solution was transferred *via* canula to another dry flask fitted with a dropping funnel containing 4-*n*-heptylbenzoyl chloride (3.05 mL, 12.80 mmol) in 10 mL THF. This acid chloride solution was added dropwise over 30 min during which time the solution turned green/blue. After stirring for another 30 min, the solution was poured into 900 mL of 1M HCl and extracted with methylene chloride (4 x 250 mL). The organic phases were combined, concentrated to 250 mL, and washed with 10% NaHSO₃ (aq.). After drying with MgSO₄, filtering, and concentrating the filtrate, the yellow oil was purified by flash chromatography (2% EtOAc in Hex) two times to give a yellow oil. Yield: 0.65 g (25%). (Characterization data matches that shown below for the alternative route.)

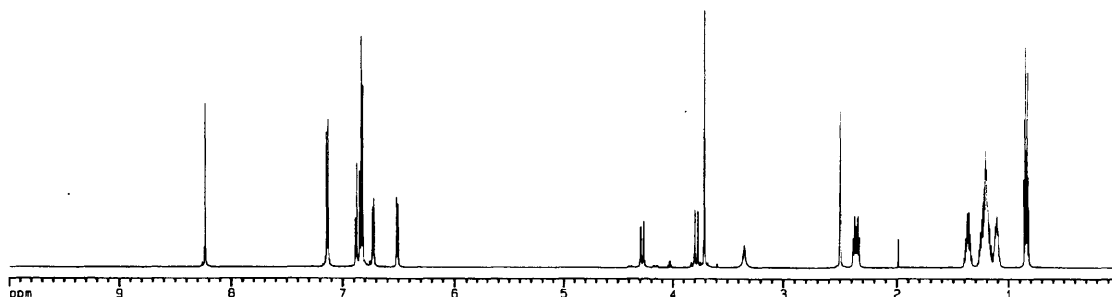
***N*-heptyl benzil (3.4f).** (R = *p*-*n*-heptylphenyl via *p*-*n*-heptylbenzoic acid) Under anhydrous conditions, lithium [\approx 30 wt. % in mineral oil, high sodium], (8.40 g, 363.12 mmol) was added directly to 500 mL of THF. To this mixture, 4-*n*-heptylbenzoic acid (20 g, 90.78 mmol) was added. Mechanical stirring and sonication over 16 h produced a

brown mixture that was quenched, after chilling, by pouring carefully into ice cold 1.5 N HCl (aq., 1000 mL). The aqueous mixture was washed with hexane (4 x 250 mL) and the combined organic phases were dried with Na₂SO₄. Filtration and concentration provided a dark yellow oil which was easily purified by flash chromatography (0 → 5% EtOAc in Hex) to give a light yellow oil. Yield: 11.30 g (61%). ¹H NMR (CDCl₃, 600 MHz) δ 7.88 (m, 4Har), 7.29 (m, 4Har), 2.67 (t, 4H, *J* = 7.72 Hz), 1.62 (m, 4H), 1.27 (m, 16H), 0.87 (t, 6H, *J* = 7.03 Hz) ppm; ¹³C NMR (CDCl₃, 600 MHz) δ 194.94, 151.31, 131.13, 130.34, 129.34, 36.33, 31.85, 31.12, 29.29, 29.20, 22.72, 14.15 ppm; IR (CDCl₃) 2927.19, 2855.57, 1672, 1604.58 cm⁻¹; HRMS (FAB) [M+H]⁺ Calc'd for C₂₈H₃₉O₂⁺ 407.2950, found 407.2961.



PMB-Glycoluril (3.3f). (R = *p-n*-heptylphenyl) Benzil **3.4f** (11.18 g, 27.49 mmol), PMB-urea (14.86 g, 82.49 mmol), 7 mL of TFA, and 150 mL of benzene were combined. The mixture was refluxed using a Dean-Stark apparatus to remove water. After 24 h, TLC indicated complete consumption of **3.4f**, so the brown solution was

concentrated in vacuo and purified twice by flash chromatography (50 -> 60 -> 70% EtOAc in Hex) to give a white foam. Yield: 10.8 g (54%). [Note: trituration of the foam with hexane may be necessary for further purification.] mp 154 °C. ¹H NMR (DMSO-*d*₆, 600 MHz) δ 8.23 (s, 2H), 7.13 (d, 4Har, *J* = 8.65 Hz), 6.83 (m, 8Har), 6.73 (d, 2Har, *J* = 8.18 Hz), 6.51 (d, 2Har, *J* = 8.29 Hz), 4.28 (d, 2H, *J* = 16.56 Hz), 3.78 (d, 2H, *J* = 16.56 Hz), 3.71 (s, 6H), 2.36 (m, 4H), 1.37 (m, 4H), 1.20 (m, 16H), 0.84 (m, 6H) ppm; ¹³C NMR (DMSO-*d*₆, 600 MHz) δ 160.52, 158.11, 142.87, 142.43, 134.70, 131.186, 130.49, 128.09, 128.04, 127.82, 127.47, 127.11, 113.57, 90.43, 79.52, 54.97, 44.19, 34.54, 34.45, 31.31, 31.28, 30.91, 30.68, 28.58, 28.51, 28.34, 28.31, 22.14, 22.09, 13.89, 13.85 ppm; IR (CDCl₃) 3264.24, 2925.92, 2854.10, 1701.04, 1512.90, 1459.17, 1246.05 cm⁻¹; HRMS (FAB): Calc'd for [M+Cs]⁺ C₄₆H₅₈N₄O₄•Cs⁺ 863.3512, found 863.3537.



Chapter 4 **A Modular Approach to Self-Assembling Systems**

4.1 Introduction

Despite the availability of more soluble, *cis*-bisprotected glycolurils, alkylation reactions with bisbenzylic bromides still proved difficult (Section 3.4). Persistent solubility problems following alkylation and spacer incompatibility with PMB deprotection conditions ended attempts to use these new glycolurils as a “quick fix” to the challenges of capsule syntheses. A new strategy that removed protecting groups prior to spacer coupling was necessary. In addition, we sought to eliminate the use of polybrominated spacers whose numerous shortcomings were articulated in Section 2.2.

Faced with similar challenges in the syntheses of supramolecular structures, several other groups adopted “modular” strategies that employed versatile molecular building blocks.¹ These new, convergent approaches resulted in simplified syntheses, higher yields, and increased structural diversity. In this chapter, we describe the development of novel building blocks based upon glycolurils.

4.2 Nolte Methodology

The first modular strategy we examined was derived from Nolte *et al.* As shown in Figure 4-1, Nolte used glycolurils as scaffolds for molecular cages and clips such as

¹ For recent reviews, see: (a) Higler, I.; Timmerman, P.; Verboom, W.; Reinhoudt, D.N. *Eur. J. Org. Chem.* **1998**, 2689-2702. (b) Higler, I.; Verboom, W.; Reinhoudt, D.N. Synthetic Receptors: A Modular Approach to Large Structures. In *Crystallography of Supramolecular Compounds*; Tsoucaris, G., Atwood, J.L., Lipkowski, J., Eds.; Kluwer Academic Publishers: Dordrecht, 1996; pp 347-368.

host **4.5**.² The short reaction sequence begins with treatment of diphenyl glycoluril **4.1** with formaldehyde followed by acid to give diether **4.2**. Conversion to tetracetate **4.3** is then accomplished using acetic anhydride. Under acidic conditions, carbocationic intermediates form and add to sufficiently electron-rich aromatics such as **4.4**. The resulting cleft-like structures bind aromatic guests within their hydrophobic pockets.

This strategy was an attractive alternative to our glycoluril alkylation methodology involving bis-benzylic bromides. If a mono-ether derivative of **4.2** could be synthesized, this new module might alkylate aromatic spacers to cleanly provide capsule monomers. Fortunately, the development of the *cis*-bisprotected glycolurils facilitated the evaluation of this *umpolung* approach to monomer synthesis.

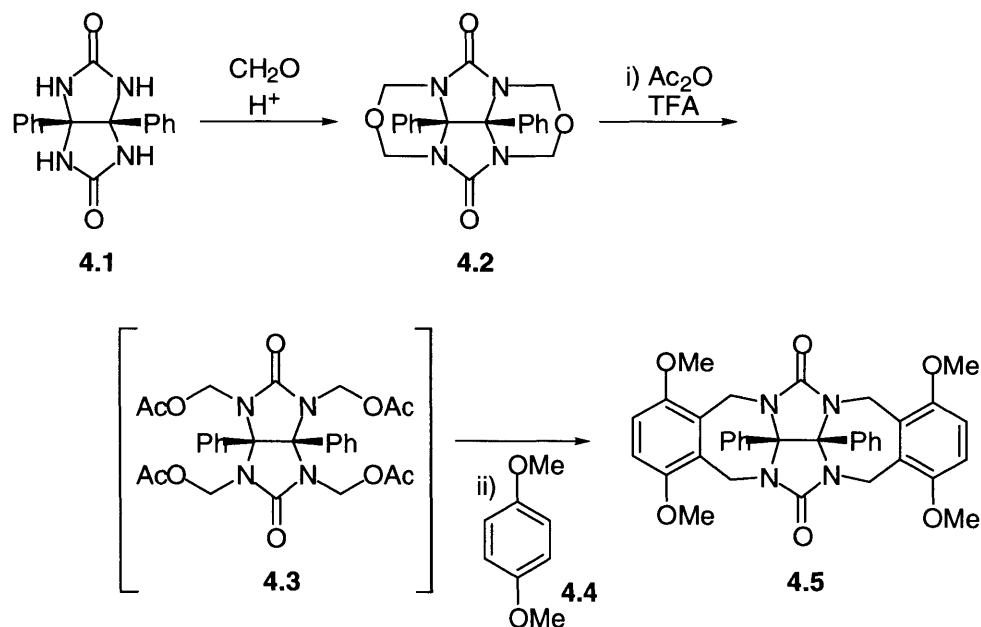


Figure 4-1. Nolte methodology for the synthesis of glycoluril clefts.

² Sijbesma, R.P.; Nolte, R.J.M. In *Molecular Clips and Cages Derived from Glycoluril*; Weber, E., Ed.; Topics in Current Chemistry 175; Springer-Verlag: New York, 1995; pp 25-56

Figure 4-2 illustrates how this methodology was employed in a new Jelly Doughnut synthesis. Subjecting glycoluril **3.3f** to the conditions described above gave the mono-ether **4.6** in good yield. Since the PMB groups could react under the aromatic substitution conditions, they were removed by CAN oxidation to give **4.7**. The alkylation of triphenylene using this Nolte-like module was then attempted,³ but no Jelly Doughnut was recovered. Evidently, the triphenylene spacer was not sufficiently electron-rich to participate in the substitution reaction. However, Dr. Daniel Mink⁴ proved the validity of this approach by synthesizing a Tennis Ball derivative from electron-rich spacer **4.4** and glycoluril module **3.3a**.

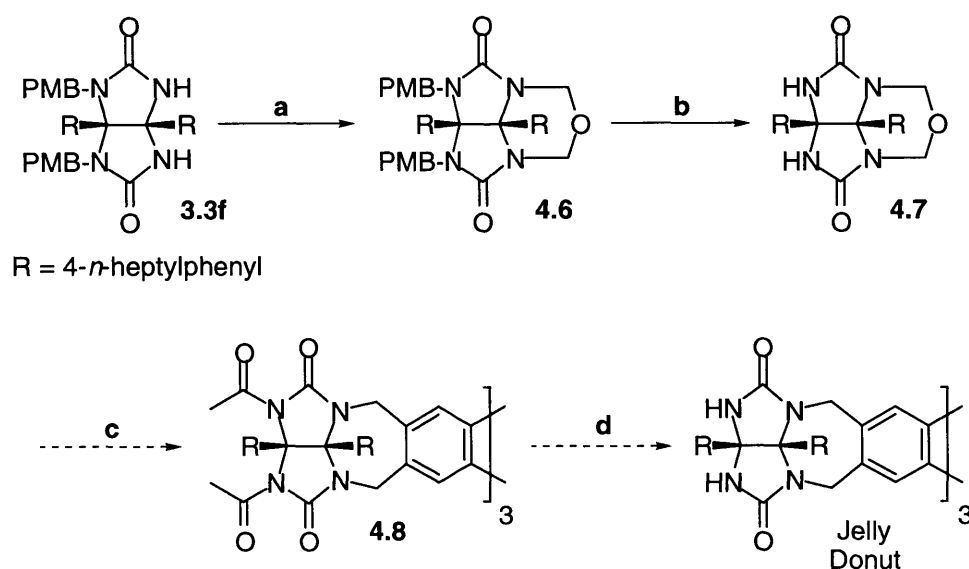


Figure 4-2. Synthesis and use of Nolte-like glycoluril modules: a) i. $(\text{CH}_2\text{O})_n$, KOH, DMSO; ii. conc. HCl, Δ ; b) CAN, CH_3CN , H_2O ; c) i. Ac_2O , TFA (1:1); ii. triphenylene, Δ ; d) KOH, MeOH.

³ Besides converting the ether to the diacetate, treatment with Ac_2O /TFA was expected to acylate the unprotected face of the glycoluril as well. We planned to remove these groups later by hydrolysis.

⁴ Mink, D. Unpublished results.

4.3 New Modules

While the Nolte-like methodology worked for the Tennis Ball, it was limited by a dependence upon electron-rich spacers. Therefore, alternative modular strategies were explored. Figure 4-3 introduces a new module **4.9** bearing a fused six-membered ring formed from the reaction of a 1,3-biselectrophile (“modular element”) with protected glycoluril **3.3**. In addition to the relative ease of formation compared to a seven-membered ring (Chapter 2), this new heterocycle should present substituents in well-defined orientations. For instance, an equatorial substituent at the 5-position could connect to suitable spacers through a single, freely-rotating bond (thereby eliminating isomer problems). Furthermore, the modular element could contribute greater size and shape diversity to the final capsules.

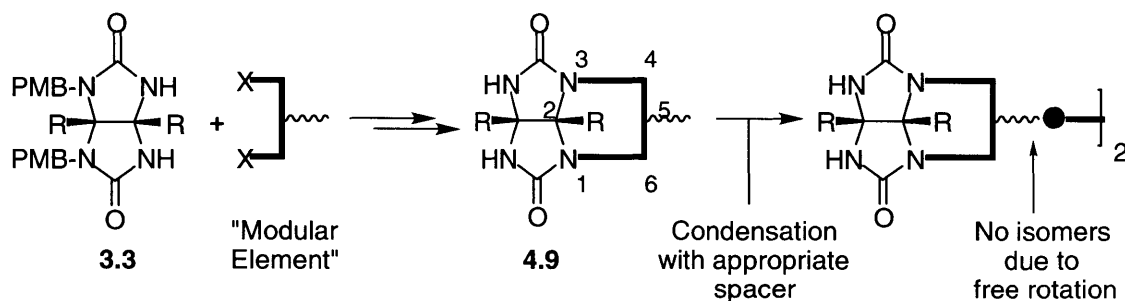


Figure 4-3. A modular strategy could provide easier syntheses, no isomers after condensation, and capsules with diverse sizes and shapes.

4.4 Hydroxyl Module

Our initial efforts focused on glycoluril module **4.15** bearing an equatorial hydroxyl group at the 5-position. Alkylation of glycoluril **3.3f**⁵ with methylal dichloride using relatively mild conditions ($\text{Cs}_2\text{CO}_3/\text{CH}_3\text{CN}$) gave **4.10** in high yield. However,

following removal of the PMB-protecting groups, Lemieux-Johnson oxidation⁶ of alkene **4.11** did not give desired ketone **4.12**. Instead, a mixture of acetals was isolated possibly due to inductive destabilization of the transitory ketone. Recently, Dave et al. reported a similar synthesis in which they found ketones at the 5-position to exist as hydrates.⁷ Although they describe a conversion to the ketone by azeotropic removal of water, we pursued an alternative route to **4.15**.

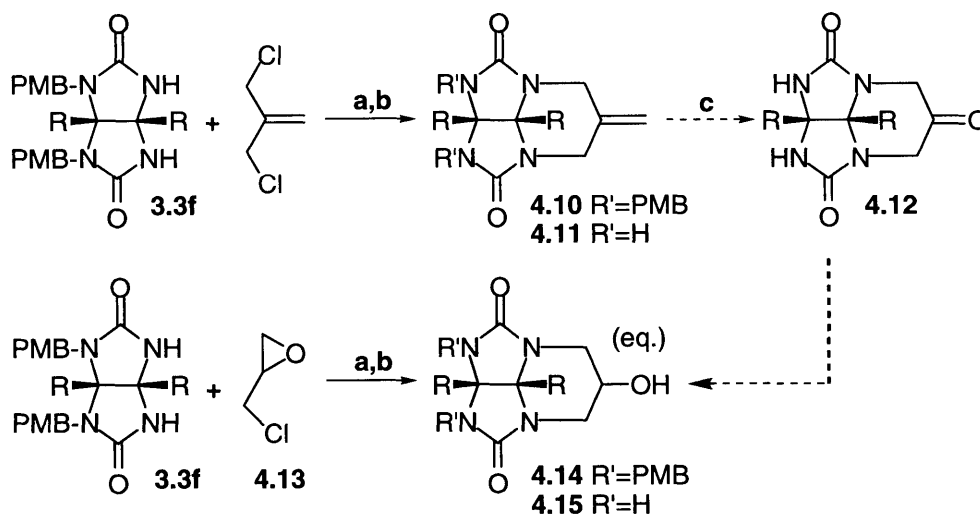


Figure 4-4. Synthesis of the hydroxyl module: a) Cs_2CO_3 , CH_3CN , reflux; b) CAN , $\text{CH}_3\text{CN}/\text{H}_2\text{O}$ (5:1); c) OsO_4 , NaIO_4 , THF , H_2O . [R = 4-*n*-heptylphenyl; PMB = *p*-methoxybenzyl.]

Substituting epichlorohydrin **4.13** for methallyl dichloride gave the PMB-protected hydroxyl module **4.14** as a mixture of equatorial and axial isomers (1:1) in high yield.⁸ Column purification provided the desired equatorial isomer which was then deprotected to give **4.15**. Unfortunately, this module exhibited poor reactivity with a

⁵ While only glycoluril **3.3f** is shown, several others were evaluated as detailed in the Experimental section.

⁶ Ireland, R.E.; Maienfisch, P. *J. Org. Chem.* **1988**, *53*, 640.

⁷ Dave, P.R.; Forohar, F.F.; Kaselj, M.; Gilardi, R.; Trivedi, N. *Tetrahedron Lett.* **1999**, *40*, 447-450.

variety of electrophilic spacers (e.g. 1,3,5-benzenetricarbonyl trichloride).⁹ The nucleophilicity of the secondary hydroxyl group in **4.15** may be reduced by steric interactions imposed by the proximal R group.

Despite these setbacks, our studies with the hydroxyl module encouraged us to continue for two reasons. First, the improved solubility of modular elements over polybrominated spacers meant that the harsh alkylation conditions used previously could be avoided. Second, the isomers produced after condensation with epichlorohydrin were easily distinguished and separated. Figure 4-5 shows the two isomers isolated following alkylation (and deprotection). Both isomers give characteristic ¹H NMR chemical shifts and splitting patterns (J_{H-H}) for the methylene protons on the fused six-membered rings. For instance, calculations¹⁰ predicted that the methylene equatorial protons on the desired isomer (Figure 4-5A) should appear downfield of the axial methylene protons as a doublet of doublet (dd). The axial protons, in contrast, should appear to be a triplet (t) or a widely-dispersed doublet of doublet. Fortunately, ¹H NMR spectra of both isomers matched neatly with our calculated expectations and made isomer assignments trivial. We anticipated that similarly substituted glycoluril modules would be structurally identified in the same way.

⁸ A collaborator, Dr. Arne Lutzen, identified epichlorohydrin as a modular element alternative and used it to synthesize hydroxyl module **4.15**.

⁹ Dr. Lutzen attempted numerous coupling reactions to no avail (unpublished results).

¹⁰ (a) Vicinal coupling constants were calculated using MacroModel v5.5; see: Mohamadi, F.; Richards, N.G.J.; Guida, W.C.; Liskamp, R.; Caulfield, C.; Chang, G.; Hendrickson, T.; Still, W.C. *J. Comput. Chem.* **1990**, *11*, 440. (b) Geminal coupling constants and relative chemical shifts were estimated according to literature values; see Pretsch, E.; Clerc, T.; Seibl, J.; Simon, W. In *Spectral Data for Structure Determination of Organic Compounds, 2nd edition (Engl. Transl. by K. Biemann)*; Fresenius, W., Huber, J.F.K., Pungor, E., Rechnitz, G.A., Simon, W., West, Th. S., Eds.; Chemical Laboratory Practice; Springer-Verlag: New York, 1989; p I-145.

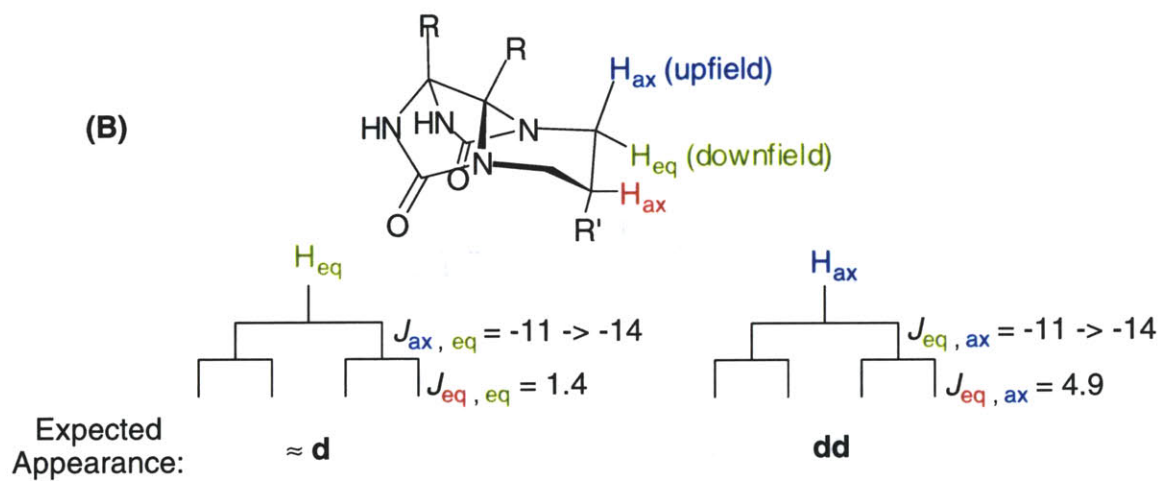
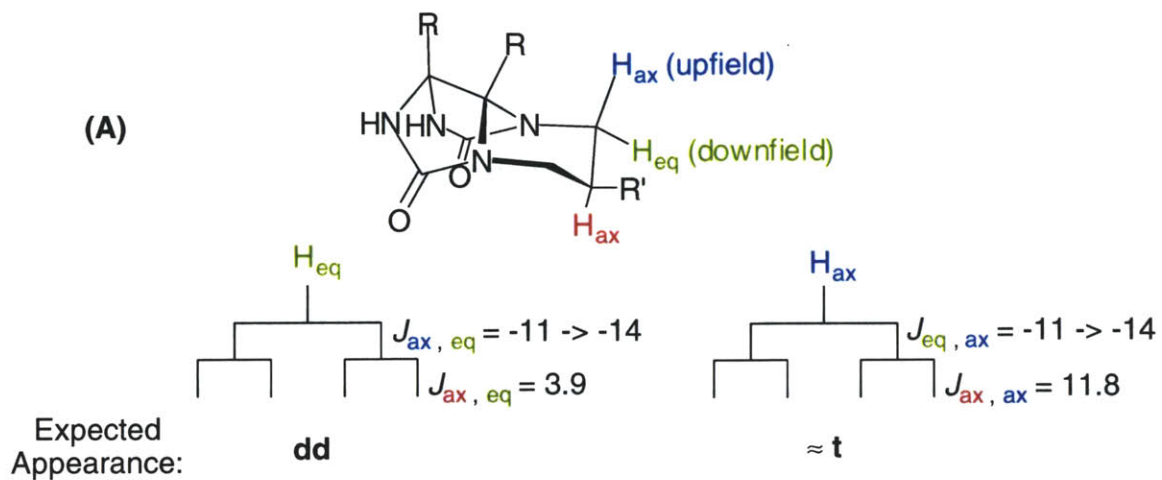


Figure 4-5. Calculated $^1\text{H} - ^1\text{H}$ coupling constants for the methylene protons on glycoluril modules similar to compound 4.15.

4.5 Acid Module

Given the low reactivity of the hydroxyl module, we designed other candidates with electrophilic or enhanced nucleophilic character. One target capable of fulfilling both roles was acid module **4.20**. Our first choice for the modular element was commercially-available acid **4.16a**. While alkylation of the glycoluril proceeded in almost quantitative yield, the geometric isomers proved resistant to separation (Figure 4-6).

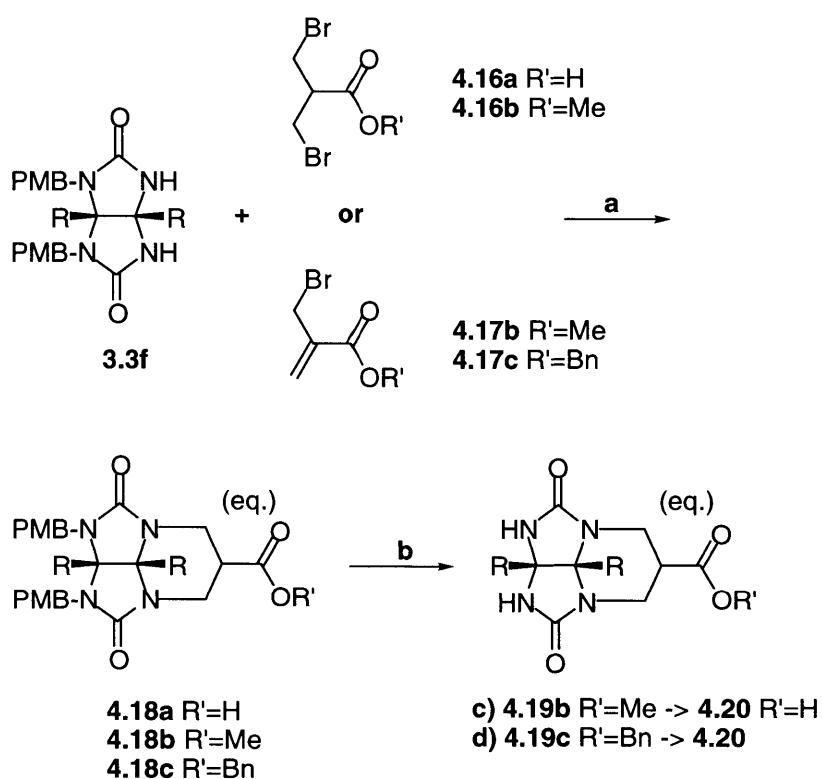


Figure 4-6. Acid module synthesis: a) CS_2CO_3 , CH_3CN , reflux; b) CAN, CH_3CN/H_2O (5:1); c) LiI, 2,6-lutidine, reflux; d) H_2 , Pd/C, EtOH.

Fortunately, replacing acid **4.16a** with modular elements **4.16b** or **4.17b** gave ester **4.18b** as a mixture of easily separable and identifiable isomers in good yield.¹¹ CAN deprotection gave **4.19b** and LiI-mediated demethylation¹² provided the equatorial acid **4.20** in high yield. The acid module was also available *via* benzyl acrylate **4.17c** which was synthesized in three steps as shown in Figure 4-7.¹³ Following alkylation and PMB-deprotection, the benzyl ester was cleaved by hydrogenolysis to give **4.20**.

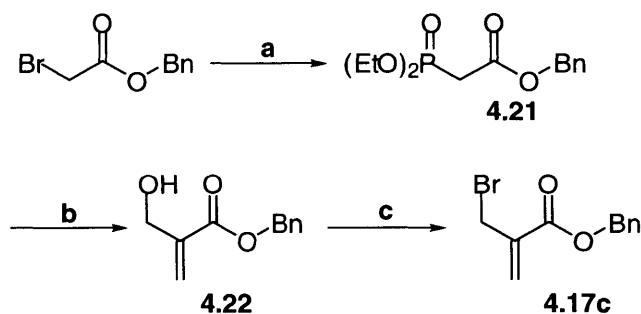


Figure 4-7. Synthesis of benzyl acrylate **4.17c**: a) $\text{P}(\text{OEt})_3$, Δ ; b) HCOH , K_2CO_3 ; c) PBr_3 , Et_2O .

¹¹ Additional **4.18b** and **4.18c** could be isolated after equilibrating their axial isomers under the alkylation conditions overnight followed by column purification.

¹² Since epimerization of the 5-position was possible, we chose demethylation conditions to prevent isomerization in the conversion of **4.19b** to **4.20**. See: Elsinger, F.; Schreiber, J.; Eschenmoser, A. *Helv. Chim. Acta* **1960**, *43*, 113-118.

¹³ The synthesis and use of benzyl acrylate **4.17c** was done in collaboration with Dr. Tomas Szabo.

4.6 Amine Module

Although hydroxyl module **4.15** proved ineffective in coupling reactions, we hoped that its amine counterpart would exhibit greater reactivity. The synthesis of the amine module **4.25** is outlined in Figure 4-8.¹⁴ Ester **4.18b** was demethylated under LiI conditions to provide acid **4.18a** and then converted to carbamate **4.23** using a modified Curtius rearrangement.¹⁵ Removal of the PMB groups followed by hydrogenolysis gave **4.25** in good overall yield.

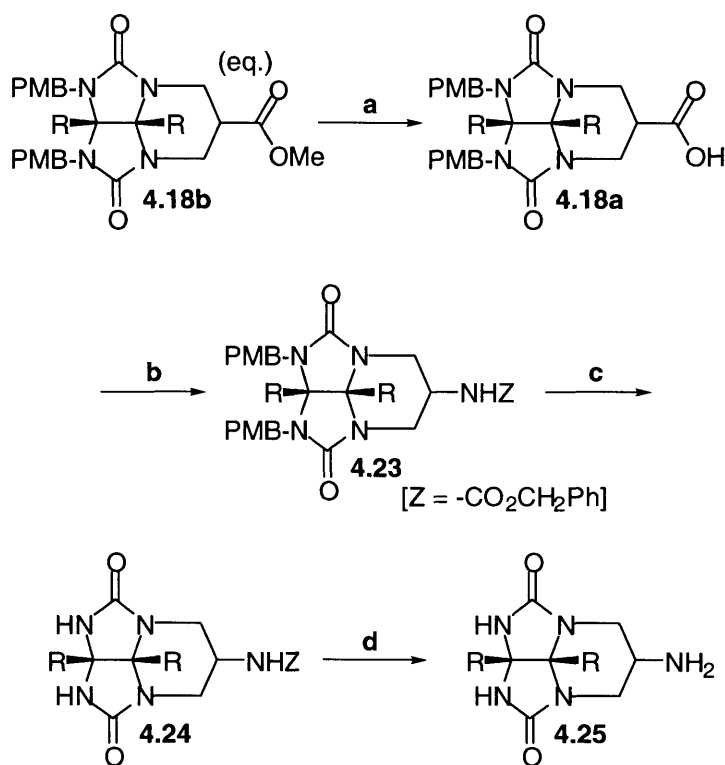


Figure 4-8. Amine module synthesis: a) LiI, 2,6-lutidine, reflux; b) i. DPPA, toluene; ii. BnOH, reflux; c) CAN, CH₃CN/H₂O (5:1); d) H₂, Pd/C, EtOH/EtOAc/AcOH (49:49:2).

¹⁴ The development of the amine module was done in collaboration with Dr. Tomas Szabo.

¹⁵ Shiori, T.; Ninomiya, K.; Yamada, S. *J. Am. Chem. Soc.* **1972**, *94*, 6203-6205.

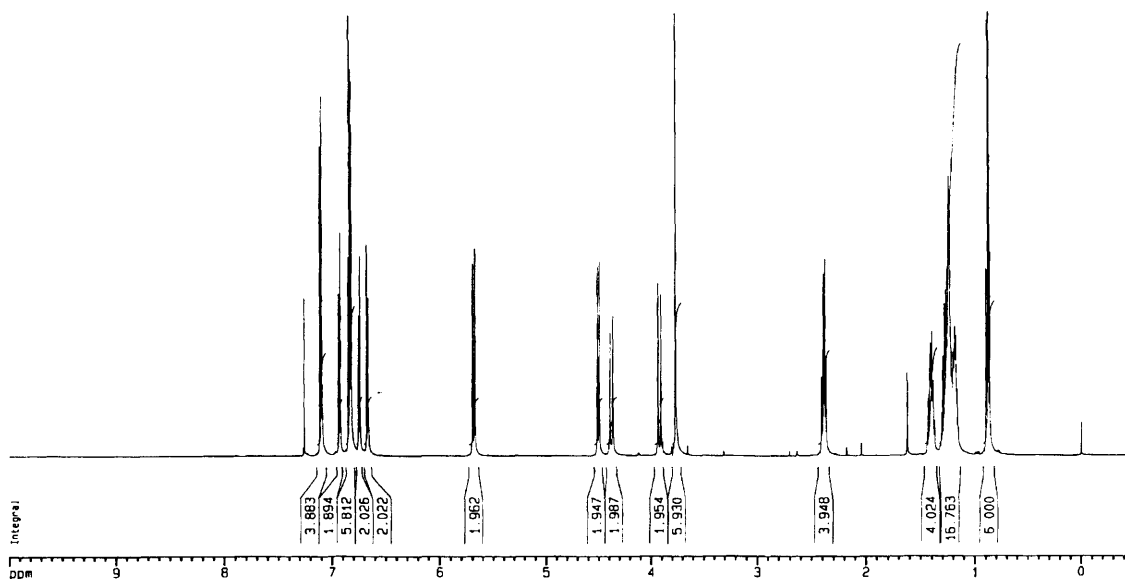
4.7 Experimental

4.7.1 Apparatus, Materials, and Methods

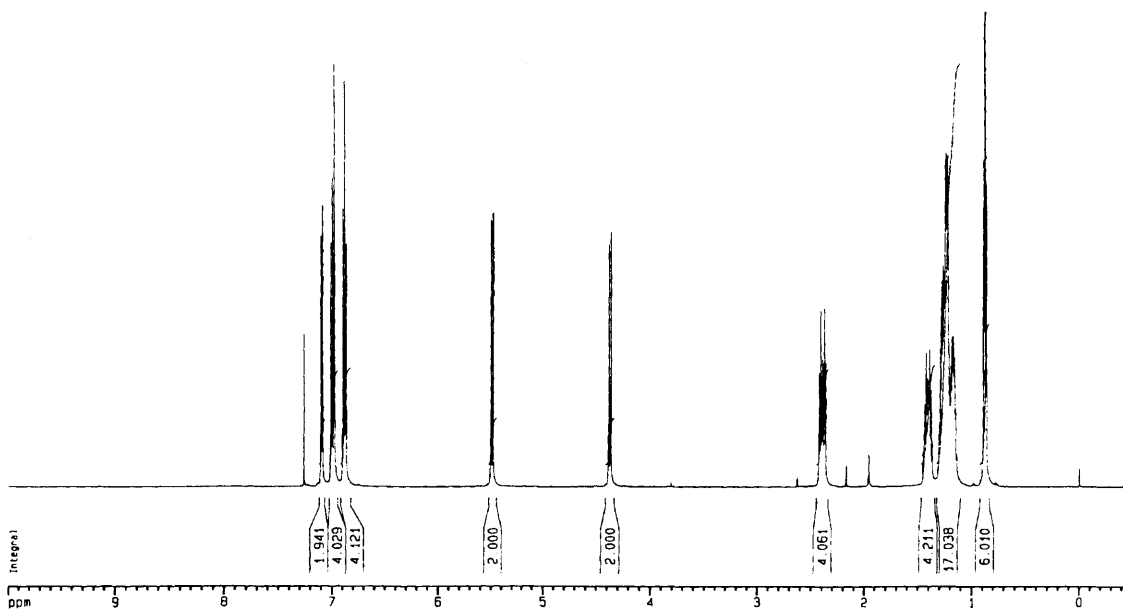
See Section 2.5.1

4.7.2 Procedures (¹H NMR spectra follow each preparation.)

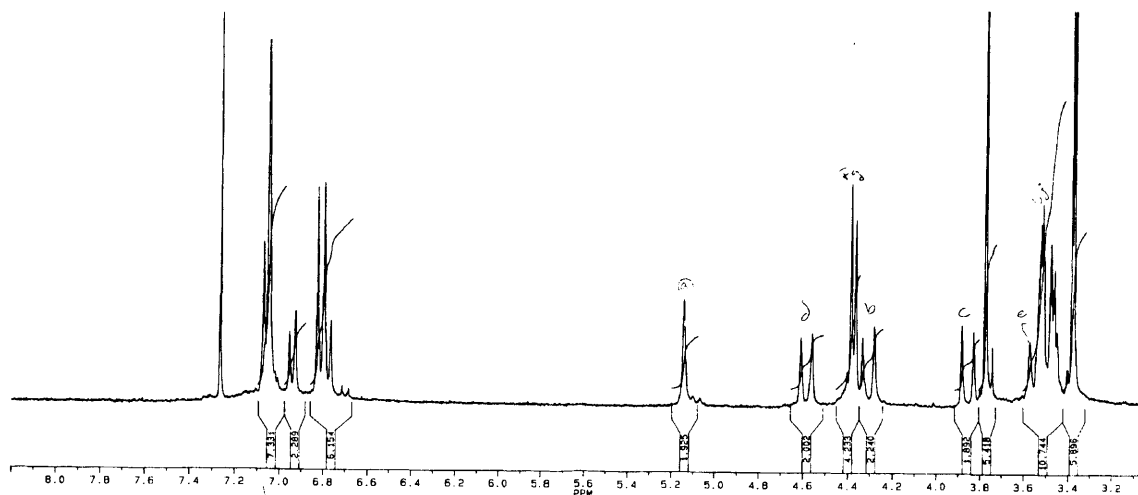
PMB-Glycoluril Ether (4.6). (R = 4-*n*-heptylphenyl) Glycoluril **3.3f** (2.500 g, 3.42 mmol) and paraformaldehyde (0.257 g, 8.55 mmol) were dissolved in 20 mL DMSO. The solution was brought to pH \approx 10 using 1 N KOH (aq.), placed under N₂, and stirred for 16 h. The pH was lowered to \approx 1 with conc. HCl, heated at 100 °C for 2 h, and then cooled. The solution was diluted with CHCl₃ (150 mL), washed with 3 x 100 mL brine, dried over Na₂SO₄, filtered, and concentrated in vacuo. Purification by flash chromatography (25 -> 30 -> 35% EtOAc in Hex) gave a white foam. Yield: 1.49 g (56%). ¹H NMR (CDCl₃, 600 MHz) δ 7.10 (d, 4Har, *J* = 8.64 Hz), 6.93 (d, 2Har, *J* = 8.24 Hz), 6.83 (m, 6Har), 6.74 (d, 2Har, *J* = 8.25 Hz), 6.67 (d, 2Har, *J* = 8.29 Hz), 5.69 (d, 2H, *J* = 10.90 Hz), 4.51 (d, 2H, *J* = 10.91 Hz), 4.38 (d, 2H, *J* = 16.22 Hz), 3.92 (d, 2H, *J* = 16.24 Hz), 3.78 (s, 6H), 2.39 (m, 4H), 1.41 (m, 4H), 1.25 (m, 16H), 0.88 (m, 6H) ppm; ¹³C NMR (CDCl₃, 600 MHz) δ 159.51, 159.01, 144.50, 144.29, 131.07, 129.70, 129.36, 129.01, 128.63, 128.44, 128.42, 127.84, 114.22, 88.73, 79.67, 72.50, 55.38, 45.89, 35.49, 35.37, 31.93, 31.91, 31.45, 31.35, 29.22, 29.14, 22.79, 22.77, 14.19, 14.18 ppm.



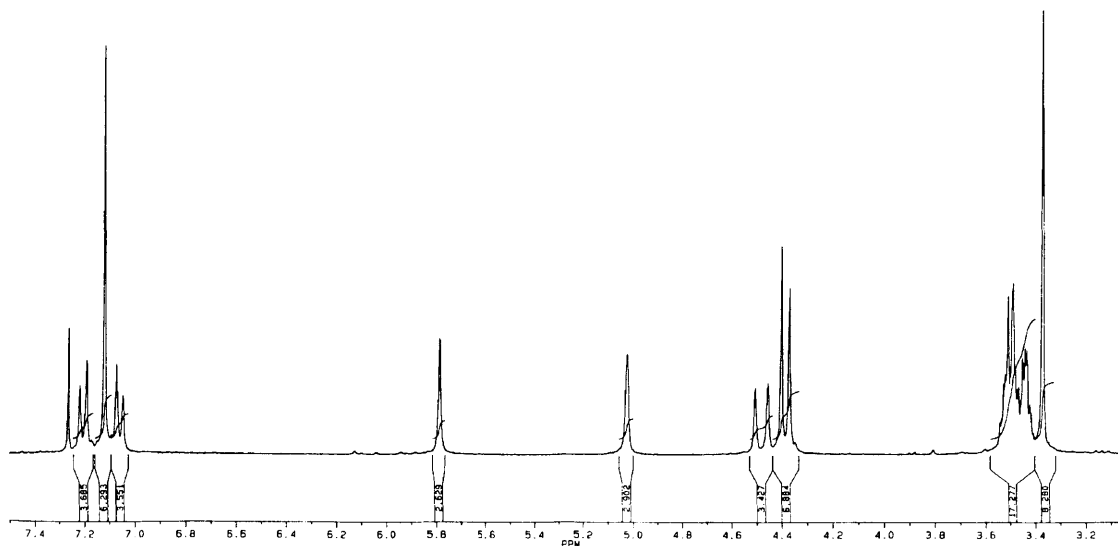
Glycoluril Ether (4.7). (R = 4-*n*-heptylphenyl) Glycoluril **4.6** (1.49 g, 1.92 mmol) was dissolved in 50 mL CH₃CN. Water (10 mL) was added followed by ≈ 3 mL THF to give a homogenous solution. CAN (10.53 g, 19.22 mmol) was added with stirring and the reaction was monitored by TLC (5% MeOH in CH₂Cl₂). After 2 h, the reaction was complete and 150 mL water was added followed by thorough sonication. Filtration and washing with water produced a white precipitate which was purified by flash chromatography (2 → 3 → 4 → 5% MeOH in CH₂Cl₂) to give a white, granular powder. Yield: 0.72 g (70%). ¹H NMR (CDCl₃, 600 MHz) δ 7.10 (d, 2H, *J* = 8.24 Hz), 7.00 (d, 2H, *J* = 8.20 Hz), 6.98 (s, 2H), 6.88 (m, 4H), 5.49 (d, 2H, *J* = 10.89 Hz), 4.37 (d, 2H, *J* = 10.94 Hz), 2.40 (m, 4H), 1.39 (m, 4H), 1.24 (m, 16H), 0.88 (m, 6H) ppm; ¹³C NMR (CDCl₃, 600 MHz) δ 159.61, 144.26, 144.13, 133.21, 130.93, 128.65, 128.36, 127.85, 127.55, 82.08, 79.16, 71.86, 35.44, 35.38, 31.93, 31.38, 31.34, 29.21, 29.15, 22.78, 14.19 ppm.



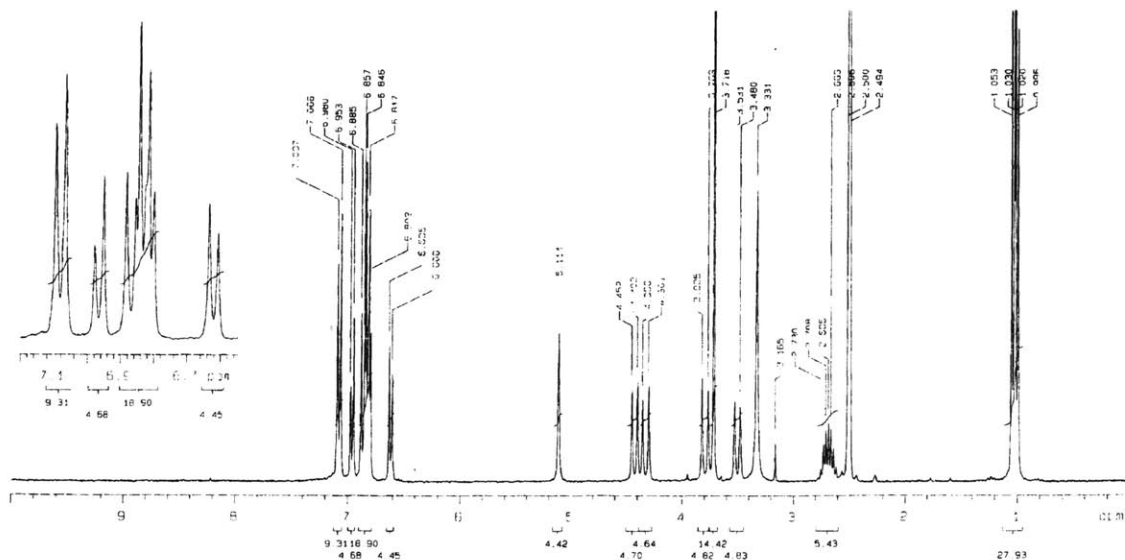
PMB-Protected Alkene (4.10a). (R = *p*-Me-C₆H₅) Under anhydrous conditions, dissolved glycoluril **3.3a** (2.00 g, 3.55 mmol) in DMSO (60 mL) with mild heating. After cooling to rt, added KO^tBu (0.80 g, 7.11 mmol) and allowed the mixture to stir for a few minutes. Methallyl dichloride (0.45 mL, 3.90 mmol) was added dropwise over 1 min and the resulting solution was stirred at rt for 1 h. The reaction mixture was then poured into a mixture of water (700 mL) and conc. HCl (100 mL) which gave a white precipitate that was collected by filtration. The precipitate was then stirred in refluxing MeOH for 30 min, cooled, and collected again by filtration to give a white powder. Yield: 0.67 g (31%). ¹H NMR (DMSO-*d*₆, 250 MHz) δ 6.94 (m, 14Har), 6.63 (d, 2Har, *J* = 8.2 Hz), 5.11 (s, 2H), 4.42 (d, 2H, *J* = 15.1 Hz), 4.27 (d, 2H, *J* = 16.6 Hz), 3.75 (m, 8H), 3.46 (d, 2H, *J* = 15.0 Hz), 2.15 (s, 3H), 2.11 (s, 3H) ppm.



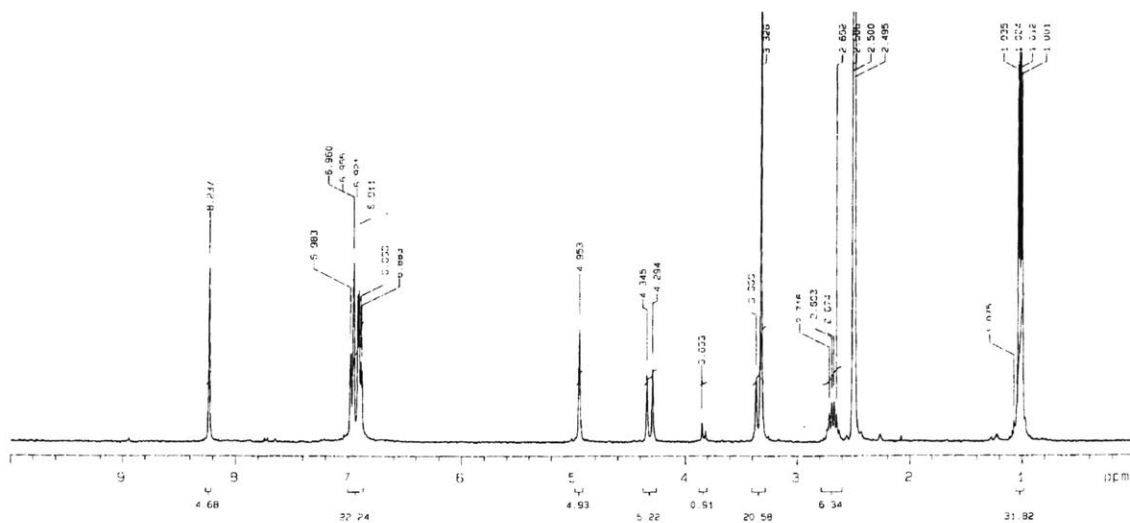
Glycoluril Alkene (4.11c). (R = $-\text{CH}_2\text{OCH}_2\text{CH}_2\text{OCH}_3$) PMB-Glycoluril **4.10c** (2.58 g, 3.38 mmol) was dissolved in a mixture of $\text{CH}_3\text{CN} / \text{H}_2\text{O}$ (5:1; 120 mL). CAN (18.56 g, 33.85 mmol) was added and the solution stirred for 4 h. The orange mixture was poured into water (200 mL) and extracted with toluene (100 mL) and CH_2Cl_2 (2 x 100 mL). The organic layers were combined and concentrated *in vacuo*. Trituration of the resulting residue with CHCl_3 left an insoluble material that was removed by filtration. The evaporated filtrate was then triturated with ether and filtered to give a white powder that was purified further by trituration with acetone. Yield: 0.64 g (36%). ^1H NMR (CDCl_3 , 300 MHz) δ 7.20 (d, 2H, $J = 8.3$ Hz), 7.12 (m, 4H), 7.06 (d, 2H, $J = 8.2$ Hz), 5.79 (s, 2H), 5.02 (s, 2H), 4.48 (d, 2H, $J = 15.2$ Hz), 4.40 (s, 2H), 4.37 (s, 2H), 3.48 (m, 10H), 3.37 (s, 3H), 3.36 (s, 3H) ppm.



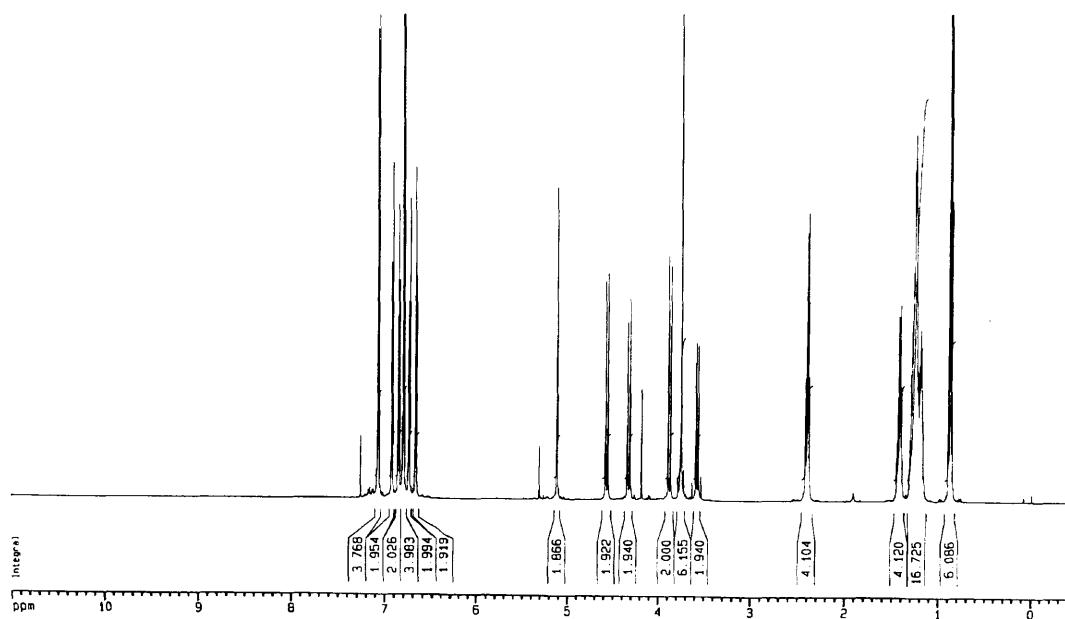
PMB-Protected Alkene (4.10e). (R = 4-isopropylphenyl) Under anhydrous conditions, glycoluril **3.3e** (4.00 g, 6.46 mmol) was dissolved in 150 mL DMSO. Solutions of KO^tBu (1.45 g, 12.93 mmol) and methallyl dichloride (823 μ L, 7.11 mmol) were prepared using 10 mL DMSO each. One half of the base solution was added to the reaction flask immediately and the remainder of both solutions was added dropwise *via* syringe pump over 2 h. After complete addition, the now cloudy mixture was allowed to stir for 3 h. The reaction mixture was poured into 1.35 N HCl solution (1.35 L), stirred for 2 minutes, then filtered. The precipitate was washed thoroughly with water, dried on the filter, and then taken up in 75 mL methanol. Refluxing the mixture for 30 m followed by cooling and filtration provided a white powder. Yield: 2.75 g (63%). ¹H NMR (DMSO-*d*₆, 300 MHz) δ 7.08 (d, 4H, J = 8.7 Hz), 6.97 (d, 2H, J = 8.1 Hz), 6.85 (m, 8H), 6.62 (d, 2H, J = 8.1 Hz), 5.11 (s, 2H), 4.43 (d, 2H, J = 15.0 Hz), 4.33 (d, 2H, J = 16.5 Hz), 3.80 (d, 2H, J = 16.8 Hz), 3.72 (s, 6H), 3.51 (d, 2H, J = 15.3 Hz), 2.69 (m, 2H), 1.02 (m, 12H) ppm.



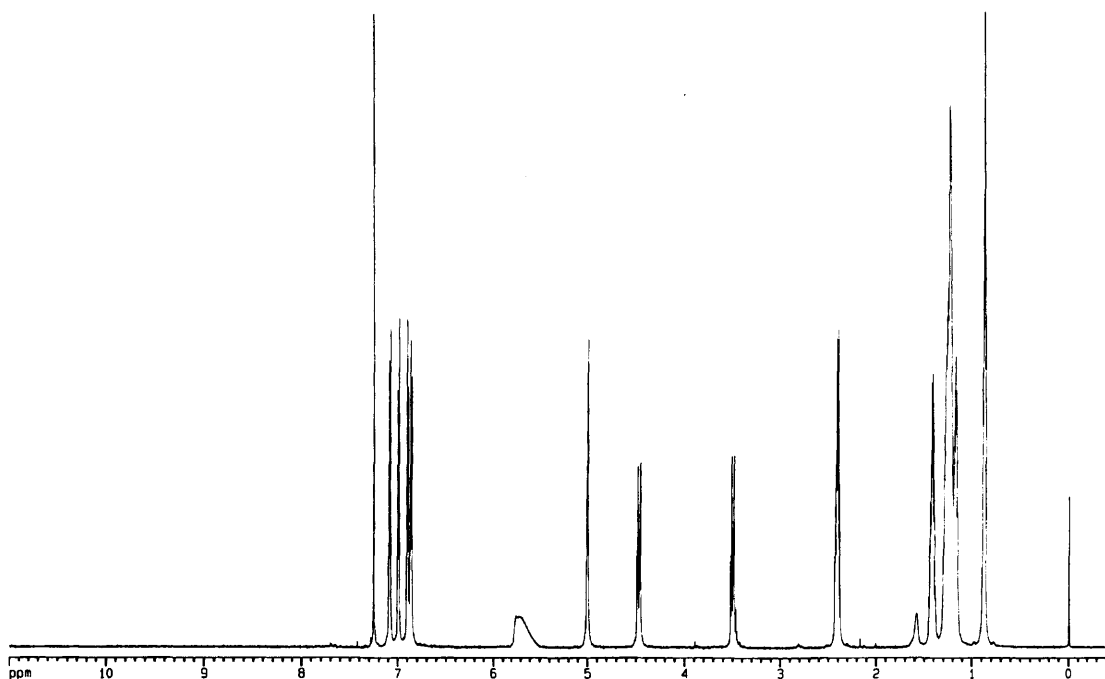
Glycoluril Alkene (4.11e). (R = 4-isopropylphenyl) The alkylated, protected glycoluril **4.10e** (3.18 g, 4.74 mmol) was dissolved in 125 mL of a CH₃CN / H₂O / THF (3.75 : 1.5: 1) solution. CAN (26.00 g, 47.42 mmol) was added and the dark orange solution was allowed to stir for 3 h. After precipitating out the crude in 1 L water and filtering, the precipitate was triturated thoroughly with diethyl ether and filtered again to give, after drying, a white powder. Yield: 1.29 g (63%). ¹H NMR (DMSO-*d*₆, 300 MHz) δ 8.24 (s, 2H), 6.92 (m, 8Har), 4.95 (s, 2H), 4.32 (d, 2H, *J* = 15.3 Hz), 3.35 (m, 2H), 2.68 (m, 2H), 1.02 (m, 12H) ppm.



PMB-Glycoluril Alkene (4.10). (R = 4-*n*-heptylphenyl) A mixture of glycoluril **3.3f** (2.50 g, 3.42 mmol), Cs₂CO₃ (2.23 g, 6.84 mmol), 45 mL CH₃CN was stirred at reflux for 30 min to give a uniform suspension. After cooling the mixture somewhat, methallyl dichloride (593 μ L, 5.13 mmol) was added dropwise over 1 min with stirring. The mixture was returned to reflux and, after 18 h, TLC indicated complete consumption of **5**. After cooling to room temperature, the reaction mixture was poured into 200 mL 1M HCl (aq.) followed by extraction with 2 x 100 mL ether. The organic layer was then washed with 2 x 100 mL H₂O, dried over Na₂SO₄, filtered, and concentrated in vacuo to give a slightly crude, white foam. Yield: 2.42 g (91%). ¹H NMR (CDCl₃, 600 MHz) δ 7.07 (d, *J* = 8.64 Hz, 4Har), 6.93 (d, *J* = 8.29 Hz, 2Har), 6.86 (d, *J* = 8.27 Hz, 2Har), 6.81 (m, 4Har), 6.75 (d, *J* = 8.27 Hz, 2Har), 6.68 (d, *J* = 8.36 Hz, 2Har), 5.12 (s, 2H), 4.58 (d, *J* = 15.20 Hz, 2H), 4.34 (d, *J* = 16.25 Hz, 2H), 3.89 (d, *J* = 16.19 Hz, 2H), 3.76 (s, 6H), 3.58 (d, *J* = 15.01 Hz, 2H), 2.41 (m, 4H), 1.42 (m, 4H), 1.25 (m, 16H), 0.88 (m, 6H) ppm.



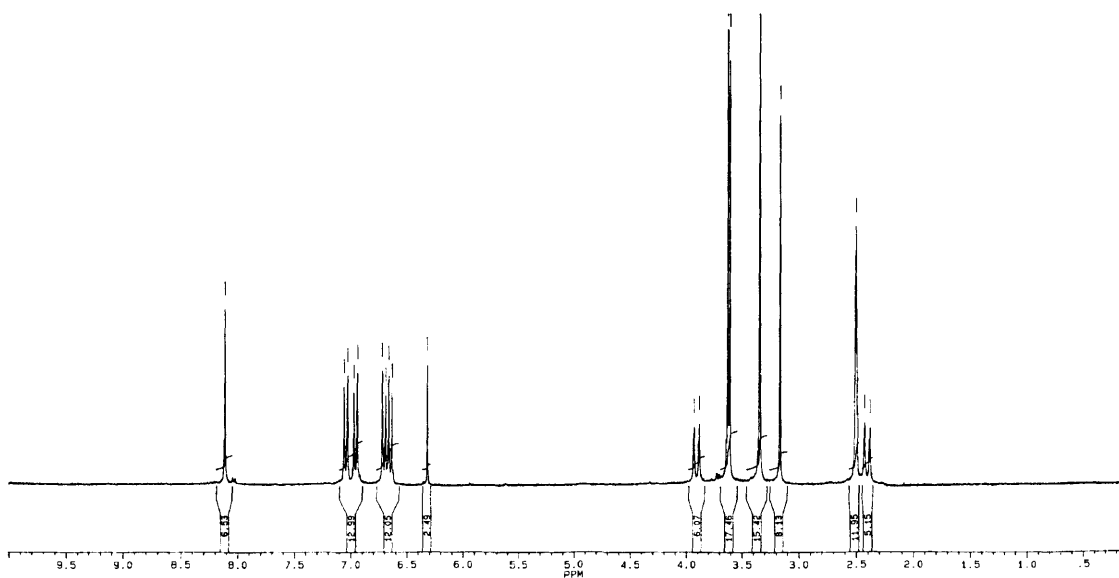
Glycoluril Alkene (4.11). (R = 4-*n*-heptylphenyl) Alkene **4.11** (2.42 g, 3.09 mmol) was dissolved in 30 mL of a mixture of CH₃CN / H₂O / THF (7 : 1.5 : 1). To this clear, colorless solution was added CAN (7.45 g, 13.59 mmol) and the yellow solution was allowed to stir overnight at room temperature. Upon pouring the reaction mixture into 200 mL H₂O, a precipitate formed which was collected by filtration. This precipitate was taken up in 100 mL CH₂Cl₂, washed with 2 x 75 mL 1N KOH (aq.), dried over Na₂SO₄, filtered, and concentrated in vacuo. The resulting residue was taken up in 75 mL of refluxing ether and a clear solution was obtained upon the addition of a few drops of MeOH. A slightly crude, white precipitate was collected after cooling by filtration. Yield: 0.93 g (56%). ¹H NMR (CDCl₃, 600 MHz) δ 7.09 (d, 2Har, *J* = 8.16 Hz), 7.00 (d, 2Har, *J* = 8.00 Hz), 6.90 (d, 2Har, *J* = 8.04 Hz), 6.87 (d, 2Har, *J* = 8.04 Hz), 5.70 (s, 2H), 5.00 (s, 2H), 4.48 (d, 2H, *J* = 14.94 Hz), 3.51 (d, 2H, *J* = 14.54 Hz), 2.41 (m, 4H), 1.42 (m, 4H), 1.24 (m, 16H), 0.88 (m, 6H) ppm.



Oxidative Cleavage¹⁶ (4.12g). (R = 4-methoxyphenyl) Alkene **4.12g¹⁷** (0.35 g, 0.86 mmol) was dissolved in 50 mL THF and 20 mL water and placed under a nitrogen atmosphere. An OsO₄ solution in water (4 wt. %; 211 μL) was added to the reaction solution and allowed to stir in the dark for 3 min. Then NaIO₄ (0.55 g, 2.59 mmol) was added and the clear, brown solution was allowed to stir in the dark until all starting material was consumed as monitored by TLC (90% CHCl₃ / 10% MeOH). After evaporating the THF, 100 mL of water was added and the precipitate was triturated thoroughly. A white precipitate was isolated by filtration and this crude was further purified by stirring in refluxing methanol for 30 minutes followed by filtration after cooling. The precipitate was dried thoroughly under vacuum to give a fine white powder. Yield: 0.25 g (65%). ¹H NMR (DMSO-*d*₆, 300 MHz) δ 8.11 (s, 2H), 7.04 (d, 2Har, *J* = 8.8 Hz), 6.96 (d, 2Har, *J* = 8.8 Hz), 6.70 (d, 2Har, *J* = 8.8 Hz), 6.64 (d, 2Har, *J* = 8.9 Hz), 6.32 (s, 1H), 3.90 (d, 2H, *J* = 13.9 Hz), 3.63 (s, 3H), 3.61 (s, 3H), 3.16 (s, 3H), 2.40 (d, 2H, *J* = 13.9 Hz) ppm; ¹³C NMR (DMSO-*d*₆, 300 MHz) δ 158.9, 158.8, 130.0, 128.8, 128.7, 126.3, 113.7, 112.8, 90.4, 81.4, 77.8, 55.0, 48.0, 44.6 ppm; HRMS (FAB) Calc'd for [M+Cs]⁺ C₂₂H₂₄N₄O₆•Cs⁺ 573.0750, found 573.0762.

¹⁶ Step c in Figure 4-4. Analytical data for this compound suggest the ketone was isolated as a methyl hemiacetal.

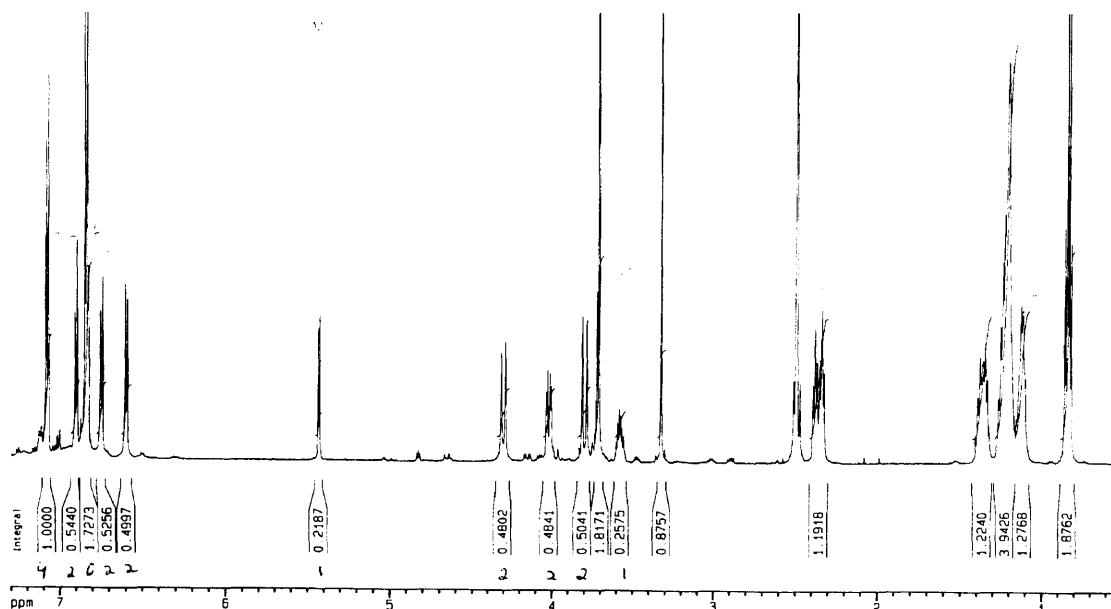
¹⁷ Synthesized by R.M. Grotzfeld by condensation of unprotected glycoluril (R = 4-methoxyphenyl) with methallyl dichloride.



PMB-Glycoluril Hydroxyl (4.14).⁸ A mixture of glycoluril **3.3f** (5.57 g, 7.6 mmol) and CsCO₃ (5.45 g, 16.72 mmol) in 100 mL of acetonitrile was heated at reflux for 30 min. Epichlorohydrin **4.13** (0.65 mL, 8.36 mmol) was then added and the mixture heated at reflux for 22 h. After cooling the reaction mixture was quenched with water and partitioned between water and dichloromethane. The layers were separated and the aqueous phase extracted with two additional portions of dichloromethane. The combined organic phase was washed with brine, dried over MgSO₄, filtered and concentrated to provide the crude product. Column chromatography (50% EtOAc/Hex) provided 1.58 g (26 %) of the axial hydroxy module and 1.88 g (31 %) of the equatorial hydroxy module.

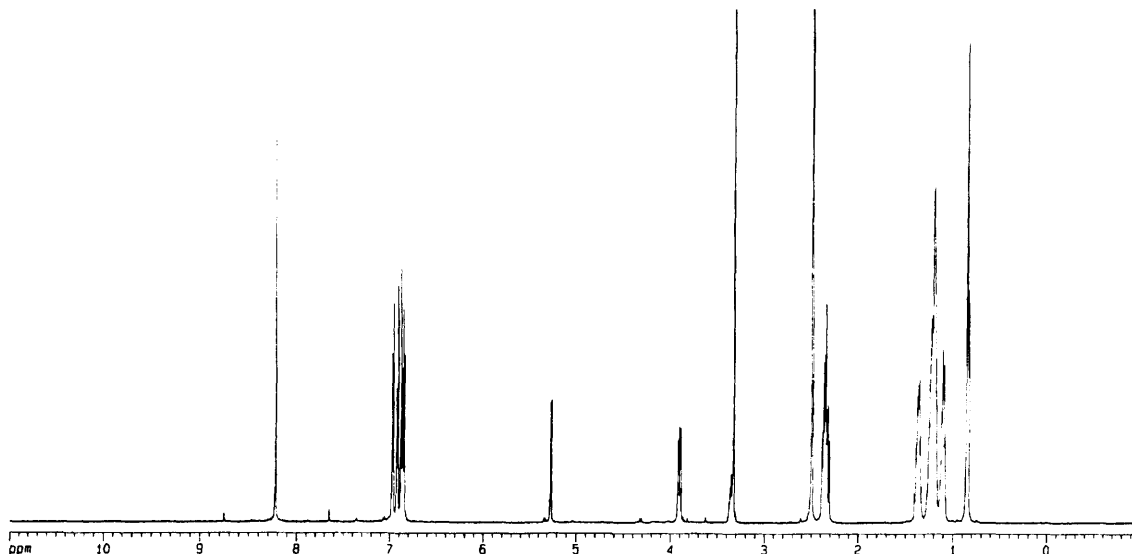
[PMB Equatorial hydroxy module **4.14**] ¹H NMR (DMSO-*d*₆, 600 MHz) δ 7.09 (d, 4Har, *J* = 8.6 Hz), 6.91 (d, 2Har, *J* = 8.2 Hz), 6.87 (m, 6Har), 6.75 (d, 2Har, *J* = 8.1 Hz), 6.60 (d, 2Har, *J* = 8.2 Hz), 5.43 (d, 1H, *J* = 5.1 Hz), 4.31 (d, 2H, *J* = 16.5 Hz), 4.02 (dd, 2H, *J* = 13.4, 5.0 Hz), 3.80 (d, 2H, *J* = 16.6), 3.73 (s, 6H), 3.60 (m, 1H), 2.49 (m [under solvent peaks], 2H), 2.39 (t, 2H, *J* = 7.5 Hz), 2.34 (t, 2H, *J* = 7.5 Hz), 1.37 (m,

4H), 1.22 (m, 12H), 1.12 (m, 4H), 0.85 (m, 6H) ppm; MS (ESI) Calc'd for C₄₉H₆₂N₄O₅ 787, found 788 [M+H]⁺ and 786 [M-H]⁻.



Hydroxyl Module (4.15).⁸ A solution of the PMB-protected equatorial hydroxy module **4.14** (1.47 g, 1.87 mmol) in CH₃CN/THF/H₂O (4:2:1) was treated with CAN (8.19 g, 14.94 mmol) and stirred at room temperature. When the starting material was consumed, the reaction mixture was concentrated and partitioned between water and dichloromethane. The layers were separated and the aqueous phase extracted with two additional portions of dichloromethane. The combined organic phase was washed with brine, dried over MgSO₄, filtered and concentrated to provide the crude product. Trituration with diethyl ether and filtration gave a white powder. Yield: 0.560 g (55 %). ¹H NMR (CDCl₃, 300 MHz) δ 8.22 (s, 2H), 6.97 (d, 2Har, *J* = 8.2 Hz), 6.92 (d, 2Har, *J* = 8.2 Hz), 6.88 (d, 2Har, *J* = 8.2 Hz), 5.26 (d, 1H, *J* = 5.1 Hz), 3.90 (dd, 2H, *J* = 13.5, 5.1 Hz), 3.45 (m, 1H), 2.35 (m, 6H), 1.36 (m, 4H), 1.21 (m, 12H), 1.11 (m, 4H), 0.85 (m, 6H) ppm; ¹³C NMR (DMSO-*d*₆, 151 MHz) δ 158.97, 142.29, 142.08, 134.57, 131.15, 128.09,

127.31, 127.25, 127.19, 81.70, 78.10, 60.74, 44.12, 40.05, 34.54, 34.49, 31.28, 30.87, 30.73, 28.52, 28.38, 28.34, 22.14, 13.95 ppm; MS (ESI) Calc'd for C₃₃H₄₆N₄O₃ 547, found 548 [M+H]⁺ and 545 [M-H]⁻.

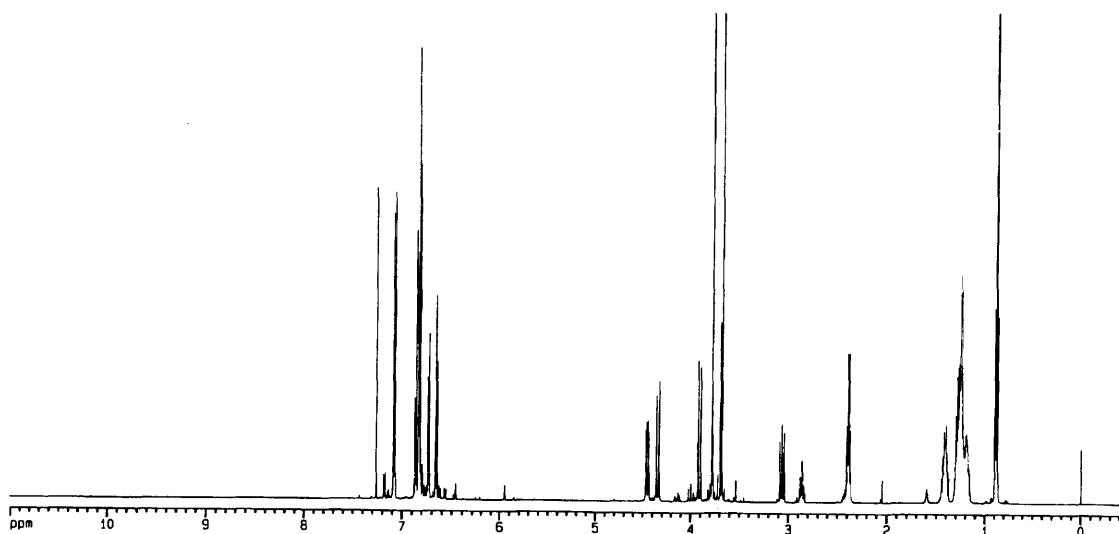


PMB-Glycoluril Methyl Ester (4.18b). Glycoluril **3.3f** (12.57 g, 17.20 mmol) and Cs₂CO₃ (23.53 g, 72.22 mmol) were mixed in 250 mL CH₃CN with vigorous stirring and mild heating to give a fine, white suspension. Methyl 2-(bromomethyl)acrylate **4.17b**¹⁸ (2.95 mL, 20.63 mmol) was added slowly with stirring over 2 minutes and then the mixture was refluxed overnight. After cooling, the mixture was poured into 300 mL of 1M HCl (aq.) and extraction was accomplished with 2 x 300 mL ether. The combined organics were washed with 2 x 200 mL 1M HCl (aq.) and 200 mL brine. The organic phase was dried over Na₂SO₄, filtered, and concentrated *in vacuo*. Purification by flash chromatography (30 -> 70% EtOAc in Hex) separated the equatorial ester isomer **4.18b**

¹⁸ Dibromide **4.16b** can be used interchangeably with acrylate **4.17b**.

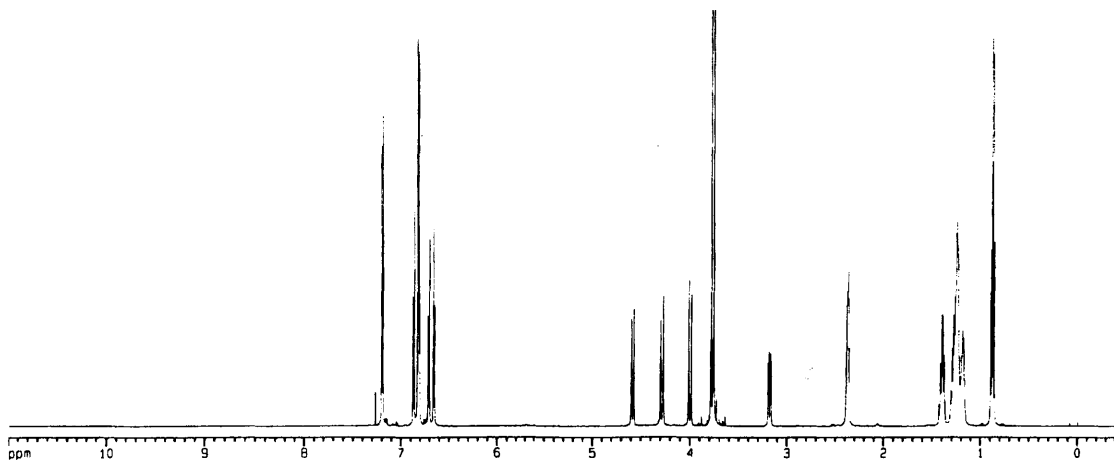
(1st spot by TLC) from the axial isomer (2nd spot). Eluent concentration gave white foams. Combined yield: 10.59 g (72%).

[Equatorial ester **4.18b**: 8.14 g (57%).] ¹H NMR (CDCl₃, 600 MHz) δ 7.08 (d, 4Har, *J* = 8.59 Hz), 6.82 (m, 8Har), 6.66 (d, 2Har, *J* = 8.29 Hz), 6.62 (d, 2Har, *J* = 8.35 Hz), 4.45 (dd, 2H, *J* = 14.33, 4.58 Hz), 4.35 (d, 2H, *J* = 16.24 Hz), 3.91 (d, 2H, *J* = 16.27 Hz), 3.78 (s, 6H), 3.68 (s, 3H), 3.07 (m, 2H), 2.87 (m, 1H), 2.40 (m, 4H), 1.41 (m, 4H), 1.24 (m, 16H), 0.88 (m, 6H) ppm; ¹³C NMR (CDCl₃, 600 MHz) δ 171.37, 159.65, 158.96, 144.38, 144.10, 130.21, 130.12, 129.48, 129.01, 128.94, 128.73, 128.42, 128.35, 127.68, 114.21, 114.06, 88.63, 80.97, 55.39, 52.24, 45.90, 40.34, 38.24, 35.52, 35.38, 31.95, 31.92, 31.47, 31.37, 29.25, 29.13, 22.79, 14.19 ppm; HRMS (FAB) Calc'd for [M+Cs]⁺ C₅₁H₆₄N₄O₆•Cs⁺ 961.3880, found 961.3915.



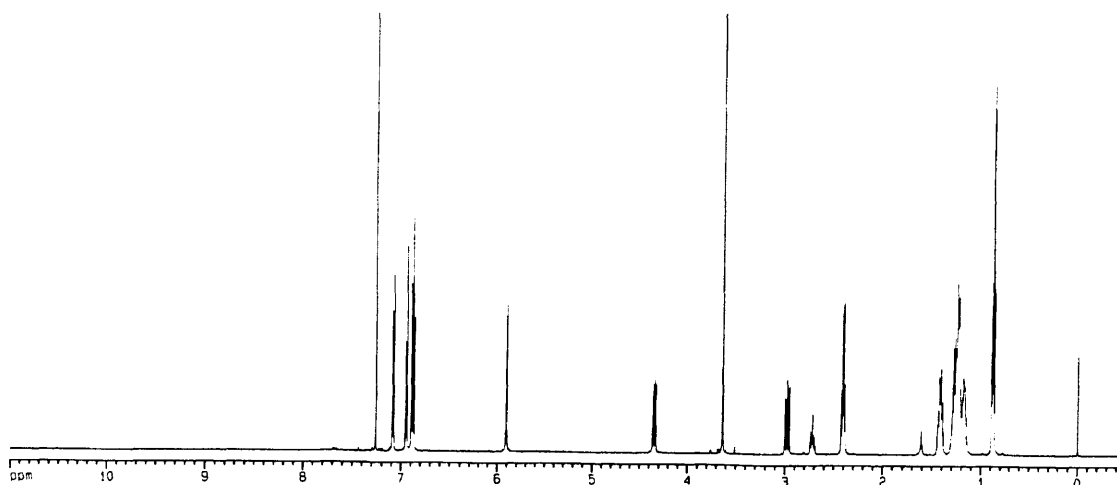
[Axial ester: 2.08 g (15%).] ¹H NMR (CDCl₃, 600 MHz) δ 7.19 (d, 4H, *J* = 8.64 Hz), 6.83 (m, 8Har), 6.71 (d, 2Har, *J* = 8.27 Hz), 6.65 (d, 2Har, *J* = 8.24 Hz), 4.59 (d, 2H, *J* = 14.20 Hz), 4.28 (d, 2H, *J* = 16.26 Hz), 4.00 (d, 2H, *J* = 16.28 Hz), 3.79 (s, 3H), 3.78 (s, 6H), 3.19 (dd, 2H, *J* = 14.68, 4.3 Hz), 2.37 (m, 5H), 1.39 (m, 4H), 1.25 (m, 16H), 0.88

(m, 6H) ppm; ^{13}C NMR (CDCl_3 , 600 MHz): δ 172.94, 159.84, 158.86, 144.06, 143.84, 130.78, 130.56, 130.18, 129.32, 128.97, 128.60, 128.21, 127.86, 113.97, 88.82, 80.66, 55.39, 52.56, 46.29, 39.44, 36.13, 35.48, 35.36, 31.95, 31.91, 31.48, 31.38, 29.26, 29.23, 29.15, 22.80, 22.78, 14.20, 14.18 ppm; HRMS (FAB) Calc'd for $[\text{M}+\text{Cs}]^+$ $\text{C}_{51}\text{H}_{64}\text{N}_4\text{O}_6 \cdot \text{Cs}^+$ 961.3880, found 961.3861.



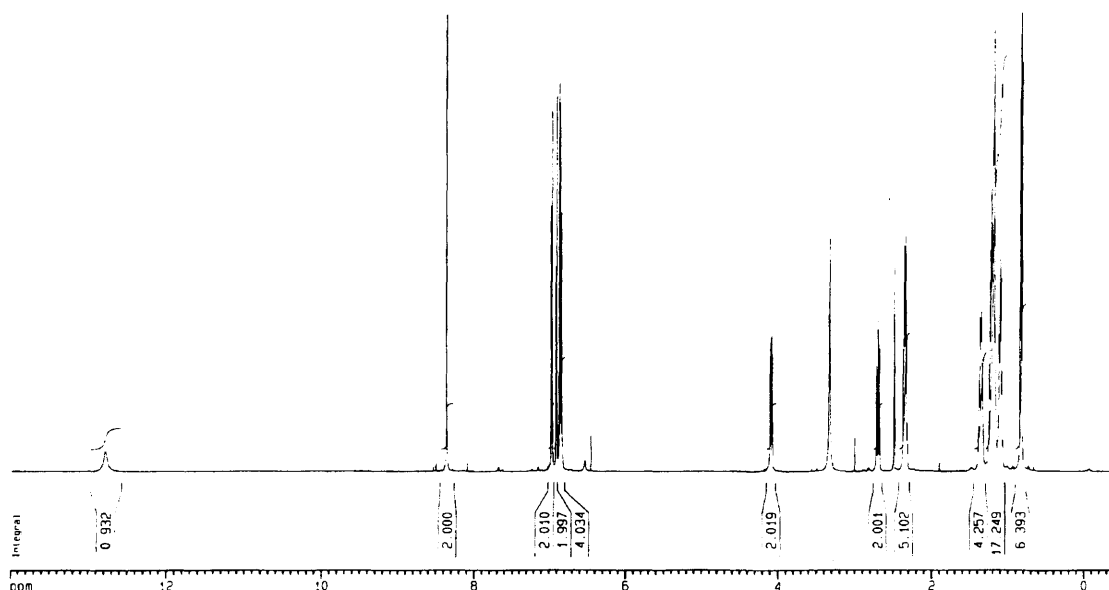
Glycoluril Methyl Ester (14.19b). Glycoluril **4.18b** (8.14 g, 9.82 mmol) was dissolved in 230 mL CH_3CN . While heating gently, water (45 mL) was added and the solution was allowed to cool to rt slowly. CAN (23.68g, 43.20 mmol) was added to the slightly cloudy solution and this mixture was allowed to stir overnight. TLC indicated complete disappearance of **7a** so the flask's contents were poured into 600 mL EtOAc. This phase was washed with 1M HCl (aq.) (3 x 100 mL), 0.5M KOH (aq.) (2 x 100 mL), saturated NaHCO_3 solution (aq.) (100 mL), and brine (2 x 100 mL). The organic phase was dried over Na_2SO_4 , filtered, and concentrated *in vacuo*. The residue was dissolved in a minimum amount of hot ether and, after refrigeration overnight, a white precipitate was collected by filtration. Yield: 1.33 g (23%). mp 160 °C; ^1H NMR (CDCl_3 , 600 MHz) δ 7.09 (d, 2Har, $J = 8.26$ Hz), 6.95 (d, 2Har, $J = 8.29$ Hz), 6.88 (m, 4Har), 5.91 (s, 2H),

4.35 (dd, 2H, $J = 14.4, 4.6$ Hz), 3.64 (s, 3H), 2.98 (m, 2H), 2.72 (m, 1H), 2.41 (m, 4H), 1.42 (m, 4H), 1.24 (m, 16H), 0.88 (m, 6H) ppm; ^{13}C NMR (CDCl_3 , 600 MHz) δ 171.20, 159.20, 144.36, 144.27, 133.37, 129.94, 128.85, 128.46, 127.68, 127.40, 83.52, 78.67, 52.22, 39.89, 37.85, 35.47, 35.39, 31.94, 31.40, 29.24, 29.22, 29.16, 29.12, 22.81, 22.79, 14.20 ppm; IR (CDCl_3) 3255.88, 2951.54, 2925.14, 2854.42, 1736.43, 1691.82, 1465.60, 1432.07 cm^{-1} ; HRMS (FAB) Calc'd for $[\text{M}+\text{H}]^+$ $\text{C}_{35}\text{H}_{48}\text{N}_4\text{O}_4$ 589.3754, found 589.3738.



Acid Module (4.20). (*via* Demethylation) Ester **4.19b** (1.30 g, 2.21 mmol) and $\text{LiI}\cdot 3\text{H}_2\text{O}$ (0.88 g, 4.42 mmol) were dissolved in 75 mL of 2,6-lutidine (Aldrich Sure-Seal) under N_2 atmosphere. The yellow solution was refluxed in the dark. After 16 h, TLC (5% $\text{MeOH}/\text{CH}_2\text{Cl}_2$) indicated complete disappearance of 11b. The mixture was cooled to room temperature, poured into 400 mL EtOAc , and washed with 4 x 200 mL 1M $\text{HCl}_{(\text{aq})}$. The organic layer was dried with Na_2SO_4 , filtered, and concentrated *in vacuo* to give an off-white foam. Yield: 1.21 g (95%). ^1H NMR (DMSO-d_6 , 600 MHz) δ 12.79 (s, 1H), 8.37 (s, 2H), 6.98 (d, 2Har, $J = 8.3$ Hz), 6.92 (d, 2Har, $J = 8.3$ Hz), 6.86 (m, 4Har), 4.10 (dd, 2H, $J = 14.2, 4.6$ Hz), 2.71 (t, 2H, $J = 13.0$ Hz), 2.36 (m, 5H), 1.37 (m, 4H), 1.20 (m, 16H), 0.84 (m, 6H) ppm; ^{13}C (DMSO-d_6 , 151 MHz) δ 172.30, 158.83,

142.61, 142.35, 134.57, 131.15, 128.30, 127.47, 127.44, 127.33, 81.70, 78.25, 37.37, 34.58, 34.51, 31.30, 31.27, 30.88, 30.73, 28.53, 28.40, 28.35, 22.13, 13.91 ppm; HRMS (FAB) Calc'd for [(M-H)+(2Cs⁺)]⁺ C₃₄H₄₅N₄O₄•Cs₂⁺ 839.1549, found 839.1520.

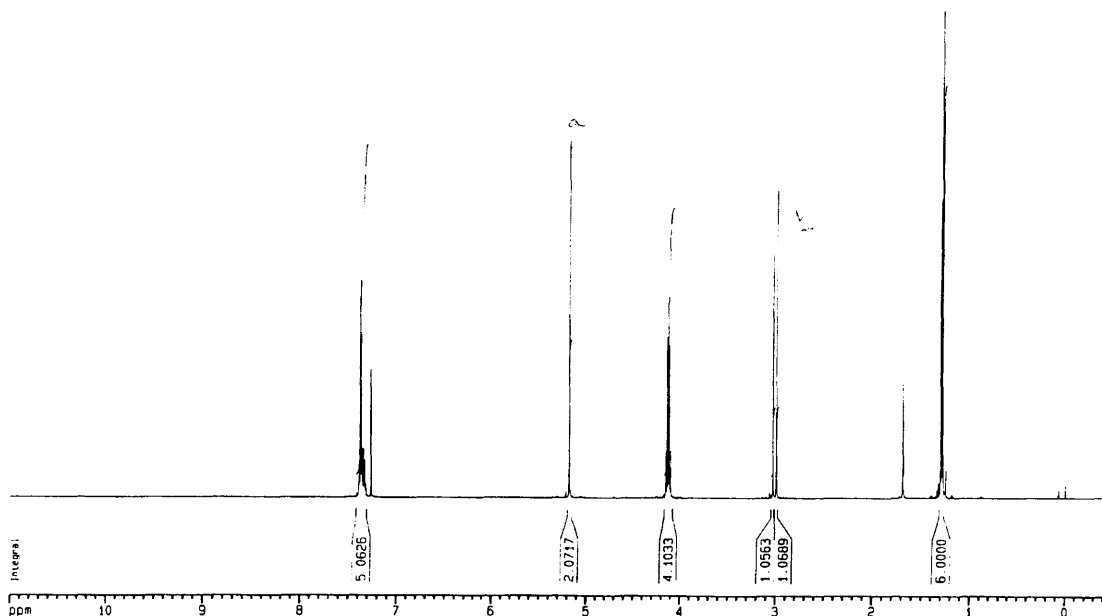


Benzyl *O,O*-diethylphosphonoacetate (4.21).¹⁹ Benzyl 2-bromoacetate (23.76 mL, 150 mmol) and triethylphosphite (28.29 mL, 165 mmol) were mixed and heated gradually to distill off ethylbromide (bp ≈ 42 °C). After the distillation was complete, the mixture was heated to 200 °C for 1 h and then allowed to cool to rt. Fractional vacuum distillation provided the crude product (bp = 130 °C, 0.1 mm Hg). Further purification was accomplished through a second distillation to give the desired product as a clear oil. Yield: 37.35 g (87%). ¹H NMR (CDCl₃, 600 MHz) δ 7.37 (m, 5H_{ar}), 5.18 (s, 2H), 4.13 (m, 4H), 3.03 (s, 1H), 3.00 (s, 1H), 1.30 (m, 6H) ppm; ¹³C NMR (CDCl₃, 151 MHz) δ 166.04 (d, J_{C,P} = 6.3 Hz), 135.628, 128.85, 128.71, 67.46, 62.90 (d, J_{C,P} = 6.2 Hz), 34.93,

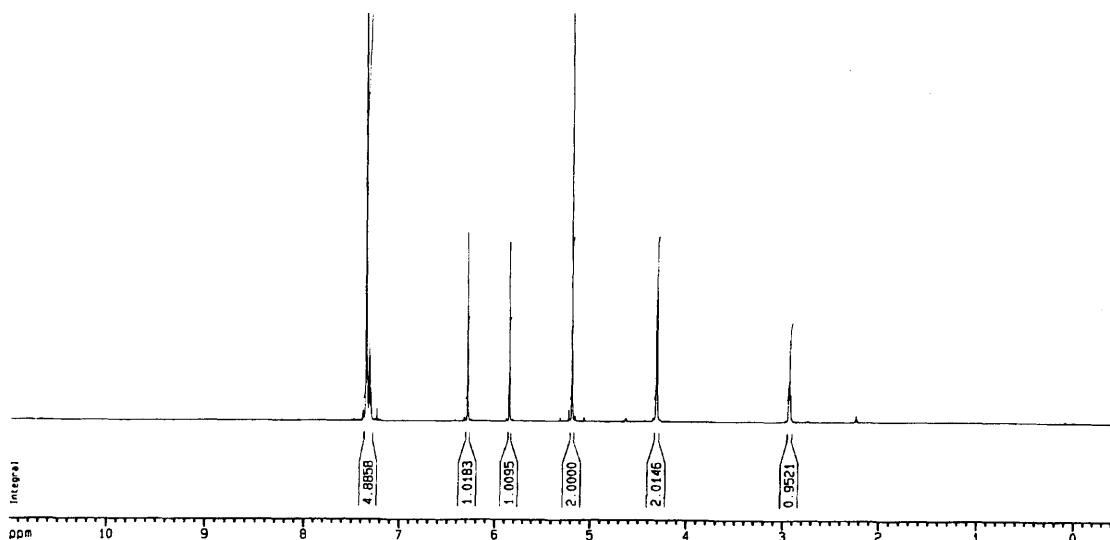
¹⁹ Martin, D.J.; Griffin, C.E. *J. Org. Chem.* **1965**, *30*, 4034-4038.

34.04, 16.36 (d, $J_{C,P} = 6.3$ Hz) ppm; ^{31}P NMR (CDCl_3 , 225 MHz) δ 20.69 (m) ppm;

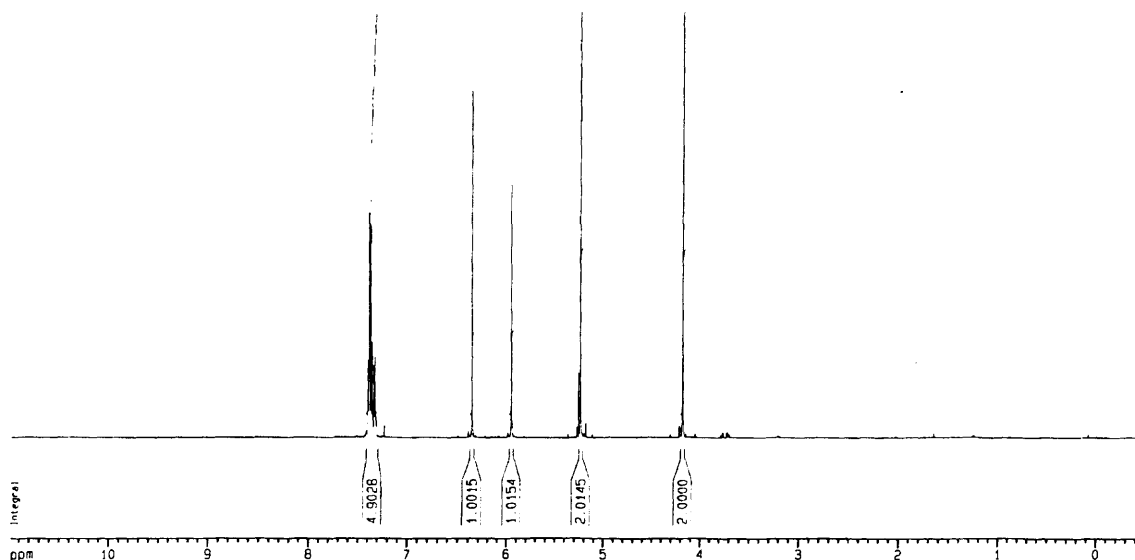
HRMS (FAB) Calc'd for $[\text{M}+\text{H}]^+$ $\text{C}_{13}\text{H}_{20}\text{O}_5\text{P}^+$ 287.1048, found 287.1041.



Benzyl 2-(hydroxymethyl)acrylate (4.22). Phosphonate **4.21** (37.35 g, 130.5 mmol) and formaldehyde [37% in H_2O] (48.90 mL, 652.4 mmol) were mixed with efficient stirring and cooled in an ice bath. A solution of K_2CO_3 (36.07 g, 260.97 mmol) in H_2O (45 mL) was added dropwise over 45 min and, after complete addition, the mixture allowed to stir at rt for 2 h. The mixture was poured into ether (300 mL) and washed with H_2O (3 x 200 mL). The organic layer was dried with Na_2SO_4 , filtered, and concentrated *in vacuo*. Flash chromatography of the residue (25% EtOAc/Hex) gave a green oil which was further purified by vacuum distillation to give a clear oil (bp = 113 °C, 0.1 mm Hg). Yield: 8.01 g (32%). ^1H NMR (CDCl_3 , 600 MHz) δ 7.32 (m, 5H), 6.29 (m, 1H), 5.85 (m, 1H), 5.19 (s, 2H), 4.32 (m, 2H), 2.94 (m, 1H) ppm; ^{13}C NMR (CDCl_3 , 151 MHz) δ 166.35, 139.59, 135.84, 128.78, 128.50, 128.28, 126.15, 66.61, 62.11 ppm; HRMS (FAB) Calc'd for $[\text{M}+\text{H}]^+$ $\text{C}_{11}\text{H}_{13}\text{O}_3^+$ 193.0865, found 193.0872.



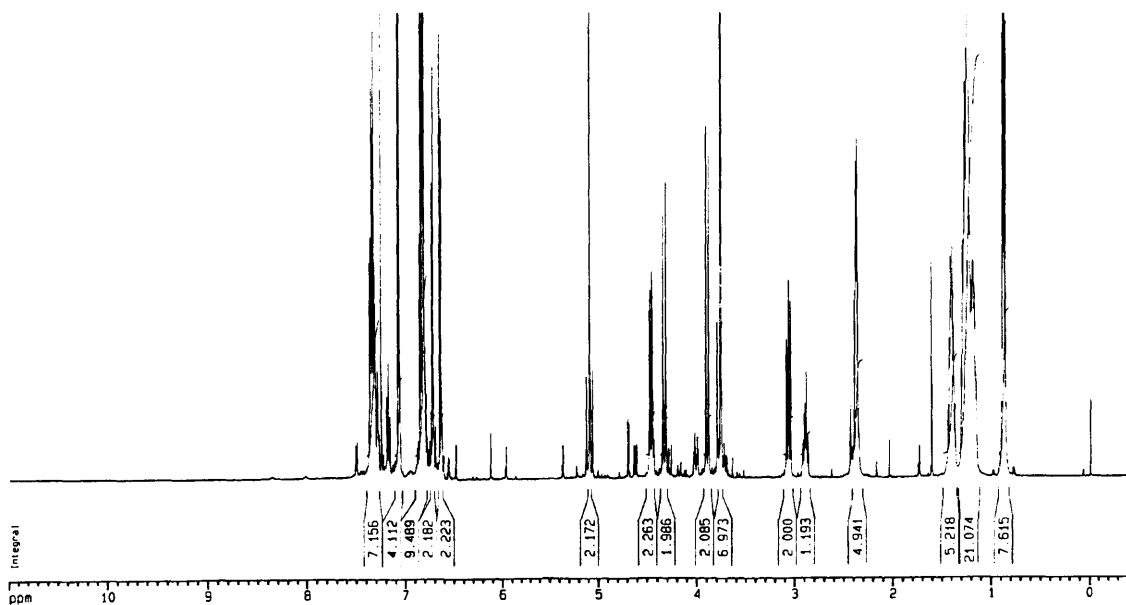
Benzyl 2-(bromomethyl)acrylate (4.17c). Under anhydrous conditions, alcohol **4.22** (8.01 g, 41.67 mmol) was dissolved in ether (50 mL) and cooled in an ice/salt bath. PBr_3 (1.98 mL, 20.84 mmol) was dissolved in ether (7 mL) and added dropwise over 5 min to the chilled reaction mixture. After complete addition, the mixture was allowed to stir at rt for 6 h. The reaction flask was cooled to 0 °C and H_2O (50 mL) was added slowly with stirring. The mixture was then diluted with hexane (150 mL) and washed with H_2O (2 x 100 mL). Drying with Na_2SO_4 , filtration, and rotary evaporation provided an oil which was purified further by flash chromatography (0-5% $\text{MeOH}/\text{CH}_2\text{Cl}_2$) to give a clear oil. Yield: 9.60 g (90%). ^1H NMR (CDCl_3 , 600 MHz) δ 7.37 (m, 5H), 6.37 (bs, 1H), 5.95 (bs, 1H), 5.24 (s, 2H), 4.18 (bs, 2H) ppm; ^{13}C NMR (CDCl_3 , 151 MHz) δ 166.35, 139.59, 135.84, 128.78, 128.50, 128.28, 126.15, 66.61, 62.11 ppm; IR (CDCl_3) 3057.26, 3033.70, 2955.13, 1724.01, 1328.23, 1306.12, 1221.23, 1174.15, 1115.41 cm^{-1} ; HRMS (FAB) Calc'd for $[\text{M}+\text{Na}]^+ \text{C}_{11}\text{H}_{11}\text{O}_2\text{Br}\cdot\text{Na}^+$ 276.9840, found 276.9831.



PMB-Glycoluril Benzyl Ester (4.18c). Glycoluril **3.3f** (11.24 g, 15.38 mmol) and Cs_2CO_3 (11.02 g, 33.83 mmol) were mixed in refluxing CH_3CN (300 mL) to produce a fine suspension. After cooling somewhat, benzyl acrylate **4.17c** (4.71 g, 18.45 mmol) dissolved in CH_3CN (10 mL) was added dropwise over 5 min. The mixture was returned to reflux overnight. After cooling to rt, the mixture was poured into ether (400 mL) and washed with 1M HCl_{aq} (300 mL) and brine (300 mL). Drying with Na_2SO_4 , filtration, and rotary evaporation gave an off-white foam. This residue was subjected to flash chromatography (25 → 40% EtOAc/Hex) to separate the equatorial ester isomer **4.18c** (1st spot by TLC) from the axial isomer (2nd spot). Each was isolated as a white foam. Combined yield: 11.06 g (75%).

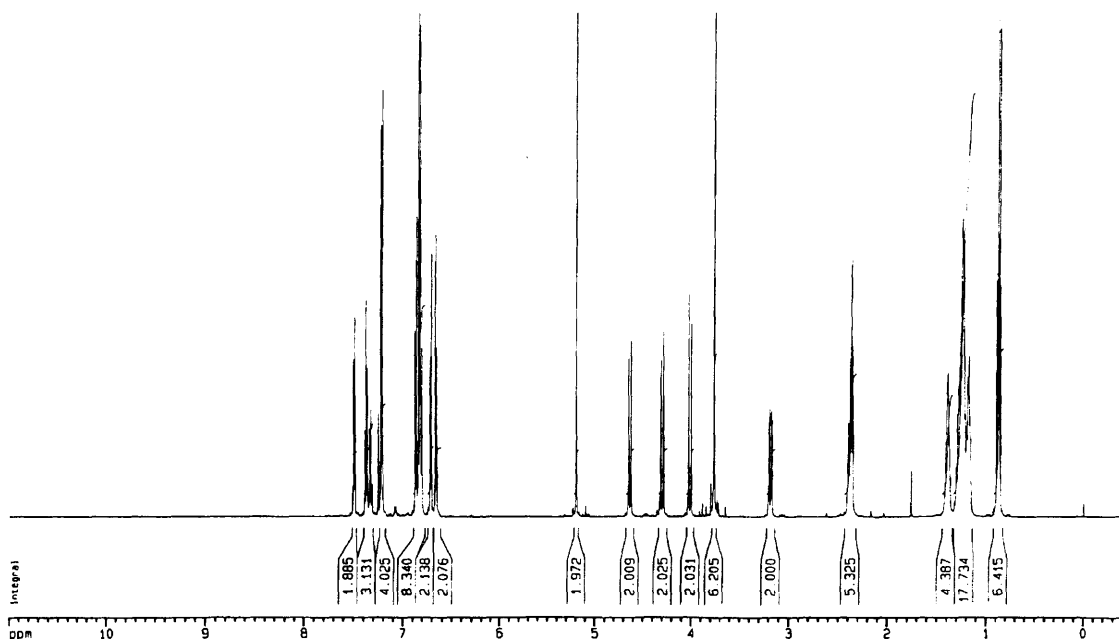
[Equatorial ester **4.18c** (slightly crude): 5.91 g (42%).] ^1H NMR (CDCl_3 , 600 MHz) δ 7.35 (m, 5Har), 7.08 (m, 4Har), 6.82 (m, 8Har), 6.73 (m, 2Har), 6.65 (m, 2Har), 5.10 (bs, 2H), 4.87 (dd, 2H, $J = 14.2, 4.7$ Hz), 4.34 (d, 2H, $J = 16.2$ Hz), 3.90 (d, 2H, $J = 16.3$ Hz), 3.77 (s, 6H), 3.08 (m, 2H), 2.89 (m, 1H), 2.38 (m, 4H), 1.41 (m, 4H), 1.24 (m, 16H), 0.88 (m, 6H) ppm; ^{13}C NMR (CDCl_3 , 151 MHz) δ 170.75, 159.65, 158.96, 144.38,

144.10, 135.52, 130.21, 130.08, 129.47, 128.96, 128.81, 128.75, 128.67, 128.42, 128.35, 127.67, 114.21, 88.65, 80.97, 67.02, 55.39, 45.90, 40.31, 38.19, 35.52, 35.38, 31.95, 31.92, 31.47, 31.37, 29.26, 29.25, 29.13, 22.80, 14.20 ppm; IR (CDCl₃) 2927.16, 2854.96, 1722.64, 1710.81, 1612.81, 1513.36, 1460.06, 1247.14, 1175.94 cm⁻¹; MS (FAB) Calc'd for [M+Cs]⁺ C₅₇H₆₈N₄O₆•Cs⁺ 1037, found 1037.



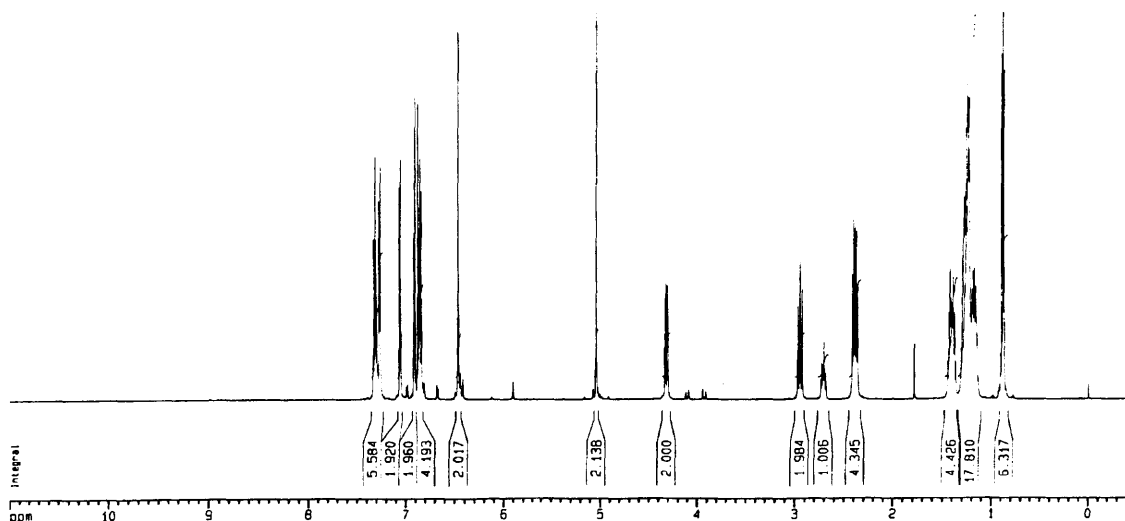
[Axial ester: 5.91 g (42%).] ¹H NMR (CDCl₃, 600 MHz) δ 7.50 (m, 2Har), 7.36 (m, 3Har), 7.22 (d, 4Har, *J* = 8.6 Hz), 6.85 (m, 8Har), 6.72 (d, 2Har, *J* = 8.3 Hz), 6.67 (d, 2Har, *J* = 8.3 Hz), 5.20 (s, 2H), 4.64 (d, 2H, *J* = 14.1 Hz), 4.31 (d, 2H, *J* = 16.3 Hz), 4.02 (d, 2H, *J* = 16.3 Hz), 3.77 (s, 6H), 3.19 (dd, 2H, *J* = 14.6, 4.3 Hz), 2.39 (m, 5H), 1.40 (m, 4H), 1.25 (m, 16H), 0.88 (m, 6H) ppm; ¹³C NMR (CDCl₃, 151 MHz) δ 172.32, 159.87, 158.84, 144.05, 143.83, 136.01, 130.72, 130.54, 129.27, 129.25, 128.93, 128.82, 128.61, 128.59, 128.20, 127.81, 113.96, 88.82, 80.66, 67.54, 55.36, 46.25, 39.45, 36.21, 35.45, 35.34, 31.92, 31.88, 31.44, 31.36, 29.23, 29.20, 29.13, 22.77, 22.75, 14.17, 14.15 ppm; IR (CDCl₃) 2927.04, 2855.03, 1735.84, 1710.15, 1612.81, 1513.21, 1458.05, 1417.67,

1284.28, 1246.83, 1175.69 cm^{-1} ; HRMS (FAB) Calc'd for $[\text{M}+\text{Cs}]^+ \text{C}_{57}\text{H}_{68}\text{N}_4\text{O}_6 \cdot \text{Cs}^+$
1037.4193, found 1037.4248.



Glycoluril Benzyl Ester (4.19c). Glycoluril **4.18c** (5.91 g, 6.52 mmol) was dissolved in $\text{CH}_3\text{CN}/\text{H}_2\text{O}$ (275 mL, 5:1) with heating. After the solution had returned to rt, added CAN (14.32 g, 26.12 mmol) and let stir overnight. The solution was poured into CH_2Cl_2 (300 mL), washed with H_2O (3 x 200 mL), and dried with Na_2SO_4 . After filtration and concentration *in vacuo*, the brown residue was subjected to flash chromatography (50 -> 70% EtOAc/Hex) to give a white powder. Yield: 2.64 g (61%). ^1H NMR (CDCl_3 , 600 MHz) δ 7.28 (m, 5Har), 7.06 (d, 2Har, $J = 8.1$ Hz), 6.91 (d, 2Har, $J = 8.2$ Hz), 6.86 (m, 4Har), 6.47 (s, 2H), 5.05 (bs, 2H), 4.32 (dd, 2H, $J = 14.2, 4.5$ Hz), 2.93 (m, 2H), 2.71 (m, 1H), 2.39 (m, 4H), 1.26 (m, 16H), 0.89 (m, 6H) ppm; ^{13}C NMR (CDCl_3 , 151 MHz) δ 170.62, 159.50, 144.14, 144.12, 135.47, 133.46, 130.01, 128.89, 128.80, 128.76, 128.72, 128.57, 128.32, 127.67, 127.44, 83.42, 78.84, 66.93, 39.79, 37.80, 35.46, 35.38, 31.93, 31.38, 31.36, 29.21, 29.16, 29.14, 22.78, 14.19 ppm; IR

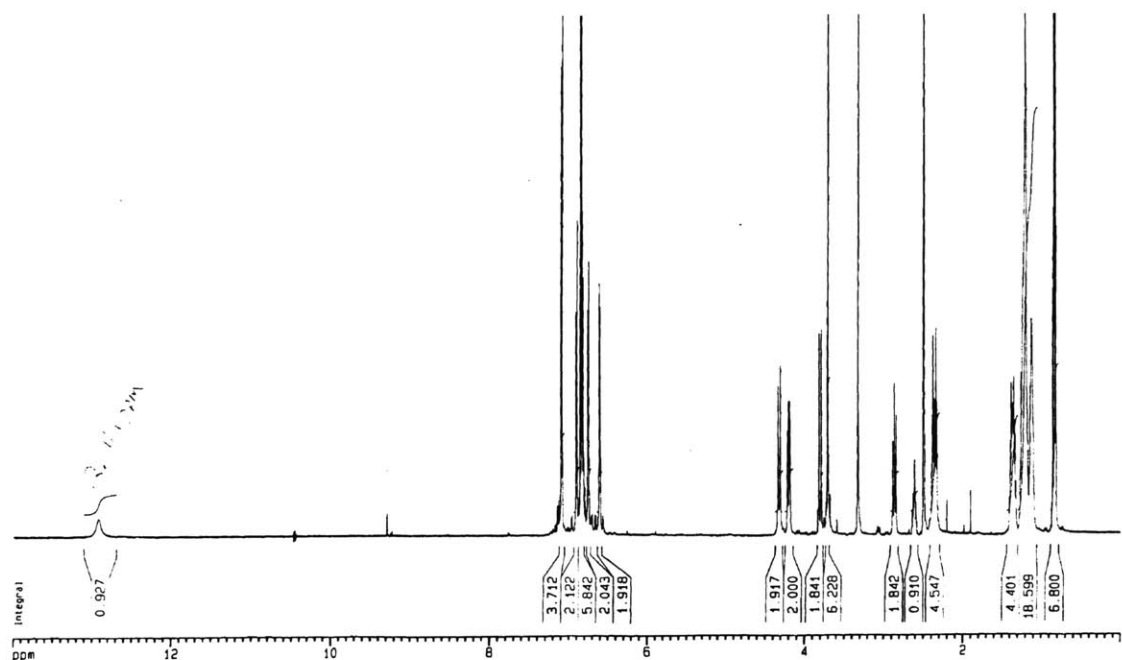
(CDCl₃) 3258.19, 2926.24, 2854.85, 1734.66, 1696.24, 1465.30, 1381.65, 1161.71 cm⁻¹;
HRMS (FAB) Calc'd for [M+H]⁺ C₄₁H₅₃N₄O₄⁺ 665.4067, found 665.4041.



Acid Module (4.20). (*via* Hydrogenolysis) Ester **4.19c** (2.54 g, 3.82 mmol) and 5% palladium on carbon (0.25 g) were mixed in EtOH (75 mL). After removal of air, the mixture was stirred under H₂ (1atm) for 3 h, filtered through celite, and the filtrate evaporated to give a white powder. Yield: 2.19 g (>99%). See demethylation method for characterization data.

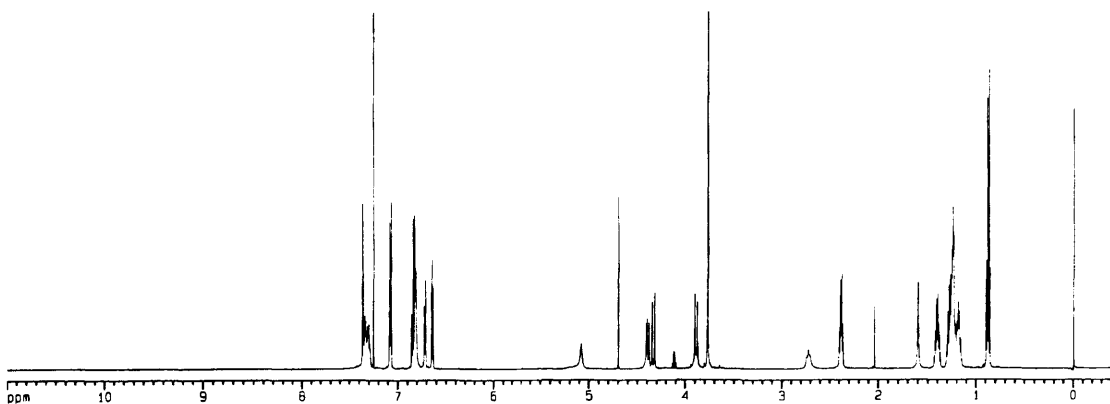
PMB-Glycoluril Acid 4.18a. Ester **4.18b** (5.55 g, 6.69 mmol) and LiI·3H₂O (2.52 g, 13.39 mmol) were dissolved in 150 mL of 2,6-lutidine (Aldrich Sure-Seal) under N₂ atmosphere. After 16 h, TLC (50 EtOAc/Hex) indicated complete disappearance of 10b. The mixture was cooled to room temperature, poured into 400 mL EtOAc, and washed with 4 x 200 mL 1M HCl_(aq.). The organic layer was dried with Na₂SO₄, filtered, and concentrated *in vacuo*. The residue was further purified by flash chromatography (10% MeOH/CH₂Cl₂) to give an off-white foam. Yield: 4.66 g (85%). ¹H NMR (DMSO-d₆, 600 MHz) δ 12.92 (s, 1H), 7.10 (d, 4Har, *J* = 8.6 Hz), 6.91 (d, 2Har, *J* = 8.2 Hz), 6.86 (d, 4Har, *J* = 8.7 Hz), 6.83 (d, 2Har, *J* = 8.2 Hz), 6.76 (d, 2Har, *J* = 8.1 Hz), 6.10 (d,

2Har, $J = 8.2$ Hz), 4.33 (d, 2H, $J = 16.6$ Hz), 4.21 (dd, 2H, $J = 14.0, 4.5$ Hz), 3.81 (d, 2H, $J = 16.6$ Hz), 3.72 (s, 6H), 2.87 (t, 2H, $J = 13.0$ Hz), 2.61 (m, 1H), 2.38 (t, 2H, $J = 7.6$ Hz), 2.35 (t, 2H, $J = 7.6$ Hz), 1.37 (m, 4H), 1.17 (m, 16H), 0.85 (m, 6H) ppm; ^{13}C (DMSO- d_6 , 151 MHz) δ 171.86, 158.70, 158.23, 143.42, 143.14, 130.32, 129.97, 129.55, 128.49, 128.20, 128.06, 127.98, 127.23, 113.78, 87.54, 55.02, 44.55, 37.55, 34.61, 34.44, 31.29, 31.24, 30.77, 30.67, 28.55, 28.50, 28.47, 28.38, 22.14, 22.09, 13.92, 13.88 ppm; IR (CDCl $_3$) 3435.49, 2926.78, 2854.85, 1722.68, 1715.10, 1612.84, 1513.41, 1465.89, 1246.94, 1177.69, 889.34 cm^{-1} ; HRMS (FAB) Calc'd for $[\text{M}+\text{Cs}]^+ \text{C}_{50}\text{H}_{62}\text{N}_4\text{O}_6 \cdot \text{Cs}^+$ 947.3724, found 947.3691.



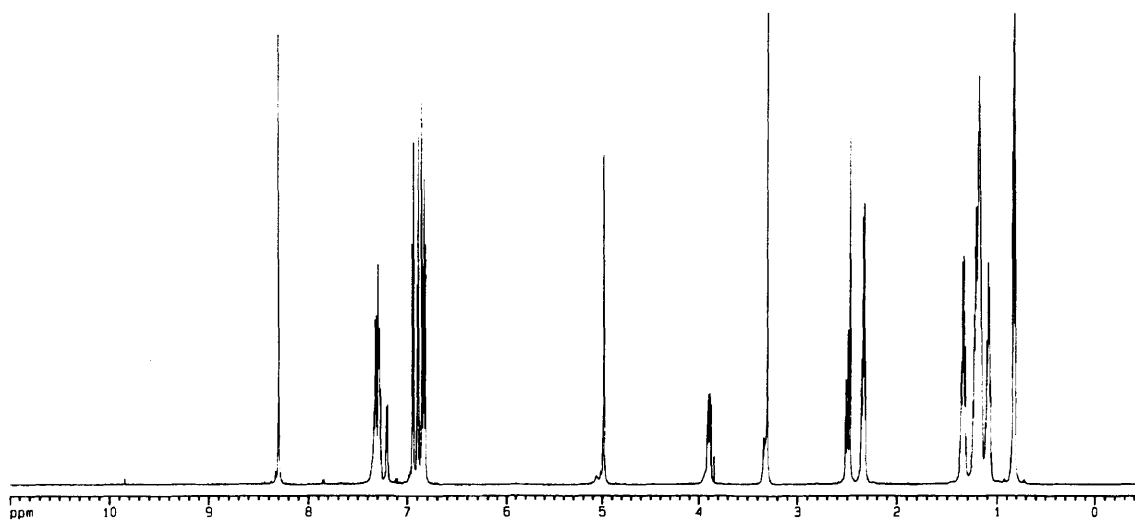
PMB-Glycoluril Carbamate (4.23). Under anhydrous conditions, acid **4.18a** (4.63 g, 5.68 mmol), DPPA (1.47 mL, 6.82 mmol), and triethylamine (0.95 mL, 6.82 mmol) were mixed in dry toluene (60 mL) under N_2 for 30 min at 25 °C. Benzyl alcohol (0.82 mL, 7.95 mmol) was added and the mixture refluxed for 4 h. After cooling, the mixture was concentrated *in vacuo* to a brown residue which was triturated with EtOAc

and filtered to provide a clear oil after rotary evaporation of the filtrate. Flash chromatography (35% EtOAc/Hex) gave an off-white foam. Yield: 4.13 g (79%). ^1H NMR (CDCl_3 , 600 MHz) δ 7.35 (m, 5Har), 7.08 (d, 4Har, $J = 8.6$ Hz), 6.84 (m, 8Har), 6.72 (d, 2Har, $J = 8.2$ Hz), 6.64 (d, 2Har, $J = 6.64$ Hz), 5.08 (s, 2H), 4.70 (s, 1H), 4.40 (dd, 2H, $J = 13.7, 5.2$ Hz), 4.34 (d, 2H, $J = 16.23$ Hz), 3.89 (m, 3H), 3.77 (s, 6H), 2.73 (t, 2H, $J = 11$ Hz), 2.38 (m, 4H), 1.40 (m, 4H), 1.24 (m, 16H), 0.89 (m, 6H) ppm; ^{13}C NMR (CDCl_3 , 151 MHz) δ 159.62, 158.96, 155.49, 144.37, 144.13, 136.43, 130.23, 130.03, 129.55, 128.97, 128.89, 128.78, 128.54, 128.40, 127.98, 127.72, 127.30, 114.24, 88.61, 80.73, 67.24, 65.61, 55.41, 45.93, 43.69, 43.64, 42.96, 42.94, 35.52, 35.39, 31.95, 31.93, 31.47, 31.37, 29.25, 29.15, 22.80, 14.19 ppm; IR (CDCl_3) 2951.54, 2926.51, 2854.51, 1722.64, 1709.48, 1513.12, 1462.15, 1440.88, 1417.11, 1302.31, 1245.83, 1177.61, 1034.78, 890.44, 775.25 cm^{-1} ; HRMS (FAB) Calc'd for $[\text{M}+\text{Cs}]^+ \text{C}_{57}\text{H}_{69}\text{N}_5\text{O}_6 \cdot \text{Cs}^+$ 1052.4302, found 1052.4342.

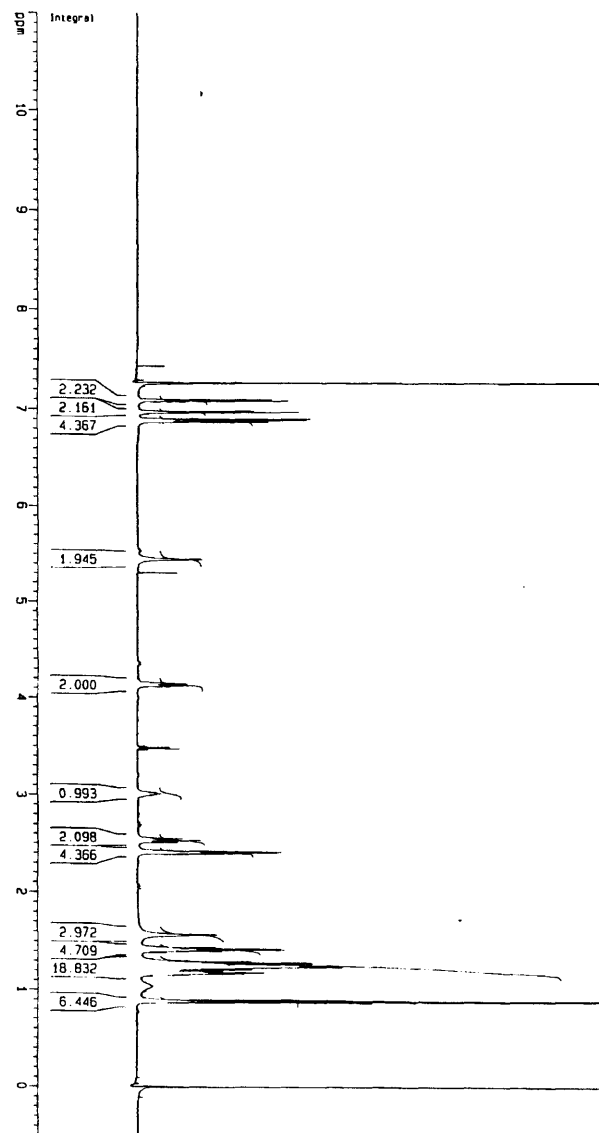


Glycoluril Carbamate (4.24). Carbamate **4.23** (6.97 g, 7.58 mmol) was dissolved in 250 mL CH_3CN . Water (50 mL) was added slowly and the temperature maintained at 25 $^\circ\text{C}$ by use of a heat gun. To the clear solution was added CAN (18.28 g, 33.35 mmol) and the resulting orange solution was covered from light and stirred under

N₂ for 16 h without additional heating. The reaction mixture was poured into 1 M HCl_{aq} and then extracted with 400 mL EtOAc. The organic layer was washed again with 2 x 300 mL 1M HCl_{aq}, dried with Na₂SO₄, filtered and concentrated in vacuo. The residue was subjected to flash chromatography (2 --> 10% MeOH/CH₂Cl₂) which gave a crude foam. Further purification was accomplished with ether trituration and filtration giving lustrous white crystals. Yield: 3.67 g (71%). ¹H NMR (DMSO-*d*₆, 600 MHz) δ 8.30 (s, 2H), 7.30 (m, 5Har), 7.21 (d, 1H, *J* = 8.1 Hz), 6.95 (d, 2Har, *J* = 8.3 Hz), 6.90 (d, 2Har, *J* = 8.2 Hz), 6.85 (d, 2Har, *J* = 8.3 Hz), 6.83 (d, 2Har, *J* = 8.3 Hz), 4.99 (s, 2H), 3.89 (dd, 2H, *J* = 13.3, 4.5 Hz), 3.33 (m, 1H), 2.51 (m, 2H), 2.34 (m, 4H), 1.35 (m, 4H), 1.19 (m, 12H), 1.12 (m, 4H), 0.83 (m, 6H) ppm; ¹³C NMR (DMSO-*d*₆, 151 MHz) δ 159.01, 155.68, 142.58, 142.31, 137.04, 134.60, 131.24, 128.54, 128.27, 128.02, 127.95, 127.46, 127.40, 127.34, 81.64, 78.27, 65.59, 43.13, 41.64, 34.51, 34.48, 31.26, 30.84, 30.71, 28.50, 28.49, 28.39, 28.31, 22.11, 22.09, 13.88 ppm; IR (CDCl₃) 3271.56, 2942.73, 2926.03, 2854.97, 1727.04, 1694.25, 1465.40, 1441.84, 1248.67, 915.87 cm⁻¹; HRMS (FAB) Calc'd for [M+Cs]⁺ C₄₁H₅₃N₅O₄•Cs⁺ 812.3152, found 812.3182.



Amine Module (4.25). Carbamate **4.24** (2.67 g, 3.93 mmol) and palladium (5%) on activated carbon (0.67 g) were mixed in 80 mL of an EtOAc/EtOH/AcOH mixture (49:49:2). The air was evacuated and replaced by H₂ three times and then the mixture was allowed to stir under 1 atm H₂. After 4 h, TLC indicated (10% MeOH/CH₂Cl₂ with 0.5% NEt₃ added) complete consumption of **4.24**. The mixture was filtered through celite and the filtrate was concentrated *in vacuo*. Flash chromatography of the residue using the TLC solvent mixture provided a hygroscopic white powder after isolation. Yield: 1.89 g (88%). ¹H NMR (CDCl₃, 600 MHz) δ 7.08 (d, 2Har, *J* = 8.0 Hz), 6.96 (d, 2Har, *J* = 8.0 Hz), 6.88 (m, 4Har), 5.85, (s, 2H), 4.12 (m, 2H), 2.99 (m, 1H), 2.52 (t, 2H, *J* = 12.0 Hz), 2.41 (m, 4H), 1.91 (s, 2H), 1.42 (m, 4H), 1.22 (m, 16H), 0.88 (m, 6H) ppm; ¹³C NMR (CDCl₃, 151 MHz) δ 159.64, 144.25, 144.13, 133.56, 130.21, 128.77, 128.41, 127.74, 127.42, 83.57, 78.71, 77.71, 45.64, 44.21, 35.47, 35.40, 31.95, 31.94, 31.41, 29.24, 29.22, 29.15, 29.12, 22.81, 22.79, 14.21 ppm; IR (CDCl₃) 3347.32, 3217.04, 2956.18, 2925.00, 2854.04, 1681.63, 1467.64, 1441.27, 1102.17, 912.32 cm⁻¹; HRMS (FAB) Calc'd for [M+H]⁺ C₃₃H₄₈N₅O₂ 546.3808, found 546.3828.



Chapter 5

Flexible, Dimeric Assemblies

“Flexiballs”

5.1 Introduction

In this chapter, we discuss the synthesis and study of several new self-assembling capsules incorporating the glycoluril modules presented in Chapter 4. Since the modules could be synthesized rapidly and in multigram quantities, the only remaining challenge to efficient capsule production was the identification of suitable spacers. The amine and acid linking sites on the modules prompted consideration of spacers capable of coupling *via* amide and ester bonds.

5.2 Benzene-Based Spacers.¹

Monomer **5.1**, available from the condensation of acid module **4.20** with triamine spacer **5.2**,² provided the first test of our modular strategy (Figure 5-1). While **5.1** gave a first-order ¹H NMR spectrum in highly competitive solvents like DMSO-*d*₆, the spectrum was broad and concentration dependent in CDCl₃ (Figure 5-2). The absence of sharp signals or a single downfield resonance for the glycoluril NH's indicated that **5.1** existed as a disordered aggregate in non-competitive solvents rather than as a discrete dimer.³ This was surprising considering that modeling predicted **5.1** would dimerize *via* twelve nearly ideal hydrogen bonds giving a structure similar to the Jelly Doughnut, but much larger (cavity volume $\approx 500 \text{ \AA}^3$).⁴

¹ This work was done in collaboration with Dr. Tomas Szabo.

² Synthesis adapted from a literature preparation: Weitzel, F.L.; Raymond, K.N. *J. Am. Chem. Soc.* **1979**, *101*, 2728-2731.

³ Rebek, J., Jr. *Chem. Soc. Rev.* **1996**, 255-264.

⁴ All modeling and volume calculations were performed as described in previous chapters. Here, pore blocking was necessary to define a cavity. This involved replacing the equatorial hydrogens on each module's six-membered ring with a cyclopropyl group.

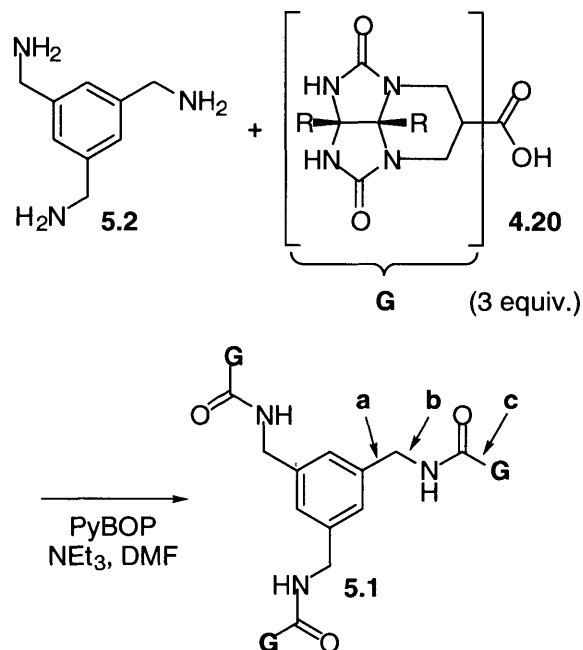


Figure S-1. Synthesis of monomer **5.1**. In the monomer, three bonds per arm (a,b,c) can rotate freely.

Raymond and co-workers also used triamine **5.2** as a platform for an analog of enterobactin, a bacterial iron-sequestering agent.⁵ Despite close structural similarities to the natural product, their mimic demonstrated a 10^6 lower affinity for ferric iron. They determined that greater rotational freedom in the mimic resulted in the lower binding affinity. However, this deficit was mitigated by introducing ethyl groups at the 2,4, and 6 positions of the spacer. Static gearing effects then enforced a *syn*-1,3,5 / *syn*-2,4,6 conformation by severely restricting rotation about the $C_{\text{ar}} - \text{CH}_2$ bond (bond **a** in Figure S-1) resulting in a 10^4 increased binding affinity.

⁵ Stack, T.D.P.; Hou, Z.; Raymond, K.N. *J. Am. Chem. Soc.* **1993**, *115*, 6466-6467.

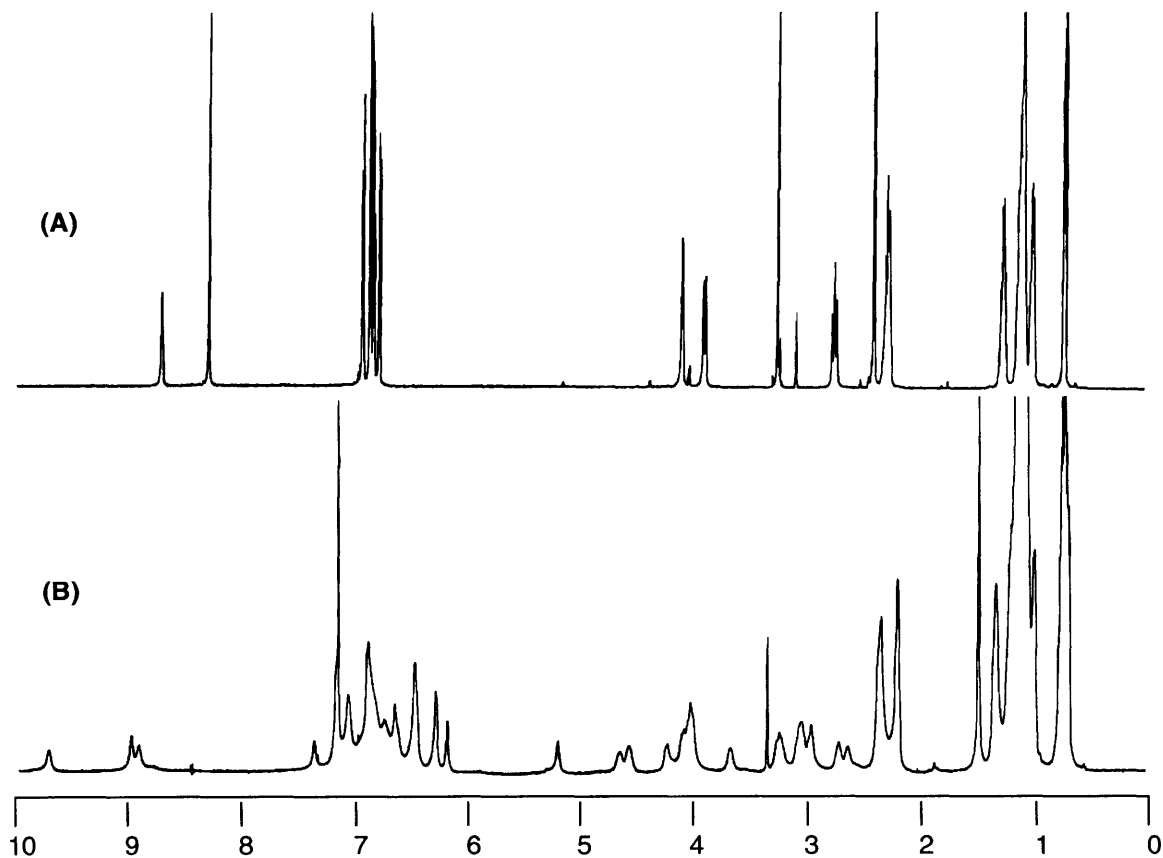


Figure 5-2. ^1H NMR spectra (600 MHz) of **5.1** in (A) $\text{DMSO-}d_6$ and (B) CDCl_3 .

Locking rotation of the three **a** bonds could lower the entropic cost of organizing **5.1** into a 1,3,5-*syn* arrangement by up to 5.5 kcal/mol.⁶ Therefore, we utilized three hindered spacers (**5.4**, **5.6**, and **5.8**) for use with the acid and amine modules (Figure 5-3). Repetitive bromomethylation of **5.3** gave spacer **5.4**. Treatment of the tribromide with NaN_3 or NaCN provided triazide **5.5** or trinitrile **5.7**⁷ respectively. Reduction of **5.5** under Staudinger conditions gave the known triamine **5.6**⁸ and hydrolysis of **5.7** produced the novel triacid **5.8**.

⁶ Page, M.I.; Jencks, W.P. *Proc. Nat. Acad. Sci. USA* **1971**, *68*, 1678-1683.

⁷ Walsdorff, C.; Saak, W.; Pohl, S. *J. Chem. Research (S)* **1996**, 282-283.

⁸ Metzger, A.; Lynch, V.M.; Anslyn, E.V. *Angew. Chem. Int. Ed. Engl.* **1997**, *36*, 862-865.

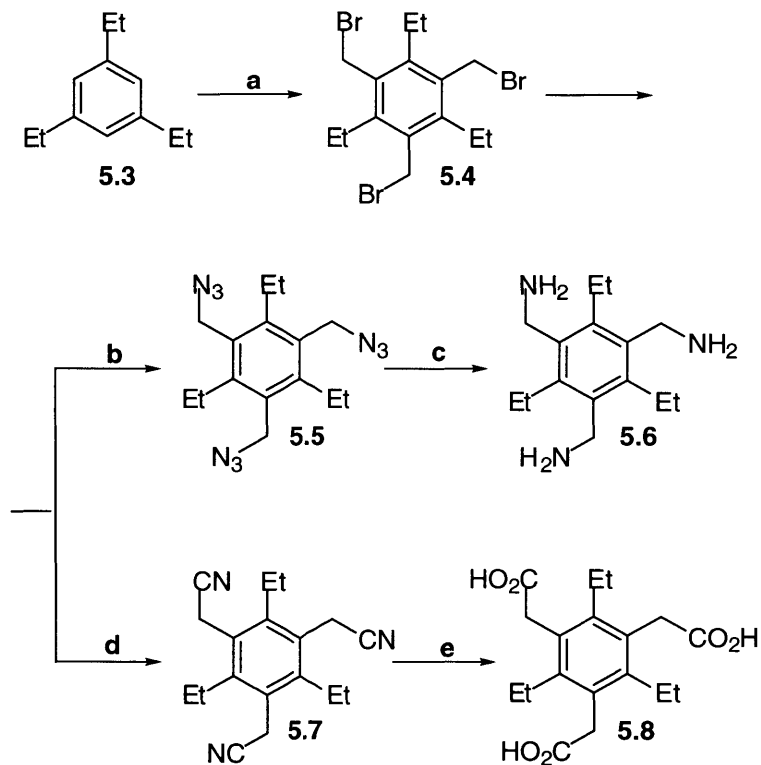


Figure 5-3. Synthesis of hindered spacers: a) i. HBr, CH₂O, AcOH; ii. CH₂O, KBr, H₂SO₄; b) NaN₃, DMF; c) PPh₃, THF, H₂O; d) NaCN, DMF; e) conc. HCl, AcOH.

Figure 5-4 illustrates the condensations of the various spacers with appropriate glycoluril modules. Using standard coupling techniques, triamide monomers **5.9** and **5.10** were synthesized in good yields. In addition, triester **5.11** was available from the reaction of tribromide **5.4** with the acid module under mild conditions. All three monomers were evaluated for their dimerization and complexation abilities.

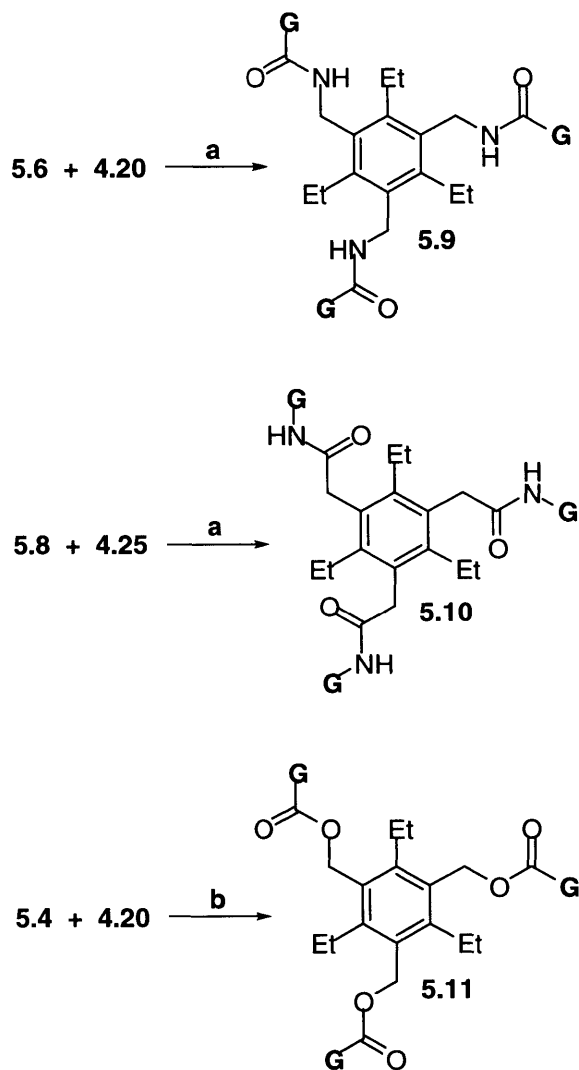


Figure 5-4. Triethylbenzene-Flexiball syntheses: a) EDC, HOBT, NEt_3 , DMF; b) Cs_2CO_3 , CH_3CN , DMF.

5.3 Triethylbenzene-Flexiballs

5.3.1 Amide Flexiballs⁹

In contrast to monomer **5.1**, amide monomers **5.9** and **5.10** exist exclusively as discrete dimers in non-competitive solvents.¹⁰ For example, the ^1H NMR spectrum of **5.9**

⁹ Reproduced in part with permission from Szabo, T.; O'Leary, B.M.; Rebek, J., Jr. *Angew. Chem., Int. Ed. Engl.* **1998**, *37*, 3410-3413. Copyright 1998 Wiley-VCH.

in CDCl₃ (Figure 5-5A) showed only sharp resonances (including a far downfield shift for the glycoluril NH's) to the limit of detection in our 600 MHz instrument.

Furthermore, no concentration dependence was observed for any shifts in solvents used for this study. These indicators of large dimerization constants were supported by mass spectroscopic (MALDI) detection of dimer **5.9•5.9** and other mass spectral evidence (*vide infra*). Although twelve degrees of rotation (bonds **b** and **c**) per dimer are restricted somewhat upon assembly, these capsules still possess significant flexibility over previous systems. Hence, we will refer to capsules made from glycoluril modules as “flexiballs.”

¹⁰ If preorganization of monomers **5.9** – **5.11** is worth up to 5.5 kcal/mol in comparison to monomer **5.1**, the dimers arising from the former group could be up to 11 kcal/mol more stable than **5.1•5.1**.

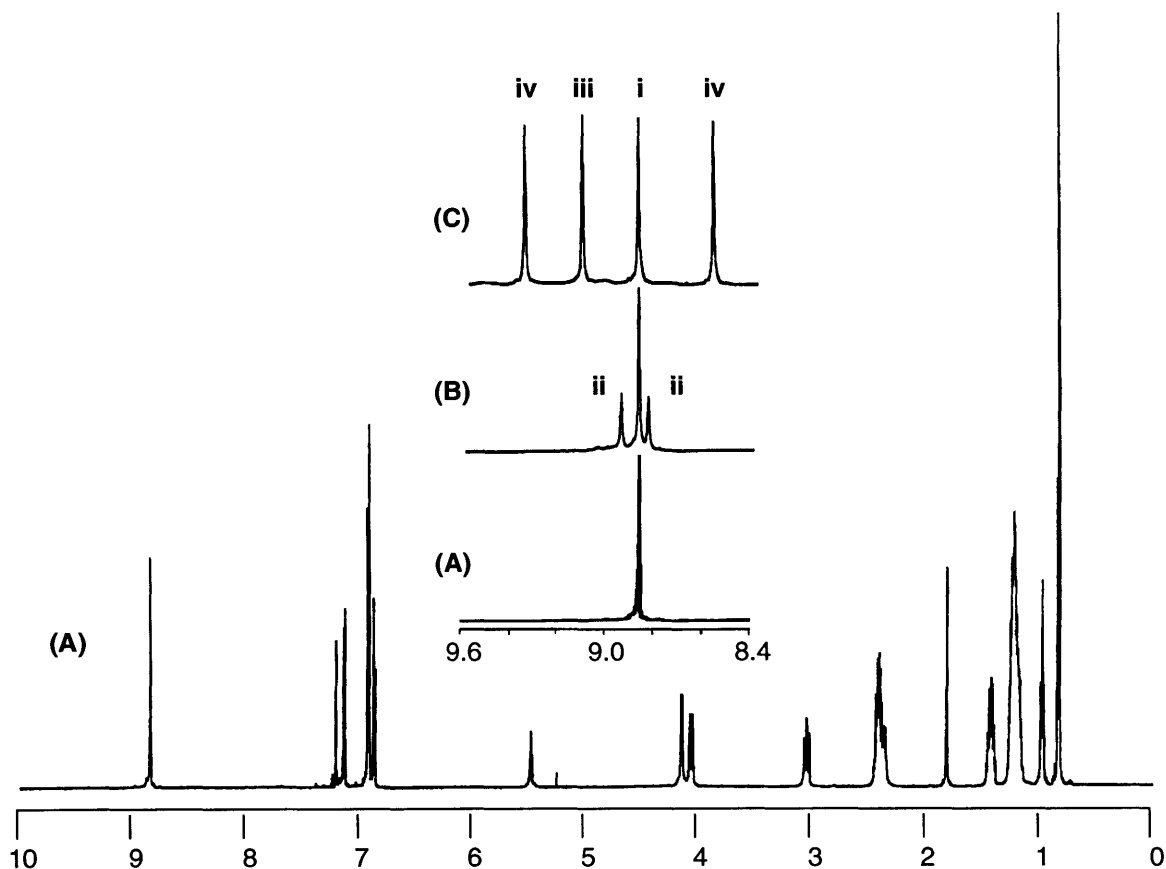


Figure 5-5. (A) Full ^1H NMR spectra (600 MHz, CDCl_3) of **5.9•5.9**. Inset shows the glycoluril NH region for samples containing monomers (A) **5.9** [dimer **5.9•5.9** = i]; (B) **5.1** and **5.9** [heterodimer **5.1•5.9** = ii]; and (C) **5.9** and **5.10** [dimer **5.10•5.10** = iii; heterodimer **5.9•5.10** = iv].

Other proof of dimeric assemblies came from ^1H NMR detection of heterodimer formation upon mixing the various monomers. Acting as a rigid template, monomer **5.9** complexed the less rigid monomer **5.1** and formed heterodimer **5.1•5.9** (Figure 5-5B). Monomer **5.10**, with inverted amide connectivity, behaved similarly to **5.9•5.9** in terms of dimerization, but showed markedly different solubility and guest binding properties (*vide*

infra). This monomer also formed a heterodimer (**5.9•5.10**) upon mixing with **5.9** to give a nearly statistical distribution of dimeric species (Figures 5-5C).¹¹

Computer modeling of complex **5.9•5.9**, with pores blocked, reveals a rugby-ball shaped cavity measuring approximately 490 Å³.⁴ All six of the amide carbonyls point outward while the amide NH's point into the cavity. Dimer **5.10•5.10** has a related structure, but features a smaller, more spherical cavity (434 Å³) because the six carbonyls point into the cavity. Figure 5-6 shows a calculated representation of the heterodimer **5.9•5.10**, the halves of which allude to the structures of the respective homodimers.

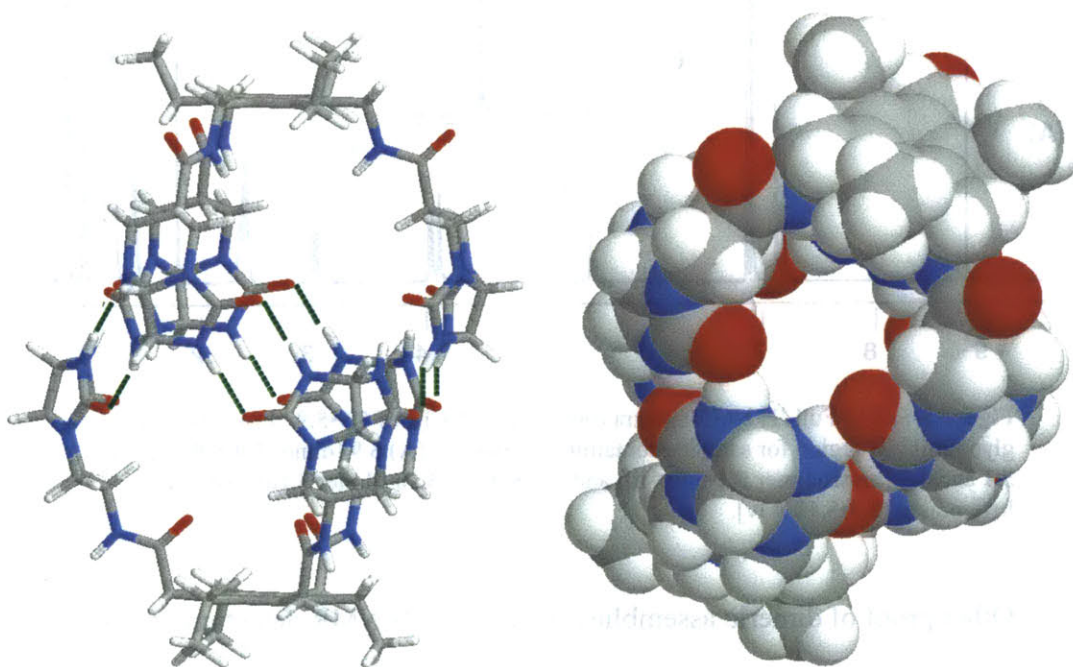


Figure 5-6. Computed polytube and CPK models of the heterodimer composed of **5.9**(top)•**5.10**(bottom) from which the structures of the homodimers may be inferred.

As seen for the Jelly Doughnut dissolved in a CDCl₃ / C₆D₆ solution, mixtures of two deuterated solvents are expected to produce at least two sets of signals for dissolved

¹¹ As calculated from peak integrations, the heterodimer and homodimers were statistically distributed upon mixing [**5.9•5.9** : **5.10•5.10** : **5.9•5.10** = 1:1:2].

capsules. However, similar experiments with hosts **5.9•5.9** and **5.10•5.10** failed to give this result.¹² This suggested that small solvent molecules rapidly move between the capsule interior and exterior resulting in an averaging of complexes on the NMR time scale. The mechanism of this exchange probably depends upon the breathing dynamics of these flexible capsules. Too fast to measure by NMR, these motions might increase the pore sizes enough to permit easy passage of solvent molecules through the dimer, akin to the flow of water through a sieve.

Previous studies identified solvent release as a significant driving force for encapsulation,^{13,14} but the large holes in these sieve-like molecules led us to doubt their utility as hosts. If solvents could enter and depart at will, entropic gains from guest encapsulation might be too small to make the process favorable. Indeed, this idea was supported by the fact that **5.9•5.9** had little or no affinity for a variety of guests while dissolved in CDCl₃. Dimer **5.10•5.10**, however, was eventually found to encapsulate several guests in this solvent (Table 5-1).

¹² For a discussion of this concept, see ref. 13. Solvent systems used in the present study included CDCl₃/C₆D₆, CDCl₃/mesitylene-*d*₁₂, *p*-xylene-*d*₁₀/mesitylene-*d*₁₂, and *p*-xylene-*d*₁₀/C₆D₆.

¹³ Kang, J.; Rebek, J., Jr. *Nature* **1996**, *382*, 239-241.

¹⁴ Meissner, R.; Garcias, X.; Mecozzi, S.; Rebek, J., Jr. *J. Am. Chem. Soc.* **1997**, *119*, 77-85.



$$K_a = \frac{[\text{Host}\cdot\text{Guest}]}{[\text{Host}\cdot\text{Solvent}_n] [\text{Guest}]} \quad \text{Eq. (2)}$$

<u>Solvent (volume, Å³)</u>	<u>5.9•5.9</u>	<u>5.10•5.10</u>
<u>Guest (volume, Å³)</u>	<u>K_a (x 10⁻⁶ M⁻¹)</u>	<u>K_a (x 10⁻⁶ M⁻¹)</u>
<u>CDCl₃ (71)</u>		
[2.2]paracyclophane (195)	0	510
ferrocene (146)	0	2700
1,1'-dimethylferrocene (178)	0	5800
ferrocenemethanol (170)	[a]	>>25000 [b]
1,1'-ferrocenedimethanol	[d]	24000
ferrocenecarboxylic acid (170)	0	8600
(1S)-(-)-camphor (159)	0	550
1-adamantaneethanol (184)	1.4	1500
<u>mesitylene-d₁₂ (124)</u>		
[2.2]paracyclophane (195)	2.0	[c]
ferrocene (146)	0	[c]
1,1'-ferrocenedimethanol	>>25000 [b]	[c]
(1S)-(-)-camphor (159)	92	[c]
1-adamantaneethanol (184)	4.6	[c]

Table 5-1. Apparent binding constants (K_a) for **5.9•5.9** and **5.10•5.10**: [a] not evaluated; [b] too large to measure accurately; [c] insoluble host; [d] This guest appeared to break up dimer **11•11** in this solvent.

How can this discrepancy be explained? One possible answer rests with size and shape differences between the two cavities. In a recent report from our lab discussing size complementarity in liquid state host-guest systems, an ideal packing coefficient (PC) was proposed.⁴ For the dimers described here, binding affinities can be understood

through evaluating ideal PCs (0.59 ± 0.09) and shape congruence between cavity and guest.¹⁵

Dimer **5.10•5.10** readily encapsulated ferrocene as indicated by a ¹H NMR spectrum showing a new set of host peaks and a new peak for encapsulated ferrocene *downfield* of the “free” guest.¹⁶ These characteristics indicate that ferrocene was too large to move freely through the dimer and was trapped in the sieve (slow exchange). Integration of these peaks revealed one ferrocene per new host corresponding to a PC of only 0.34.¹⁷ This small PC suggests an unfavorable complex due to insufficient “solvation” of the cavity. However, co-inclusion of one or two chloroforms *on average* (fast exchange) with each ferrocene would increase the PC to a more comfortable 0.50 or 0.66, respectively. While speculative, this scenario appears feasible by molecular modeling.

In contrast, dimer **5.9•5.9** does not encapsulate ferrocene even at large exterior concentrations of this compound. Encapsulation of two chloroforms and one ferrocene gives a favorable PC of 0.59, but an ideal PC does not automatically translate into a good fit. Shape is a major consideration, i.e. a square peg may have the same volume as a round hole, but the different shapes preclude a good fit. The rugby-ball shaped cavity of **5.9•5.9** is presumably filled on average with four chloroforms (PC = 0.58). These solvent molecules can be thought of as small spheres. Replacing two of these with a larger

¹⁵ Cavity volumes likely are underestimated due to the necessary hole-blocking method used in calculations (see ref. 4). Therefore, PCs will appear larger than the reported ideal (0.55 ± 0.09). The best binders in this study gave an apparent average PC = 0.59 ± 0.09 . [PC = vol. guest(s) / vol. cavity].

¹⁶ The twelve phenyl groups of the glycolurils present their edges to the cavity which accounts for the downfield shifts of guests' signals from their “free” positions.

¹⁷ Ferrocene derivatives were modeled using MacSpartan Plus and their volumes were calculated using MacroModel.

sphere (like free-tumbling ferrocene) may not be favorable because this new guest may not be able to “solvate” the tapered ends of the cavity as well as chloroform.

While almost every prospective guest shunned the cavity of **5.9•5.9** in CDCl₃, the story changed upon switching to one of the largest deuterated solvents available, mesitylene-*d*₁₂ (Table 5-1).¹⁸ Calculation of PCs showed that the included guests plus one mesitylene gave values in the upper end of the ideal range. Unsurprisingly, the better binders tended to be more complementary in shape *and* possessed functionality capable of hydrogen bonding to polar surfaces within the cavity. In short, **5.9•5.9** preferred these guests to the poorer solvation offered by large, disc-shaped mesitylenes.¹⁹ However, as indicated in Table 5-1, none of these guests could compete as well against chloroform solvation of the interior.

What is the mechanism of encapsulation? A clue is given by the heterodimerization of the two capsules. The disproportionation of **5.9•5.9** and **5.10•5.10** to the heterodimer requires the complete dissociation of a dimeric capsule *via* the eventual disruption of 12 hydrogen bonds. This process reaches equilibrium in chloroform over the course of hours. The common finding that encapsulation equilibrium is reached within minutes for all viable guests suggests a mechanism of guest uptake not dependent upon complete dissociation. Instead, modeling shows that opening one glycoluril “flap” by breaking 4 hydrogen bonds creates a pore large enough to accommodate the passage of most guests.²⁰

¹⁸ Dimer **5.10•5.10** displayed very poor solubility and dimer **5.9•5.9** was only moderately soluble in mesitylene-*d*₁₂. This could result from the poor shape complementarity of two encapsulated mesitylenes (PCs = 0.57 and 0.51, respectively) with the cavities.

¹⁹ K.T. Chapman, W.C. Still, *J. Am. Chem. Soc.* **1989**, *111*, 3075-3077.

²⁰ T. Szabo, G. Hilmersson, J. Rebek Jr., *J. Am. Chem. Soc.* **1998**, *120*, 6193-6194.

5.3.2 Ester Flexiball

Triester **5.11** also dimerizes to form a capsule (**5.11•5.11**), although the broad signal for the glycoluril NH protons (Figure 5-7A) suggests a less symmetric or less tightly bound assembly than with the amide flexiballs. Despite this, the ester capsule still forms heterodimers upon mixing with **5.9•5.9** or **5.10•5.10**. Furthermore, upon addition of an *N*-methylquinuclidium salt ($\text{NMQ}^+\text{BF}_4^-$), the signals sharpen dramatically presumably due to guest-induced stabilization of the capsule (Figure 5-7B).¹⁴

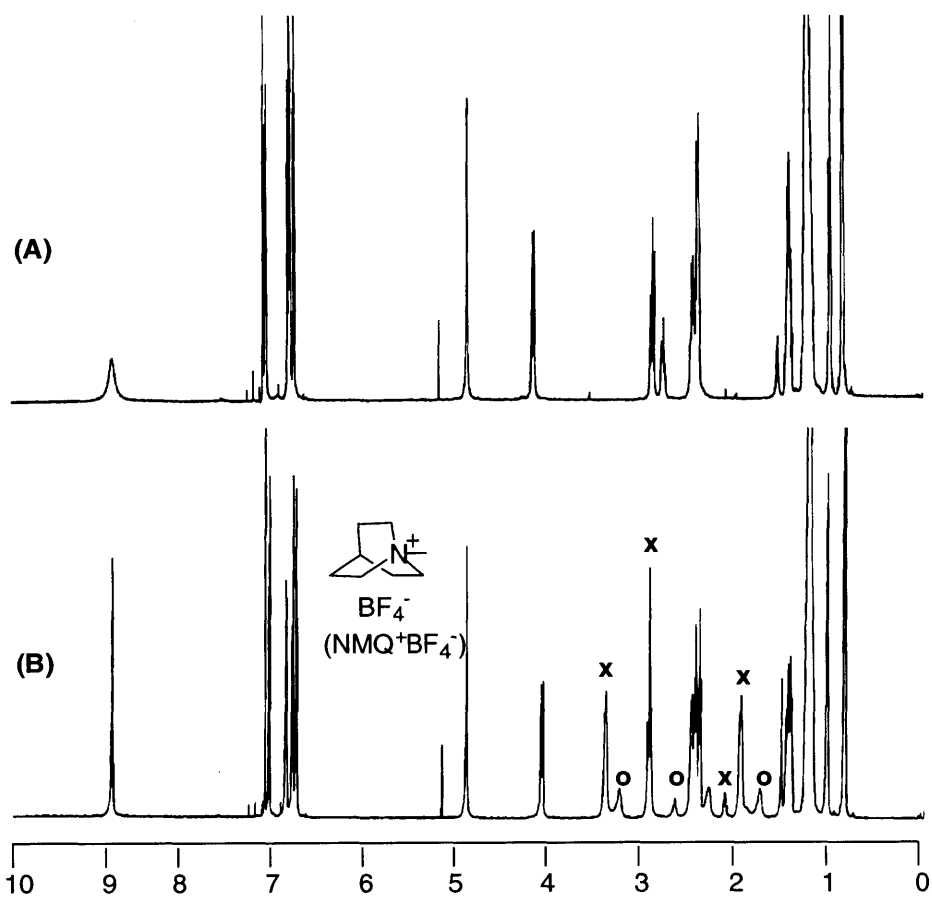


Figure 5-7. ¹H NMR (600 MHz, CDCl_3) of ester flexiball **5.11•5.11** (A) alone and (B) with ≈ 3 equivalents of $\text{NMQ}^+\text{BF}_4^-$. Some signals attributed to the guest are marked (x = free; o = encapsulated). Integration of peaks indicates a 1:1 capsule to guest ratio. ¹⁹F NMR gave no direct evidence of BF_4^- encapsulation although it is likely that both the cation and anion are encapsulated as ion pairs in solution.

Several guests similar to $\text{NMQ}^+\text{BF}_4^-$ were evaluated by both electrospray-ionization mass spectrometry²¹ (ESI-MS) and ^1H NMR with the ester flexiball. ESI-MS competition experiments showed modest encapsulation selectivities as listed in Figure 5-8. Using the same guests, ^1H NMR studies²² gave results in agreement with the MS data as discussed more thoroughly later in the chapter.

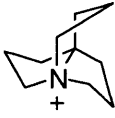
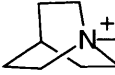
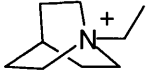
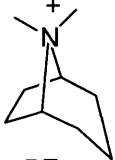
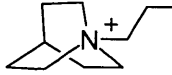
MS:		>		≥		≥		>	
	BF_4^-		BF_4^-		BF_4^-		BF_4^-		BF_4^-
Vol./PC:	162 / 0.33		138 / 0.28		154 / 0.31		153 / 0.31		170 / 0.35
NMR:	Encap.		Encap.		Encap.		Disrupts Dimer		Broad peaks

Figure 5-8. Guest selectivities observed with the ester flexiball by ESI-MS (CH_2Cl_2 solutions) and ^1H NMR (600 MHz, CDCl_3). In the ESI-MS studies, selectivity was determined by relative peak intensities recorded from multiple-guest solutions. In the NMR studies, K_a values could not be attained (where encapsulation occurred) because of poor solubility of the free salts in CDCl_3 and extremely high binding values (i.e. only one set of capsule peaks seen). Volumes (\AA^3) and PC values are given as relative references only since calculation of ion volumes is imprecise using MacroModel. [Consideration of the BF_4^- anion adds 35\AA^3 to volume and 0.07 to PC values.]

5.4 Larger Flexiballs

5.4.1 Calix[4]arene Flexiball

To date, either two or three glycolurils have served as the hydrogen bonding units in monomers with C_2 or C_3 rotational axes, respectively. The resulting self-complementary surfaces produced dimers with D_{2d} or D_{3d} symmetry. However, these symmetry groups are insufficient for larger capsules due to increased spacing between the

²¹ ESI-MS experiments were carried out in collaboration with Dr. Christoph A. Schalley.

²² ^{19}F NMR experiments gave no indication of BF_4^- anion inclusion, although inclusion of the whole salt is likely due to ion-pairing.

glycolurils. Therefore, spacers with C_4 axes were designed which could form dimers with D_{4d} symmetry.

One such spacer was tetraminocalix[4]arene **5.12**.²³ Condensation of acid module **4.20** with **5.12** gave monomer **5.13** in good yield (Figure 5-9). Modeling predicted that monomers in cone conformation (C_{4v}) would dimerize *via* 16 hydrogen bonds to give the desired capsule. However, ^1H NMR spectra in non-competitive solvents showed numerous signals for protons expected to be equivalent in a C_{4v} structure (including several downfield glycoluril NH peaks). This suggested that the required conformation was inaccessible due to intramolecular hydrogen bonds enforcing a pinched-cone (C_{2v}) structure.

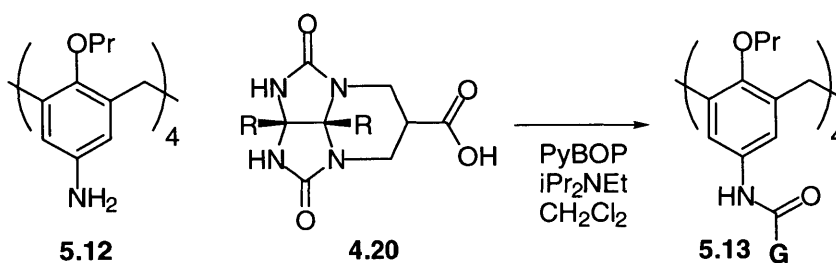


Figure 5-9. Synthesis of calixarene-based monomer **5.13**.

5.4.2 Cavitand Flexiball²⁴

Monomer **5.13**, like triamide monomer **5.1**, was simply too flexible to permit capsule formation. Our experience with **5.1** suggested that increased pre-organization of the large spacer might lead to assembly. Therefore, we replaced the calixarene spacer

²³ Calixarene **5.12** was synthesized from the tetranitro derivative (Verboom, W.; Durie, A.; Egberink, R.J.M.; Asfari, Z.; Reinhoudt, D.N. *J. Org. Chem.* **1992**, *57*, 1313-1316) as described in the Experimental section.

²⁴ The synthetic aspects of this work were done in collaboration with Dr. Arne Lutzen. The solution-phase encapsulation studies were carried out by Dr. Adam R. Renslo.

5.12 with a rigid, bowl-shaped cavitand²⁵ **5.14** as shown in Figure 5-10. Coupling the tetrahydroxy cavitand²⁶ **5.14** with four equivalents of acid module **4.20** as shown provided monomer **5.15** in 48% yield.

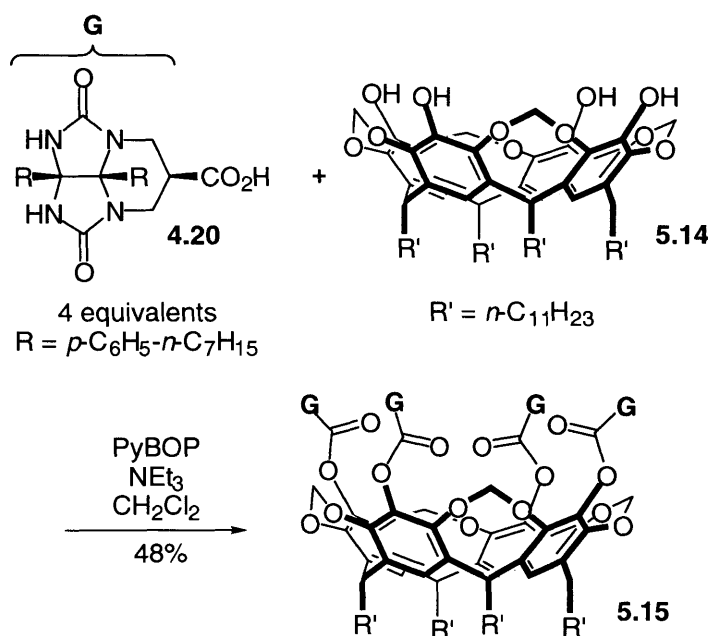


Figure 5-10. Synthesis of cavitand flexiball monomer **5.15**.

Molecular modeling of **5.15** predicted that the self-complementary shape and recognition surfaces of the C_{4v} symmetric monomer would encourage dimerization to produce a D_{4d} symmetric capsule **5.15•5.15** (Figure 5-11). Figure 5-12A shows the ¹H NMR spectrum of **5.15** in a 1:3 mixture of DMSO-*d*₆ and CDCl₃ and, under these conditions, the hydrogen bond donors are bound to DMSO and the monomers do not assemble. The glycoluril N-*H* protons give a signal at $\delta = 8.1$ ppm. In less competitive solvents such as mesitylene-*d*₁₂ (Figure 5-12B), a significant downfield shift of $\Delta\delta \approx 1.7$

²⁵ Cram, D. J.; Cram, J. M. In *Container Molecules and Their Guests*; Stoddart, J. F., Ed.; Monographs in Supramolecular Chemistry; Royal Society of Chemistry: Cambridge, 1994.

ppm for the N-H resonance indicates the formation of an assembly. In addition, the highly symmetric structure shown in Figure 5-11 is supported by the simple set of signals in the rest of the spectrum.²⁷

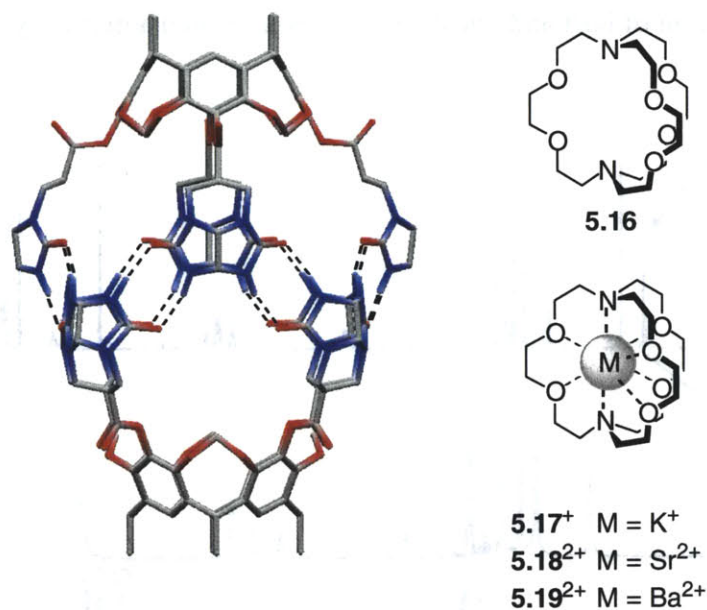


Figure 5-11. Structural model of cavitand-based flexiball **5.15•5.15** and guests **5.16** – **5.19²⁺**.

The cavity of **5.15•5.15** features a volume of ca. 950 Å³—the largest yet prepared by our group. Given this large size, identifying suitable guests for this flexiball proved challenging. After screening a number of candidates, Adam Renslo found that large cryptand / cryptate guests (**5.16** – **5.19²⁺**) were readily encapsulated in mesitylene-*d*₁₂ solution. The guest volumes range from 390 – 420 Å³ which translate into packing coefficients of ca. 0.45 – a value shy of ideal for neutral guests in previous capsules.

²⁶ (a) Cram, D. J.; Karch, S.; Kim, H.-E.; Knobler, C. B.; Maverick, E. F.; Ericson, J. L.; Helgeson, R. C. *J. Am. Chem. Soc.* **1988**, *110*, 2229. (b) Cram, D. J.; Jaeger, R.; Deshayes, K. *J. Am. Chem. Soc.* **1993**, *115*, 10111.

²⁷ All chemical shifts were concentration independent within the range of 0.1 to 10 mM.

Titration of free cryptand **5.16** into a solution of the flexiball (Figure 5-12C) led to the appearance of a new set of peaks for **5.15**•**5.15** and the disappearance of the original dimer. Three signals for encapsulated **5.16** (filled circles in Figure 5-12C) were identified at positions downfield of the signals for free **5.16** (open circles) by $\Delta\delta \approx 0.6$ ppm and integration of host and guest resonances indicated a highly symmetric 1:1 complex.

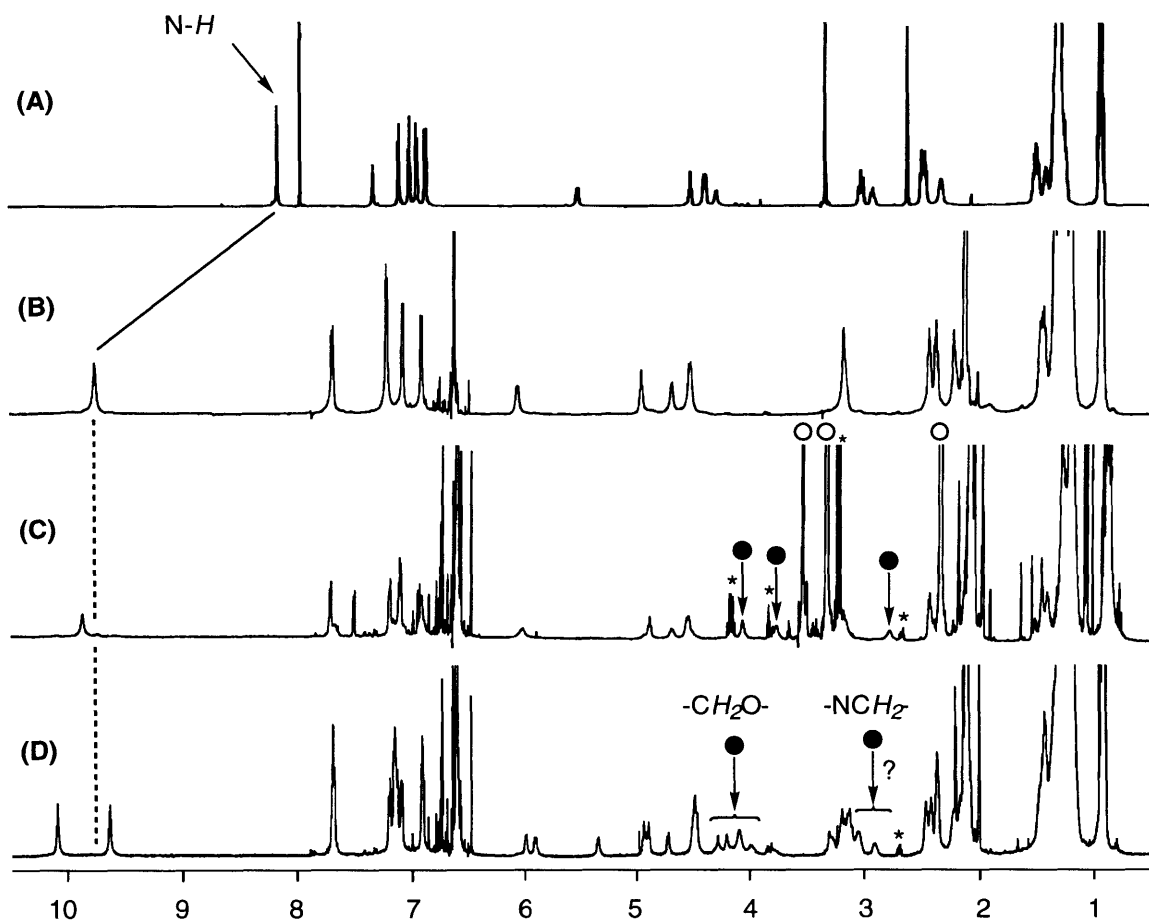


Figure 5-12. $^1\text{H-NMR}$ spectra (600 MHz) of (A) **5.15** in $\text{DMSO-}d_6/\text{CDCl}_3$ (1:3); **5.15** in mesitylene- d_{12} (B) alone, (C) with excess **5.16**, and (D) with $\text{5.17}^+\text{SCN}^-$. Solvent impurities are denoted by asterisks and were shown not to participate in encapsulation processes. See text for other label descriptions.

The capsule also encapsulated the K^+ -filled cryptate 5.17^+ . While the thiocyanate salt $\text{5.17}^+\text{SCN}^-$ is not soluble in mesitylene- d_{12} , addition of the cavitand dimer to a

suspension of 5.17^+SCN^- rendered the salt soluble and gave the 1H NMR spectrum shown in Figure 5-12D. Signals for the $-CH_2O-$ protons of the encapsulated cryptate are visible at $\delta = 3.95 - 4.20$ ppm, downfield of the signals given by the encapsulated cryptand by $\Delta\delta \approx 0.3$ ppm due to deshielding of the cryptate by the K^+ ion inside.²⁸ Again, signal integration gave the expected 1:1 stoichiometry. However, the signals for host and guest were now split into two sets and no signals for the solvent-filled capsule were present. We interpret that the splitting results from desymmetrization of the complex due to restricted guest motion within the capsule, i.e. the two halves of the capsule are in different magnetic environments.

The cryptate cation alone is not expected to cause such desymmetrization, but the combination of the cryptate and anion can do so:²⁹ one occupies the upper half and the other the lower, with slow exchange of their positions on the NMR timescale. As mentioned previously, the cation alone would give a rather small packing coefficient, but this value increases to almost 0.50 upon co-inclusion of the anion. Complexation of the full ion pair 5.17^+SCN^- was supported by using isotopically labeled salt $5.17^+S^{13}CN^-$. Predictably, the ^{13}C NMR spectrum of the salt without the capsule showed no signals due to the salt's insolubility. In the presence of the capsule, however, an intense signal for the $S^{13}CN^-$ anion arose at 132.5 ppm suggesting the whole salt is solubilized by

²⁸ The $-NCH_2-$ protons are likely to be buried under the capsule signals at $\delta \approx 3$ ppm as shown in Figure 5-12D. In this case, they experience a $\Delta\delta$ similar to that of the $-CH_2O-$ signals.

²⁹ The simultaneous binding of anions and cations has been described a number of times and ion pairs less frequently. For a recent review, see: Antonisse, M.M.G; Reinhoudt, D.N; *Chem. Commun.* 443-448 (1998).

encapsulation. In contrast, the much larger salt **5.17**⁺ B(*p*-ClPh)₄⁻ gave no sign of encapsulation despite its greater solubility in mesitylene.³⁰

Double-inclusion of host-guest complexes has been a rare phenomenon limited to the solid-state complexation of coronates and cryptates by cyclodextrins.^{31,32} The solution phase flexiball – cryptate systems reported here represent novel complexes-within-complexes reminiscent of simple Russian *Matroschka* dolls. These “second-sphere” supramolecular capsules hint at the multilayer complexity which future systems may demonstrate.

5.5 Capsule Characterization by ESI-MS²¹

5.5.1 Introduction

Recently, our group described an electrospray ionization mass spectrometric (ESI-MS)^{33,34} protocol for the structural characterization of capsules using quaternary ammonium ions as guests.³⁵ These complexes are easily electrosprayed from non-

³⁰ Computational modeling found a packing coefficient of 0.85 for the proposed complex. This value exceeds that found in many super-dense solids.

³¹ Vögtle, F.; Müller, W.M. *Angew. Chem., Int. Ed. Engl.* **1979**, *18*, 623-624.

³² Kamitori, S.; Hirotsu, K.; Higuchi, T. *J. Am. Chem. Soc.* **1987**, *109*, 2409-2414.

³³ For reviews on the application of MS to noncovalent interactions, see: (a) Vicenti, M.; Pelizzetti, E.; Dalcanale, E.; Soncini, P. *Pure Appl. Chem.* **1993**, *65*, 1507. (b) Vicenti, M.; Minero, C.; Pelizzetti, E.; Secchi, A.; Dalcanale, E. *Pure Appl. Chem.* **1995**, *67*, 1075. (c) Vicenti, M. *J. Mass Spectrom.* **1995**, *30*, 925. (d) Przybylski, M.; Glocker, M. O. *Angew. Chem., Int. Ed. Engl.* **1996**, *35*, 806. (e) Brodbelt, J. S.; Dearden, D. V. in: *Comprehensive Supramolecular Chemistry*, Atwood, J. L.; Davies, J. E. D.; MacNicol, D. D.; Vögtle, F., Lehn, J.-M. (eds.), vol. 8, p. 567, Pergamon Press, Oxford: 1996. (f) Smith, R. D.; Bruce, J. E.; Wu, Q.; Lei, Q. P. *Chem. Soc. Rev.* **1997**, *26*, 191.

³⁴ For examples of MS studies on hydrogen-bonded supramolecular complexes, see: (a) Russell, K. C.; Leize, E.; Van Dorsselaer, A.; Lehn, J.-M. *Angew. Chem., Int. Ed. Engl.* **1995**, *34*, 209. (b) Cheng, X.; Gao, Q.; Smith, R. D.; Simanek, E. E.; Mammen, M.; Whitesides, G. M. *J. Org. Chem.* **1996**, *61*, 2204. (c) Jolliffe, K. A.; Crego Calama, M.; Fokkens, R.; Nibbering, N. M. M.; Timmerman, P.; Reinhoudt, D. N. *Angew. Chem., Int. Ed.* **1998**, *37*, 1247. (d) Ma, S.; Rudkevich, D. M.; Rebek, J., Jr. *J. Am. Chem. Soc.* **1998**, *120*, 4977. (e) Scherer, M.; Sessler, J.L.; Moini, M.; Gebauer, A.; Lynch, V. *Chem. Eur. J.*, **1998**, *4*, 152.

³⁵ (a) Schalley, C. A.; Rivera, J. M.; Martín, T.; Santamaría, J.; Siuzdak, G.; Rebek, J., Jr. *Eur. J. Org. Chem.*, in press. (b) Schalley, C.A.; Martín, T.; Obst, U.; Rebek, J., Jr. *J. Am. Chem. Soc.* **1999**, *121*, 2133. (c) Schalley, C.A.; Castellano, R. K.; Brody, M. S.; Rudkevich, D. M.; Siuzdak, G.; Rebek, J., Jr. *J. Am.*

competitive solvents and characterized by isotope pattern analysis to provide information about elemental composition and charge state. Furthermore, experiments studying the formation of heterodimers and guest encapsulation selectivities provide compelling evidence for the structures of these host-guest complexes in solution. Finally, collision experiments confirm that the capsular structure is retained in the gas phase.

The capsules presented here differ from those examined earlier in several aspects that complicate mass spectral characterizations. First, their cavity sizes far surpass those studied previously by MS which made the identification of suitable guests challenging. Second, the large molecular masses for these hosts (e.g. $m/z = 6888$ amu for cavitand flexiball **5.15•5.15**) extend beyond the mass range of our instruments ($m/z < 4000$). Third, as described earlier, capsules generated using our modular approach exhibit greater flexibility than previous capsules. This could hasten guest release in the gas phase and obscure collision experiments. Finally, amide flexiballs **5.9•5.9** and **5.10•5.10** are isobaric species given their identical elemental composition and ester flexiball **5.11•5.11** differs only by 6 amu from its amide analogs. These small mass differences could hinder the quantitative detection of heterodimers because of poor separation of capsular isotope patterns.

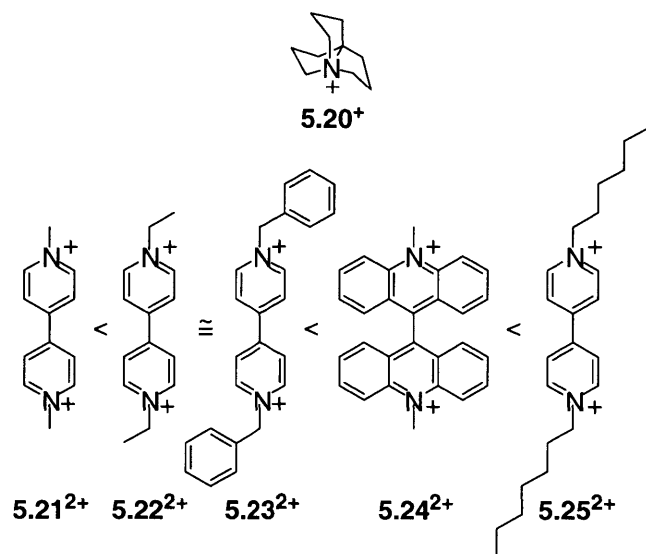


Figure 5-13. Other guests used in ESI-MS encapsulation studies (counter ions = BF_4^-). Rankings reflect the results of competition experiments with the ester flexiball **5.11•5.11**.

5.5.2 ESI-MS of Triethylbenzene Flexiballs

As shown in Figure 5-14, masses corresponding to flexiballs **5.9•5.9**, **5.10•5.10**, and **5.11•5.11** encapsulating monocationic guest **5.20⁺** were detected at the far limit of our range (Figure 5-14A-C). In fact, the only intense signals correspond to 1:1 complexes of flexiballs to guest [i.e. $[\mathbf{5.20}^+@5.9\cdot5.9]$ ($m/z = 3990$), $[\mathbf{5.20}^+@5.10\cdot5.10]$ ($m/z = 3990$) and $[\mathbf{5.20}^+@5.11\cdot5.11]$ ($m/z = 3996$)].³⁶

A very similar result was found for the complexes containing doubly-charged **5.25²⁺**. Now well within our detection window, the base peaks in these spectra correspond to $[\mathbf{5.25}^{2+}@5.9\cdot5.9]$ ($m/z = 2097$), $[\mathbf{5.25}^{2+}@5.10\cdot5.10]$ ($m/z = 2097$) and $[\mathbf{5.25}^{2+}@5.11\cdot5.11]$ ($m/z = 2100$). Some ions of low abundance are detected which correspond to the protonated monomers and monomer-guest complexes.

³⁶ The following nomenclature has been employed: $[\mathbf{5.20}^+@5.9\cdot5.9]$ means that guest ion **5.20⁺** is encapsulated (indicated by the “@” sign) within the dimer of flexiball **5.9•5.9**. In contrast, $[\mathbf{5.20}^+\cdot5.9]$ indicates that **5.20⁺** and monomer **5.9** form a complex with a structure that is not further specified.

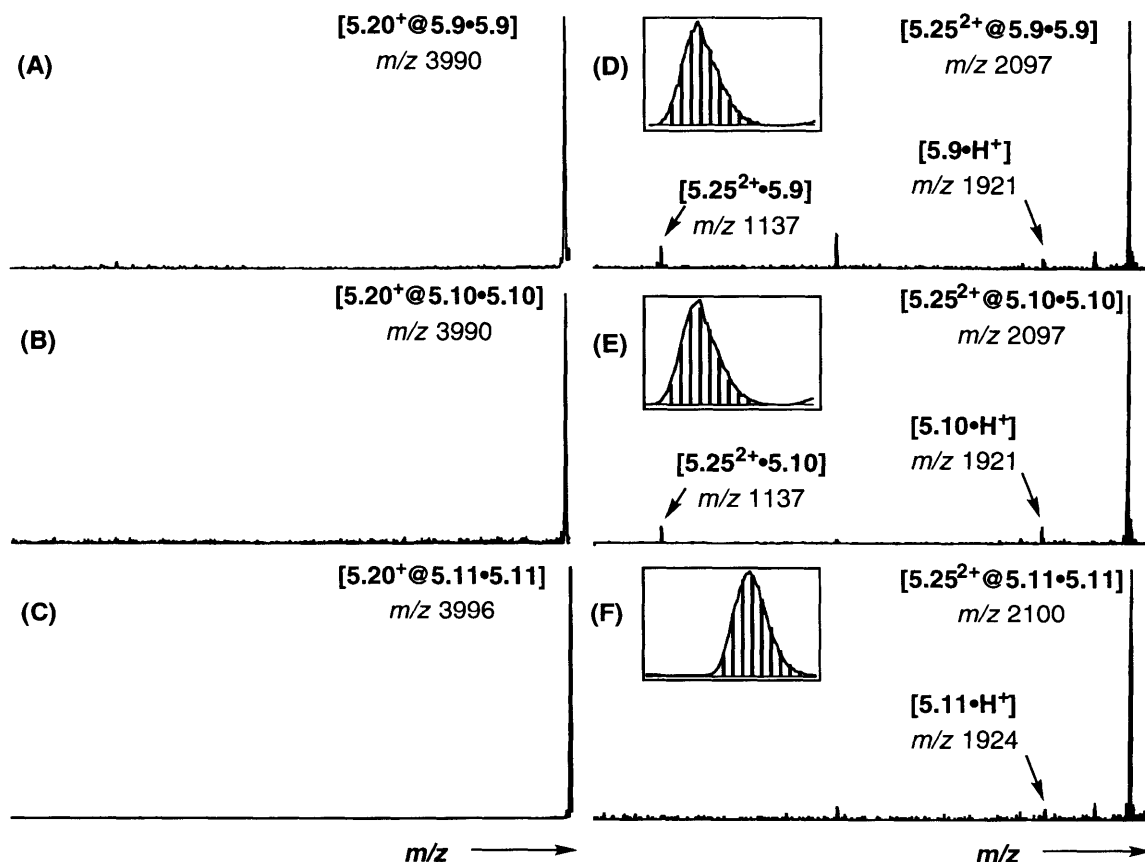


Figure 5-14. ESI mass spectra of CHCl_3 solutions of 5.20^+BF_4^- (75 μM) as the guest salt with (A) **5.9** (50 μM), (B) **5.10** (50 μM), and (C) **5.11** (50 μM) ($m/z = 1900 - 4000$ amu) and acetone solutions of $5.25^{2+}(\text{BF}_4^-)_2$ (75 μM) as the guest salt with (D) **5.9** (50 μM), (E) **5.10** (50 μM), and (F) **5.11** (50 μM) ($m/z = 1000 - 2150$ amu). The insets show the measured isotope patterns together with those calculated on the basis of natural abundancies for the dicationic capsules ($m/z = 2093 - 2108$ amu).

The dicationic guests $5.21^{2+} - 5.25^{2+}$ were not soluble enough in CHCl_3 for use in these studies. Therefore, acetone was chosen as the solvent for the dicationic complexes, despite concerns that this solvent might inhibit capsule formation. The measured isotope patterns of the capsule ions (insets in Figure 5-14) are not resolved into separate isotope peaks, ruling out ions with only one charge. (Monocations in this mass range should easily be separated with the resolving power of $m/\Delta m = 2000$ provided by our instrument.) In addition, the measured curve fits almost perfectly to the intensities

calculated³⁷ for the doubly-charged complexes based on natural isotope abundancies which confirms the correct composition of the complexes.

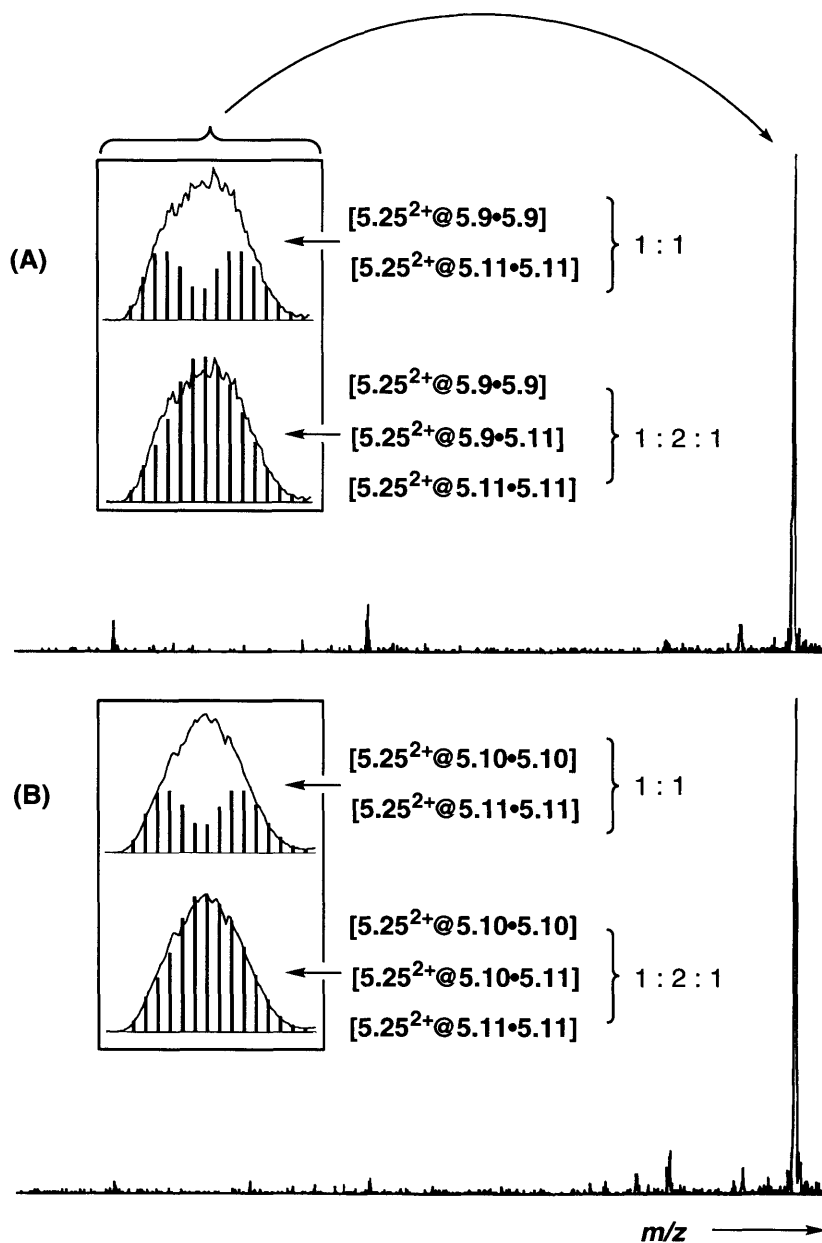


Figure 5-15. ESI mass spectra of acetone solutions of $5.25^{2+}(\text{BF}_4^-)_2$ (75 μM) as the guest salt with (A) **5.9** (25 μM) and **5.11** (25 μM); and (B) **5.10** (25 μM) and **5.11** (25 μM) ($m/z = 1000 - 2150$). The insets (corresponding to the large peaks) compare the measured isotope pattern with those calculated for either a 1:1 mixture of the two homodimers or a statistical 1:2:1 ratio of the homo- and heterodimers.

³⁷ Isotope patterns calculated using Isotope Pattern Calculator v.1.6.6.

Two experiments provide evidence of the hydrogen-bonded nature of these capsules. First, addition of highly competitive solvents to the sample solutions disrupts the assemblies. For example, upon addition of methanol, new signals appear for the protonated monomers and dimers at the expense of the capsule signals. The proton-bridged dimer does not contain a guest suggesting a nonspecific structure rather than capsular. Second, heterodimers can be detected by MS (Figure 5-15). Due to the small mass difference of $\Delta m/z = 3$ for doubly charged [5.25²⁺@5.9•5.9] or [5.25²⁺@5.10•5.10] compared to [5.25²⁺@5.11•5.11], the isotope patterns of the homodimers overlap somewhat. Despite this, comparison of the measured signal shapes of acetone solutions containing equimolar amounts of 5.9 and 5.11 (Figure 5-15A) or 5.10 and 5.11 (Figure 5-15B) reveals a good fit with the isotope patterns calculated for a 1:2:1 ratio of the homo- and heterodimers. In contrast, the pattern calculated for the two homodimers alone does not fit at all. This not only provides qualitative evidence for the formation of heterodimers, but also mimics the statistical distribution found in solution and further supports the hydrogen-bonded nature of these complexes.

In order to gather evidence for the specific capsular structure of these host-guest complexes in solution, competition experiments were performed with doubly-charged ammonium ions 5.21²⁺ – 5.25²⁺. Figure 5-13 illustrates their binding abilities with ester flexiball 5.11•5.11.³⁸ The general similarity of these guests should result in similar properties if non-specific binding occurs. However, selectivity in guest binding would support an encapsulation scenario within the cavity of the capsules.

³⁸ See section 5.3.2 for similar studies with singly-charged ammonium ions.

While guest selectivity was observed for these systems, it was less pronounced than in previously studied capsules.³⁵ For instance, the best guest, **5.25**²⁺, was only about 15 times better than **5.21**²⁺. In view of the flexibility of the capsule monomer, this result is not surprising. As supported by molecular modeling, the capsule can adapt to the shape of guests and accommodate even large guests such as **5.23**²⁺ or **5.24**²⁺ in a significantly deformed capsule. In the series of *n*-alkyl substituted paraquat salts, **5.21**²⁺ and **5.22**²⁺ were too small to be good guests. While they bear appropriate lengths, their small widths preclude sufficient van der Waals contacts with the capsule walls.

Surprisingly, the long *n*-heptyl sidechains featured by **5.25**²⁺ did not hamper the assembly. As determined from the competition experiments, their presence seems quite favorable and modeling suggests two possible scenarios for encapsulation of **5.25**²⁺. First, the sidechains might fold in yielding a shape more congruent with that of the cavity than possible with **5.21**²⁺ or **5.22**²⁺. However, several degrees of rotational freedom would be lost which makes this model unlikely from an entropic standpoint. Alternatively, the sidechains might protrude through holes in the capsule walls. Regardless of which mode operates, the size selectivity observed in these experiments – although modest – points to a capsular structure and strongly supports our solution phase studies.

5.5.3 ESI-MS Characterization of the Cavitand Flexiball

The cavitand flexiball **5.15•5.15** shares several characteristics with the benzene flexiballs: a high molecular mass (monomer = 3444 amu), a large cavity volume (ca. 950 Å³), flexible binding sites, and sizeable holes in the capsule walls. Due to our limitations in mass range, its characterization could not be achieved with monocations as guests.

However, as with the smaller flexiballs, dication guests lowered the m/z ratios to well within our detection limits.

Three examples are shown in Figure 5-16. Two belong to the series of doubly charged ammonium ions and the third was chosen as analog for the potassium cryptate used in the NMR experiments described above. The base peaks in the first two spectra (Figure 5-16A and B) correspond to $[5.25^{2+}@5.15\cdot5.15]$ ($m/z = 3622$) and $[5.24^{2+}@5.15\cdot5.15]$ ($m/z = 3637$). They are accompanied by less intense signals for the monomer-guest complexes which follows the pattern found for the smaller flexiballs. Similar mass spectra were obtained using salts $5.21^{2+} - 5.23^{2+}$ (BF_4^- counterions) as guests.

Figure 5-16C shows the ESI-MS recorded from an acetone solution of **5.15** and cryptate $5.18^{2+}(\text{ClO}_4^-)_2$. The base peak corresponds to the cryptate dication encapsulated in the capsule dimer ($[5.18^{2+}@5.15\cdot5.15]$, m/z 3677) and the only other signal is significantly less intense and corresponds to the monomer-guest complex $[5.18^{2+}\cdot5.15]$ (m/z 1955). A very similar spectrum with signals for $[5.19^{2+}\cdot5.15]$ (m/z 1980) and $[5.19^{2+}@5.15\cdot5.15]$ (m/z 3702) was obtained with $5.19^{2+}(\text{Cl}^-)_2$ as the guest salt.

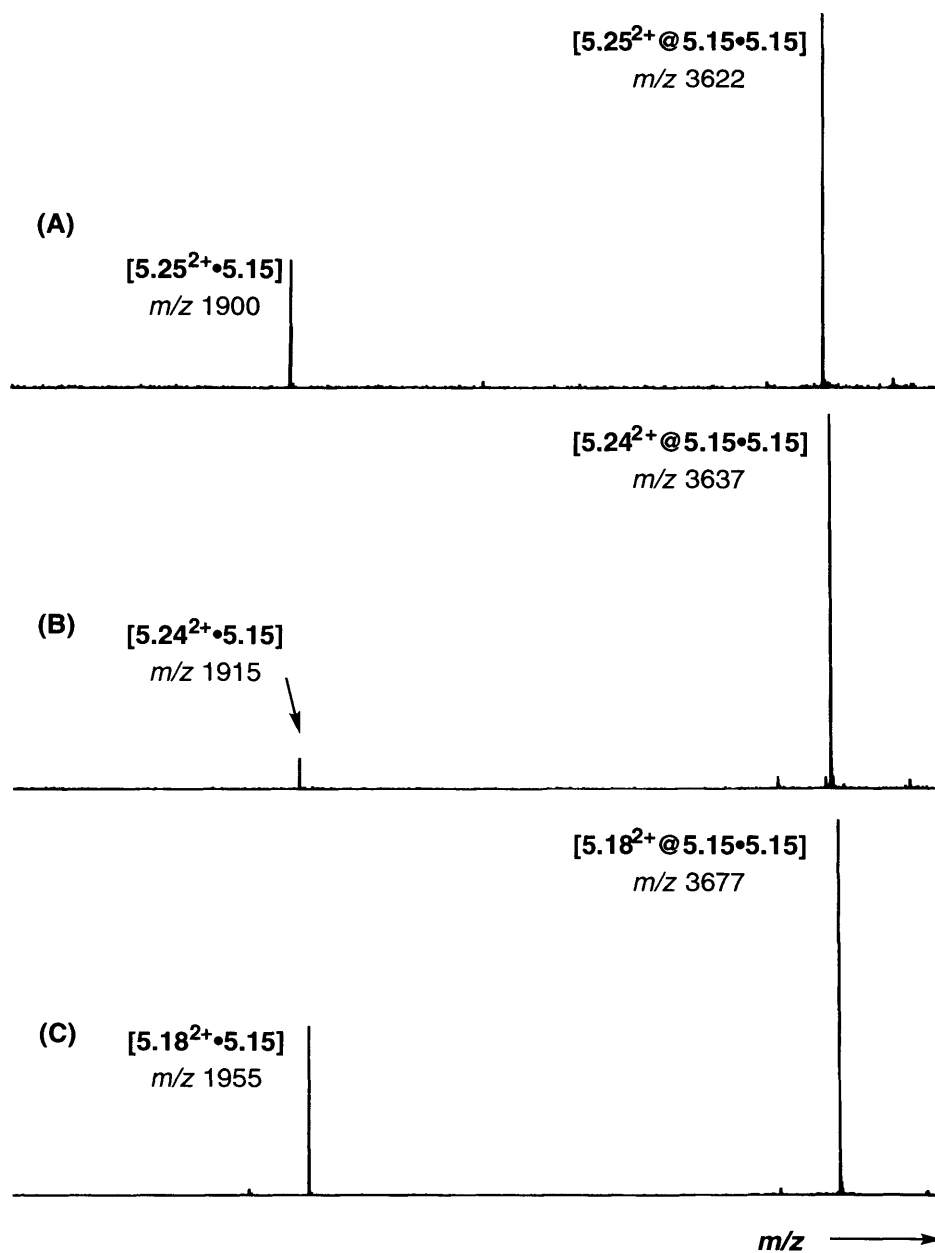


Figure 5-16. ESI mass spectra of an acetone solution of cavitand flexiball monomer **5.15** ($50\ \mu\text{M}$) with (A) $5.25^{2+}(\text{BF}_4^-)_2$ ($75\ \mu\text{M}$), (B) $5.24^{2+}(\text{BF}_4^-)_2$ ($75\ \mu\text{M}$), and (C) $5.18^{2+}(\text{ClO}_4^-)_2$ ($75\ \mu\text{M}$) as the guest salts. The intensities have been maximized by switching on the acceleration voltage to $-10\ \text{V}$ (for details see text).

5.5.4 Ion-Pairing in ESI-MS Experiments

Interestingly, the absolute intensity of the $[5.18^{2+}@5.15\cdot5.15]$ signal increased substantially upon performing collisional activation of the ions at acceleration voltages of

-10 to -20 V. (In comparison, the spectra of the triethylbenzene flexiballs did not change at all when subjected to collisions.) We believe that this finding results from ion pair encapsulation. In the electrospray process, singly charged complexes [(5.18²⁺ ClO₄⁻)@5.15•5.15] could be formed and would possess an *m/z* far beyond the mass range of the spectrometer. However, collisional activation could eject the remaining small anion through one of the holes in the capsule walls. This escape produces [5.18²⁺@5.15•5.15] and magnifies the intensity of the small signal already present in the absence of collisions. In contrast, the cavity volume of the benzene flexiballs is roughly half that of the cavitand flexiball. Therefore, the ammonium ions occupy the vast majority of available space and the dications are formed more easily during the normal electrospray process (i.e. without collisions).

5.6 Experimental

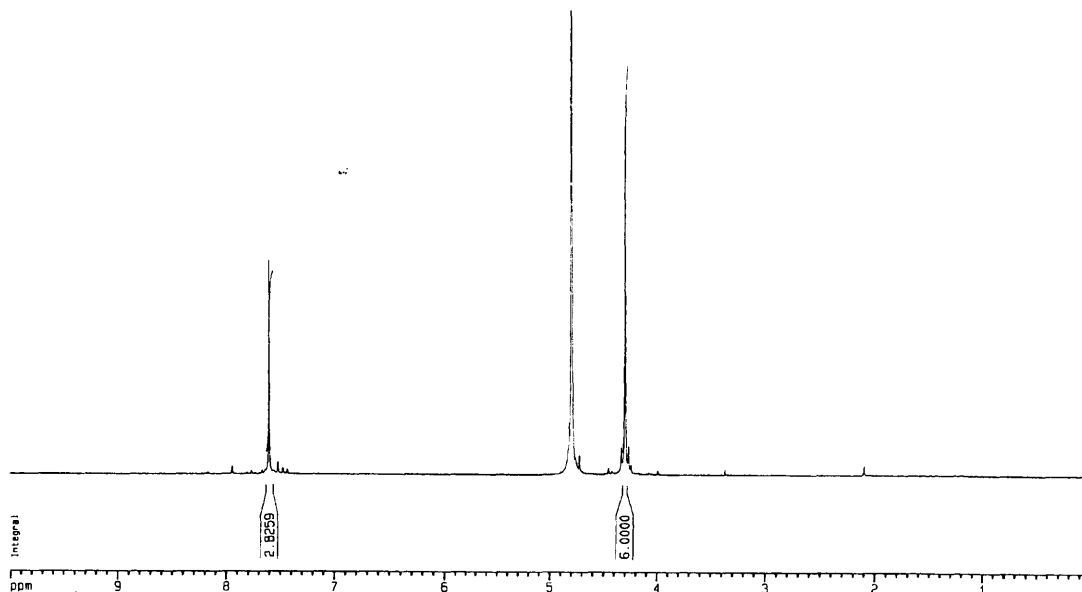
5.6.1 Apparatus, Materials, and Methods.

MS encapsulation and competition experiments performed were carried out using standard techniques.³⁵ For all other experimental details, see section 2.5.1.

5.6.2 Procedures (¹H NMR spectra follow each preparation.)

Triamine Spacer (5.2).² Ground and oven-dried (150 °C, 3 d) 1,3,5-tricarboxamidobenzene (3.82 g, 18.44 mmol) was mixed with 140 mL of 1M BH₃ in THF under anhydrous conditions (N₂) and then refluxed for 6 d. Dry THF was added occasionally to maintain solvent level. After this time, the mixture was cooled to 0 °C and concentrated HCl (15 mL) was added slowly with stirring. The mixture was then brought to reflux for another 3 h followed by removal of the THF *in vacuo*. The residue was thoroughly triturated with H₂O and filtered followed by evaporation of the filtrate.

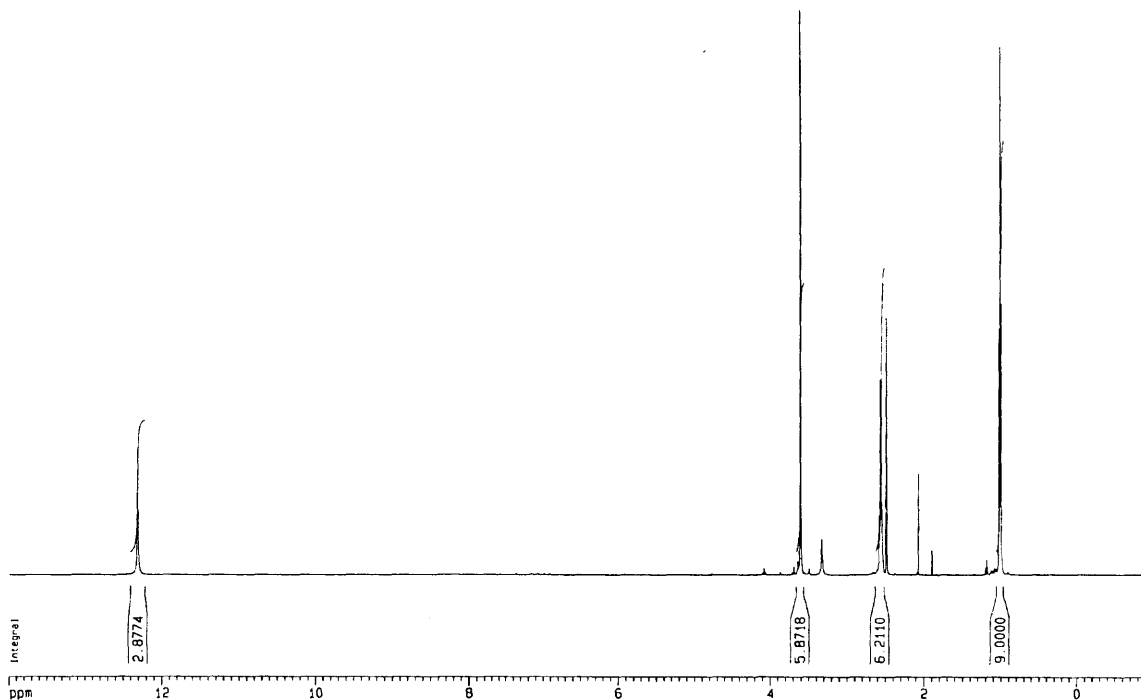
This residue was diluted with MeOH (50 mL), the MeOH removed by evaporation, and the process repeated three more times to volatilize all borates. A minimum of MeOH (10 mL) was used to dissolve the crude product followed by addition of EtOH (25 mL) and ether (200 mL) which gave a white precipitate that was < 90% pure by ^1H NMR. The precipitate was then dissolved in 3N KOH (100 mL), washed with EtOAc (3 x 100 mL), and the combined organic phases concentrated to 50 mL. This solution was saturated with HCl gas and then left overnight in the refrigerator which produced white flakes isolated by filtration. Yield: 0.51 g (10%). ^1H NMR (D_2O , 600 MHz) δ 7.61 (s, 3H), 4.3 (s, 6H) ppm; ^{13}C NMR (D_2O , 151 MHz) δ 134.74, 129.81, 42.04 ppm; HRMS (FAB): Calc'd for $[\text{M}+\text{H}]^+$ $\text{C}_9\text{H}_{16}\text{N}_3$ 166.1344, found 166.1349.



Monomer (5.1). Acid module **4.20** (1.15 g, 2.00 mmol), triamine **5.2** (0.11 g, 0.40 mmol), PyBOP (1.04 g, 2.00 mmol), and NEt_3 (0.56 mL, 4.00 mmol) were mixed in 20 mL DMF for 24 h at room temperature. The solvent was removed in vacuo and the residue taken up in EtOAc (40 mL). Washing this solution with 1M HCl (2 x 40 mL)

followed by drying (Na_2SO_4), filtering, and evaporation gave a brown foam. Two purifications by flash chromatography (0 -> 15% MeOH/ CH_2Cl_2) gave an off-white foam which was triturated thoroughly with MeOH. Filtration provided a clean, white powder. Yield: 0.27 g (36%). ^1H NMR ($\text{DMSO-}d_6$, 600 MHz) δ 8.75 (t, 3H, $J = 5.7$ Hz), 8.34 (s, 6H), 7.00 (d, 6Har, $J = 8.1$ Hz), 6.93 (m, 9Har), 6.90 (d, 6Har, $J = 8.2$ Hz), 6.84 (d, 6Har, $J = 8.2$ Hz), 4.17 (d, 6H, $J = 5.3$ Hz), 3.96 (dd, 6H, $J = 13.6, 3.9$ Hz), 2.84 (m, 6H), 2.40 (m, 15H), 1.38 (m, 12H), 1.24 (m, 36H), 1.14 (m, 12H), 0.85 (m, 18H) ppm; ^{13}C NMR ($\text{DMSO-}d_6$, 600 MHz) δ 170.02, 158.65, 142.32, 142.05, 139.39, 134.63, 131.25, 128.08, 127.35, 127.15, 125.00, 81.56, 78.12, 41.89, 40.11, 40.05, 38.53, 34.65, 34.61, 31.32, 31.31, 30.99, 30.83, 28.62, 28.54, 28.46, 22.19, 22.14, 13.94 ppm; IR (CDCl_3) 3392.04, 3280.44, 2955.17, 2925.37, 2854.28, 1720.67, 1686.10, 1549.23, 1466.79, 1445.38, 1378.69, 1229.84, 1105.70 cm^{-1} ; HRMS (FAB) Calc'd for $[\text{M}+\text{Cs}]^+$ $\text{C}_{111}\text{H}_{147}\text{N}_{15}\text{O}_9\cdot\text{Cs}^+$ 1967.0561, found 1967.0713. [For ^1H NMR spectrum, see Figure 5-2A.]

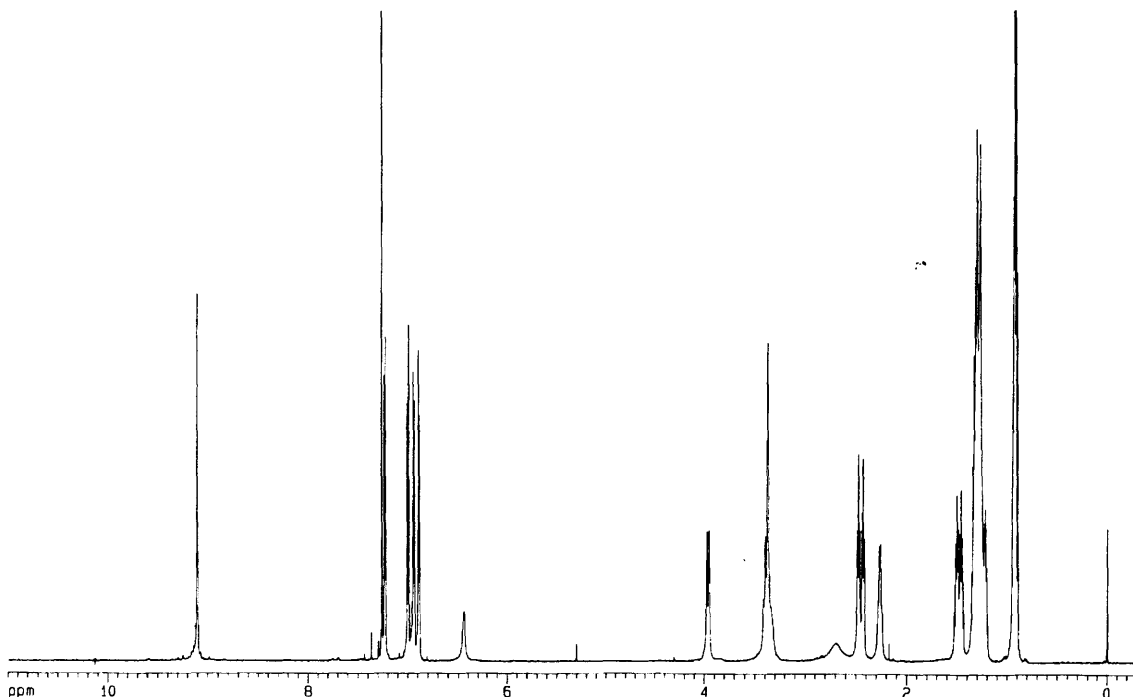
Triacid Spacer (5.8). Trinitrile **5.7** (0.28 g, 1.00 mmol) was mixed in conc. HCl (10 mL) and glacial acetic acid (10 mL). The mixture was refluxed overnight, cooled to rt, and the volatiles removed by rotary evaporation. The residue was triturated with acetone and the resulting white precipitate collected by filtration. Yield: 0.31 g (92%). ^1H NMR ($\text{DMSO-}d_6$) δ 12.32 (s, 3H), 3.62 (s, 6H), 2.57 (q, 6H, $J = 15.0, 7.4$ Hz), 1.03 (t, 9H, $J = 7.5$ Hz) ppm; ^{13}C NMR ($\text{DMSO-}d_6$, 151 MHz) δ 173.34, 140.89, 129.44, 34.78, 23.06, 14.06 ppm; HRMS (FAB) Calc'd for $[\text{M}+\text{Na}]^+$ $\text{C}_{18}\text{H}_{24}\text{O}_6\cdot\text{Na}^+$ 359.1471, found 359.1466.



Amide Ball Monomer (5.9). Triamine **5.6** (0.05 g, 0.20 mmol), acid module **4.20** (0.57 g, 1.00 mmol), HOBt (0.14 g, 1.00 mmol), and EDC (0.19 g, 1.00 mmol) were mixed in 20 mL dry DMF under N₂ atm. To this mixture was added NEt₃ (140 μL, 1.00 mmol) and the solution was stirred at rt for 6 h. The solvent was removed *in vacuo* and the filtrate taken up in EtOAc (50 mL). This solution was washed with 1M HCl_(aq.) (2 x 15 mL), dried with Na₂SO₄, filtered, and evaporated to give an off-white foam. This residue was subjected to flash chromatography (0 → 5% MeOH/CH₂Cl₂) and, after isolation, further purified by precipitation from a minimum of CHCl₃ (3 mL) with MeOH (15 mL). Filtration gave a white powder. Yield: 0.26 g (68%). ¹H NMR (CDCl₃, 600 MHz) δ 8.87 (s, 12H), 7.19 (d, 12Har, *J* = 8.3 Hz), 6.98 (d, 24Har, *J* = 8.1 Hz), 6.93 (d, 12Har, *J* = 8.0 Hz), 5.47 (s, 6H), 4.21 (s, 12H), 4.13 (dd, 12H, *J* = 14.2, 3.4 Hz), 3.12 (t, 12H, *J* = 12.9 Hz), 2.48 (m, 42H), 1.51 (m, 24H), 1.30 (m, 96H), 1.06 (t, 18H, *J* = 7.6 Hz), 0.92 (m, 36H) ppm; ¹³C NMR (CDCl₃, 151 MHz) δ 170.42, 161.03, 144.17, 143.87,

143.81, 133.89, 131.72, 130.97, 128.64, 128.36, 127.77, 127.58, 82.91, 80.17, 41.01, 40.89, 37.94, 35.57, 32.02, 31.53, 31.43, 29.84, 29.33, 29.25, 23.30, 22.87, 22.85, 16.35, 14.26 ppm; MS (MALDI) a) (monomer) Calc'd for [M_{avg}] C₁₁₇H₁₅₉N₁₅O₉ 1920, found 1922, b) (dimer) Calc'd for [M_{avg}] C₂₃₄H₃₁₈N₃₀O₁₈ 3839, found 3842. [For ¹H NMR spectrum, see Figure 5-5A. For other MS results, see text.]

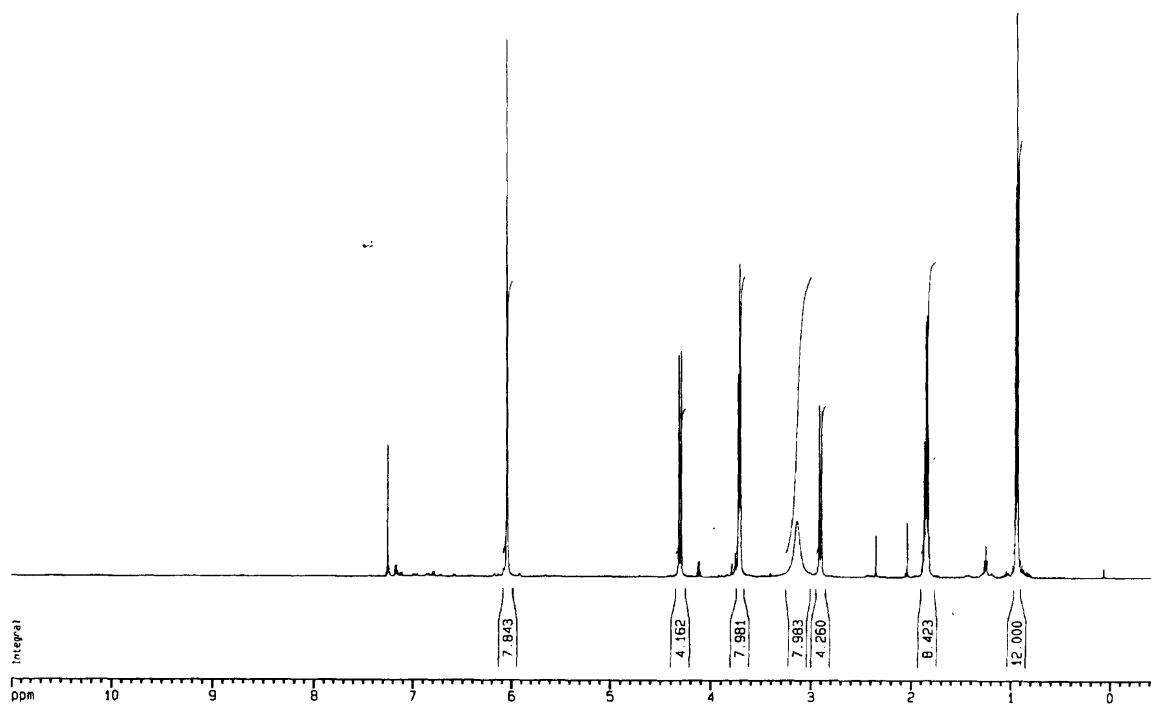
Inverted Amide Ball Monomer (5.10). Triacid **5.8** (0.67 g, 0.20 mmol), amine module **4.25** (0.55 g, 1.00 mmol), HOBt (0.14 g, 1.00 mmol), and EDC (0.19 g, 1.00 mmol) were mixed in 20 mL dry DMF under N₂ atm. To this mixture was added NEt₃ (140 μL, 1.00 mmol) and the solution was stirred at rt for 24 h. The solvent was removed *in vacuo* and the filtrate taken up in CH₂Cl₂ (50 mL). This solution was washed with 1M HCl_(aq.) (2 x 15 mL), dried with Na₂SO₄, filtered, and evaporated to give an off-white foam. This residue was subjected to flash chromatography (0 -> 7% MeOH/CH₂Cl₂) which gave a white powder after isolation. Yield: 0.19 g (49%). ¹H NMR (CDCl₃, 600 MHz) δ 9.10 (s, 12H), 7.22 (d, 12Har, *J* = 8.2 Hz), 7.00 (d, 12Har, *J* = 8.1 Hz), 6.94 (d, 12Har, *J* = 8.2 Hz), 6.89 (d, 12Har, *J* = 8.1 Hz), 6.49 (s, 6H), 3.96 (m, 12H), 3.39 (m, 30H), 2.48 (t, 12H, *J* = 7.6 Hz), 2.43 (t, 12H, *J* = 7.7 Hz), 2.27 (m, 12H), 1.48 (m, 24H), 1.28 (m, 96H), 0.92 (m, 54H) ppm; MS (ESI) see text.



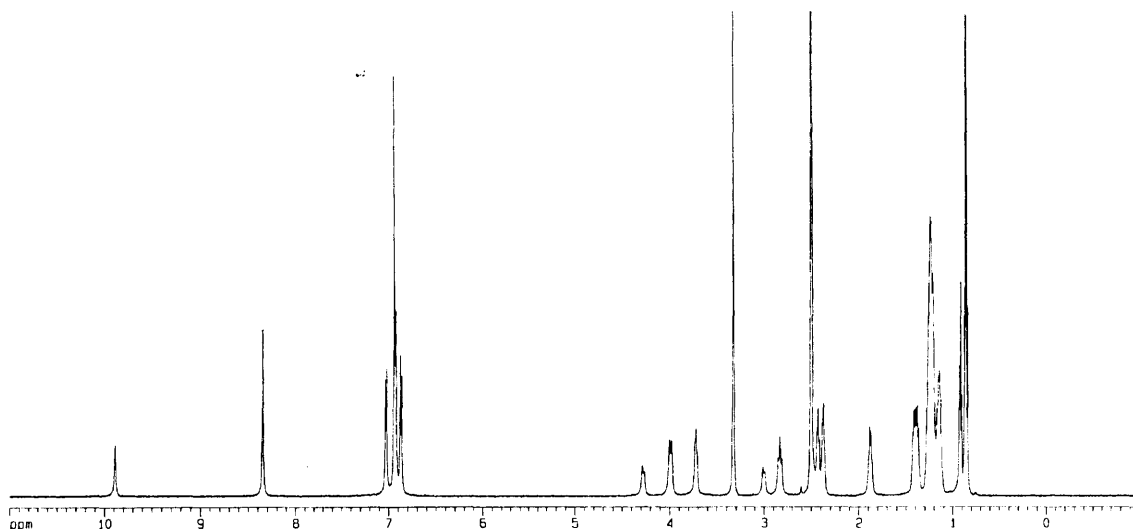
Ester Ball Monomer (5.11). Tribromide **5.4** (0.88 g, 0.20 mmol), acid module **4.20** (0.57 g, 1.00 mmol), Cs₂CO₃ (0.33 g, 1.00 mmol), CH₃CN (20 mL), and DMF (20 mL) were mixed at 100 °C for 2 h. After cooling, the solvents were removed by evaporation and the residue taken up in CH₂Cl₂ / *t*-BuOH (4:1, 25 mL). Washing with 1M HCl_(aq.) and drying with Na₂SO₄ followed by filtration and evaporation gave a brown foam. This residue was subjected to flash chromatography (0 → 5% MeOH/CH₂Cl₂) and, after isolation, further purified by precipitation from a minimum of CHCl₃ (3 mL) with MeOH (15 mL). Filtration gave a white powder. Yield: 0.20 g (52%). ¹H NMR (CDCl₃, 600 MHz) δ 8.90 (s, 12H), 7.23 (d, 12Har, *J* = 8.1 Hz), 6.97 (m, 24H), 6.91 (d, 12Har, *J* = 8.0 Hz), 4.99 (s, 12H), 4.27 (dd, 12H, *J* = 14.0, 3.8 Hz), 2.96 (t, 12H, *J* = 12.9 Hz), 2.84 (m, 6H), 2.50 (m, 36H), 1.50 (m, 24H), 1.30 (m, 96H), 1.05 (t, 18H, *J* = 7.7 Hz), 0.92 (m, 36H) ppm; ¹³C NMR (CDCl₃, 151 MHz) δ 172.22, 160.55, 146.91, 143.60, 143.46, 134.64, 131.38, 129.48, 128.52, 128.24, 127.89, 127.70, 82.64, 79.90, 60.58,

40.15, 38.24, 35.58, 35.57, 32.01, 31.53, 31.47, 29.36, 29.33, 29.26, 23.17, 22.85, 16.32, 14.25 ppm; MS (ESI) see text. [For ^1H NMR spectrum, see Figure 5-7A.]

Tetraamino Calixarene (5.12). 5,11,17,23-Tetranitro-25,26,27,28-tetrapropoxy-calix[4]arene²³ (0.50 g, 0.65 mmol) was suspended in 50 mL toluene with efficient stirring. A 2 mL aliquot of Raney Nickel (50% slurry in H_2O) was placed in a small test tube, washed with 3 x 5 mL EtOH and 3 x 5 mL toluene, and transferred to the reaction flask with some toluene. The air in the flask was removed under aspirator, replaced with hydrogen, and this process repeated twice more. While under 1 atm H_2 , the mixture was brought to 40 °C and stirred for 3 h. After cooling to rt, the supernatant was removed and filtered through packed celite. A slightly crude, off-white foam was isolated after evaporation. Yield: 0.251 g (59%). ^1H NMR (CDCl_3 , 600 MHz) δ 6.06 (s, 8H), 4.31 (d, 4H, $J = 13.22$ Hz), 3.73 (t, 8H, $J = 7.46$ Hz), 3.15 (s, 8H), 2.92 (d, 4H, $J = 13.25$ Hz), 1.86 (m, 8H), 0.95 (t, 12H, 7.44 Hz) ppm.



Calixarene Ball Monomer (5.13). Tetraaminocalixarene **5.12** (0.10 g, 0.15 mmol), acid module **4.20** (0.35 g, 0.61 mmol), and PyBOP (0.32 g, 0.61 mmol) were mixed in dry CH₂Cl₂ (50 mL) followed by addition of dry (Aldrich Sure-Seal) iPr₂NEt (214 μL, 1.23 mmol) under anhydrous conditions (N₂). After stirring 18 h at rt, TLC (10% MeOH / CH₂Cl₂) indicated complete consumption of **5.12**. More CH₂Cl₂ (100 mL) was added and the solution washed with brine (100 mL), 1 M HCl_(aq.) (3 x 100 mL), and saturated NaHCO_{3(aq.)} (2 x 100 mL). The organic layer was dried with Na₂SO₄, filtered, and concentrated by evaporation. The resulting brown residue was sonicated thoroughly with MeOH, filtered, and the precipitate was collected. Dissolving the precipitate in a minimum of CHCl₃ (3 mL), precipitation with CH₃CN (25 mL), sonication of the precipitate, and filtration gave an off-white powder. Yield: 0.23 g (52%). ¹H NMR (DMSO-d₆, 600 MHz) δ 9.88 (s, 4H), 8.34 (s, 8H), 7.03 (d, 8Har), 6.93 (m, 24Har), 6.87 (d, 8Har, *J* = 8.3 Hz), 4.28 (d, 4H, *J* = 12.1 Hz), 3.99 (m, 8H), 3.73 (m, 8H), 3.00 (d, 4H, *J* = 11.3 Hz), 2.83 (t, 8H, *J* = 12.6 Hz), 2.43 (t, 8H, *J* = 7.5 Hz), 2.38 (t, 8H, *J* = 7.4 Hz), 1.88 (m, 8H), 1.40 (m, 16H), 1.22 (m, 64H), 0.92 (t, 12H, *J* = 7.4 Hz), 0.86 (m, 24H) ppm; ¹³C NMR (DMSO-d₆, 151 MHz) δ 168.58, 158.83, 152.18, 142.49, 142.26, 134.83, 134.19, 132.81, 131.36, 128.19, 127.51, 127.33, 120.07, 81.65, 78.15, 76.64, 34.63, 34.54, 31.35, 31.26, 30.90, 30.84, 28.63, 28.48, 28.39, 22.54, 22.16, 22.09, 13.88, 13.86, 10.03 ppm; MS (MALDI) Calc'd for [Mavg] C₁₇₆H₂₂₈N₂₀O₁₆ 2878, found 2878.



Cavitand Ball Monomer (5.15). A mixture of the tetrahydroxy cavitand **5.14**²⁶ (0.597 g, 0.48 mmol) and acid module **4.20** (1.112 g, 1.94 mmol, 4 equiv.) was dried in high vacuum for two hours. The mixture was then dissolved in 120 mL of dichloromethane and treated with PyBOP (1.07 g, 1.94 mmol, 4 equiv.) and Et₃N (0.54 mL). The mixture was stirred at room temperature under nitrogen overnight and then quenched with brine and extracted with ethyl acetate. The organic layer was washed with 2 N hydrochloric acid twice, sat'd. sodium bicarbonate solution twice, and with brine. The organic layer was dried over MgSO₄ and concentrated. Column chromatography (80% EtOAc/Hex) gave the desired compound. Yield: 0.795 g (48%). ¹H NMR (acetone-d₆, 600 MHz) δ 9.097 (s, 16 H), 7.425 (s, 8 H), 7.419 (d, *J* = 7.3 Hz, 16 H), 7.113 (d, *J* = 7.3 Hz, 16 H), 7.074 (d, *J* = 8.0 Hz, 16 H), 7.047 (d, *J* = 8.0 Hz, 16 H), 5.903 (m, 8 H), 4.635 (t, *J* = 8.0 Hz, 8 H), 4.461 (m, 8 H), 4.361 (d, *J* = 11.7 Hz, 16 H), 3.248 (m, 8 H), 3.054 (m, 16 H), 2.610 (t, *J* = 7.6 Hz, 16 H), 2.524 (t, *J* = 7.7 Hz, 16 H), 2.275 (m, 16 H), 1.613 (m, 16 H), 1.531 (m, 16 H), 1.34 – 1.22 (m, 272 H), 0.918 (m, 48 H), 0.844 (m, 24 H) ppm; MS (MALDI) Calc'd for C₂₁₂H₂₈₈N₁₆O₂₄⁺ [M+H]⁺ 3446, found 3446. [For ¹H NMR spectrum, see Figure 5-12.]

Chapter 6 **Ferric Iron Sequestering Agents**

6.1 Introduction

As discussed in Chapter 1, most supramolecular capsules utilize hydrogen bond networks for assembly. While nature relies heavily upon hydrogen bonds in many biological structures, other intermolecular forces also make significant contributions to structure and function. Coulombic, hydrophobic, and metal-ligand interactions all play important roles in large biomolecules. In order to mimic the rich functional diversity of such systems, synthetic capsules must incorporate these interactions as well. This chapter briefly examines a new class of iron-sequestering agents as an introduction to related capsules incorporating both metal-ligand interactions and hydrogen bonds.

A limiting factor in the growth of many microorganisms is the supply of iron, a key component in many cellular oxidation and reduction processes. For instance, intestinal bacteria require exterior ferric iron concentrations of at least 5×10^{-7} M in order to survive. However, the near insolubility of iron hydroxide at physiological pH provides a much lower equilibrium concentration of free iron ($[\text{Fe}^{3+}] \approx 10^{-18}$). Therefore, bacteria secrete iron-sequestering agents, called siderophores, which extract iron from the surrounding environment and return it to the microbe.¹

¹ Vögtle, F. *Supramolecular Chemistry*; John Wiley and Sons: New York, 1993; pp 84-106.

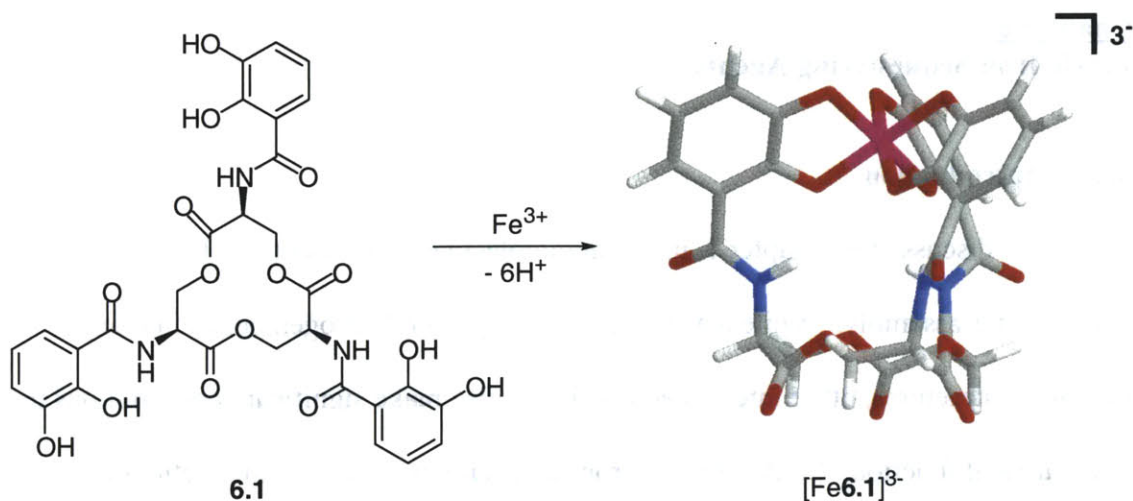


Figure 6-1. Structural diagram of enterobactin **6.1** and calculated structure of complex $[\text{Fe6.1}]^{3-}$.

Of the roughly 200 natural siderophores characterized, enterobactin **6.1** has been the most heavily studied (Figure 6-1).² Enterobactin is composed of a cyclic triester of L-serine functionalized with three catecholamides and, although no crystal structure exists for the ferric iron complex, numerous studies³ support a structure similar to the model shown in Figure 6-1.⁴ The formation constant for this complex ($K_f \approx 10^{49}$) is extremely high and surpasses that for any known iron chelator. Given this fact and the importance of siderophores to a variety of pathogens, enterobactin has served as the primary model for a variety of synthetic siderophores. Used in the study of membrane receptors for enterobactin, these analogs may eventually lead to a new class of antibiotics.¹

Iron chelation therapy represents another potential use for synthetic siderophores. Adult humans contain approximately 4–5 grams of iron held within a variety of proteins

² For reviews of these studies, see: (a) Raymond, K.N. *Pure Appl. Chem.* **1994**, *66*, 773-781 and (b) Raymond, K.N. Cass, M.E.; Evans, S.L. *Pure Appl. Chem.* **1987**, *59*, 771-778.

³ Karpishin, T.B.; Raymond, K.N. *Angew. Chem. Int. Ed. Engl.* **1992**, *31*, 466-468 and references therein.

⁴ All structural models were created as described in section 7.2.

such as hemoglobin and ferritin.⁵ However, despite the body's heavy dependence upon iron, larger amounts are toxic. Common causes of excessive iron levels include vitamin overdosing (especially in young children) and the regular blood transfusions required by patients with refractory anemias. Since the body can only remove a maximum of one milligram of iron per day, iron levels accumulate in such patients. Heart, liver, and pancreatic damage result and death eventually occurs due to cardiac failure or arrhythmia. One drug, deferoxamine, is currently approved to treat iron poisoning, but its significant shortcomings (i.e. prohibitive cost and intravenous administration) make the development of alternatives compelling.⁶

We identified several C_3 -symmetric platforms which, if properly functionalized, could serve as useful iron-sequestering agents.⁷ Using computer modeling,⁴ ligands capable of binding ferric iron as octahedral complexes were designed. The syntheses of these ligands and preliminary binding studies are reported here.

6.2 Truxene-Based Ligand

Truxene **6.2** served as the platform for the first ligand. Previously, we considered truxene an attractive spacer for self-assembling capsules, but the inability to introduce substituents solely in a *syn* fashion was a concern.⁸ Recently, however, an efficient protocol for the preparation of *syn*-trialkylated truxenes was reported, so we adapted this method for the synthesis of a truxene-based ligand (Figure 6-2). Alkylation of truxene using 3-bromomethylveratrole proceeded smoothly to give triveratrole **6.3** as a mixture of

⁵ Stryer, L. *Biochemistry*, 3rd ed.; W.H. Freeman: New York, 1988.

⁶ Hoffbrand, A.V. *J. Lab. Clin. Med.* **1998**, *131*, 290-291.

⁷ For a review of C_3 symmetric receptors, see: Moberg, C. *Angew. Chem. Int. Ed. Engl.* **1998**, *37*, 248-268.

syn and *anti* isomers. After refluxing this mixture with base in tert-butanol, the *syn* isomer was easily isolated in good yield. Boron tribromide demethylation gave a racemic mixture of tricatechol ligand **6.4** in quantitative yield.

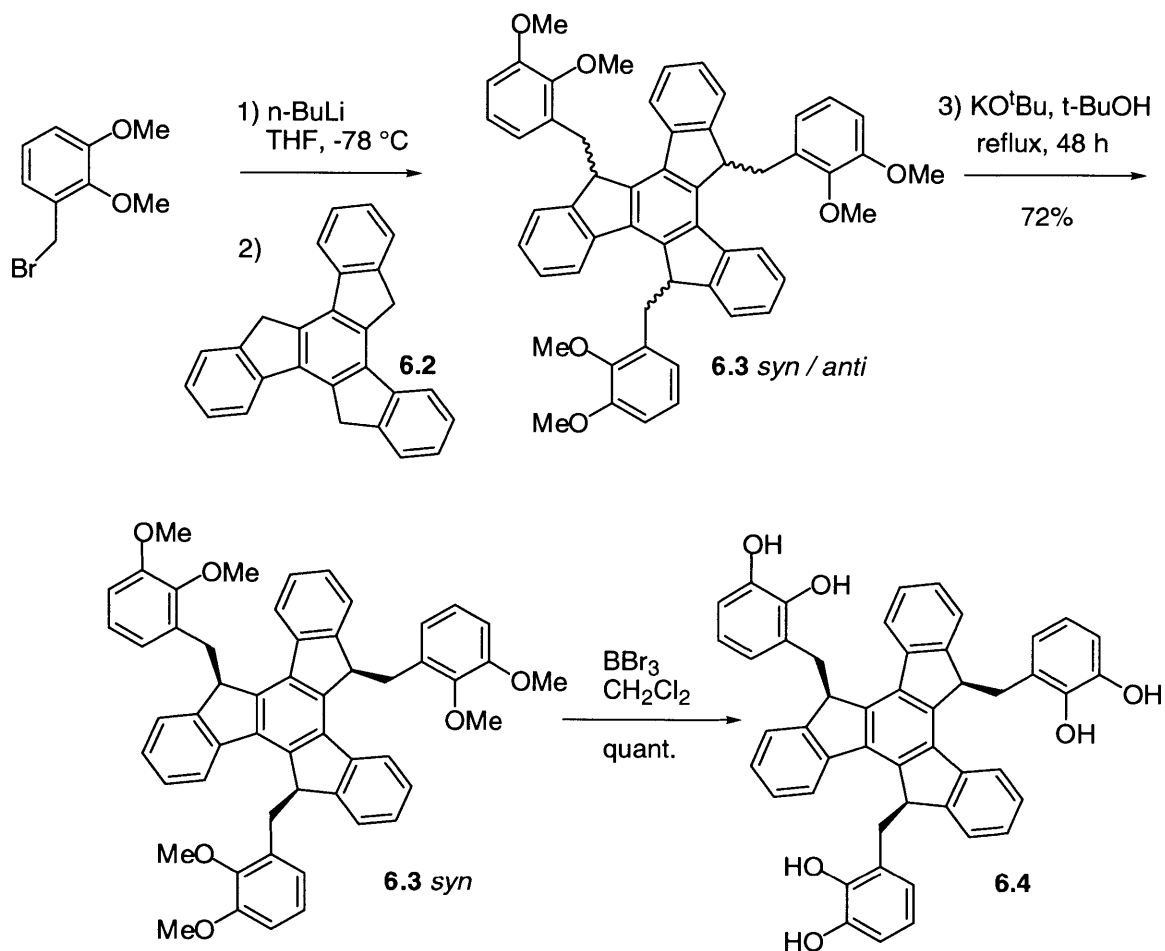


Figure 6-2. Synthesis of truxene-based ligand **6.4**.

Various NMR experiments with ligand **6.4** and gallium(III)⁹ gave inconclusive results due to complex precipitation. However, the iron(III) complex was synthesized as described in the Experimental section and easily detected by ESI-MS (Figure 6-3). The

⁸ Previous attempts to introduce substituents at the benzylic positions of truxene gave primarily *anti* isomers; see: (a) Dehmlow, E.V.; Kelle, T. *Synth. Commun.* **1997**, *27*, 2021 and (b) Sbrogio, F.; Fabris, F.; De Lucchi, O. *Synlett* **1994**, 761-762.

major peak in the spectrum corresponds to the mono-anion¹⁰ $2\text{H}^+\cdot[\text{Fe6.4}]^{3-}$ and only a trace peak remains for the free ligand. Given these results, we speculate that ligand **6.4** forms a complex with ferric iron similar to the calculated model shown in the figure.¹¹

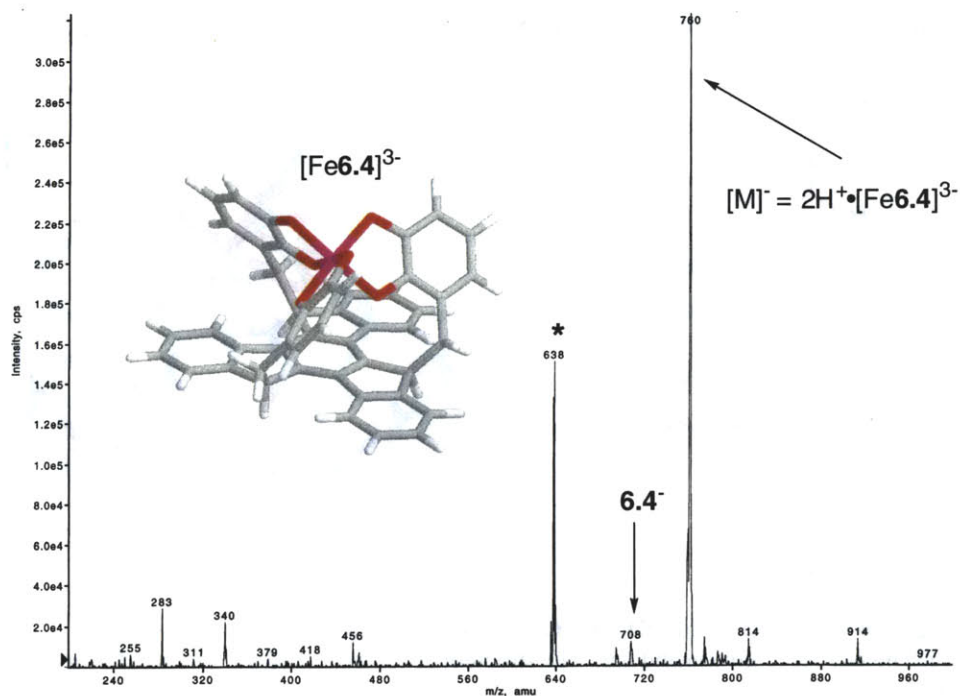


Figure 6-3. Negative ESI mass spectrum and calculated structure [see ref. 11] of complex $[\text{Fe6.4}]^{3-}$. Only trace amounts of the free ligand (mono-deprotonated **6.4**) remain. The peak denoted with an asterisk is an unknown impurity.

6.3 Pseudopeptide-Based Ligand

Recently, our group introduced the pseudopeptide platform **6.5** with C_3 symmetry.¹² Intramolecular hydrogen bonds confer some rigidity to this platform and enforce a bowl shape with side chains all presented above the face of the molecule.

⁹ Gallium(III) is generally used instead of iron(III) in NMR studies of catechol-ligand complexes because the former produces diamagnetic complexes while the iron complexes are paramagnetic.

¹⁰ Ligand-metal complexes will be designated according to the following generalization: positive counterion·[metal **ligand**_n]·negative counterion. For simplicity, this labeling scheme does not change when protons are lost upon complex formation.

While reminiscent of the enterobactin core, platform **6.5** is larger and modeling predicted that introducing the ligands used in enterobactin (2,3-catecholamides) onto **6.5** would produce a poor mimic. However, 3,4-catecholamides provide adequate ligand spacing and the calculated structure of the corresponding iron complex is shown in Figure 6-4.

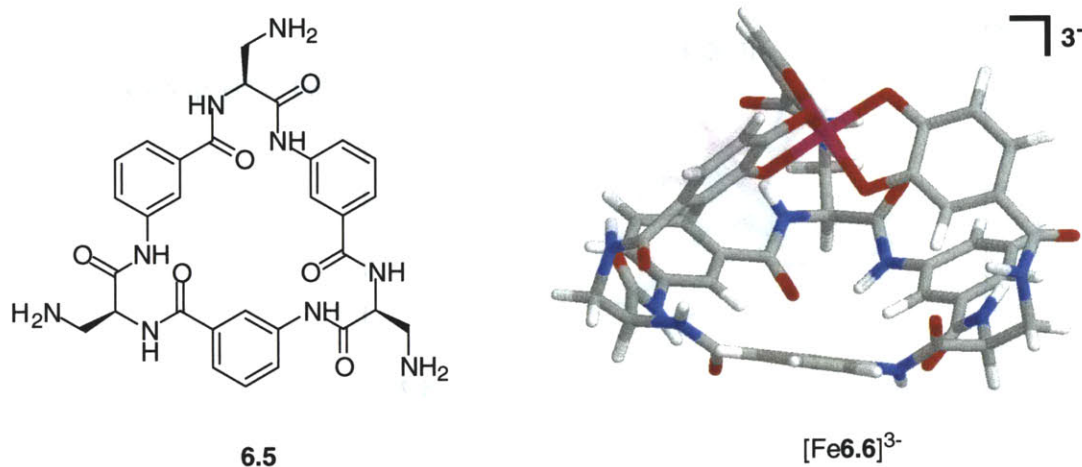


Figure 6-4. Pseudopeptide platform **6.5** can be functionalized with three 3,4-catecholamides to give ligand **6.6**. The structure of complex $[\text{Fe6.6}]^{3-}$ predicted from modeling is shown.

Figure 6-5 illustrates our progress toward the synthesis of ligand **6.6**. We chose acetate protecting groups for the catechol units in order to avoid harsh deprotection conditions. Given that catechol-containing compounds can be unstable and the limited availability of platform **6.5**, we postponed the removal of these protecting groups until the commencement of animal trials (*vide infra*).

¹¹ Since ligand **6.4** exists as a racemic mixture and the ferric iron complex can form a right- or left handed helix, complex $[\text{Fe6.4}]^{3-}$ is expected to exist as a mixture of diastereomers. A diastereomer containing a right-handed (or Δ) helix is shown in Figure 6-3.

¹² Rasmussen, P.H.; Rebek, J., Jr. *Tetrahedron Lett.* **1999**, *40*, 3511-3514.

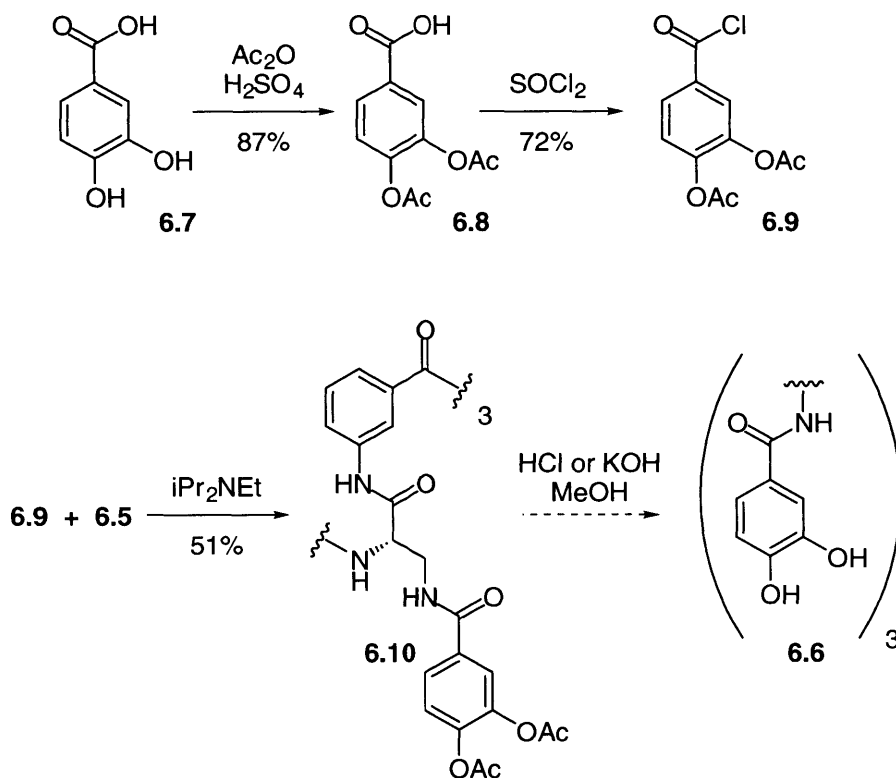


Figure 6-5. Synthesis of ligand 6.6.

6.4 Triphenylene-Based Ligand

Platform 6.11, described recently by our group, contains the familiar triphenylene and possesses C_{3v} symmetry (Figure 6-6).¹³ This platform is exceptionally rigid and points substituents directly toward the C_3 axis of the molecule. As with the pseudopeptide platform, triphenylene 6.11 is larger than enterobactin and must be substituted with 3,4-catecholamides in order to form an octahedral iron complex. The partial synthesis of ligand 6.14 starting from 6.11 is shown in Figure 6-6. We again retained the acetate protecting groups until ready to perform further studies.

¹³ Platform 6.11 was synthesized analogously to other triphenylene platforms as described in Waldvogel, S.R.; Wartini, A.R.; Rasmussen, P.H. Rebeck, J., Jr. *Tetrahedron Letters* 1999, 40, 3515-3518. (Dr. Siegfried Waldvogel, unpublished results)

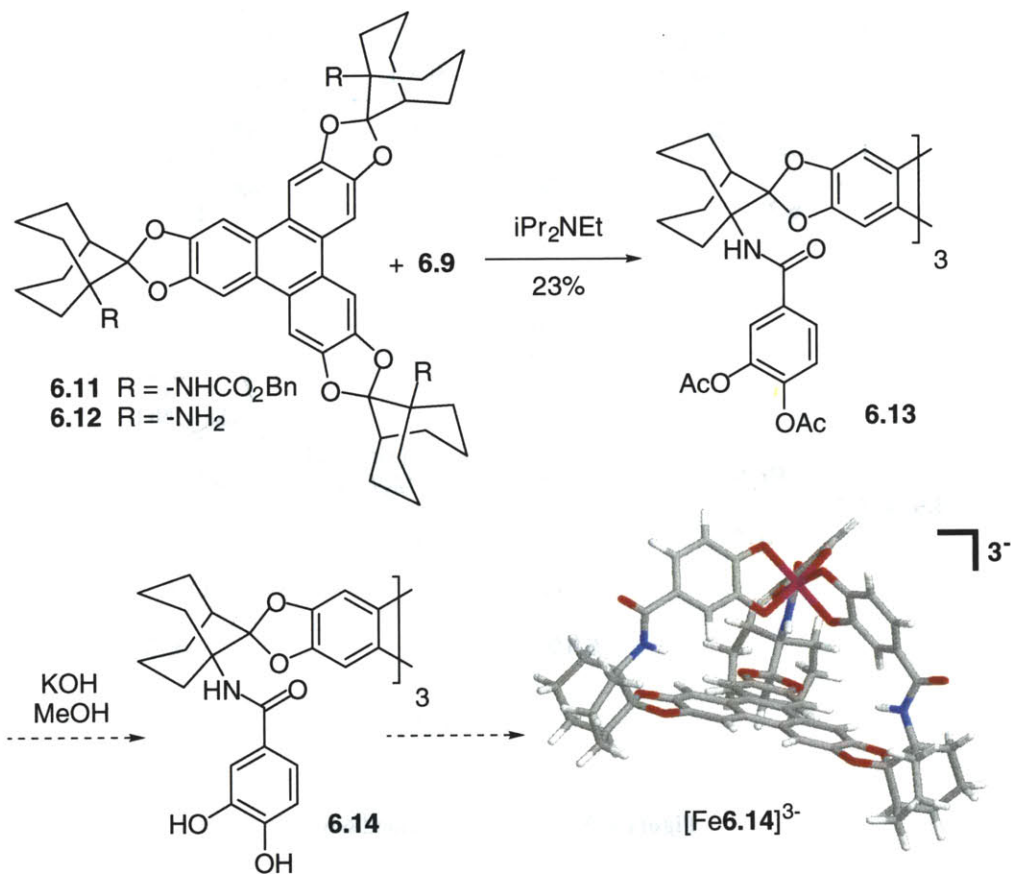


Figure 6-6. Synthesis of ligand 6.14 and calculated structure of complex [Fe6.14]³⁻.

6.5 Future Work

In the near future, animal studies using these novel agents will begin in collaboration with other groups at Scripps. After feeding rats these compounds, their urine and feces will be analyzed by mass spectrometry to determine if the ligands or, hopefully, the corresponding ferric iron complexes are secreted.¹⁴ If positive results are obtained, the toxicity and efficacy profiles of these compounds will be evaluated in rat models as well.

¹⁴ Harrison, P.M.; Arosio, P. *Biochim. Biophys. Acta* **1996**, *1275*, 161-203.

6.6 Experimental

6.6.1 Apparatus, Methods, and Materials

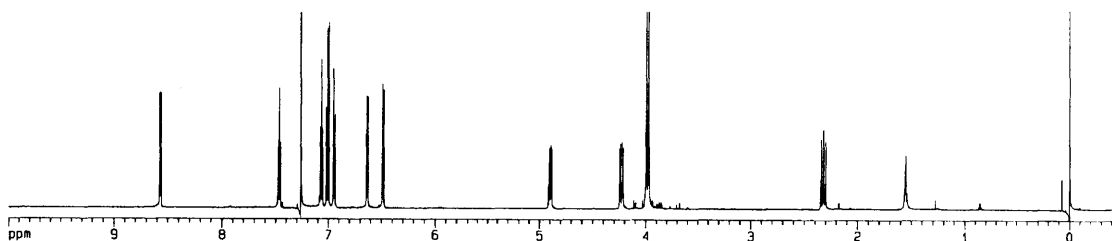
See section 2.5.1.

6.6.2 Procedures

Truxene triveratrole (6.3). Under anhydrous conditions, truxene **6.2** (2.00 g, 5.84 mmol) and THF (200 mL) were mixed at $-78\text{ }^{\circ}\text{C}$. While stirring the truxene mixture vigorously, n-BuLi [1.6 M in Hex] (11.3 mL, 18.11 mmol) was added dropwise *via* syringe. After 4 h, the temperature was gradually raised to $-10\text{ }^{\circ}\text{C}$ and the mixture became homogenous turning from orange to dark red. 3-Bromomethylveratrole¹⁵ (4.72 g, 20.44 mmol) was dissolved in THF (40 mL) and added dropwise to the truxene solution *via* an addition funnel. Following complete addition (5 min), the reaction flask was removed from its cooling bath and stirred at rt for 1 h. The resulting slurry was poured into EtOAc (500 mL), washed with brine (3 x 500 mL), dried (Na_2SO_4), and filtered. The filtrate was evaporated and dried under vacuum to give **6.3** (4.55 g, 98%) as a crude mixture of its *syn* and *anti* isomers. This was mixed with ^tBuOH (250 mL) and KO^tBu (1.28 g, 11.48 mmol) and the mixture was refluxed for 48 h. After cooling, roughly 200 mL of ^tBuOH was removed by rotary evaporation and the slurry was poured into 1M HCl_{aq.} (300 mL). Extraction with CH₂Cl₂ (400 mL), subsequent washing of the organic layer with 1M HCl_{aq.} (3 x 300 mL), drying (Na_2SO_4), and filtration gave a brown solution which was concentrated *in vacuo*. The residue was sonicated thoroughly using MeOH (200 mL) to give a homogenous precipitate which was collected by filtration. Repeating this trituration step gave **6.3** as dark yellow powder. Yield: 3.33 g (72%). ¹H NMR

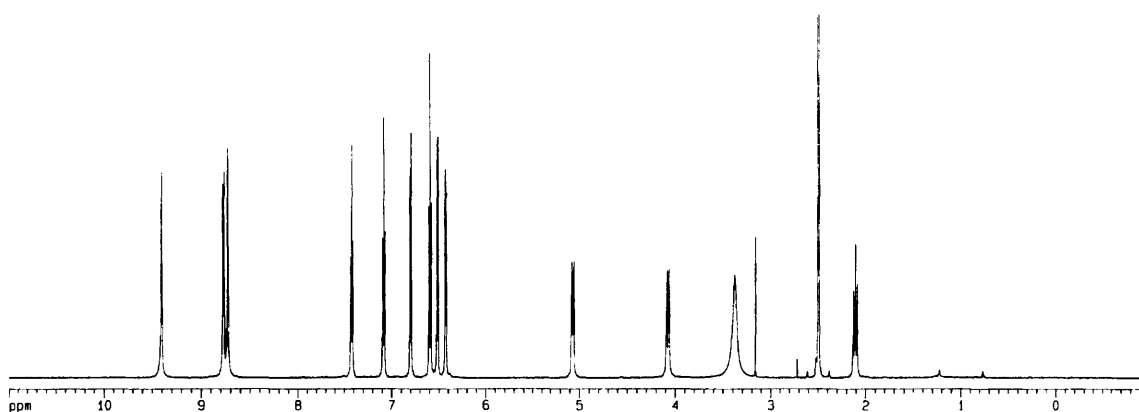
¹⁵ See compound 7.14.

(CDCl₃, 600 MHz) δ 8.57 (d, 3H, $J = 6.7$ Hz), 6.46 (m, 3H), 6.07 (m, 3H), 6.01 (t, 3H, $J = 6.8$ Hz), 6.94 (m, 3H), 6.63 (dd, 3H, $J = 6.5, 1.1$ Hz), 6.48 (d, 3H, $J = 6.4$ Hz), 4.90 (dd, 3H, $J = 11.6, 4.3$ Hz), 4.23 (dd, 3H, $J = 13.5, 4.4$ Hz), 3.99 (s, 9H), 3.98 (s, 9H), 2.32 (m, 3H) ppm; ¹³C NMR (CDCl₃, 151 MHz) δ 152.84, 148.21, 146.47, 141.94, 140.70, 136.30, 133.98, 126.37, 126.23, 125.48, 124.61, 123.51, 122.95, 111.18, 61.06, 56.01, 46.23, 35.29 ppm; IR (CDCl₃) 3036.90, 2932.57, 2828.90, 1583.81, 1472.80, 1428.30, 1296.90, 1268.27, 1222.69, 1076.80, 1008.08, 745.11 cm⁻¹; HRMS (FAB) Calc'd for [M+Cs]⁺ C₅₄H₄₈O₆•Cs⁺ 925.2505, found 925.2528.



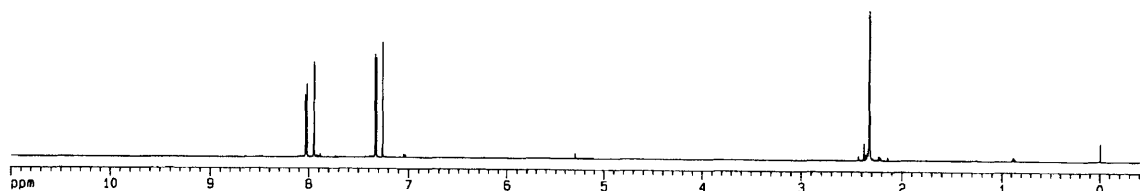
Truxene tricatechol (6.4). Under anhydrous conditions, triveratrole **6.3** (0.50 g, 0.63 mmol) was dissolved in CH₂Cl₂ (75 mL). Three freeze-pump-thaw cycles were performed to remove oxygen, then the solution was cooled to -78 °C. With efficient stirring, BBr₃ (1.25 mL, 13.24 mmol) was added dropwise over 1 min. The resulting black solution was allowed to slowly rise to rt and then stirred for an additional 48 h. The flask was cooled again to -78 °C and thoroughly sparged (N₂) MeOH (15 mL) was added dropwise over a few minutes. The bath was removed and the mixture stirred for 2h at rt. Under O₂ free conditions, volatiles were removed by evaporation and the dry residue taken up in sparged MeOH (30 mL). After refluxing the brown solution for 15 min, the volatiles were removed again by evaporation. This process was repeated a total of 12 times to remove all borates. The resulting brown residue was dried under high vacuum. [Note: tricatechol **6.4** decomposes slowly in solution, but is quite stable when

dry even in air.] Yield: 0.44 g (98%). ^1H NMR (DMSO- d_6 , 600 MHz) δ 9.41 (s, 3H), 8.78 (d, 3Har, $J = 6.8$ Hz), 8.73 (s, 3H), 6.42 (t, 3Har, $J = 6.5$ Hz), 6.09 (t, 3Har, $J = 6.4$ Hz), 6.80 (m, 3Har), 6.60 (t, 3Har, $J = 6.6$ Hz), 6.52 (d, 3Har, $J = 6.5$ Hz), 6.43 (d, 3Har, $J = 6.3$ Hz), 5.07 (dd, 3H, $J = 11.4, 3.8$ Hz), 4.08 (dd, 3H, $J = 13.4, 3.6$ Hz), 2.11 (t, 3H, $J = 12.7$ Hz) ppm; ^{13}C NMR (DMSO- d_6 , 151 MHz) δ 146.34, 144.98, 144.10, 141.31, 139.53, 135.80, 126.22, 126.44, 125.55, 125.32, 123.26, 122.41, 118.46, 114.03, 45.01, 35.14 ppm; HRMS (FAB) Calc'd for $[\text{M}+\text{Na}]^+ \text{C}_{48}\text{H}_{36}\text{O}_6 \cdot \text{Na}^+$ 731.2410, found 731.2388.



Ferric iron-truxene ligand complex ($[\text{Fe6.4}]^{3+} \cdot 3(\text{HNEt}_3)^+$). Truxene ligand **6.4** (10.0 mg, 0.014 mmol) and $\text{Fe}(\text{acac})_3$ (4.9 mg, 0.014 mmol) were dissolved in DMSO (15 mL). To this reddish solution was added ≈ 12 equiv. NEt_3 (24 μL , 0.17 mmol). After stirring briefly (2 min), the solution became darker. A sample for mass spectrometry was immediately prepared by removing a small aliquot (100 μL) of the solution and diluting it with MeOH (500 μL) to give a sample concentration of 150 μM . MS (ESI) Calc'd for $[\text{M}]^- (2\text{H}^+ \cdot [\text{Fe6.4}]^{3-}) \text{C}_{48}\text{H}_{32}\text{O}_6 \cdot \text{Fe}^-$ 760, found 760. [See Figure 6-3 for spectrum.]

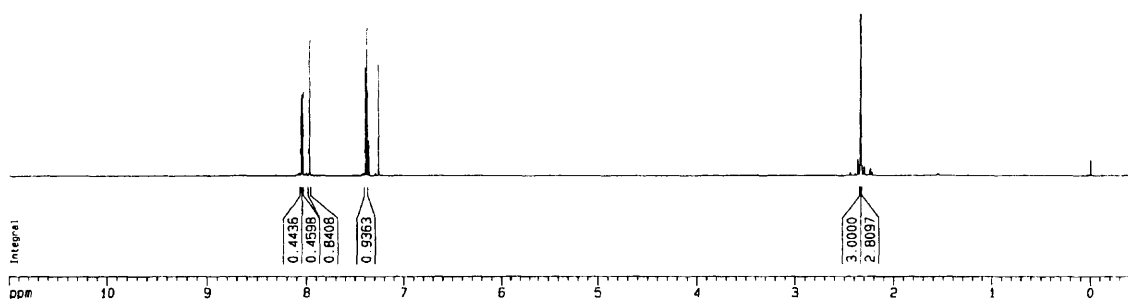
3,4-Diacetoxybenzoic acid (6.8).¹⁶ 3,4-Dihydroxybenzoic acid **6.7** (10.0 g, 64.88 mmol) and Ac₂O (13.5 mL, 142.74 mmol) were mixed vigorously under N₂ to give a fine slurry. Four drops of conc. H₂SO₄ were added and the slurry became a clear yellow solution. Within a few minutes, a thick white precipitate developed and ether (70 mL) was added. The resulting slurry was allowed to stir under N₂ for 16 h and then was poured over 200 g of ice. The mixture was extracted with CH₂Cl₂ (3 x 200 mL) and the combined organics were then washed with water (2 x 150 mL). Drying (Na₂SO₄), filtration, and concentration of the filtrate provided a yellowish precipitate. Trituration with hexane, cooling overnight, and filtration gave an off-white powder. Yield: 13.38 g (87%). ¹H NMR (CDCl₃, 600 MHz) δ 12.02 (broad s, 1H), 8.03 (dd, 1H, *J* = 8.6, 1.9 Hz), 6.95 (d, 1H, *J* = 2.2 Hz), 6.32 (d, 1H, *J* = 8.3 Hz), 2.33 (s, 3H), 2.32 (s, 3H) ppm; ¹³C NMR (CDCl₃, 151 MHz) δ 170.48, 168.21, 166.87, 146.93, 142.29, 129.01, 126.96, 125.92, 123.90, 20.92, 20.79 ppm; HRMS (FAB) Calc'd for [M+H]⁺ C₁₁H₁₁O₆⁺ 239.0556, found 239.0558.



3,4-Diacetoxybenzoyl chloride (6.9). Under anhydrous conditions, acid **6.8** (2.00 g, 8.40 mmol) and thionyl chloride (4.06 mL, 54.80 mmol) were heated at reflux overnight. The clear yellow solution was cooled to rt and volatiles were removed by rotary evaporation. The resulting oil was diluted with C₆H₆ (100 mL) and washed with

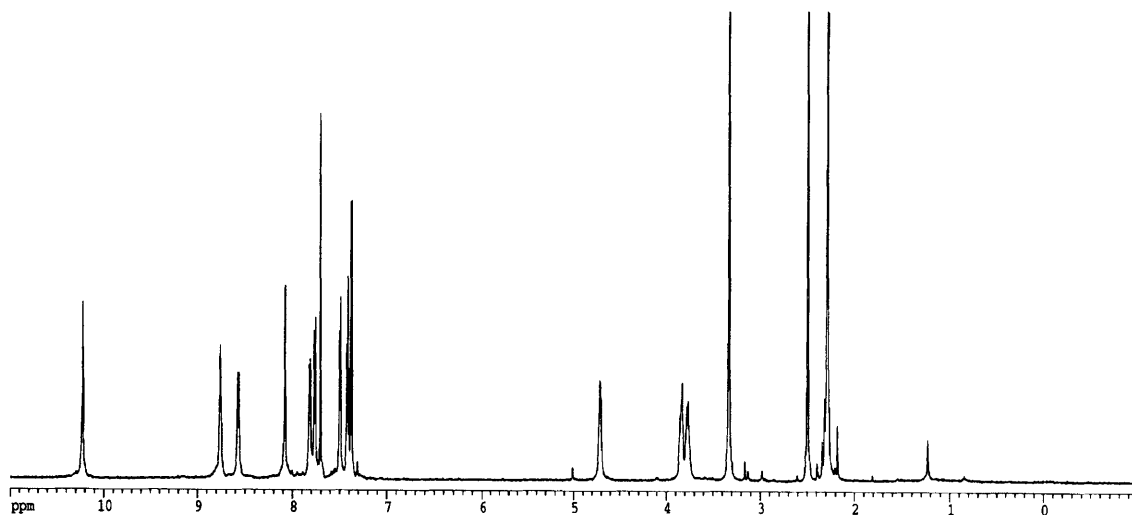
¹⁶ Prepared analogously to the 2,3-substituted isomer: Bergeron, R.J.; McGovern, K.A.; Channing, M.A.; Burton, P.S. *J. Org. Chem.* **1980**, *45*, 1589-1592.

sat. $\text{NaHCO}_{3(\text{aq})}$ (3 x 75 mL). Drying (Na_2SO_4), filtration, and evaporation of the residue gave an oil which solidified upon refrigeration. Yield: 1.55 g (72%). ^1H NMR (CDCl_3 , 600 MHz) δ 8.05 (dd, 1Har, $J = 8.7, 2.0$ Hz), 6.97 (d, 1Har, $J = 2.2$ Hz), 6.39 (d, 1Har, $J = 8.7$ Hz), 2.34 (s, 3H), 2.81 (s, 3H) ppm; ^{13}C NMR (CDCl_3 , 600 MHz) δ 166.99, 166.51, 166.94, 148.18, 142.55, 131.64, 130.04, 126.96, 124.27, 20.91, 20.76 ppm; IR (CDCl_3) 1775.50, 1756.06, 1258.37, 1195.51, 1174.79, 1106.87 cm^{-1} ; HRMS (FAB) Calc'd for $[\text{M}]^+ \text{C}_{11}\text{H}_9\text{O}_5\text{Cl}^+$ 256.0139, found 256.0148.

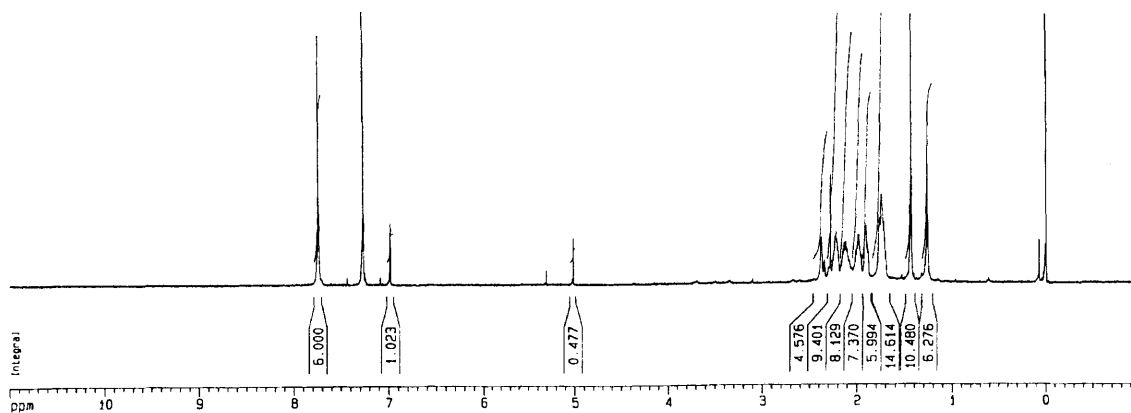


Pseudopeptide platform (hexaacetate) (6.10). Triamine **6.5** (30.0 mg, 0.0487 mmol), acid chloride **6.9** (56.2 mg, 0.219 mmol), and Hünig's base (51 μL , 0.29 mmol) were stirred in DMF (10 mL) under anhydrous conditions for 16 h. The resulting clear solution was poured into CH_2Cl_2 (100 mL) and washed with 1M HCl_{aq} (2 x 100 mL). Drying (Na_2SO_4), filtration, and concentration of the filtrate gave a yellow oil. Water (10 mL) was added and the cloudy mixture was freeze-dried to remove residual DMF. After triturating the residue thoroughly with MeOH, a white precipitate was collected by filtration. This precipitate was further purified by trituration in refluxing MeOH (10 min) which, after filtration, gave an off-white powder. Yield: 31.5 mg (51%). ^1H NMR ($\text{DMSO}-d_6$, 600 MHz) δ 10.22 (s, 3H), 8.75 (m, 3H), 8.57 (d, 3Har, $J = 6.3$ Hz), 8.08 (s, 3H), 6.82 (d, 3Har, $J = 8.0$ Hz), 6.77 (m, 3Har), 6.70 (d, 3Har, $J = 1.9$ Hz), 6.49 (d, 3Har, $J = 6.6$ Hz), 6.41 (t, 3Har, $J = 6.9$ Hz), 6.37 (d, 3Har, $J = 8.4$ Hz), 4.71 (m, 3H), 3.85 (m,

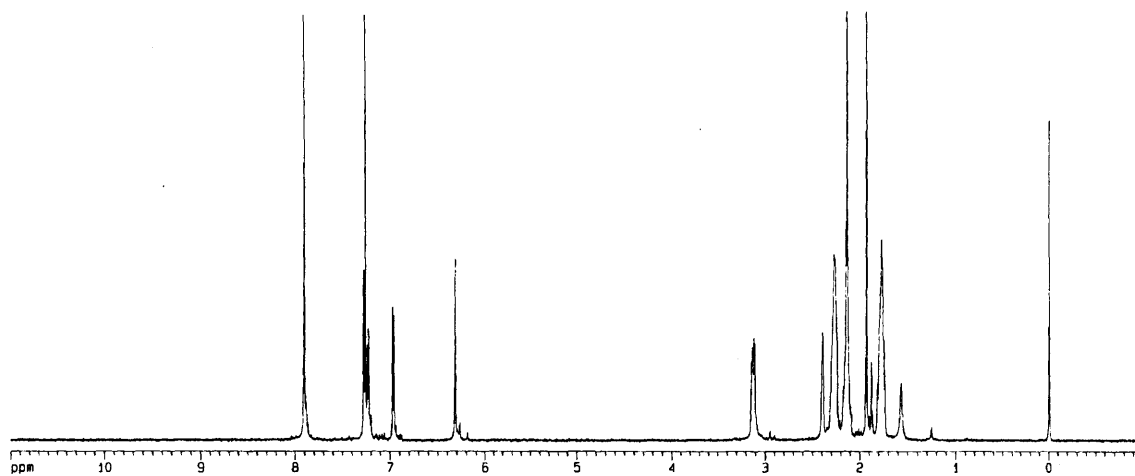
3H), 3.75 (m, 3H), 2.29 (bs, 18H) ppm; ^{13}C NMR (DMSO- d_6 , 151 MHz) δ 168.84, 168.24, 168.05, 166.12, 165.43, 144.33, 141.78, 138.88, 135.20, 132.93, 128.72, 125.68, 123.65, 122.88, 122.43, 122.34, 119.04, 54.65, 40.35, 20.37, 20.29 ppm.



Triphenylene triamine (6.12). Tricarbamate **6.11** (0.30 g, 0.26 mmol) and $\text{Pd}(\text{OH})_2$ [20% w/w on carbon] (20 mg) were mixed in MeOH (25 mL) and EtOAc (25 mL). Following replacement of air by H_2 (1 atm), the mixture was stirred overnight. Filtration through Celite and concentration *in vacuo* gave a brown residue. Yield: 0.19 g (100%). ^1H NMR (CDCl_3 , 600 MHz) δ 6.73 (s, 6H), 2.37 (m, 3H), 2.21 (m, 6H), 2.12 (m, 6H), 1.98 (m, 6H), 1.88 (m, 6H), 1.73 (m, 12H), 1.26 (s, 6H) ppm; HRMS (FAB) Calc'd for $[\text{M}+\text{Cs}]^+$ $\text{C}_{45}\text{H}_{51}\text{N}_3\text{O}_6\cdot\text{Cs}^+$ 862.2832, found 862.2862.



Triphenylene platform (hexaacetate) (6.13). Under anhydrous conditions, triamine **6.12** (0.19 g, 0.26 mmol) and acid chloride **6.9** (0.91 g, 3.55 mmol) were dissolved in THF (50 mL). Hünig's base (775 μ L, 4.45 mmol) was added and the brown solution heated at reflux for 48 h. The resulting yellow solution concentrated *in vacuo* and the residue taken up in CH₂Cl₂ (100 mL). This solution was washed with 0.5 N HCl_{aq.} (2 x 100 mL), dried (Na₂SO₄), filtered, and rotary evaporated. Flash chromatography (0 \rightarrow 4% MeOH/CH₂Cl₂) of the residue gave the crude product which was further purified by trituration with refluxing ether to give a white precipitate. The product was collected by filtration. Yield: 85.2 mg (23%). ¹H NMR (CDCl₃, 600 MHz) δ 6.91 (s, 6H), 6.28 (d, 3Har, J =1.9 Hz), 6.23 (dd, 3Har, J = 8.5, 2.0 Hz), 6.97 (d, 3Har, J = 8.3 Hz), 6.32 (s, 3H), 3.13 (dd, 6H, J = 13.8, 5.8 Hz), 2.40 (m, 3H), 2.27 (m, 12H), 2.15 (m, 6H), 2.13 (s, 9H), 1.93 (s, 9H), 1.75 (m, 12H) ppm; ¹³C NMR (CDCl₃, 151 MHz) δ 166.92, 166.80, 165.48, 146.63, 144.55, 142.25, 134.66, 125.07, 124.74, 123.64, 122.94, 121.73, 102.27, 59.59, 38.18, 33.63, 28.45, 21.14, 20.59, 20.32 ppm; IR (CDCl₃) 2992.75, 2926.79, 2888.02, 1774.89, 1672.29, 1495.71, 1456.59, 1371.58, 1245.39, 1203.76, 1106.38 cm⁻¹; HRMS (FAB) Calc'd for [M+Cs]⁺ C₇₈H₇₅N₃O₂₁•Cs⁺ 1522.3947, found 1522.4032.



Chapter 7 Toward Glycoluril Modules as Transition-Metal Ligands

7.1 Introduction

Helicates are supramolecular complexes composed of one or more organic ligands arranged in a helical fashion about one or more metals. For example, Figure 7-1 shows a simple triple stranded helicate formed from three dicatechol ligands **7.1** and two equivalents of the metal gallium(III).¹ Even in the presence of other competing ligands, dinuclear helicate $K_6 \cdot [Ga_2 7.1_3]$ spontaneously self-assembles under the appropriate conditions due to careful ligand design.^{2,3}

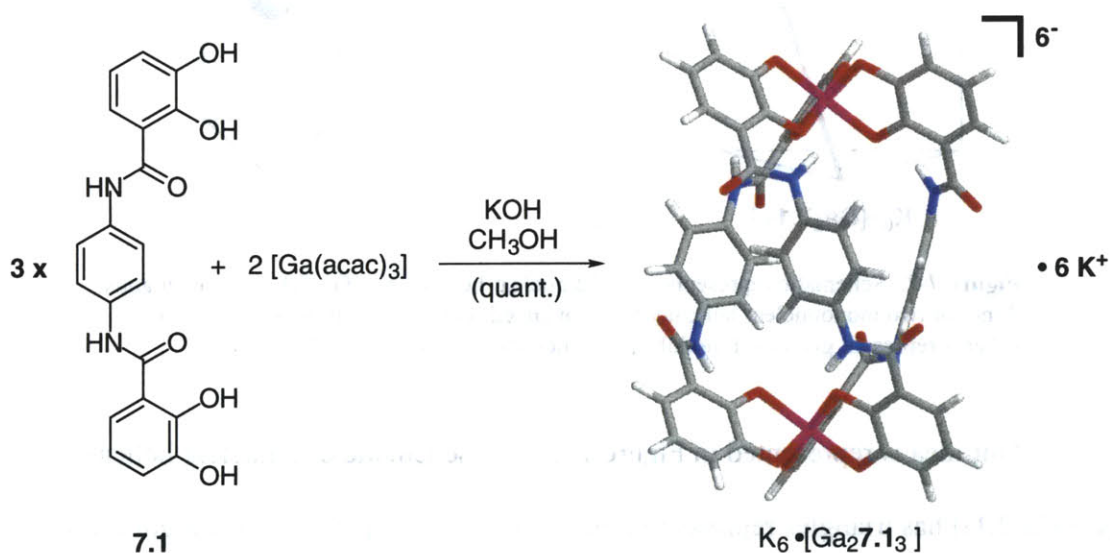


Figure 7-1. An example of dinuclear, triple-stranded helicate formation.

¹ Caulder, D.L.; Raymond, K.N. *Angew. Chem. Int. Ed. Engl.* **1997**, *36*, 1440-1442.

² See Chapter 6, ref. 10 for a description of complex labeling.

³ Piguet, C.; Bernardinelli, G.; Hopfgartner, G. *Chem. Rev.* **1997**, *97*, 2005-2062.

Since supramolecular complexes containing metals have potential as catalysts⁴ and sensors,⁵ we were interested in creating capsules which simultaneously bound both transition metals and organic guests. Although helicates are attractive possibilities due to their defined structures, their small interiors limit their utility as hosts.^{6,7} Therefore, we initiated the development of a conceptually-new class of hydrogen-bonded capsules containing mononuclear helicates as spacer units.

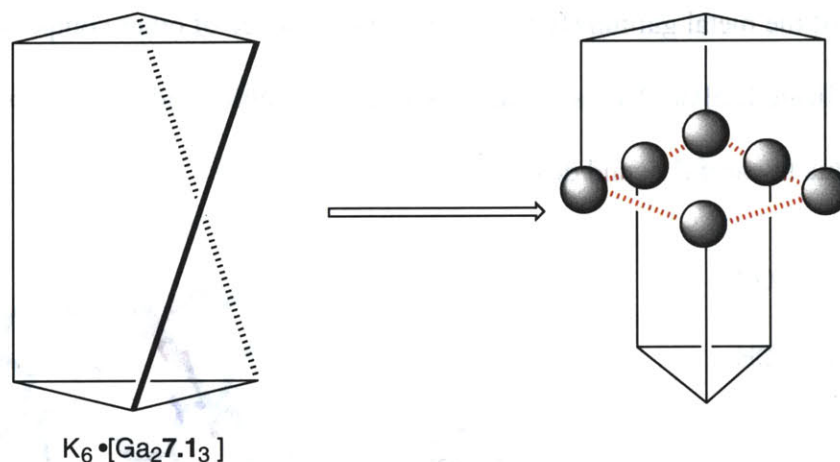


Figure 7-2. Schematic representation of dinuclear helicate $K_6 \bullet [Ga_{27.13}]$ and analogous dimer of two mononuclear helicates functionalized with glycoluril modules. [Gray spheres represent glycoluril modules; red lines show hydrogen bond seam.]

Our idea is represented in Figure 7-2. The schematic of dinuclear helicate $K_6 \bullet [Ga_{27.13}]$ has triangles representing the two metal complexes and straight lines corresponding to the covalent spacers between ligand sites. We planned to replace the covalent linkages between metal centers with a seam of hydrogen bonds provided by our

⁴ (a) Reetz, M.T. *J. Heterocycl. Chem.* **1998**, *35*, 1065-1073. (b) Sanders, J.K.M. *Chem. Eur. J.* **1998**, *4*, 1378-1383.

⁵ Reinhoudt, D.N.; van Wageningen, A.M.A.; Huisman, B.-H. *NATO ASI Ser., Ser. C* **1996**, *485*, 1-9.

⁶ Small alkali cations have been encapsulated within helicates; see: Albrecht, M.; Schneider, M.; Rottele, H. *Angew. Chem. Int. Ed. Engl.* **1999**, *38*, 557-559.

⁷ Recently, organo-metallic cluster compounds have been developed which possess cavities capable of encapsulating small guests; see: Parac, T.N.; Caulder, D.L.; Raymond, K.N. *J. Am. Chem. Soc.* **1998**, *120*, 8003-8004.

glycoluril modules. The monomers, composed of a metal and three glycoluril modules functionalized with transition metal ligands, were designed to dimerize into a capsule in non-competitive solvents. The resulting cavity should be large enough to encapsulate a variety of guests.

7.2 Design Considerations

Since our molecular modeling techniques predicted capsule formation in other systems with reasonable accuracy, we modeled systems derived from glycoluril ligand modules as well.⁸ Our program of choice, MacroModel (v5.5), was incapable of producing or minimizing transition metal complexes,⁹ so the metal complexes described in this chapter were created using MacSpartan Plus and then read into MacroModel as PDB files. The complexes were then functionalized with glycoluril modules and manually docked to give a capsule. Prior to minimization, the metals were replaced with “dummy” atoms and the ligand-metal complexes were frozen into octahedral geometries¹⁰ using the program’s standard tools. Bond angles and distances for the complexes were found in the literature for similar helicates and then defined for our complexes.¹¹ With the metal-complexes frozen in their ideal configurations, minimizations were performed and the resulting structures analyzed as usual.

⁸ Except as noted in this section, modeling was performed as described in previous chapters.

⁹ Although the MacroModel manual described routines for modeling transition-metal complexes, we found the protocols to be inadequate.

¹⁰ Other types of complexes were also evaluated, but only octahedral complexes provided adequate spacing between adjacent glycoluril units.

¹¹ In the “Energy” window, the “VDWB” button automatically identifies a coordination sphere after selecting the dummy atom. Next, van der Waals parameters were set using the “VDWE” button. [r_O = *trans* bond lengths (e.g. 3.98 Å for *trans* oxygens in a octahedral tricatechol-gallium(III) complex); Σ = repulsive potential (a value of 0.55 was found to be adequate).] If necessary, bond torsions in the transition metal complexes were also frozen using the “FxTor” button.

7.3 Dipyridyl Ligand Modules

The first ligand module we synthesized was dipyridyl module **7.3** (Figure 7-3). As detailed in the Experimental section, alkylating amine module **4.25** with the bromomethyldipyridyl **7.2** proceeded in low yield because of the spacer's polymerization tendency. However, enough material was isolated to evaluate the ligand module's complexation behavior.

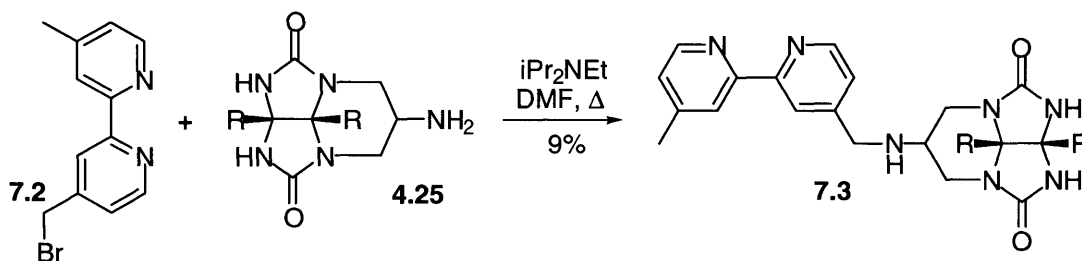


Figure 7-3. Synthesis of dipyridyl ligand module **7.3**.

Metals such as iron(II) readily form octahedral complexes in the presence of 2,2'-dipyridyl and complexes utilizing linked dipyridyls have been used extensively to form triple-stranded helicates.^{3,12} Modeling indicated that the mononuclear helicate $[Fe7.3_3] \cdot 2PF_6$ formed from **7.2** (3 equiv.) and iron(II) could dimerize to form a hydrogen-bonded assembly $[(Fe7.3_3)_2] \cdot 4PF_6$ as shown in Figure 7-4. While most helicates are water soluble, we predicted that $[Fe7.3_3] \cdot 2PF_6$ would dissolve in relatively non-polar organic solvents due to its numerous lipophilic groups. It was hoped that dimer formation would drive $[Fe7.3_3] \cdot 2PF_6$ to the all *fac* isomer (as shown) rather than the probable mixture of *fac* and *mer* isomers in the absence of dimerization.¹³

¹² Constable, E.C. *Tetrahedron* **1992**, *48*, 10013-10059.

¹³ The rate of exchange between *fac* and *mer* isomers depends upon metal, ligand, solvent, and counter-ion. Equilibration to the desired *fac* isomer can take anywhere from minutes to days. See: Kramer, R.; Lehn, J.-M.; Marquis-Rigault, A. *Proc. Natl. Acad. Sci.* **1993**, *90*, 5394-5398. Charbonniere, L.J.; Williams, A.F.; Frey, U.; Merbach, A.E.; Kamalaprija, P.; Schaad, O. *J. Am. Chem. Soc.* **1997**, *119*, 2488-2497.

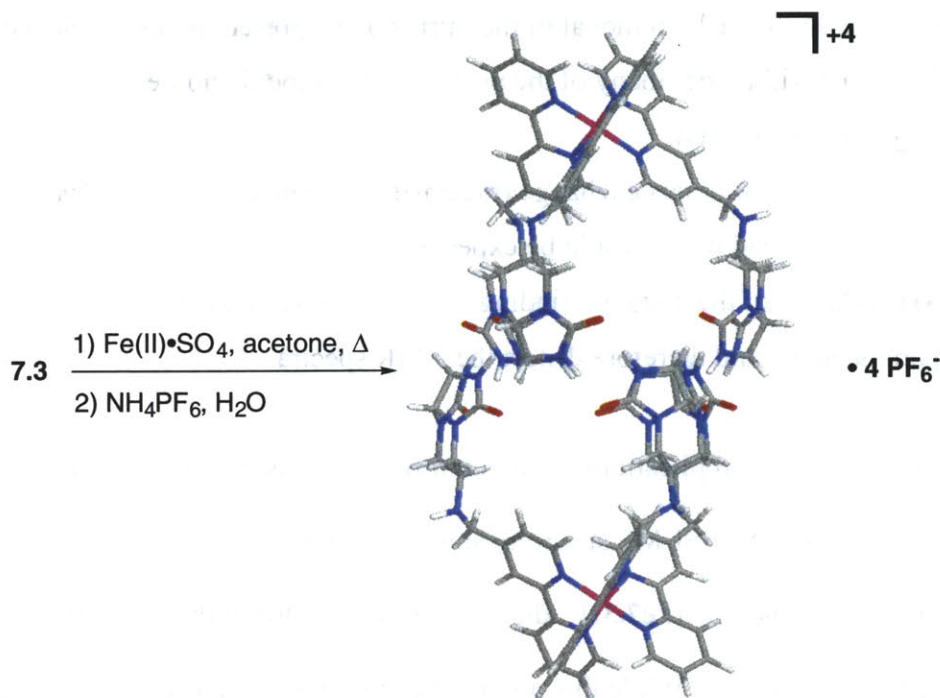


Figure 7-4. Synthesis of mononuclear helicate [Fe7.3₃]•2PF₆ and computed structure of the hydrogen-bonded dimer [(Fe7.3₃)₂]•4PF₆. Modeling found twelve hydrogen bonds between the glycouril units. Several groups, including the 4'-methyls on the dipyridyls, have been removed for clarity.

Complex [Fe7.3₃]•2PF₆ was synthesized according to standard literature procedures.¹⁴ Although soluble in common organic solvents, the ¹H-NMR spectra of the complex in CDCl₃ and DMSO-d₆ showed only broad peaks even after long equilibration times (i.e. several days). The likely reasons for such disappointing spectra are:

- 1) Complex [Fe7.3₃]•2PF₆ probably exists as a mixture of *fac* and *mer* geometric isomers in the absence of a driving force to favor the *fac* isomer (i.e. strongly favored dimer).
- 2) Each geometric isomer has two enantiomers (right- and left-handed helices). While the enantiomers will share the same chemical shifts overall, the helical nature of the compounds desymmetrizes each

¹⁴ Serr, B.R.; Andersen, K.A.; Elliot, C.M.; Anderson, O.P. *Inorg. Chem.* **1988**, *27*, 4499-4504. Since sulfate counterions may disturb dipyridyl helicates because of ion-pairing, we converted our complexes to hexafluorophosphate salts as described in the referenced work.

glycoluril module by removal of the mirror plane present in uncomplexed **7.3**. This will render many of the protons in the module non-equivalent (e.g. glycoluril NHs).

3) If these enantiomers exchange (racemize) at a rate close to the NMR timescale, broad peaks would be expected.

4) Oxidation of the metal or binding of oxygen may make the complexes paramagnetic and therefore distort the NMR spectra.

Despite these complications, complex formation was confirmed by mass spectrometry (ESI). An ESI-MS spectrum showed a single peak ($m/z = 1120$) corresponding to either the $[\text{Fe7.3}_3]^{2+}$ dication (mass = 2240) or the dimer $[(\text{Fe7.3}_3)_2]^{4+}$ tetracation (mass = 4480). While this provided compelling evidence for monomer formation, our protocols for capsule characterization depend heavily upon ^1H NMR so we continued with those studies.

In an effort to template the *fac* complex, amide flexiball monomer **5.9** was mixed with complex $[\text{Fe7.3}_3]\cdot 2\text{PF}_6$. Although modeling indicated that heterodimer $\mathbf{5.9}\cdot[\text{Fe7.3}_3]\cdot 2\text{PF}_6$ could be formed (Figure 7-5), no such product was identified by NMR or MS. Therefore, we decided to eliminate the possibility of geometric isomers in hopes of simplifying our characterizations.

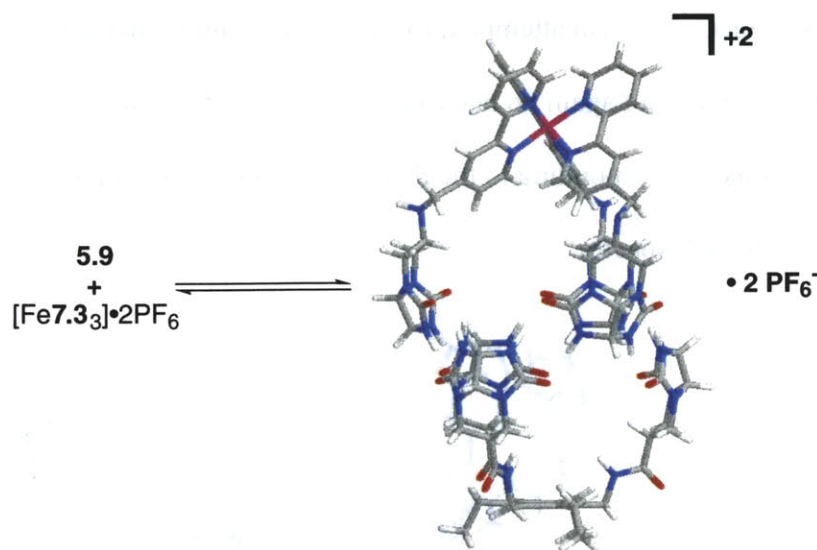


Figure 7-5. Possible heterodimer $5.9 \cdot [Fe7.3_3] \cdot 2PF_6$ formed between complex $[Fe7.3_3] \cdot 2PF_6$ and amide flexiball monomer 5.9.

Alkylating two acid modules¹⁵ with 4,4'-bisbromomethyldipyridyl 7.4 gave the new ligand module 7.5 (Figure 7-6). The increased symmetry of this ligand precludes the possibility of geometric isomers upon complex formation. Indeed, the spectra of complex $[Fe7.5_3] \cdot 2PF_6$ were much simpler than those for $[Fe7.3_3] \cdot 2PF_6$,¹⁶ however no tell-tale signs of capsule formation were evident. (As shown in Figure 7-7, the complex $[Fe7.5_3] \cdot 2PF_6$ was expected to exist as a linear, hydrogen-bonded polymer in non-

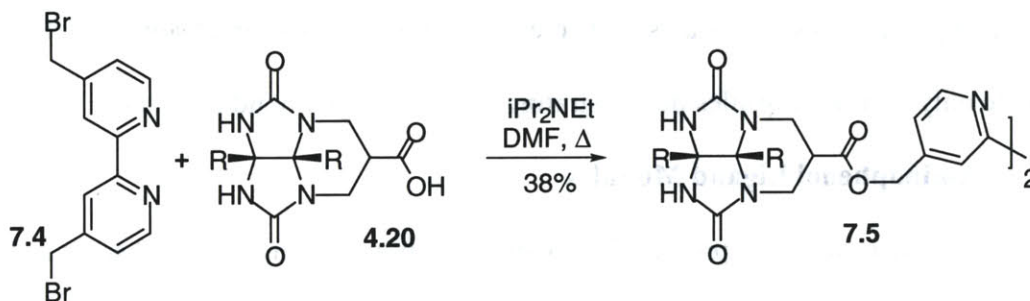


Figure 7-7. Synthesis of the dimodular dipyridyl ligand 7.5.

¹⁵ Acid modules were used rather than amine modules because of higher yields.

competitive solvents.) We also attempted to form a heterodimer using amide flexible monomer **5.9** as before, but again no heterodimer was found. However, as with $[\text{Fe}7.3_3] \cdot 2\text{PF}_6$, peaks corresponding to the dicationic mononuclear helicate $[\text{Fe}7.5_3]^{2+}$ were found by ESI-MS spectra.

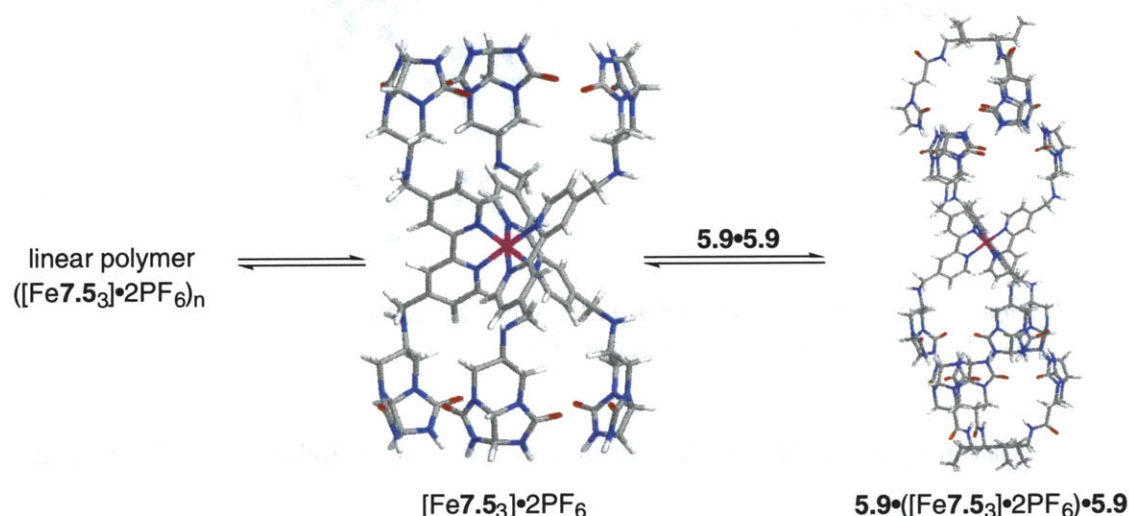


Figure 7-7. Possible aggregation states of helicate $[\text{Fe}7.5_3] \cdot 2\text{PF}_6$.

Our results support the formation of the desired helicates, but it seems clear that no capsule formation occurred with either complex. Although modeling predicted capsule formation, the hydrogen-bond angles and lengths found were less ideal than those in other glycoluril-based capsules.¹⁷ Therefore, we refined our target selections to include only helicate capsules demonstrating ideal hydrogen-bond networks.

7.4 Aminophenol Ligand Modules

One helicate dimer predicted to display an optimal hydrogen bond seam is derived from the aminophenol ligand module **7.6** (Figure 7-8). Although relatively few helicates

¹⁶ In addition, the removal of oxygen from these NMR samples was attempted by repetitive “freeze-pump-thaw” cycles as described in Derome, A.E. In *Modern NMR Techniques for Chemistry Research*; Baldwin, J.E., Ed.; Organic Chemistry Series 6; Pergamon Press: New York, 1987; pp 112-113.

based on aminophenol exist,¹⁸ we were attracted to this ligand because of two unique properties. First, triple helicates formed with aminophenol derivatives (3 equiv.) and a triply-charged metal such as gallium(III) are neutral. Besides having increased solubility in non-polar solvents, a neutral helicate would require no counter-ions. Therefore, complications due to ion-pairing (as discussed for the dipyridyl modules) are reduced.

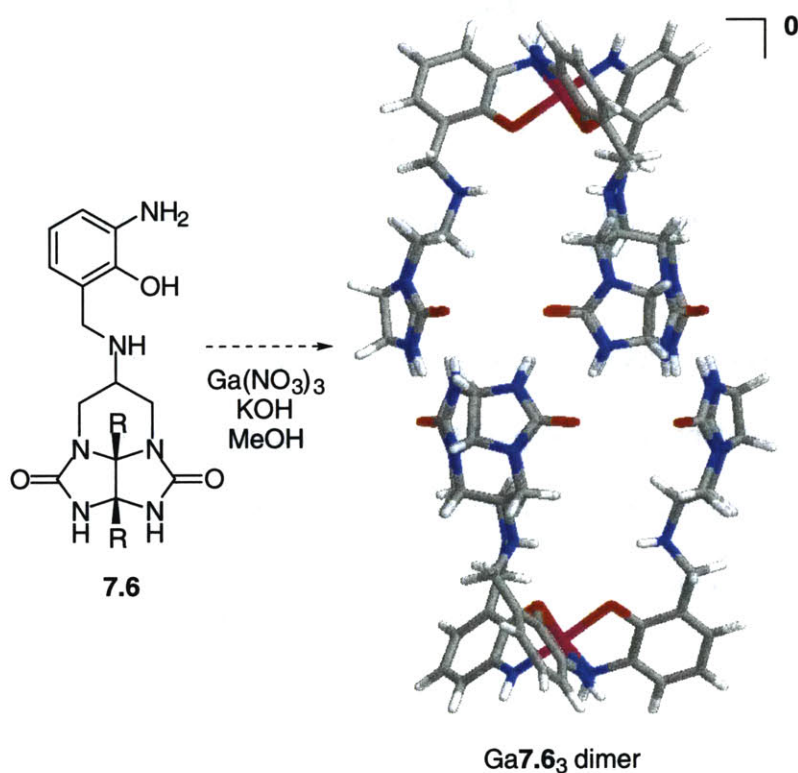


Figure 7-8. Aminophenol ligand 7.6 and proposed gallium(III) helicate shown as the dimer. Due to modeling limitations, a proton on each aniline nitrogen has been omitted.

Second, in an octahedral complex, aminophenol ligands prefer a *fac* orientation because of the *trans*-influence.¹⁹ This is a thermodynamic phenomenon which positions weakly donating ligands *trans* to strongly donating ligands in a complex as shown in Figure 7-9.

¹⁷ See section 1.4.

¹⁸ For an example with leading references, see: Albrecht, M.; Frohlich, R. *J. Am. Chem. Soc.* **1997**, *119*, 1657-1661.

In aminophenol ligands, this corresponds to the more weakly donating amines preferring a *trans* orientation to the more strongly donating phenols. This should produce a *fac* complex as shown in Figure 7-8 and remove complications caused by geometric isomerization.

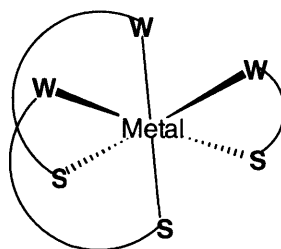


Figure 7-9. The *trans*-influence preferentially orients weaker ligands (W) *trans* to stronger ones (S) in an octahedral complex.

The synthesis of **7.6** is outlined in Figure 7-10 and detailed in the Experimental section.²⁰ The last deprotection step (BBr₃ demethylation) proceeded in low yield due to instability of the final product. Unfortunately, ligand **7.6** decomposed readily which prevented complexation studies.

¹⁹ (a) Appleton, T.G.; Clark, H.C.; Manzer, L.E. *Coord. Chem. Rev.* **1973**, *10*, 355-422. (b) Enemark, E.J.; Stack, T.D.P. *Angew. Chem. Int. Ed. Engl.* **1995**, *34*, 997-998.

²⁰ Jonathon D. Toker assisted with the synthesis of several intermediates in Figure 7-10.

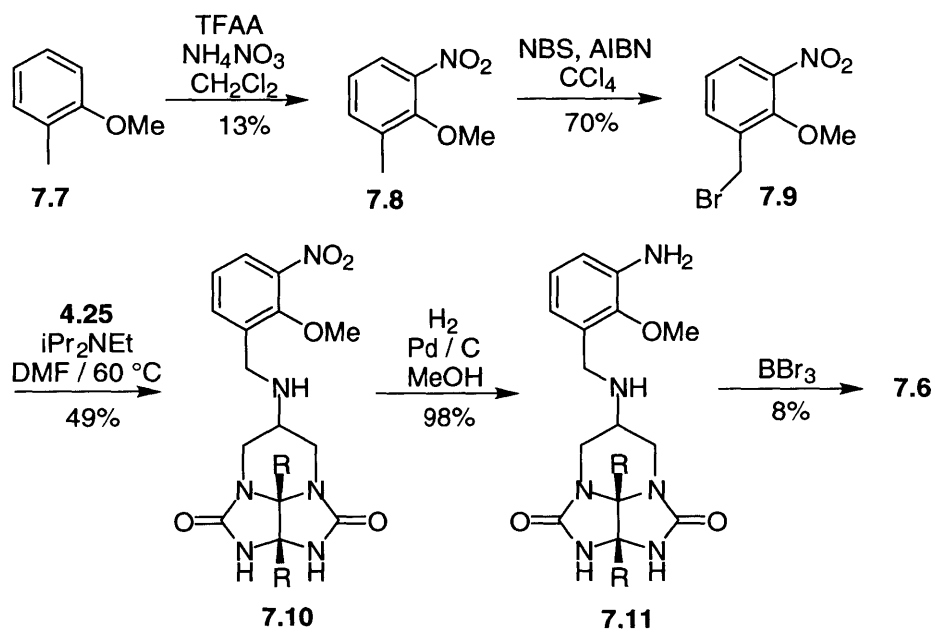


Figure 7-10. Synthesis of aminophenol ligand **7.6**.

7.5 Catechol Ligand Modules

Since calculations predicted that aminophenol helicates would be highly predisposed toward dimerization, we sought other ligand modules with similar structures and increased stability. As shown in Figure 7-11, catechol ligand module **7.12** was expected to produce helicate $\text{K}_3\cdot[\text{Ga7.12}_3]$. Modeling found that the proposed dimer $\text{K}_6\cdot[(\text{Ga7.12}_3)_2]$ possessed a network of 12 ideal hydrogen bonds, so we embarked upon the synthesis of these types of ligand modules.

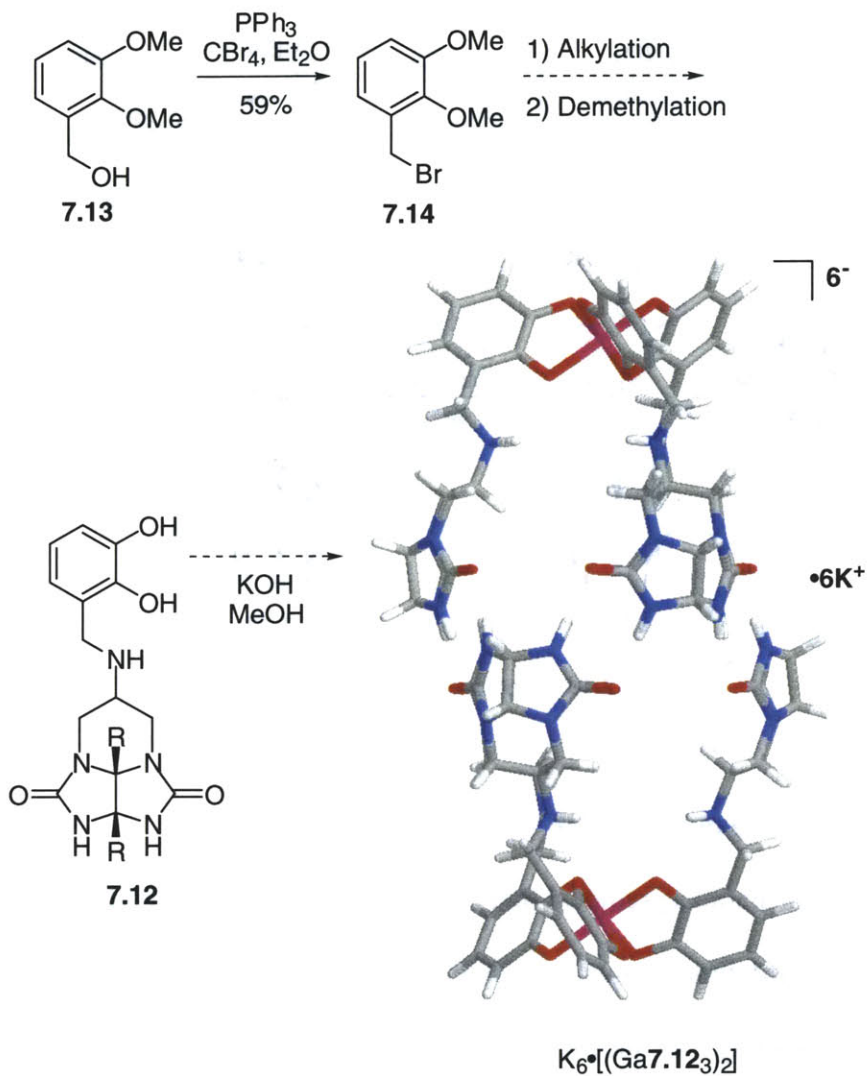


Figure 7-11. Synthesis of catechol ligand module **7.12** and proposed helicite dimer $\text{K}_6 \cdot [(\text{Ga}7.12_3)_2]$.

We began the synthesis of **7.12** as shown in Figure 7-11, but then abandoned this module because of concerns about geometric isomers in the helicites. As with the dipyriddy ligand modules, we decided to synthesize a dimodular catechol ligand based upon spacer 3,7-dimethylcatechol. In addition, we initially sought to protect the catechol oxygens as a ketal in order to avoid the harsh demethylation conditions required for the methoxy protecting groups.

Figure 7-12 illustrates our first route. Surprisingly, 3,7-dimethylcatechol **7.17** proved a difficult target. Starting from 3-methylcatechol **7.15**, a Mannich reaction proceeded in fair yield to give the morpholino catechol **7.16**.²¹ However, hydrogenolysis of this intermediate gave a poor yield despite high pressure and a large catalyst load.²² Resistance of phenolic Mannich bases to hydrogenolysis is a known phenomena that still lacks a definitive explanation.²³ Although Byck and Dawson²⁴ suggested that intramolecular hydrogen-bonding between the phenolic OH and morpholine nitrogen may contribute to the low reactivity, we find this explanation flawed given ethanol as the reaction solvent. In addition to the small amounts of **7.17** available from this route, various attempts to protect the catechol as the acetone ketal failed completely.

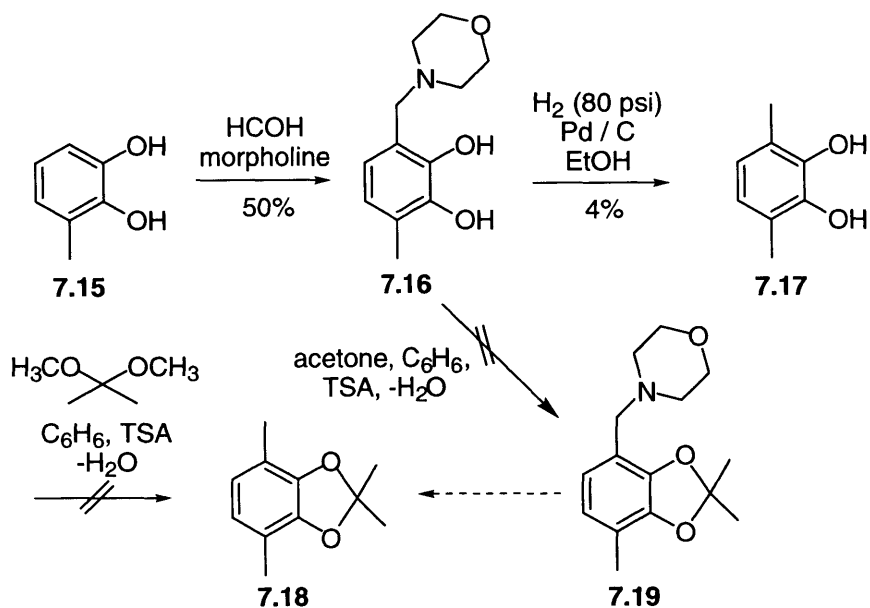


Figure 7-12. First route to 3,7-dimethylcatechol **7.17** and various attempts at ketal protection.

²¹ Prepared analogously to 3,7-bis(morpholinomethyl)catechol; see: Sinhababu, A.K.; Borchardt, R.T. *Synth. Commun.* **1982**, *12*, 983-988. See also: Helgeson, R.C.; Tamowski, T.L.; Timko, J.M.; Cram, D.J. *J. Am. Chem. Soc.* **1977**, *99*, 6411-6418.

²² Adapted from Bell, T.W.; Lein, G.M.; Nakamura, H.; Cram, D.J. *J. Org. Chem.* **1983**, *48*, 4728-4734.

²³ For a review, see Sinhababu, A.K.; Borchardt, R.T. *Synth. Commun.* **1982**, *12*, 983-988.

²⁴ Byck, J.S.; Dawson, C.R. *J. Org. Chem.* **1968**, *33*, 2451-2457.

Given the difficulties encountered above, we evaluated a different route to **7.17** and decided to retreat to methoxy protection of the catechol oxygens. Acetylation of morpholino catechol **7.16** gave triacetate **7.20** in fair yield. Hydrogenolysis was then effected at lower pressure to give diacetate **7.21** in good yield.²⁵ Acidic methanolysis gave 3,7-dimethylcatechol **7.17** which was immediately treated with MeI to give 3,7-dimethylveratrole **7.22**. Subsequent bromination and amine module alkylation gave **7.24**. Since catechol **7.17** decomposed slowly upon standing in air, we were concerned about the stability of target module **7.25**. Unfortunately, despite repeated attempts under O₂-free conditions to demethylate **7.24**, we were unable to isolate the dimodular catechol ligand because of decomposition.

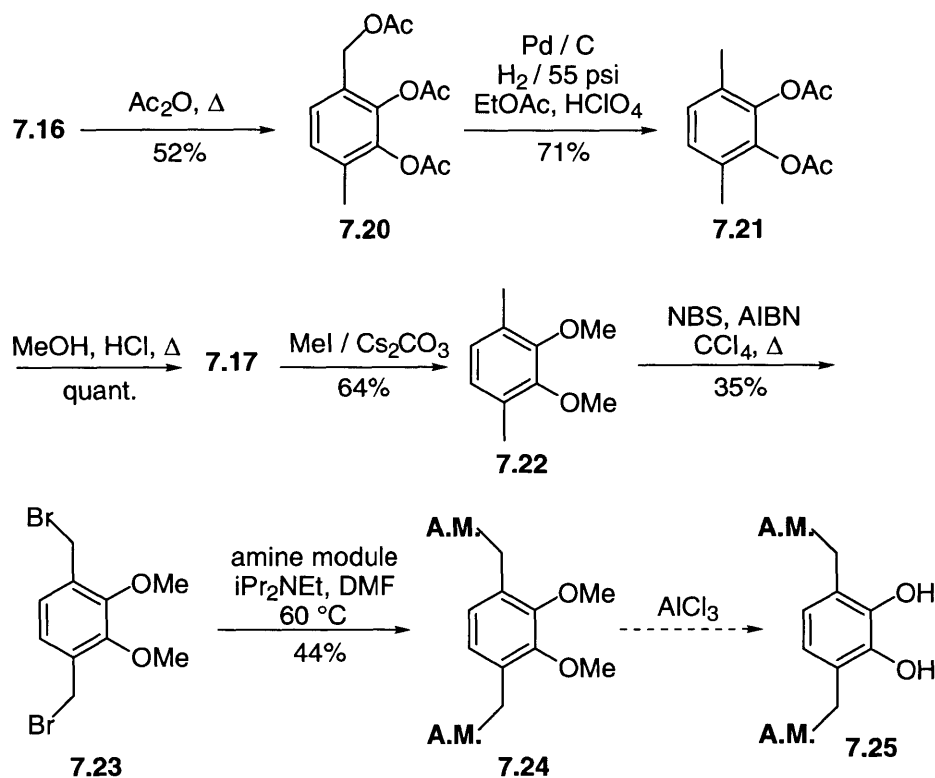


Figure 7-13. Alternative synthesis of dimodular catechol ligand **7.25** (A.M. = amine module).

²⁵ This sequence was adapted from ref. 23 which started from 3,7-bis(morpholinomethyl)catechol.

Most catechol-containing helicates possess electron-withdrawing groups (e.g. carbonyls) at the 3 and 6 positions. The donating substituents in our case probably increase the oxidation potential of these catechols and underlie the stability problems we encountered. Therefore, a catechol ligand substituted with a glycoluril module *via* an amide linkage might prove more stable. However, modeling indicated that subsequent helicates would not position the glycolurils in the orientation necessary for dimerization. Distortion of the octahedral complex, though, may permit such helicates to obtain the necessary configuration for capsule formation. Given this possibility, this new ligand will be synthesized²⁶ and studied.

7.6 Experimental

7.7.1 Apparatus, Materials, and Methods

See Section 2.5.1

7.7.2 Procedures

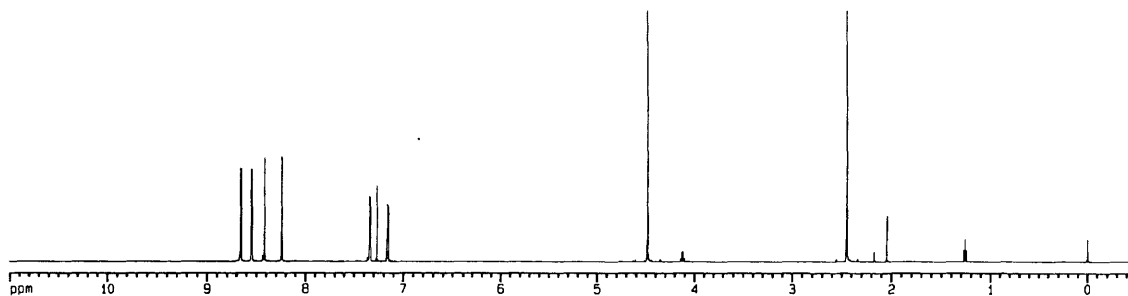
4-(Bromomethyl)-4'-methyl-2,2'-bipyridine (7.2).²⁷ Combining 4,4'-dimethyl-2,2'-bipyridine²⁸ (4.02 g, 21.82 mmol), NBS (4.04 g, 22.70 mmol), and AIBN (0.11 g, 0.65 mmol) in refluxing 100 mL CCl₄ (Aldrich, redistilled) produced a yellow heterogeneous mixture. After 3 h, reaction was cooled to rt and filtered. The filtrate was evaporated to about 15 mL with no heat applied in order to minimize polymerization. A flash chromatography purification (30% EtOAc/Hex, 1% NEt₃ added) provided a crude

²⁶ Condensation of amine module with commercially-available 2,3-dimethoxybenzoic acid followed by deprotection should provide the desired module.

²⁷ Modified from a literature preparation: Gould, S.; Stousse, G.F.; Meyer, T.J.; Sullivan, B.P. *Inorg. Chem.* **1991**, *30*, 2942-2949.

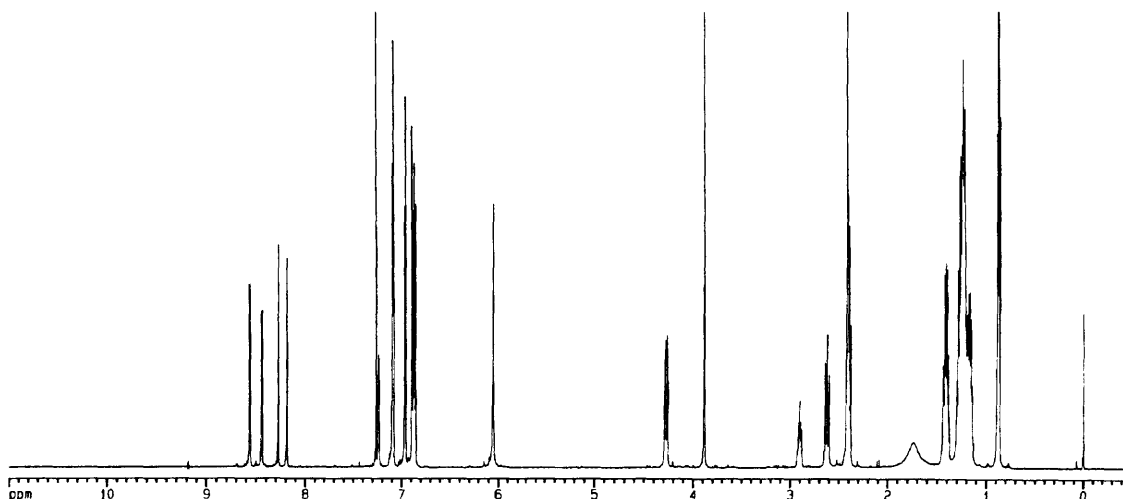
²⁸ Recrystallized from EtOAc prior to use.

sample of the desired product (2nd major spot by TLC) which was triturated with ether and filtered. The precipitate was further purified by another round of chromatography (50% EtOAc/Hex). Combination of fractions pure by TLC and evaporation (no heat) gave a lustrous white precipitate. Yield: 0.44 g (8%). ¹H NMR (CDCl₃, 600 MHz) δ 8.66 (d, 1Har, *J* = 5.0 Hz), 8.54 (d, 1Har, *J* = 4.9 Hz), 8.41 (m, 1Har), 8.24 (m, 1Har), 7.34 (dd, 1Har, *J* = 5.0, 1.7 Hz), 7.16 (m, 1Har), 4.48 (s, 2H), 2.45 (s, 3H) ppm; ¹³C NMR (CDCl₃, 151 MHz) δ 157.28, 155.64, 150.00, 149.36, 148.63, 147.51, 125.31, 123.82, 122.34, 121.26, 30.88, 21.31 ppm; IR (CDCl₃) 3048.45, 3004.40, 2951.54, 2917.29, 1595.32, 1555.36, 1457.95, 1372.35, 825.82 cm⁻¹; HRMS (FAB) Calc'd for [M+H]⁺ C₁₂H₁₂N₂Br⁺ 263.0184, found 263.0177.



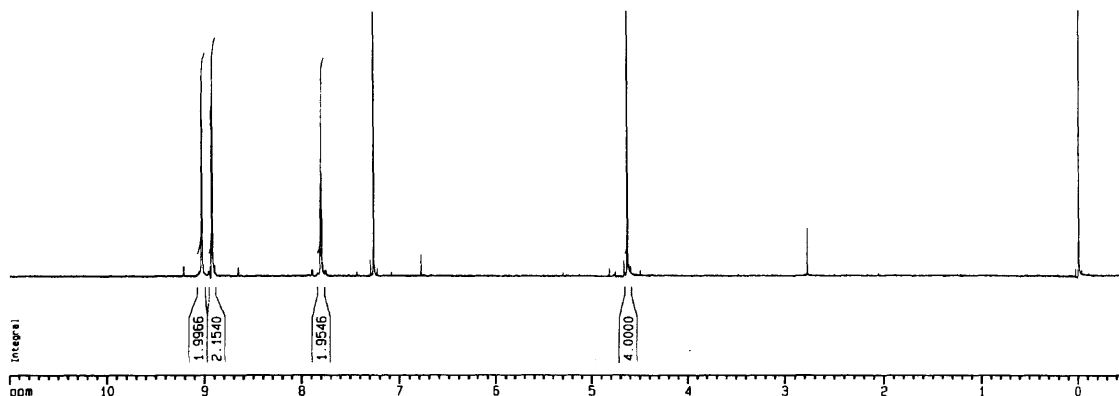
Dipyridyl glycoluril module (7.3). Amine module **4.25** (0.18 g, 0.33 mmol), compound **7.2** (0.08 g, 0.30 mmol), and dry iPr₂NEt (Aldrich Sure-Seal, ≈ 0.5 mL) were mixed in dry DMF (25 mL) at heated at 60 °C. After 16 h, TLC indicated complete disappearance of **7.2** so the solvent was removed by evaporation. The residue was taken up in CH₂Cl₂ (100 mL), washed with saturated NaHCO_{3(aq.)} (2 x 50 mL), dried with Na₂SO₄, filtered, and evaporated to brown residue. Sonication of the residue in MeOH gave a white precipitate which was then triturated with ether. Filtration gave a fine white precipitate. Yield: 0.02 g (9%). ¹H NMR (CDCl₃, 600 MHz) δ 8.56 (d, 1Har, *J* = 5.0 Hz), 8.44 (d, 1Har, *J* = 4.9 Hz), 8.27 (s, 1Har), 8.19 (s, 1Har), 7.24 (m, 1Har), 7.09 (m,

3Har), 7.96 (d, 2Har, $J=8.2$ Hz), 7.89 (d, 2Har, $J=8.2$ Hz), 7.86 (d, 2Har, $J=8.3$ Hz), 7.05 (s, 2H), 4.27 (dd, 2H, $J=13.7, 4.7$ Hz), 3.89 (s, 2H), 2.90 (m, 1H), 2.62 (t, 2H, $J=13.1$ Hz), 2.40 (m, 7H), 1.74 (bs, 1H), 1.43 (m, 4H), 1.23 (m, 16H), 0.88 (m, 6H) ppm; ^{13}C NMR (CDCl_3 , 151 MHz) δ 159.61, 157.79, 157.11, 150.19, 149.64, 149.23, 148.53, 144.18, 144.10, 133.66, 130.22, 128.77, 128.39, 127.74, 127.45, 125.02, 123.20, 122.39, 120.49, 83.89, 78.67, 50.33, 50.29, 43.70, 35.47, 35.38, 31.94, 31.42, 31.40, 29.23, 29.21, 29.16, 29.11, 22.80, 22.78, 21.28, 14.20 ppm; IR (CDCl_3) 3253.54, 2925.36, 2854.28, 1713.83, 1693.91, 1597.81, 1464.44, 1438.62, 1103.28 cm^{-1} ; HRMS (FAB) Calc'd for $[\text{M}+\text{H}]^+$ $\text{C}_{45}\text{H}_{58}\text{N}_7\text{O}_2^+$ 728.4652, found 728.4628.



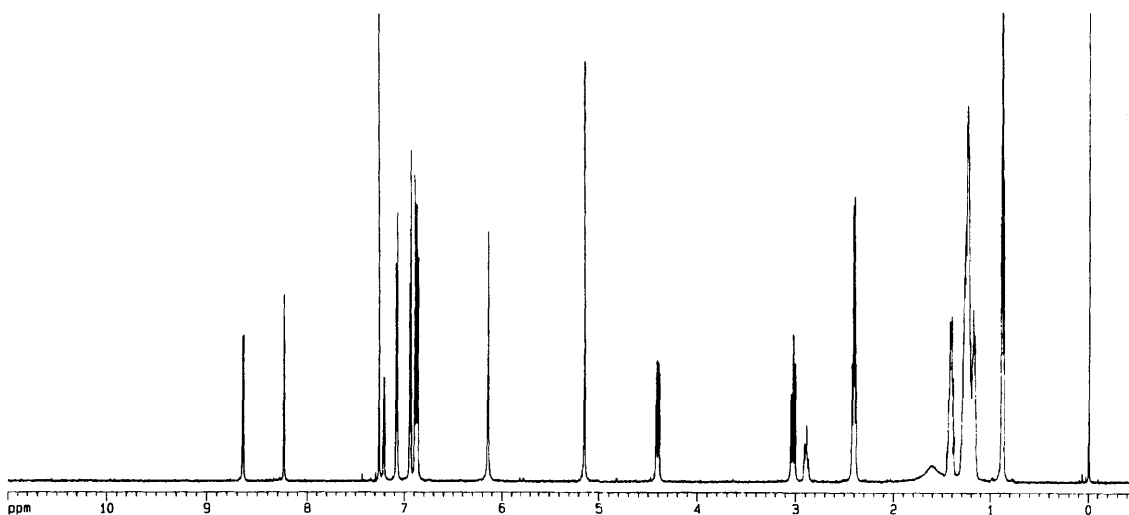
4,4'-Bis(bromomethyl)-2,2'-bipyridine (7.2). 4,4'-dimethyl-2,2'-bipyridine²⁸ (4.36 g, 23.68 mmol) and NBS (4.95 g, 27.81 mmol) were combined in 125 mL CCl_4 (Aldrich, redistilled) and the mixture refluxed for 4 h using a sunlamp. After cooling to rt, the mixture was filtered and evaporated to about 15 mL without the application of heat in order to reduce polymerization. Flash chromatography (20% acetone/ CH_2Cl_2) accomplished a crude separation and fractions containing the desired product (1st major spot by TLC) were combined and concentrated to near dryness. This residue was taken

up in CH_2Cl_2 (200 mL) and washed with 2M $\text{HBR}_{(\text{aq})}$ (2 x 150 mL) which removed most of the color from the organic phase. The organic layer was dried with Na_2SO_4 , filtered, and concentrated to near dryness. Another flash chromatography purification (2 -> 5% acetone/ CH_2Cl_2) isolated the desired product with minor impurities by TLC. These impurities were removed by dissolving the crude product in a minimum of CH_2Cl_2 (10 mL) and precipitating the product with ether (100 mL). Filtration provided a white powder. Yield: 0.31 g (4%). ^1H NMR (CDCl_3 , 600 MHz): δ 9.03 (s, 2Har), 8.92 (d, 2Har, $J = 5.4$ Hz), 7.80 (d, 2Har, $J = 5.2$ Hz), 4.63 (s, 4H) ppm. ^{13}C NMR (CDCl_3 , 151 MHz): δ 148.56, 147.98, 127.03, 125.19, 29.08 ppm. IR (CDCl_3): 2957.15, 2917.10, 1631.88, 1595.54, 1460.86, 1377.72 cm^{-1} . HRMS (FAB): Calc'd for $[\text{M}+\text{H}]^+$ $\text{C}_{12}\text{H}_{11}\text{N}_2\text{Br}_2$ 342.9268, found 342.9261.



Dimodular Dipyridyl Ligand (7.5). Acid module (0.84 g, 1.46 mmol), dibromide **7.4** (0.250 g, 0.73 mmol), and Hünig's base (0.25 mL, 1.46 mmol) were mixed under anhydrous conditions in DMF (40 mL). The reaction mixture was then stirred at 100 °C overnight under N_2 atmosphere. The solvents were removed by rotary evaporation and the residue taken up in CH_2Cl_2 (200 mL). This organic layer was washed with saturated $\text{NaHCO}_{3\text{aq}}$ (3 x 100 mL) and then rotary evaporated without prior

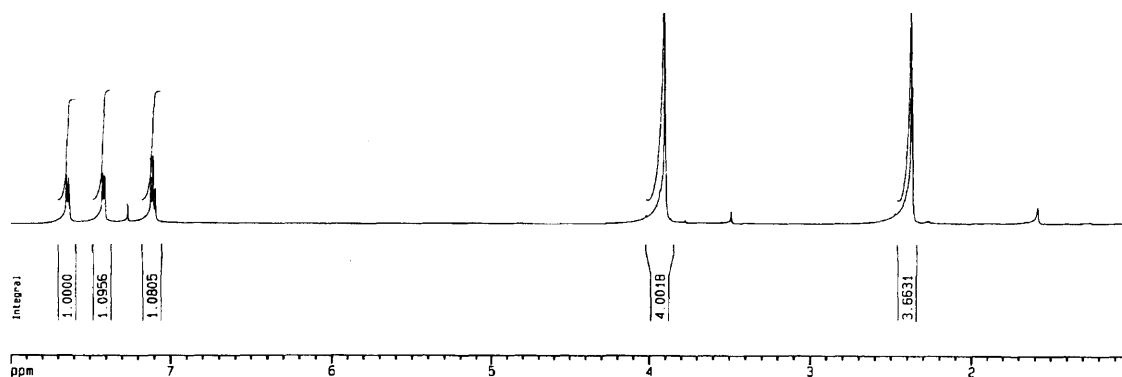
drying. The residue was sonicated briefly in MeOH (100 mL) which produced a pure white precipitate that was collected by filtration. Yield: 0.37 g (38%). ^1H NMR (CDCl_3 , 600 MHz) δ 8.64 (d, 2Har, $J = 4.9$ Hz), 8.24 (s, 2Har), 7.21 (m, 2Har), 7.08 (d, 4Har, $J = 8.2$ Hz), 7.94 (d, 4Har, $J = 8.1$ Hz), 7.88 (m, 8Har), 7.15 (s, 4H), 5.15 (s, 4H), 4.41 (dd, 4H, $J = 14.1, 4.4$ Hz), 3.03 (t, 4H, $J = 12.9$ Hz), 2.89 (m, 2H), 2.41 (m, 8H), 1.42 (m, 8H), 1.25 (m, 32H), 0.88 (m, 12H) ppm; ^{13}C NMR (CDCl_3 , 151 MHz) δ 170.33, 159.31, 157.43, 149.94, 145.20, 144.11, 144.09, 133.30, 129.84, 128.74, 128.30, 127.59, 127.34, 122.46, 120.14, 83.43, 78.87, 65.19, 39.87, 37.76, 35.56, 35.48, 32.03, 31.49, 29.33, 29.31, 29.27, 29.24, 22.91, 22.90, 14.33 ppm; IR (CDCl_3) 3251.66, 2953.88, 2925.28, 2853.98, 1734.88, 1698.27, 1463.79, 1442.87, 1378.49, 1161.06, 917.80 cm^{-1} ; HRMS (FAB) Calc'd for $[\text{M}+\text{Cs}]^+ \text{C}_{80}\text{H}_{100}\text{N}_{10}\text{O}_8\cdot\text{Cs}^+$ 1461.6780, found 1461.6863.



7-Methyl-2-nitroanisole (7.8).²⁹ In a flask fitted with a reflux condenser and drying tube were added 2-methylanisole **7.7** (12.22 g, 100 mmol) and ammonium nitrate (8.00 g, 100 mmol). After cooling with an ice bath, trifluoroacetic anhydride (50 mL,

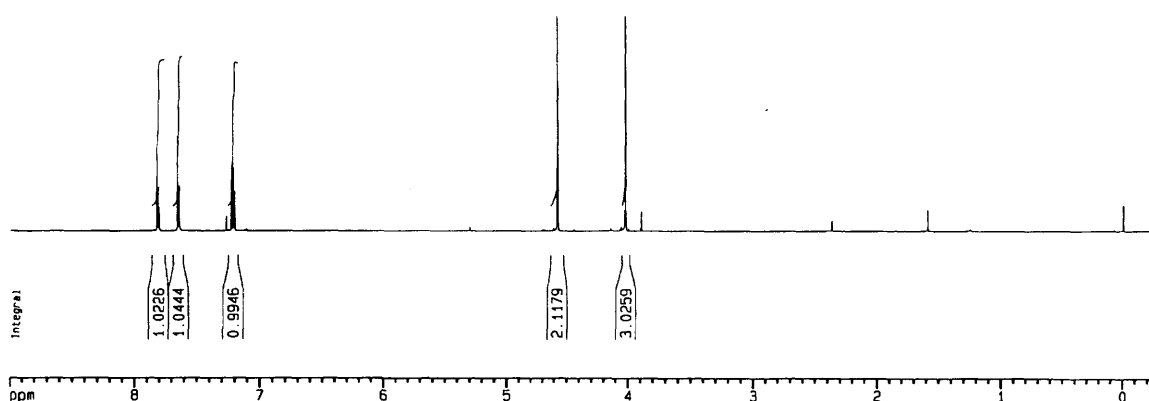
²⁹ Crivello, J.V. *J. Org. Chem.* **1981**, *46*, 3057-3060.

350 mmol) was added with stirring followed by dry CH₂Cl₂ (100 mL). The resulting yellow solution was allowed to warm to room temperature and stir for 3 h during which time the solution turned black. The reaction mixture was poured into 300 mL H₂O and then extracted with CH₂Cl₂ (3 x 100 mL). Drying with Na₂SO₄ followed by filtration and concentration in vacuo produced a black oil. Trituration with hexanes, filtration, and evaporation of the filtrate gave an orange oil which was further purified by flash chromatography (5% EtOAc/Hex) to give the desired ortho-product as a clear, orange oil. [nOe experiments verified the structure. The ortho-product gave no nOe for aromatic protons upon irradiating the methoxy group whereas the undesired para-product gave a positive nOe for one aromatic signal.] Yield: 2.1 g (13%). ¹H NMR (CDCl₃, 600 MHz) δ 7.64 (d, 1Har, *J* = 8.0 Hz), 7.41 (d, 1Har, *J* = 7.4 Hz), 7.11 (t, 1Har, *J* = 7.8 Hz), 3.90 (s, 3H), 2.37 (s, 3H) ppm; ¹³C NMR (CDCl₃, 151 MHz) δ 152.00, 135.95, 134.82, 124.03, 123.15, 62.02, 17.17 ppm; IR (CDCl₃) 2954.19, 2917.04, 2849.24, 1737.27, 1462.65, 1377.45, 1357.23, 1239.98, 1175.98, 1154.71 cm⁻¹; HRMS (FAB) Calc'd for [M+Na]⁺ C₈H₉NO₃•Na⁺ 190.0480, found 190.0487.



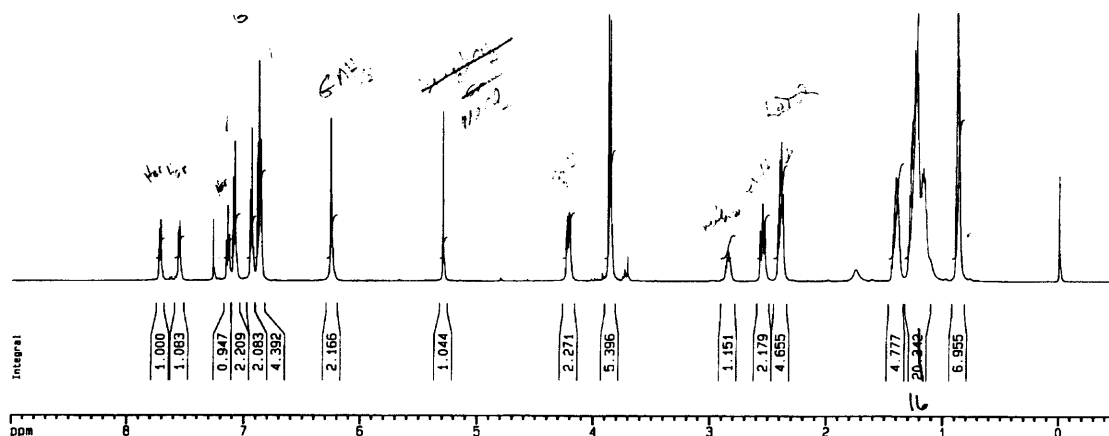
7-Bromomethyl-2-nitroanisole (7.9). NBS (2.13 g, 11.94 mmol), precursor **7.8** (1.81 g, 10.86 mmol), and AIBN (150 mg) were combined in CCl₄ (80 mL) and refluxed under N₂ overnight. After cooling, the reaction mixture was filtered and the filtrate

evaporated to give a yellow oil. Flash chromatography (5% EtOAc/Hex) gave the product as a pure yellow oil. Yield: 1.88 g (70%). ^1H NMR (CDCl_3 , 600 MHz) δ 7.81 (dd, 1Har, $J = 8.2, 1.7$ Hz), 7.65 (dd, 1Har, $J = 7.6, 1.6$ Hz), 7.22 (t, 1Har, $J = 7.9$ Hz), 4.58 (s, 2H), 4.03 (s, 3H) ppm; ^{13}C NMR (CDCl_3 , 600 MHz); δ 152.27, 137.14, 134.89, 127.22, 124.52, 124.49, 63.20, 27.13 ppm; IR (CDCl_3) 3412.63, 3004.38, 2925.11, 1713.93, 1421.62, 1362.18, 1222.17, 1092.39, 902.34 cm^{-1} ; HRMS (FAB) Calc'd for $[\text{M}+\text{H}]^+$ $\text{C}_8\text{H}_9\text{BrNO}_3^+$ 245.9766, found 245.9757.



Nitro-Methoxy Protected Ligand (7.10). Bromide **7.9** (0.11 g, 0.46 mmol), amine module **4.25** (0.25 g, 0.46 mmol), Hünig's base (0.16 mL, 0.92 mmol), and dry THF (30 mL) were combined in a flame-dried flask under N_2 atmosphere. After refluxing for 48 h, the yellow mixture was evaporated and then taken up in CH_2Cl_2 (75 mL). Washing with 1M HCl_{aq} (2 x 50 mL), saturated $\text{NaHCO}_{3\text{aq}}$ (3 x 50 mL), and brine (25 mL) followed by drying (Na_2SO_4) and filtration gave a crude yellow precipitate after evaporation. This was further purified by flash chromatography (5% MeOH/ CH_2Cl_2) giving an off-white powder. Yield: 0.16 g (49%). ^1H NMR (CDCl_3 , 600 MHz) δ 7.72 (d, 1Har, $J = 8.2$ Hz), 7.56 (dd, 1Har, $J = 7.7, 1.2$ Hz), 7.14 (t, 1Har, $J = 7.9$ Hz), 7.08 (d, 2Har, $J = 8.1$ Hz), 7.93 (d, 2Har, $J = 8.1$ Hz), 7.87 (t, 4Har, $J = 8.3$ Hz), 7.26 (s, 2H),

4.22 (dd, 2H, $J = 13.4, 4.5$ Hz), 3.87 (s, 3H), 3.86 (s, 2H), 2.85 (m, 1H), 2.55 (t, 2H, $J = 12.2$ Hz), 2.39 (m, 5H), 1.40 (m, 4H), 1.23 (m, 16H), 0.89 (m, 6H) ppm; ^{13}C NMR (CDCl_3 , 151 MHz) δ 159.71, 151.92, 143.95, 143.92, 137.25, 134.77, 133.57, 130.11, 128.62, 128.21, 127.62, 127.38, 124.82, 124.29, 83.78, 78.83, 63.11, 50.11, 45.64, 43.72, 35.52, 35.46, 32.01, 31.50, 31.47, 29.30, 29.24, 29.22, 22.88, 22.87, 14.30 ppm; IR (CDCl_3) 3225.65, 2954.10, 2927.42, 2855.45, 1724.80, 1693.54, 1531.65, 1463.85, 1440.40, 1355.08, 1247.99, 1102.09, 1082.60, 997.31, 917.92 cm^{-1} ; HRMS (FAB) Calc'd for $[\text{M}+\text{Cs}]^+$ $\text{C}_{41}\text{H}_{54}\text{N}_6\text{O}_5 \cdot \text{Cs}^+$ 843.3210, found 843.3240.



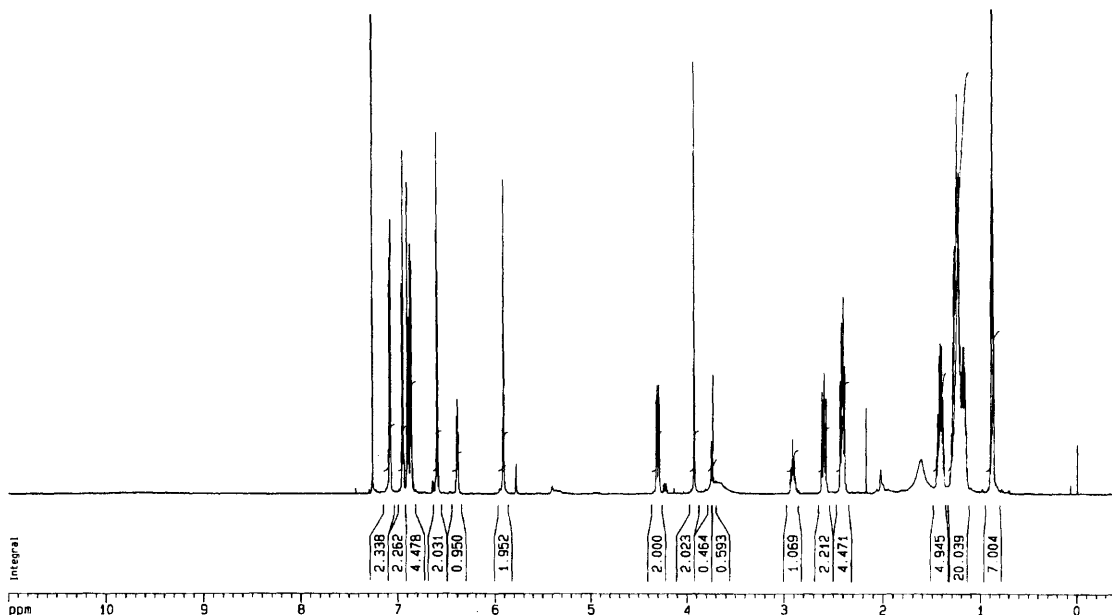
Methoxy Protected Ligand (7.11). Nitro compound **7.10** (0.14 g, 0.19 mmol), palladium on carbon (5% w/w, 0.68 g), and MeOH (15 mL) were combined with stirring. The air in the reaction flask was evacuated and replaced with H_2 (1 atm) three times and then the reaction mixture was allowed to stir under H_2 (1 atm) for 3 h. Filtration through celite and evaporation gave the product as a pure, clear oil. Yield: 0.13 g (98%). ^1H NMR (CDCl_3 , 600 MHz) δ 7.08 (d, 2Har, $J = 8.3$ Hz), 7.93 (d, 2Har, $J = 8.2$ Hz), 7.85 (m, 4Har), 7.64 (m, 1Har), 7.61 (m, 1Har), 7.34 (s, 2H), 4.20 (dd, 2H, $J = 13.5, 4.6$ Hz), 3.74 (s, 2H), 3.72 (s, 3H), 2.85 (m, 1H), 2.57 (t, 2H, $J = 12.1$ Hz), 2.39 (m, 4H), 1.41 (m, 4H), 1.24 (m, 16H), 0.88 (m, 6H) ppm; ^{13}C NMR (CDCl_3 , 151 MHz) δ 159.68, 145.59,

143.87, 143.79, 140.21, 133.70, 130.23, 128.56, 128.18, 127.64, 127.39, 125.11, 119.68, 115.89, 83.83, 78.72, 60.08, 49.97, 47.23, 43.58, 35.52, 35.45, 32.01, 31.49, 31.45, 29.89, 29.31, 29.29, 29.22, 29.20, 22.89, 22.87, 14.30 ppm; IR (CDCl₃) 2954.81, 2918.02, 2849.96, 1737.37, 1463.42, 1379.88, 1357.01, 1242.64, 1175.62 cm⁻¹; HRMS (FAB) Calc'd for [M+Cs]⁺ C₄₁H₅₆N₆O₃•Cs⁺ 813.3468, found 813.3441.



Aminophenol Ligand (7.6). Under anhydrous conditions and an N₂ atmosphere methoxy compound **7.11** (0.13 g, 0.19 mmol) was dissolved in CH₂Cl₂ (25 mL). The solution was chilled in an ice bath and BBr₃ [1N in CH₂Cl₂] (0.93 mL, 0.93 mmol) was added. The clear solution was allowed to stir at room temperature covered from light for 48 h. After cooling again in an ice bath, the solution was quenched with MeOH (25 mL) and then all of the volatiles were removed by rotary evaporation. The residue was triturated thoroughly with water (25 mL) and filtered to provide a crude precipitate. Flash chromatography (2 → 7% MeOH/CH₂Cl₂) provided a small amount of pure (>90%) product which decomposed upon exposure to air. Yield: 10 mg (8%). ¹H NMR (CDCl₃, 600 MHz) δ 7.08 (d, 2Har, *J* = 8.2 Hz), 7.95 (d, 2Har, *J* = 8.2 Hz), 7.90 (d, 2Har, *J* = 8.3 Hz), 7.87 (d, 2Har, *J* = 8.3 Hz), 7.61 (m, 2Har), 7.41 (t, 1Har, *J* = 4.5 Hz), 5.92 (s, 2H), 4.31 (dd, 2H, *J* = 13.8, 4.7 Hz), 3.93 (s, 2H), 2.91 (m, 1H), 2.60 (m, 2H),

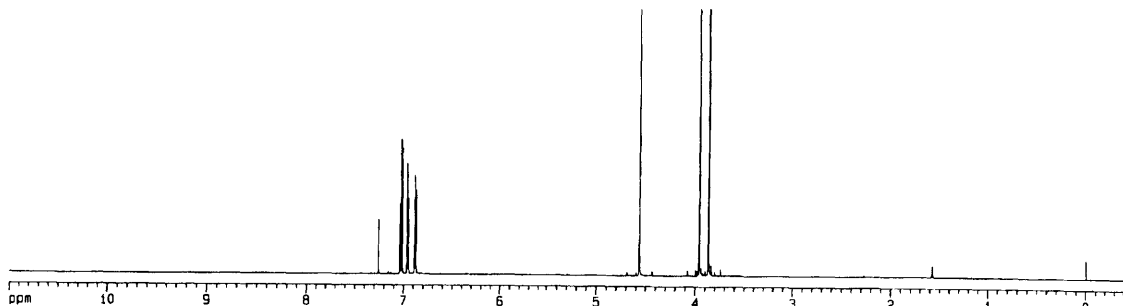
2.41 (m, 4H), 1.42 (m, 4H), 1.25 (m, 16H), 0.88 (m, 6H) ppm; ^{13}C NMR (CDCl_3 , 151 MHz): δ 159.22, 144.94, 144.21, 135.51, 133.33, 129.81, 128.80, 128.34, 127.58, 127.33, 122.05, 119.97, 118.36, 115.32, 83.72, 78.70, 50.23, 49.80, 43.35, 35.57, 35.47, 32.03, 31.50, 29.33, 29.30, 29.29, 29.22, 22.91, 22.89, 14.33 ppm; HRMS (FAB) Calc'd for $[\text{M}+\text{Cs}]^+ \text{C}_{40}\text{H}_{54}\text{N}_6\text{O}_3 \cdot \text{Cs}^+$ 799.3312, found 799.3342.



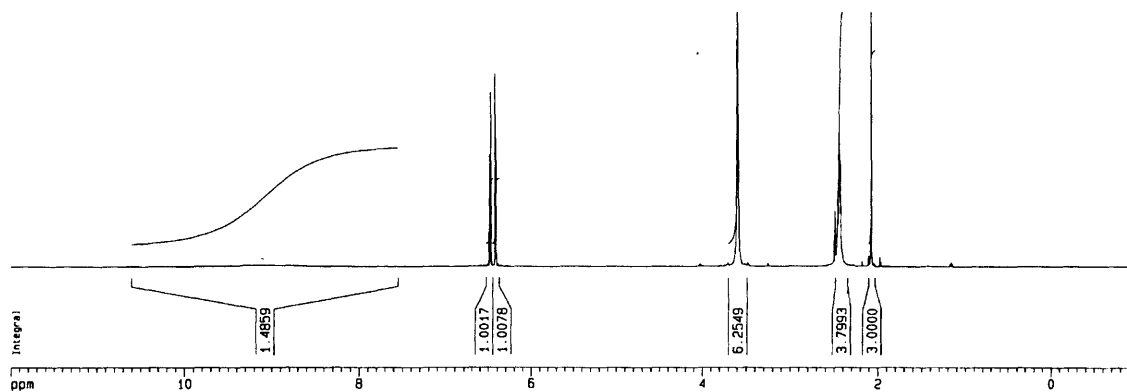
3-Bromomethylveratrole (7.14).³⁰ 2,3-dimethoxybenzyl alcohol **7.13** (12.00 g, 71.3 mmol), PPh_3 (20.98 g, 80.0 mmol), and CBr_4 (27.53 g, 80.0 mmol) were stirred in ether (150 mL) for 2 h at 25 °C. The mixture was filtered, concentrated *in vacuo*, and subjected to flash chromatography (ether) to give a waxy white solid. Yield: 9.73 g (59%). ^1H NMR (CDCl_3 , 600 MHz) δ 7.02 (m, 1Har), 7.96 (dd, 1Har, $J = 7.8, 1.5$ Hz), 7.88 (dd, 1Har, $J = 8.1, 1.3$ Hz), 4.56 (s, 2H), 3.96 (s, 3H), 3.86 (s, 3H) ppm; ^{13}C NMR (CDCl_3 , 151 MHz) δ 152.98, 147.59, 132.06, 124.35, 122.68, 113.16, 61.02, 57.00, 28.36

³⁰ Adapted from JACS **1987** 109 2738-2743 and performed by Dr. Alex Wartini. For a discussion of the Appel reaction, see: Appel, R. *Ang. Chem. Int. Ed. Engl.* **1975**, 14, 801-812.

ppm; IR (CDCl₃) 3000.98, 2963.59, 2937.60, 2833.91, 1585.61, 1481.10, 1430.35, 1311.12, 1273.19, 1234.50, 1080.69, 1069.50, 1002.19, 787.31, 745.02, 664.96 cm⁻¹.

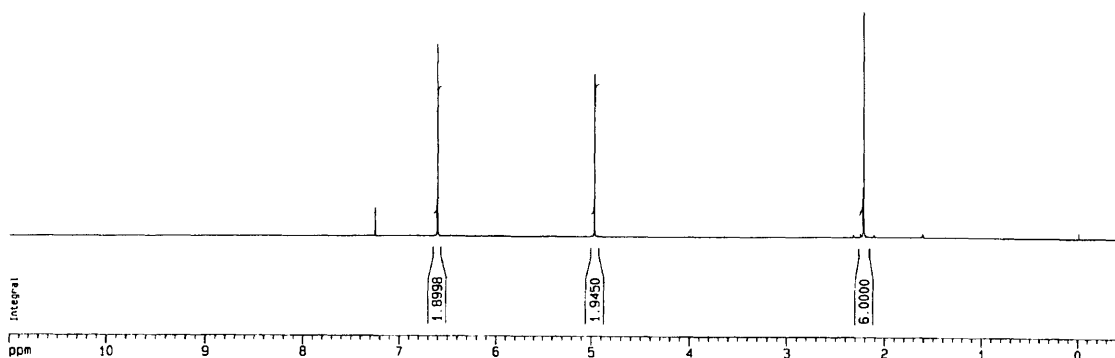


3-Methyl-7-(morpholinomethyl)catechol (7.16). Morpholine (87.00 g, 1 mol) and paraformaldehyde (30.02 g, 1 mol) were stirred in refluxing *i*PrOH (250 mL) until a clear solution developed. After cooling to room temperature, the reaction flask was then chilled to 0 °C in an ice bath. 3-Methylcatechol **7.15** (124.14 g, 1 mol) was dissolved in 400 mL *i*PrOH and then added dropwise to the chilled reaction mixture over 40 minutes with vigorous stirring. Following complete addition, the black reaction mixture was refluxed for 30 min and then cooled to rt. Removal of some *i*PrOH (\approx 100 mL) by rotary evaporation followed by overnight refrigeration resulted in the formation of a dark brown precipitate that was collected by filtration. Two recrystallizations using EtOAc gave off-white crystals which were finely ground using a mortar and pestle. Yield: 110.20 g (49%). ¹H NMR (DMSO-d₆, 600 MHz) δ 9.00 (broad, 2H), 7.48 (d, 1H, J = 7.6 Hz), 7.42 (d, 1H, J = 7.6 Hz), 3.60 (m, 10H), 2.08 (s, 3H) ppm; ¹³C NMR (DMSO-d₆, 151 MHz) δ 144.48, 142.91, 123.55, 120.34, 119.11, 118.76, 67.21, 59.89, 52.47, 15.93 ppm; HRMS (FAB) Calc'd for [M+H]⁺ C₁₂H₁₈NO₃⁺ 224.1287, found 224.1288.

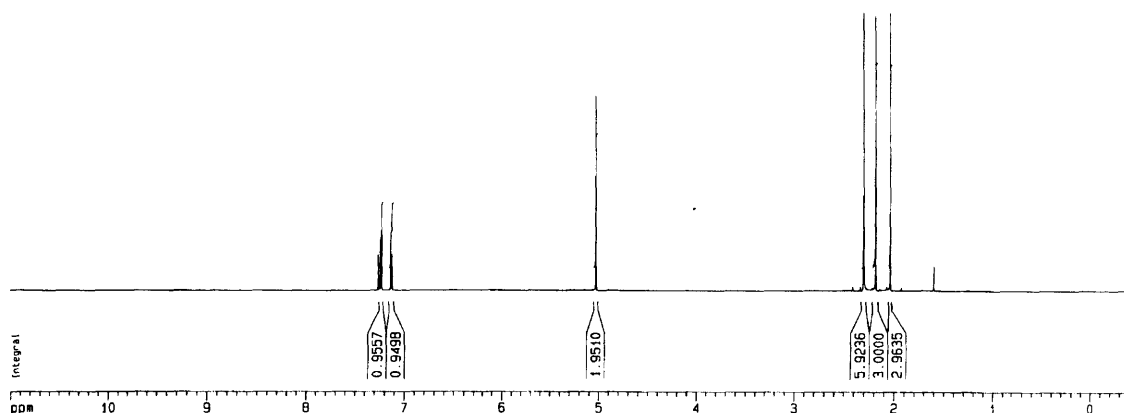


3,7-Dimethylcatechol (7.17).³¹ EtOH (200 mL) was added to a 500 mL Parr bottle and then cooled in an ice bath. Palladium [10% w/w on carbon] (7.00 g) was added slowly under an N₂ atmosphere followed by **7.16** (45.00 g, 201.55 mmol) and the reaction mixture was then allowed to rise to rt. Using a Parr shaker, the mixture was subjected to hydrogenolysis at 80 psi until hydrogen uptake ceased (48 h). Careful filtration through celite (i.e. filter cake was kept wet with EtOH) gave a black filtrate. After concentrating the filtrate down to 200 mL by rotary evaporation, CH₂Cl₂ (500 mL) was added and the solution extracted with 1 M HCl_{aq} (4 x 300 mL). The organic layer was concentrated *in vacuo* without prior drying. The residue was sublimed at 100 °C and 0.1 mm Hg to give an orange and white powder. Recrystallization from hexane and filtration provided the product as an off-white powder. Yield: 1.04g (4%). ¹H NMR (CDCl₃, 600 MHz) δ 7.61 (s, 2Har), 4.98 (s, 2H), 2.22 (s, 6H) ppm; ¹³C NMR (CDCl₃, 151 MHz) δ 141.84, 122.00, 121.74, 15.57 ppm; IR (CDCl₃) 3531.00, 3421.64, 3347.71, 3301.09, 1512.47, 1470.36, 1422.36, 1274.54, 1197.90, 1059.85, 928.35, 798.90, 665.40 cm⁻¹.

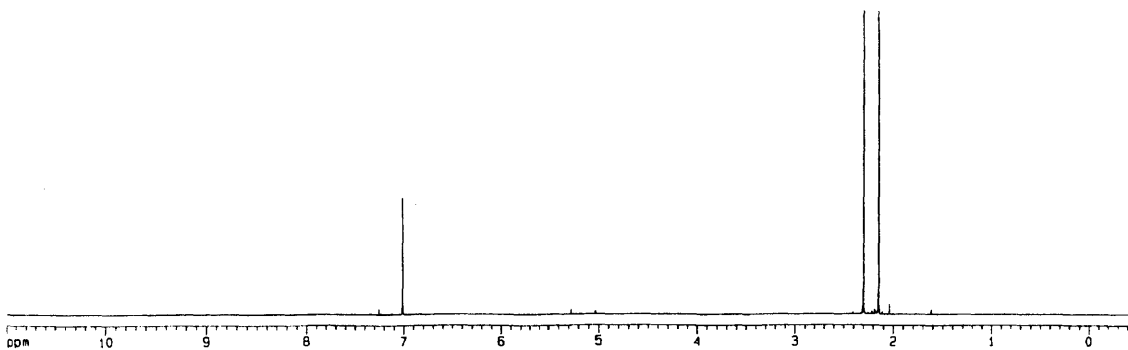
³¹ Also available in quantitative yield from the acidic methanolysis of **7.21**.



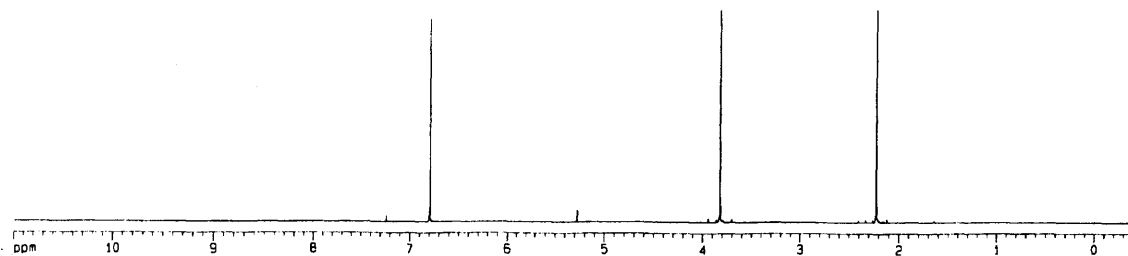
3-Acetoxymethyl-7-methylcatechol Diacetate (7.20). Morpholino catechol **7.16** (49.66 g, 222.42 mmol) was mixed in Ac₂O (250 mL, 2.65 mol) and the mixture refluxed under N₂ for 20 h. Volatiles were removed by rotary evaporation to give an orange oil. This was taken up in EtOAc (500 mL), washed with brine (2 x 250 mL), dried with Na₂SO₄, filtered, and concentrated in vacuo. The residue was dissolved in CH₂Cl₂ (500 mL), mixed with activated carbon, and filtered through celite to remove color. The filtrate was evaporated and the residue was recrystallized with refluxing EtOH (≈ 400 mL) and cooling. After collection of the off-white powder by filtration, the precipitate was recrystallized again using EtOAc. Filtration and washing with a minimum of cold EtOAc provided a clean white powder. Yield: 32.65 g (52%). ¹H NMR (CDCl₃, 600 MHz) δ 7.24 (d, 1H, *J* = 7.9 Hz), 7.13 (d, 1H, *J* = 8.1 Hz), 5.03 (s, 2H), 2.31 (m, 6H), 2.19 (s, 3H), 2.04 (s, 6H) ppm; ¹³C NMR (CDCl₃, 151 MHz) δ 170.82, 168.43, 168.14, 141.74, 141.52, 133.02, 128.47, 127.69, 127.61, 61.30, 21.04, 20.52, 17.40 ppm; IR (CDCl₃) 1777.14, 1740.17, 1430.24, 1370.72, 1204.38, 1171.26, 1072.11, 1024.92 cm⁻¹; HRMS (FAB) Calc'd for [M+Na]⁺ C₁₄H₁₆O₆•Na⁺ 303.0845, found 303.0837.



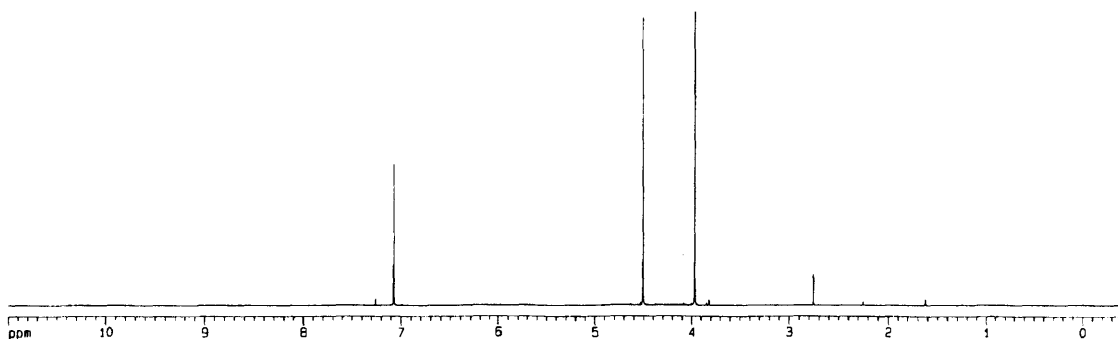
3,7-Dimethylcatechol Diacetate (7.21). Triacetate **7.20** (21.02 g, 75.00 mmol) was dissolved in 250 mL EtOAc with mild heating. This solution was transferred to a 500 mL Parr bottle and then 70% HClO₄ (2.5 mL) was added. Palladium [10% w/w on carbon] (500 mg) was suspended in EtOAc (20 mL) and then added to the reaction solution. This mixture was subjected to hydrogenolysis at 55 psi for 3 h and then filtered through celite. The filtrate was washed with water (300 mL) and saturated aq. NaHCO₃ (3 x 300 mL), dried with Na₂SO₄, filtered and concentrated in vacuo. The resulting yellowish residue was dissolved in a minimum of CH₂Cl₂ and then precipitated using hexane to give a clean white powder after filtration. Yield: 11.90 g (71%). ¹H NMR (CDCl₃, 600 MHz) δ 7.02 (s, 2H), 2.30 (s, 6H), 2.15 (s, 6H) ppm; ¹³C NMR (CDCl₃, 151 MHz) δ 168.37, 141.35, 129.52, 128.06, 20.49, 17.05 ppm; IR (CDCl₃) 1755.88, 1434.79, 1371.93, 1218.67, 1185.62, 1070.23, 868.29, 818.06 cm⁻¹ HRMS (FAB) Calc'd for [M+Na]⁺ C₁₂H₁₄O₄•Na⁺ 245.0790, found 245.0797.



3,7-Dimethylveratrole (7.22). Dimethylcatechol **7.17** (7.40 g, 53.56 mmol) was added to 250 mL acetone followed by K_2CO_3 (44.42 g, 321.38 mmol) and MeI (80 mL, 1.29 mol). The mixture was refluxed for 48 h under N_2 . After cooling, the mixture was poured into 400 mL water and 500 mL ether. After washing, the organic layer was further extracted with saturated aq. $NaHCO_3$ (3 x 300 mL), dried with Na_2SO_4 , filtered, and rotary evaporated. Trituration of the residue with hexane and cooling resulted in the formation of a black precipitate that was removed by filtration. The filtrate was then evaporated and subjected to flash chromatography (CH_2Cl_2) to give a clean white powder. Yield: 5.68 g (64%). 1H NMR ($CDCl_3$, 600 MHz) δ 7.79 (s, 2H), 3.82 (s, 6H), 2.23 (s, 6H) ppm; ^{13}C NMR ($CDCl_3$, 151 MHz) δ 151.53, 129.88, 125.52, 60.23, 15.86 ppm; IR ($CDCl_3$) 2930.53, 2861.08, 2827.10, 1492.87, 1468.88, 1405.76, 1280.05, 1228.54, 1082.13, 1034.10, 908.87, 801.23 cm^{-1} ; MS (GC/MS) Calc'd for $[M^+]$ $C_{10}H_{14}O_2^+$ 167.21, found 167.



3,7-bis(Bromomethyl)veratrole (7.23). Veratrole derivative **7.22** (5.68 g, 34.19 mmol), NBS (13.39 g, 75.21 mmol), and AIBN (561 mg) were combined in CCl₄ (250 mL) and refluxed overnight under N₂. After cooling, the reaction mixture was filtered and the filtrate concentrated by rotary evaporation. The residue was subjected to flash chromatography (10 → 30% CH₂Cl₂/Hex) which gave the desired compound as a slightly impure, clear residue. Trituration with hexane and cooling produced white, needle-like crystals which were collected by filtration. (Note: when in solution, this compound slowly decomposes). Yield: 3.91 g (35%). ¹H NMR (CDCl₃, 600 MHz) δ 7.08 (s, 2Har), 4.51 (s, 4H), 3.97 (s, 6H) ppm; ¹³C NMR (CDCl₃, 151 MHz) δ 151.62, 133.38, 125.93, 60.67, 27.86 ppm; IR (CDCl₃) 2974.43, 2938.05, 2827.18, 1463.72, 1412.05, 1282.42, 1263.79, 1241.61, 1209.49, 1057.42, 1017.09, 750.54, 680.27 cm⁻¹.



Dimodular Veratrole. Dibromide **7.24** (0.35 g, 1.07 mmol), amine module **4.25** (1.75 g, 3.21 mmol), and Hünig's base (0.56 mL, 3.21 mmol) were dissolved under anhydrous conditions in DMF (90 mL). The solution was heated to 100 °C for 24 h under N₂ and then the volatiles were removed by rotary evaporation. The residue was dissolved in CH₂Cl₂ (150 mL) and washed with saturated aq. NaHCO₃ (100 mL) and brine (100 mL), dried with Na₂SO₄, filtered, and rotary evaporated. The residue was

sonicated briefly in MeOH and then cooled overnight. The resulting white precipitate was collected by filtration. Yield: 0.59 g (44%). ^1H NMR (DMSO- d_6 , 600 MHz) δ 8.18 (s, 4H), 7.01 (s, 2Har), 7.96 (d, 4Har, $J = 8.3$ Hz), 7.91 (d, 4Har, $J = 8.3$ Hz), 7.86 (d, 4Har, $J = 8.2$ Hz), 7.84 (d, 4Har, $J = 8.4$ Hz), 4.03 (dd, 4H, $J = 13.2, 4.0$ Hz), 3.76 (s, 6H), 3.66 (s, 4H), 2.43 (m, 2H), 2.35 (m, 12H), 1.37 (m, 8H), 1.20 (m, 24H), 1.11 (m, 8H), 0.84 (m, 12H) ppm; ^{13}C NMR (DMSO- d_6 , 151 MHz) δ 158.91, 150.42, 142.18, 141.99, 134.69, 133.08, 131.46, 128.03, 127.31, 127.19, 123.65, 82.06, 78.03, 60.34, 49.53, 43.85, 42.94, 34.54, 34.50, 31.27, 30.87, 30.74, 28.53, 28.51, 28.40, 28.34, 22.15, 22.13, 13.94 ppm; IR (CDCl $_3$) 3258.18, 2954.71, 2925.72, 2854.58, 1724.97, 1694.13, 1463.97, 1439.60, 1415.39, 1247.14, 1102.11, 1018.30, 913.94 cm^{-1} ; HRMS (FAB) Calc'd for $[\text{M}+\text{Cs}]^+ \text{C}_{76}\text{H}_{104}\text{N}_{10}\text{O}_6 \cdot \text{Cs}^+$ 1385.7195, found 1385.7267.

